POLITECNICO
MILANO 1863

School of Industrial and Information Engineering

Master of Science in Chemical Engineering

Department of Chemistry, Materials and Chemical Engineering "Giulio Natta"

MODELING OF A THERMO DEASPHLATING COLUMN PROCESS: AN INDUSTRIAL CASE STUDY

Supervisor: Prof. Flavio MANENTI

Advisor: Ing. Victor BALDO, Doc. Daniele PREVITALI

M.Sc. Thesis of:

Kristiano Prifti 893005

Leonardo Palomba 894088

Academic Year 2018 – 2019

Our heartfelt thanks to professor F. Manenti, without whom this thesis would have not been possible, for the opportunity he gave us to interact with this particular yet important industrial reality of Italy. We also want to extend our thanks to Itelyum in the persons of Ing. F. Gallo, who made this work possible, and Ing. V. Baldo, who supported us along all this year long period of work, with modeling suggestions, data and information vital to our work. We also want to thank him for his patience and the willingness to help he showed whenever asked.

Our thanks go also to the rest of SuPER team which was always available to provide feedback and help on our work. In particular we wanted to thank Prof. Giulia Bozzano for the feedback she gave us on the furnace modelling and Prof. Simone Colombo for the observations made on the limits of risk analysis carried out on a simulating software such as DynSim.

Lastly, but surely not for importance, our thanks go to Doc. Daniele Previtali for its continuous support, availability, and assistance in all that is part of thesis. Thank you for always sharing your honest opinion with us and making this whole experience so much more enriching.

Preface

This thesis has been made possible through a collaboration between Politecnico di Milano and Itelyum which, in the persons of Ing. Francesco Gallo and Ing. Victor Baldo, provided experimental data and modeling advice.

Its main purpose is the development of a dynamic and stationary model of the Thermo-de-Asphalting column located in the Pieve Fissiraga (LO) plant to stand as a basis for future plant development, economic optimization and optimal procedure development for star-up, shutdown and accident management of the column.

POLITECNICO
MILANO 1863

ITELYUM

† www.polimi.it
† www.itelyum-regeneration.com

Table of Contents

List of Figures

List of Tables

Estratto

Questa tesi verte sulla modellazione stazionaria e dinamica di una colonna operante sottovuoto, che tratta oli esausti disidratati. I modelli saranno la base per successivi sviluppi e applicazioni. Il software Aspen HYSYS® V10 comprende la modellazione statica usando il suo ampio database per una caratterizzazione efficacie dei tagli di olio lubrificante, mentre SimSci DynSim® (versione 5.3.1) è usato per la modellazione dinamica, favorendo una accurata precisione nel predire il comportamento dinamico del sistema a discapito della caratterizzazione delle proprietà dei prodotti.

I modelli termodinamici BK-10 e Peng-Robinson sono stati testati, e quest'ultimo è risultato essere il migliore.

Il modello stazionario della colonna è sviluppato in Aspen HYSYS® che rappresenta la sezione impacchettata della colonna in diversi stadi teorici, mentre il ciclone alla base è implementato come un flash. La parte dinamica richiede una maggiore precisione nel descrivere l'idraulica interna alla colonna e il modello di un'unica torre non era appropriato. Perciò, la TDA è stata suddivisa in 7 parti, ognuna rappresentante una differente sezione.

I modelli di predizioni di viscosità in Aspen HYSYS® non sono sufficientemente accurati, quindi i modelli di Bingham e Bergmann-Sutton sono stati implementati in un codice VBA in Excel che automaticamente calcola le viscosità per ogni simulazione.

Il modello stazionario utilizza 31 pseudo-componenti per favorire la precisione nella caratterizzazione dei prodotti, mentre il modello dinamico utilizza solo 15 pseudo-componenti per minimizzare lo sforzo computazionale e migliorare la convergenza. Tale set di pseudo-componenti è stato modificato per ottimizzare la qualità predizione dei risultati. L'unità di preflash ha testato le differenti performance di vari set.

Excel ha analizzato la maggior parte di dati e risultati. Le librerie di Python (Pandas, NumPy e Seaborn) sono state utilizzate quando necessario (correlogrammi e schemi).

Il modello stazionario risulta predire ottimamente le condizioni operative del processo e le proprietà dei tagli prodotti, mentre il modello dinamico rappresenta accuratamente il comportamento dinamico del sistema, come validato per entrambi i casi. Infine, il modello dinamico è stato utilizzato per pianificare una nuova procedura di Startup e per simulare un caso di incidente implementando la miglior strategia di controllo nei limiti di simulazione e quantificando la portata di prodotto fuori specifica.

Abstract

This thesis concerns with the stationary and dynamic modeling of a vacuum distillation column working with dehydrated used oil. The model aims as the basis for successive optimization tasks. Aspen HYSYS® V10 carries out the stationary modeling to exploit its oil database for best property prediction, while SimSci DynSim® (version 5.3.1) performed the dynamic modelling to have an accurate prediction of the equipment behavior in spite of lower precision in predicting properties.

For the thermodynamic description of the system BK10 and Peng-Robinson equations of state were tested, and Peng-Robinson proved to be the best one.

The column model for the stationary simulation is a standard Aspen HYSYS column representing only the packed section of the Thermo De Asphalting tower, while a flash unit approximates the cyclone preceding the column. The dynamic simulation requires higher precision in the description of the internal hydraulics and a classical tower was not sufficiently detailed. Thus, the TDA was broken down in sections each representing a limited portion of the column as accurately as possible.

The performances of Aspen HYSYS internal models for viscosity were unsatisfactory and the Bergmann-Sutton and Bingham models were implemented by means of a VBA script in Excel that automated the data extraction and computation of the viscosities.

The stationary simulation adopts thirty-one pseudo-components in order to favour precision in the property prediction, whereas the dynamic simulation utilises fifteen pseudo-components so to guarantee a reasonable computational time and a better convergence. This cut set was also customized to be more precise in the description of middle cuts which are the products of the column. The quality of the approximation was tested using data from an upstream flash unit.

Excel analyzed and represented most of the data. However, when necessary (correlograms and heatmaps), Python libraries are used (Pandas, NumPy and Seaborn for visualization).

The stationary model accurately predicts the distribution of the lubricant cuts and their properties as verified by the experimental data, whereas the dynamic model correctly predicts the qualitative behaviour of the column by means of historical data validation. After validation, the dynamic model aimed to simulate a start-up procedure and a top condenser failure, as accident scenario. The devised start-up procedure confronted its performances against the procedure used presently. The accident scenario quantified the amounts of out of specification product sent to storage during transients and it was integrated with a strategy to compute the longest possible time the plant can be operated in off-spec conditions without compromising the quality of the final product.

1. Introduction

A lubricant is a substance, usually of organic nature, used to reduce friction between surfaces in mutual contact. Lubricants are formulations, which are tuned to a specific application through different proportions of base oils and specific additives. Between 5000 and 10000 different formulations cover about 90% of the market demand [1].

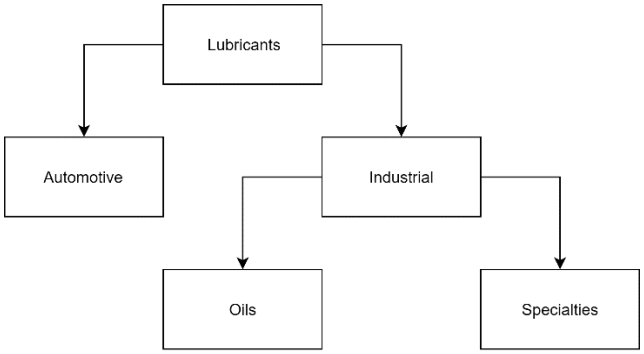

Figure 1: Lubricant classification

Lubricants are classified in automotive and industrial lubricants. Industrial lubricants are sub-divided in oils and specialties where oils refer to standard lubricant applications while specialties refer to greases, metalworking lubricants, and solid lubricant films.

In the early 50s, the most important requirements for base oils were correct viscosity and absence of acidic components, but during the 60s the attention shifted towards additives formulation and synthetic oils. By the time the 70s and 80s had passed, the first formulations based on quasi-synthetic hydrocracked oils were starting to be economically feasible. Synthetic oils, with their uniform chemical structures, offered better performance than their mineral counterparts and these decades focused on making their synthesis economically competitive. The 90s pushed the requirements for performance, environmental and health/safety even further. In spite of higher prices, the new generations of oils were required to be environmentally friendly, safe and outperform their mineral counterpart. Hydrocracked products, polyalphaolefins, and esters gained acceptance. Natural fatty oils and their oleochemical derivatives saw a renaissance in popularity due to their biodegradability. Lubricants were more and more concerned with the quality of their base oils than the formulation of their additives.

By the year 2000 in western Europe about 10 wt % of base oils were synthetic (hydrocracked oils are also considered in this category) representing 40% wt of total base oil value, furthermore, 5 wt % of lubricants were rapidly biodegradable esters [1].

1.1. Lubricants

Base oils are the main component of lubricants in volumetric terms, for standard hydraulic and compressor oils, they make up 99% of the formulation while for metalworking fluids, greases and gear lubricants they make up to 70% of the total volume [1]. Most common Base oils have a prevalently straight paraffinic nature, but crude from Venezuela, Russia or United States may have a higher Naphthenic content.

Base oils are a mixture of paraffinic, aromatic and naphthenic hydrocarbons with boiling point ranging from 350° to 520°. Their complex composition makes a detailed description of the single components impossible. Thus, they are characterized by using some key performance indicators.

Paraffinic oils are the most common ones and their innately high viscosity index makes them ideal for lubricant applications. Unfortunately, long chain linear paraffins tent to crystalize at relatively high temperatures making them inadequate for most applications. This is the reason why branched paraffins are preferred since their viscosity index is still very high, but their crystallization temperature is much lower.

Naphthenic oils are much scarcer and, due to toxicity reasons, are used only in particular applications and after going through hydrogenation and solvent extraction processes. Depending on the presence of long paraffinic chains their viscosity index might drastically change, despite still being lower than paraffinic oils. Naphthenic compounds are also worse at resisting oxidation and will degrade faster. All these drawbacks are however sometimes displaced by their better ability to solvate additives and their extremely low crystallization temperature which make them a very valid choice in cold operations were viscosity index has a secondary importance.

Non-conventional oils are obtained by hydrogen treating of standard refinery processes products and, more recently, by Fisher-Tropsch synthesis. The treatments make the oil final composition relatively independent from the crude feedstock and the quality of the final product very high (VI is usually higher than 140, better oxidation resistance, lower pour point and negligible sulfur content).

Additives are organic or inorganic compounds dissolved or suspended as solids in oil. They have three basic roles:

- Enhance base oil properties: antioxidants, corrosion inhibitors anti-foam and demulsifying agents.
- Suppress undesired oil properties: pour-point depressants and Viscosity Index improvers
- Grant new properties to the oil: extreme pressure additives, detergents, metal deactivators, and adhesion agents

MACHINE	COMMON ADDITIVES USED	PERCENT OF OIL VOLUME
Engines	Antioxidant, corrosion inhibitor, detergent/dispersant, anti-wear, anti-foam, alkalinity improver	10 - 30%
Steam turbines, compressors	Antioxidant, corrosion inhibitor, demulsifier, anti-foam	0.5 - 5%
Gears (spiral, bevel or hypoid)	Anti-wear, antioxidant, anti-foam, sometimes corrosion inhibitor, extreme pressure	1 - 10%
Gears (worm)	Extreme pressure, antioxidant, corrosion inhibitor, fatty acids	3 - 10%
Hydraulic systems	Antioxidant, anti-wear, anti-foam, corrosion inhibitor, pour-point depressant, viscosity index improver	2 - 10%

Table 1: Additive presence in various applications [24]

They are usually sacrificial, meaning that once deactivated they cannot be regenerated, but must be reintroduced in the system.

The formulation of additives is a complex process, most of them have competing positions in the oil and will improve a property while having a negative effect on another one. The mechanism through which they achieve their purposes varies depending on the specific case, but most of them are molecules that can interact with the base oil and surrounding environment.

Some examples of how they work are listed:

- Dispersants are used in engine oil to keep the engine clean and free of deposits. The way they achieve this is by having a structure with a head that interacts with the soot and a tail that is solvable in the base oil. This structure keeps the soot suspended in the oil avoiding accumulation and allowing for cleaning when the oil is changed.
- Anti-foam agents are molecules with low interfacial tension so that they weaken the oil bubble wall and make it burst faster.
- Rust and corrosion inhibitors are molecules that chemically absorb on the metal surface and avoid contact between water and the metal by physically separating them.

1.1.1. Base-Oils Properties

Base oils are made by an extremely large variety of compounds and their isomers, so they are described by their technical properties and the quantitative presence of groups of compounds with similar properties.

Stability to Oxidation is an important base oil property. If exposed for long periods to air base oils will eventually oxidise to give corrosive acids or insoluble compounds that will deposit and hinder the lubricant performance. The standard tests to verify the stability of the oil are IP 48, Differential Scanning Calorimetry – DSC, and TGA – Thermo-Gravimetric Analysis.

Cloud point and **Pour point** are the temperatures at which the oil becomes cloudy due to paraffin crystal formation and the temperature at which it stops pouring. These

two parameters are very important during cold operations and usually values as low as possible are desired.

Flash point is the temperature at which the oils vapor burns if exposed to a free flame and it is important for safety concerns on the operations.

Colour while being a rather qualitative property provides a lot of important information on the oil's conditions. To have a more objective way to measure it is converted to a numerical value through appropriate ASTM test:

- Pale – ASTM 4.5 or lighter
- Red – darker than ASTM 4.5
- Dark – ASTM greater than 8

Dark oils are usually more viscous, and this colour can also be indicative of oxidative degradation of the oil. High performance non-conventional oils are characterized by extremely clear colour.

Carbon residue is how much carbon is left once combustion has ended. Very low values are desired so that if combustion takes place no residue is left in the oil.

VCG – *Viscosity Gravity Constant* is a rough index for chemical characterization of the oil. It is calculated as a function of specific gravity and Saybolt Universal viscosity (SUV is and experimental value to be measured at 37.8° or 98.9° corresponding to the efflux time in Saybolt Universal seconds of 60 mL of oil through a Saybolt universal viscometer [2]). VGC values close to 0.8 indicate a paraffinic oil while values close to 1 an aromatic oil.

Carbon distribution in terms of aromatics, naphthenic and paraffinic is the most important characterization of the oil. It is however achieved through complex analytical means. The components are first separated by chromatography then analyzed with high ionizing voltage spectrometry (ASTM D 2786-91 for saturated fractions and ASTM 3239-91 for aromatic ones). The aromatic content can be determined by Nuclear Magnetic Resonance (ASTM 5292) [1].

The **viscosity index (VI)** is a measure of how much viscosity changes with temperature; higher VI means the lubricant viscosity is less affected by changes in temperature, which is a desired property for lubricants working in wide temperature ranges. VI is calculated as follows:

$$\boldsymbol{VI = 100 \cdot \frac{L - U}{L - H}}$$

U is the oil's kinematic viscosity at 40°C, while **L** and **H** are reference values of kinematic viscosities at 100°C for oil with **VI** of 0 and **VI** of 100 respectively [3].

Base oils themselves are categorized by the American Petroleum Institute (API) into five main groups depending on their viscosity index and sulfur content:

- **Group I** base oils are the less refined type, usually made of conventional hydro-treated petroleum base oil (VI of 80-120 and 0.03% sulfur or more)

- **Group II** base oils may be partially produced by hydrocracking and undergo purification steps to achieve sulfur contents lower than 0.03% mass fraction and a VI in the 80-120 range.
- **Group III** base oils are the best grade of non-synthetic base oil. Besides hydrocracking they undergo hydro-isomerization and hydrotreating, sulfur content is below 0.03% massive and VI is greater than 120.
- **Group IV** base oils are synthetic oils made of Poly-alpha-olefins (PAO) with a viscosity index in the range 125-200 and negligible contents of sulfur

.

Group	Origin	Composition	VI	S % [w/w]
I	Petroleum	Saturated hydrocarbons	80-120	> 0.03%
II	Petroleum	Saturated hydrocarbons	80-120	< 0.03%
III	Petroleum	Saturated hydrocarbons	>120	< 0.03%
IV	Synthetic	Poly-alpha-olefins	125-200	-

Table 2: API base oils classification

Higher grade base oils are made from synthetic oil and are tailored to specific applications.

Alongside the standard group classification some unofficial groups, marked with a "+", to identify their superior quality, exist. These oils are subjected to further treatments besides the basic ones and usually have VI in the upper bracket of the range or lower Sulphur content.

1.1.2. Standard Production and Treating

Base oils are refinery products coming from post-treatment of topping distillation residue. They are distilled in a vacuum column as intermediate cuts, their normal boiling range is about 350-530 °C. The residue of vacuum distillation can go through a de-asphalting step with propane to recover brightstock (a highly viscous base oil mixed in asphaltenes).

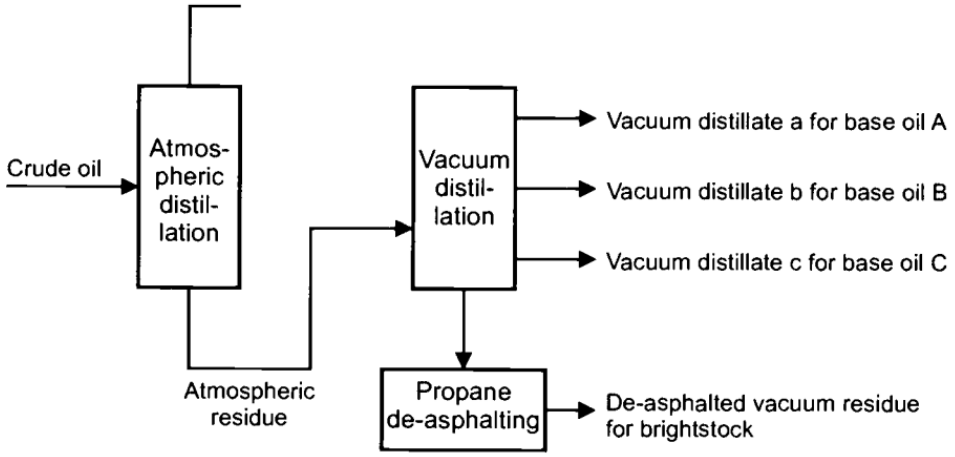

Figure 2: Flowsheet for the manufacture of suitable feeds for lube oil refining [1]

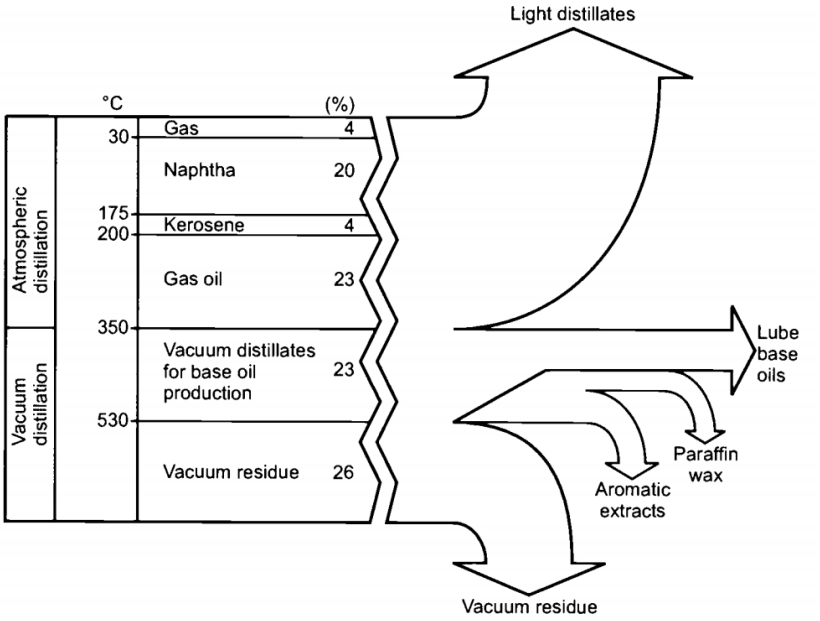

Figure 3: Yield of the various cuts in conventional lube oil refining of a typical lube crude [1]

Acid refining is the treatment with concentrated sulfuric acid (oleum) with the purpose of removing reacting oil components (mainly olefins) and reducing the aromatic content, which in turn raises the VI. Since the process requires complex neutralization follow-up steps, it is used only for the production of technical and pharmaceutical white oils.

Dewaxing removes long-chain, high melting point paraffines that crystallize at high temperature leading to high temperature pour point, poor performance, and undesired aromatic components (they lower VI). In traditional refining, dewaxing is carried out by a mix of crystallization, filtration and solvent extraction.

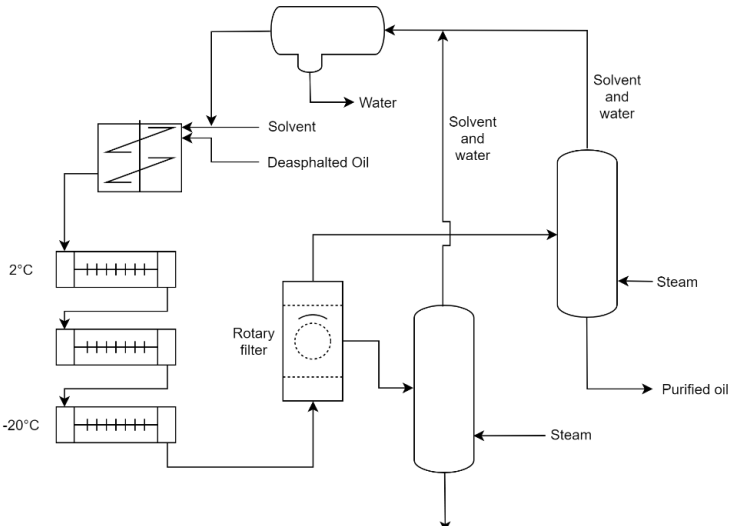

Figure 4: Dewaxing process scheme

Hydro-finishing is a mild hydrotreating process focused on improving color, odor, and ultraviolet stability. Catalyzed by either Co-Mo or Ni-Mo, uses hydrogen at temperatures close to 300°C and high pressures (depending on the severity it can go from 20 atm to 150 atm) to remove unsaturated compounds. In the case of finishing no significant amount of hydrodesulphurization is carried out.

Hydrogenation and **Hydrocracking** in the manufacture of lubricant base oils significantly influence the chemical structures of mineral oil molecules. Unstable molecules are chemically stabilized by the removal of the heteroatoms (sulfur, oxygen, nitrogen) and severe hydrogenation can convert aromatics into saturated naphthenic or paraffinic structures. Hydrocracking allows for better control on the quality of the final product, independently on the quality of the oil feedstock.

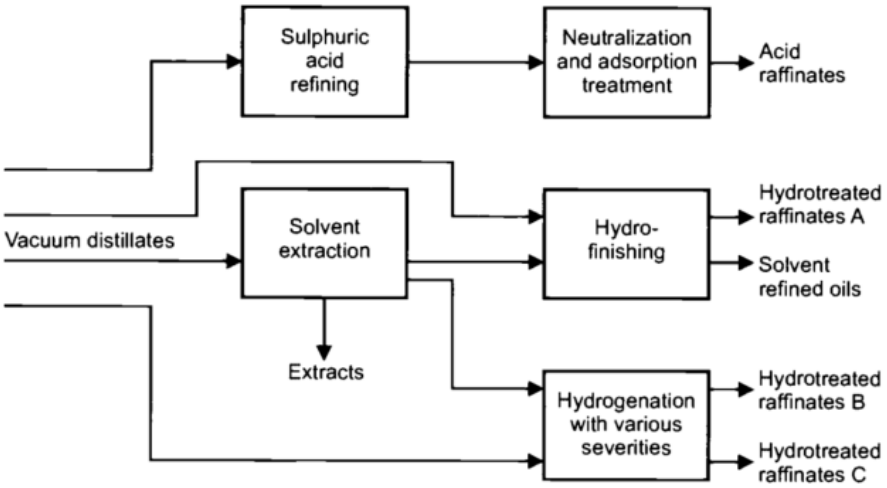

Figure 5: Base oil treatment alternatives [1]

1.1.3. End of Life

During their lifetime lubricants undergo drastic conditions such as high temperature operation, micro-dieseling (when cavitation happens and the formed bubbles contain a flammable mixture, during their collapse they will cause self-ignition in a similar fashion to what happens in diesel engines, which leads to high temperatures that degrade the oil), oxidation and contamination by dirt, water and fine particles. Over time these phenomena wear down the oil performances and make replacement necessary. Waste oil is an environmentally hazardous substance and as such it requires proper disposal procedures.

Waste oil can be disposed of in several ways:

- **Direct incineration** which however makes for a very dirty feedstock
- **Blending stock** for high sulfur fuels
- **Secondary feedstock** for catalytic crackers
- **Flux oil** for bitumen
- **Re-refining** to restore the original base oils

Growing environmental concerns over the last decades have made legislation (D.M. 392/1996 in Italy) stricter and re-refining more competitive and appealing [1].

1.1.4. Oil Regeneration Market

In 2017, according to CONOU (Consorzio Nazionale per la gestione, raccolta e trattamento di Oli minerali Usati), 406 kton of new lubricant oil was consumed in the Italian market [4]. The lubricant oil usage was split into two main sectors, the industrial and automotive.

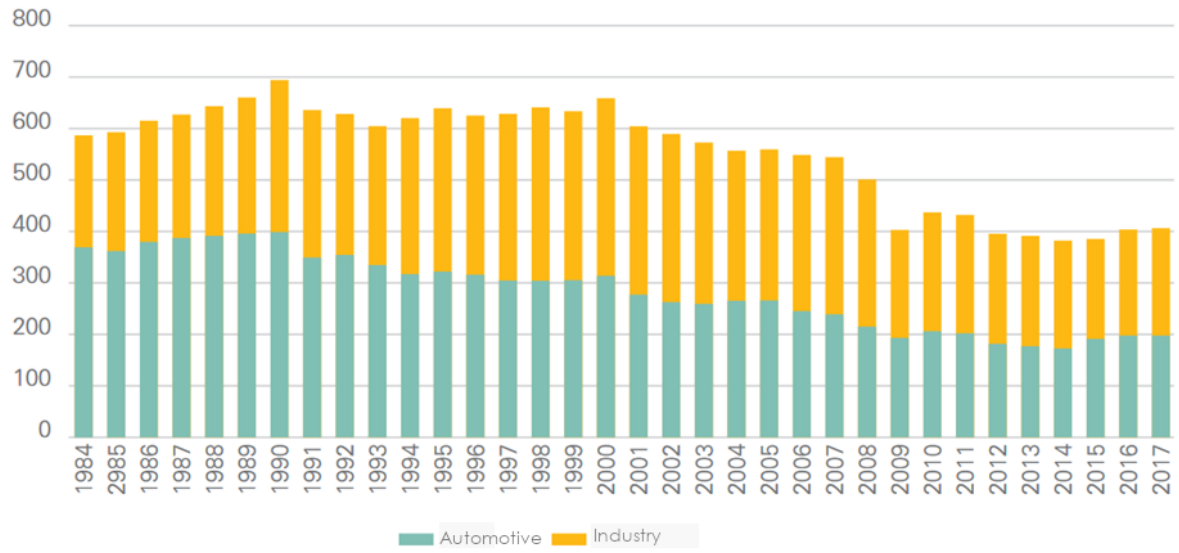

Figure 6: New lubricant oil introduced in the Italian market each year in kton [4]

Italy is an important refining center in Europe, refining 80.3 Mton of crude oil in 2017 [4] most of which (82.5% of the total) was imported from the middle east (42%), ex-Soviet Union members (34%) and Africa (18%). The greatest part of the products were fuels (close to ¾ of the whole national production) while lubricants made up a small yet important fraction: 1.7% of the total resulting in 1.36 Mton of lubricant oils produced of which 1.2 Mton were destined to export, 0.16 Mton were used internally and 0.3 Mton were imported.

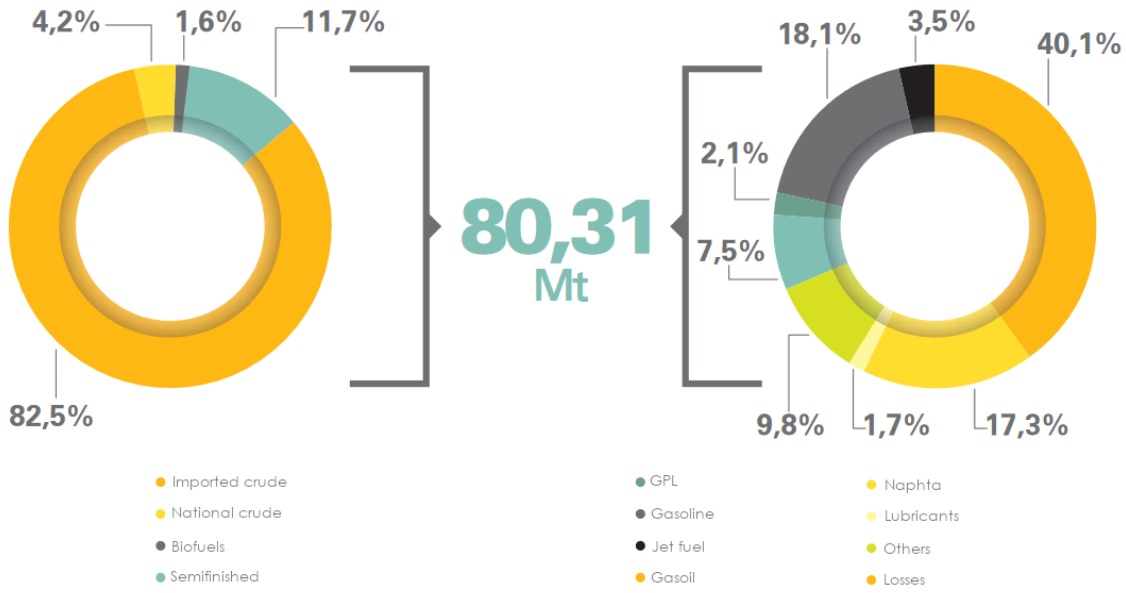

Figure 7: Refinery production distribution and raw materials in Italy in 2017 [4]

Of the new oil introduced in the market in 2017 only about 45% is collected into the waste management system while the remaining fraction was lost during usage or was impossible to collect. Of the remaining 182.7 kton, 99% is destined to regeneration while what is left is mostly used as fuel in incinerators. The efficiency with which the regeneration process can recover the base oils is about 62%, the remaining is lost to other products (gasoil and bitumen) and wastewater.

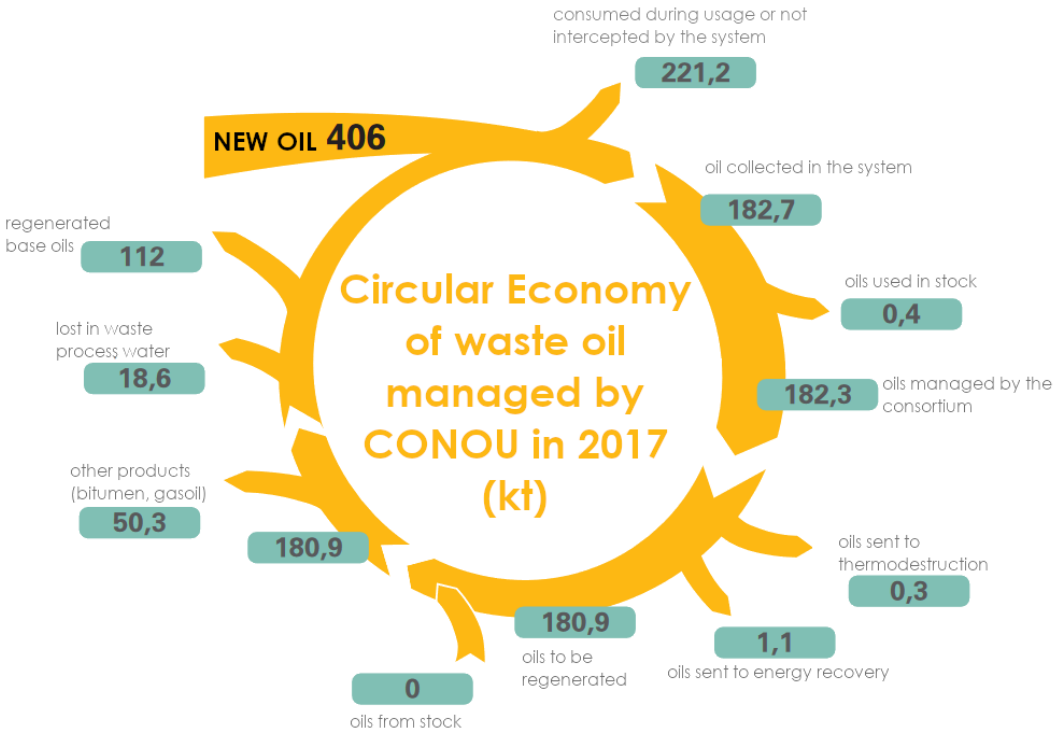

Figure 8: Circular economy of waste oils in Italy in 2017 (numbers in kton) [4]

In this contest, **Itelyum Regeneration Srl** has distinguished itself as a leader in the promotion of a circular waste oil economy both in Italy and in Europe in the last 5 decades. The history of Itelyum started in 1963 at Pieve Fissiraga as Viscolube and in recent years has seen several expansive investments in a new business line dealing in collection and treatment of special waste, a new plant in Ceccano and the introduction of a new Vacuum distillation column in the Pieve Fissiraga plant. The regeneration plants of Ceccano (FR) and Pieve Fissiraga (LO) have a combined capacity of 200 kton a year, capable of satisfying all the recycling requirements of Italy. These plants are capable, starting from a waste oil feedstock, to recover up to Group II+ base oil quality while also producing gasoil. The dynamic and stationary modeling of this column will be the theme of this thesis.

1.2. Regeneration Plant

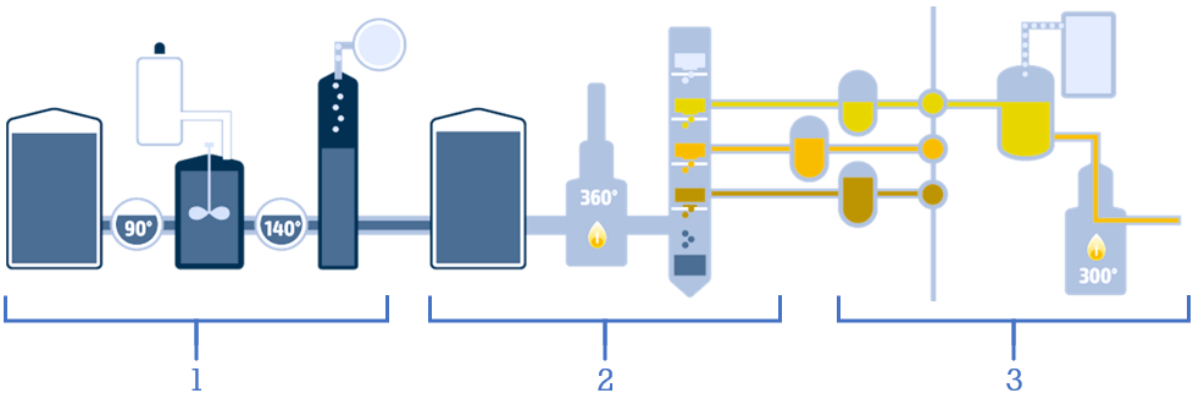

Figure 9: Plant layout general scheme

The regeneration plant can be divided into three macroscopic sections:

1. A pre-flash stage in which the oil is heated up to 140 °C to then be distilled in low vacuum conditions in order to remove light hydrocarbons and water;
2. A high temperature, deep vacuum deasphlating stage: the feedstock is heated up to 360°C in a furnace then sent to the TDA column where the heavy asphaltenes are removed at the bottom and the lubricant cuts are retrieved alongside vacuum gasoil as side products;
3. The final step consists in mixing the base oils with hydrogen and then feeding them at 300 °C to a catalytic reactor where the oil is stabilized and cleaned of any residual sulfur.

Several of these treatments are shared with refineries. However, the ever-changing feedstock requires continuous monitoring and along with it, the plant operative conditions must change to guarantee the product specifications.

The partially cracked feedstock contaminated by metals and water will need a fine-tuned pretreatment and an accurate thermodynamic characterization when modeled.

The non-conventional design of the column, featuring a sludge-vapor cyclone and an internal top condenser, will represent another challenge for the simulating software.

These factors combined with an unfortunate topology of the data will make several approximations necessary, even if these approximations will be made so that errors on the prediction of the most economically relevant products are avoided.

Vacuum distillation is used with high boiling compounds that suffer from thermal degradation to lower the operative temperatures of classical distillation. The vacuum is usually achieved either through vacuum pumps or ejectors, both of which have high operative and capital cost. Operating a vacuum column is expensive for several reasons, the main ones being:

- Lower pressures decrease vapor density, this makes an increased column diameter necessary;
- Ejectors and vacuum pumps are expensive both to purchase and operate;
- The column must be designed to withstand external pressure. Working in compression is much more complex than working in traction so particular attention has to be paid in designing the vessel (it will usually result in thicker walls);
- Working with flammable compounds. In case of a leak, air will be sucked in the column and a flammable mixture could be formed. Extra safety precautions must be implemented (seal testing);
- Low pressure drops per tray are necessary. To achieve them either structured packs are used (more expensive than standard trays) or low weir heights (will result in lower tray efficiency and thus more trays).

1.3. Simulation Software

Aspen HYSYS® is a chemical process simulator suite created by Hyprotech® and later acquired and developed by AspenTech®. It is provided with mathematical models for all the main unit operations used in the chemical industry and a framework to expand on them and the compounds included in the default library. The software is widely used in industry for steady-state simulation, process design, performance monitoring, and operation optimization. HYSYS was originally developed to model petrochemical systems characterized by the necessity of hypothetical compounds and petroleum assays, and for the reputation it holds on the market as the leader of refinery modeling, it was chosen for the steady-state modeling of the TDA.

SimSci DynSim® is a comprehensive, dynamic process simulator developed by Schneider Electric and closely integrated with PRO/II®. The main focus of DynSim is dynamic behavior, control, and operator training. The dynamic simulations carried out in DynSim enjoy state of the art algorithms optimized for robustness and accuracy and complete access to the unit operation models for better understanding of the modeling limits and parameters. The TDA plant layout comprises several refluxes and for this reason, a more robust solver than the one of HYSYS was necessary, the choice fell on DynSim for its excellent performance in dynamic simulations.

1.4. Thermo Deasphalting Column

The core of the plant and subject of this thesis is the Thermo de Asphalting column (TDA) which separates lube base oils from asphaltenes and vacuum gasoil by means of vacuum distillation. The column present in Viscolube plant is about 35 m tall with a diameter of 2.5 m and filled with 6 structured packed beds.

The column can be divided into two sections; a non-conventional cyclone and the packed column. The feed enters tangentially to the column shell, the sludge sticks to the borders decreasing its speed and falling down while the vapors can proceed to the upper packed section through a large cylindrical pipe. The pipe connecting packed section and cyclone is covered by a cap which does not allow the liquid trickling from the first packed bed to fall back in the cyclone. The liquid is instead collected in a basin and recycled back to the first pack after a purge.

All the packs, from which products are retrieved, are equipped with a basin that collects part of the liquid from above while letting some drop to the pack below. The products go through a pump-around system and are recycled to the column after a purge which is where the products are collected. VGO is cooled at 20°C and sent at the top of the 6th pack. FLS is cooled at 180°C and split into two parts, one is sent as reflux to the 4th pack the other one is further cooled at 90°C and sent to the 5th pack.

Basins designs are all different and optimized depending on the characteristics of each individual product. In Figure 10 a general representation is reported to describe how a basin works. No further details can be found in this thesis in order to protect Itelyum industrial secrets. The basins do not work as equilibrium stages, but only as storing units.

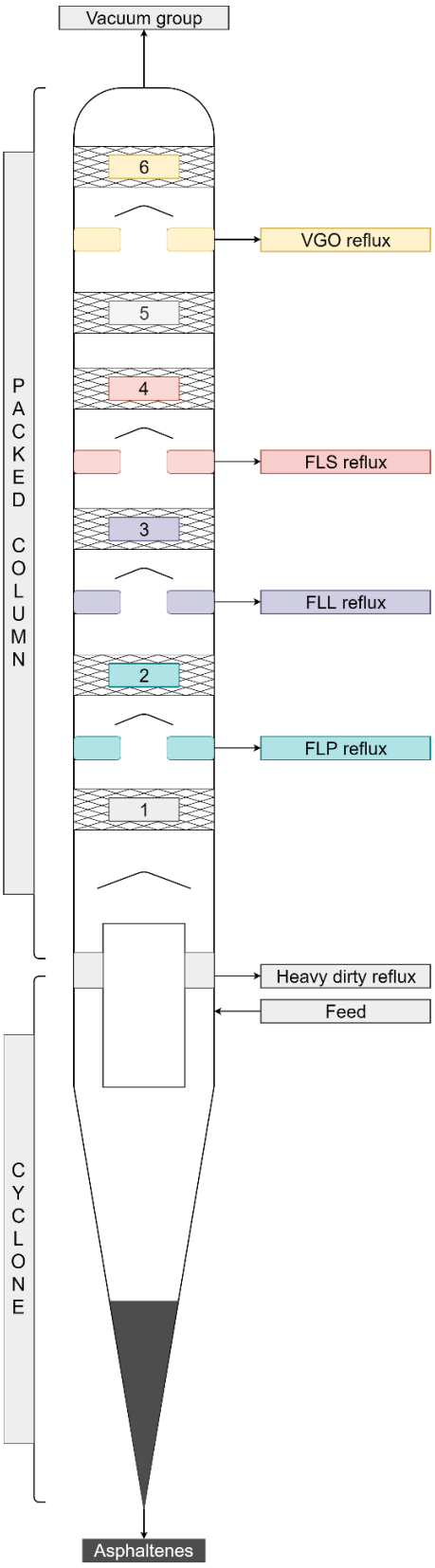

Figure 10: TDA column

The top of the column is operated with a large excess of subcooled VGO reflux to condense all the vapours that would otherwise go to the vacuum group, making the operation of the VGO pack more like a contact condenser than an equilibrium pack.

The column is not provided with a reboiler, but the feed is overheated in a furnace to 360°C and then fed to the cyclone. The cyclone allows for phase separation after heating, thus acting as a flash, which is how it will be modelled since there is no standard unit for a sludge/vapor cyclone.

The cyclone separates asphaltenes as sludge from the lighter products which raise to the column first pack as vapor.

The first pack receives vapor from the cyclone, liquid from the above FLP pack (both as reflux and directly from above) and liquid present in the lower basin through a reflux pump-around. To avoid accumulation at the column base, part of the latter liquid is purged and send to the asphaltenes treatment section.

The FLP and FLL packs work in a similar manner. Both receive liquid reflux from the above stage, the product is withdrawn from the basin and split into two streams: one is refluxed in the stage below while the other one is sent to stripping section which precedes the successive treatments.

The FLS stage is different because the withdrawn liquid is split into 3 parts: the first portion is sent to the stage below, the second is sent to the buffers, the third (most important one in terms of massive flowrate) is sent to a kettle cooler (E408). Once cooled, the stream is split again into 2 sub-streams, a fraction acts as reflux for the FLS pack and another one that is sent to a second cooling unit. E411 is an air cooler

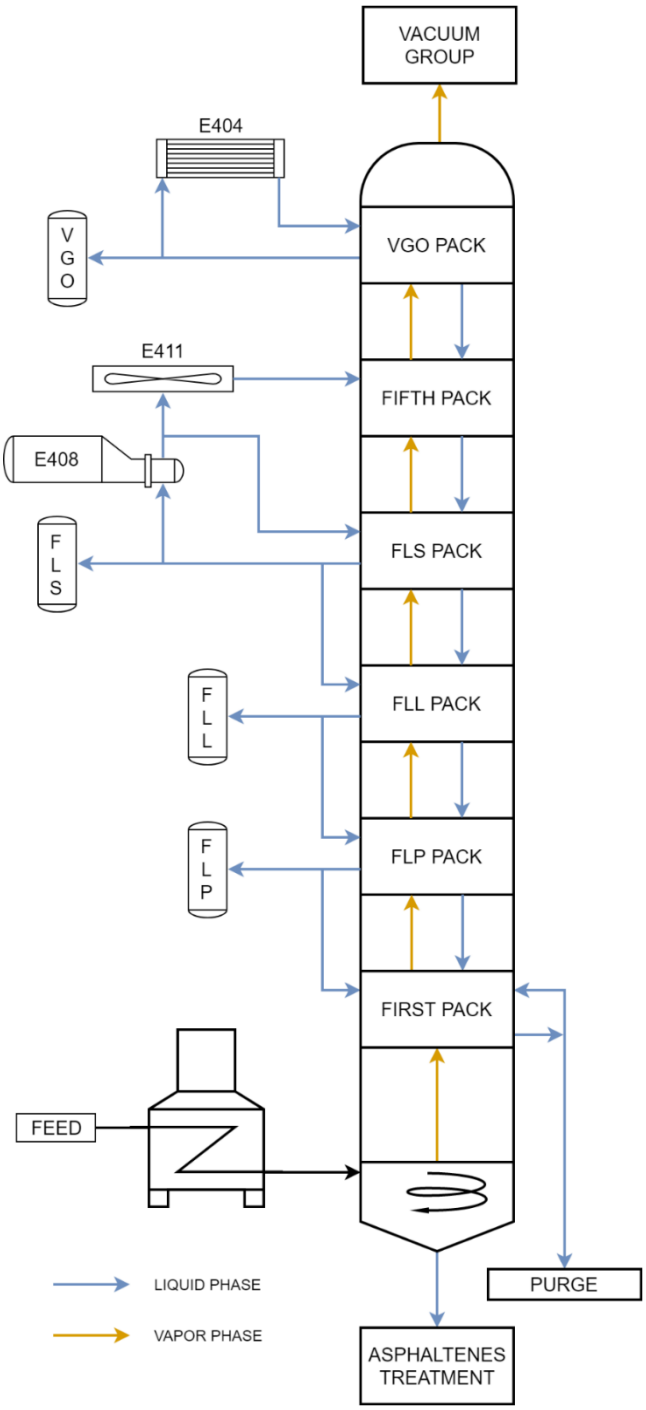

Figure 11: TDA column flowsheet with auxiliaries

that drops the temperature of the liquid by about 100°C and sends it back to the fifth pack.

The fifth pack is the only one not equipped with a basin and nothing is retrieved from it.

The VGO pack receives vapor from the fifth pack and condenses it by using a sub-cooled recycle. The reflux is made of VGO itself which is withdrawn by the basin, split into VGO product and the reflux itself. The cooler acting on the VGO stream has a thermal power that is about half of the total cooling duty provided to the column and is a straight run tube and shell unit working with water.

The vacuum in the column is kept by a vacuum group consisting of several ejectors and a vacuum pump. The vapor flow coming from the VGO pack is considered negligible thanks to the very high flowrate of subcooled VGO applied on top. This assumption is fundamental for the proper characterization of the feed and is verified once the stationary model is completed.

1.4.1. Upstream treatments

Two furnaces precede the TDA column to provide the necessary heating duty. They are operated in parallel one at the time to allow continuous operation of the plant. Their design is fundamentally different since one is a convective furnace and the other is radiative.

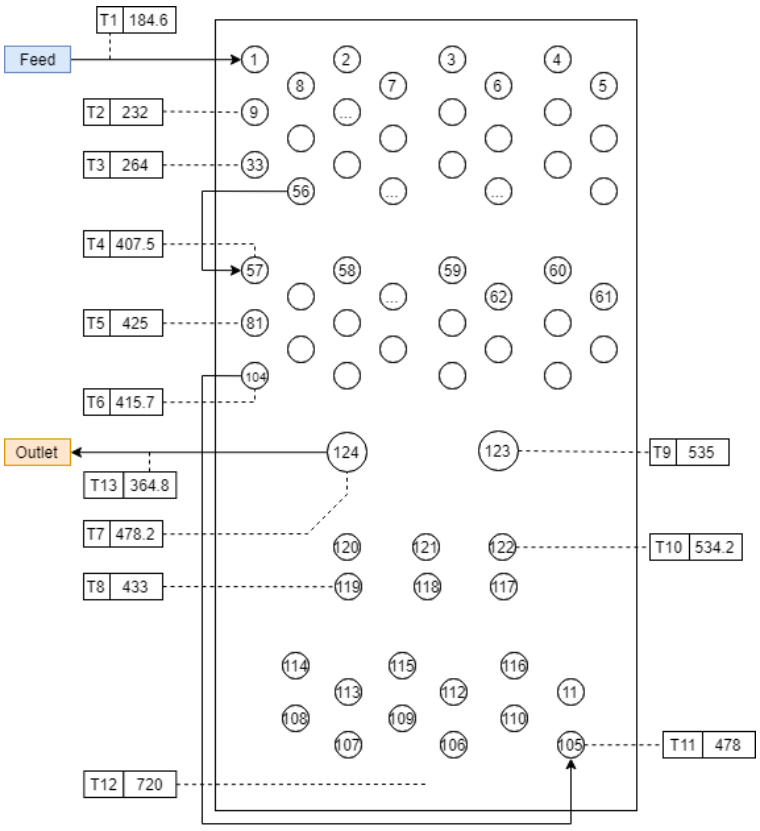

Figure 12: Furnace detailed PFD

Due to relevant amounts of coking, the radiative furnace is to be exchanged with a convective one which is less prone to coking.

The convective furnace is made of a single pipe coil to allow a contact time of about 10 min. The feed enters on top where it is preheated and then sent to the lower part where the higher temperature allows reaching the desired outlet temperature of 360°C.

The main concern with this unit is that the skin temperature of the coil near the bottom of the column is sufficiently high for relevant amounts of cocking to take place. This is the reason for which two furnaces in parallel are necessary.

The pre-flash unit is located right before the furnace and has the purpose of removing the light cuts and water present in the exhaust lubricant oil as contaminants. The feed can be simplified as a mix of:

- Lubricant cuts;
- Light gasoil formed during high-temperature operation of the lubricants;
- Water which contaminated the lubricant during its lifetime.

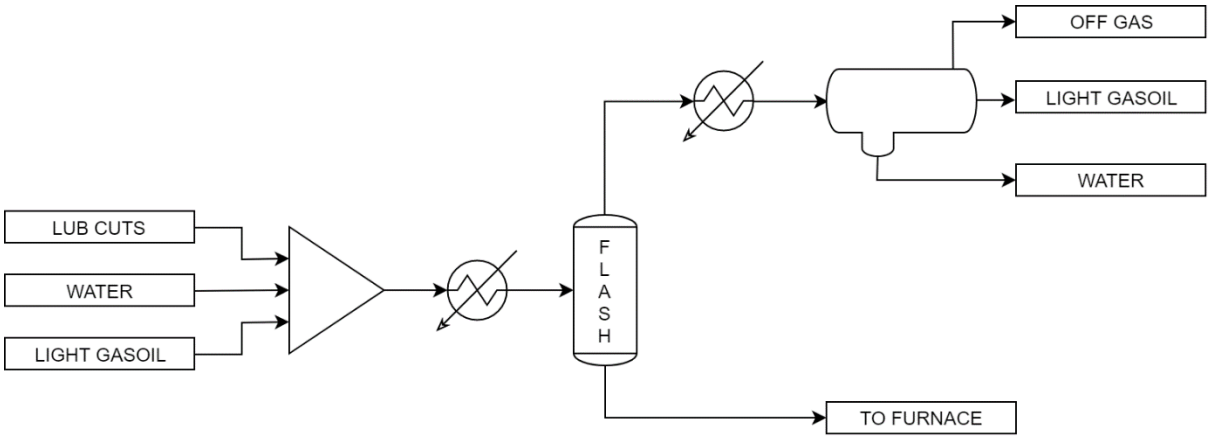

Figure 13: Pre-flash PFD

The flash is carried out at about 140°C and in moderate vacuum conditions (~380 tor). The top product of the flash is separated using a pit vessel. Small amounts of off-gas coming from dissolved hydrocarbon contaminants can be expected.

Before being fed to the furnace lubricant cuts are heated using the residual asphaltenes stream from the column recovering its heat. The degree to which this pre-heating is pushed depends on the desired outlet temperature of the asphaltenes which may vary depending on the requirements of clients.

1.4.2. Downstream treatments

The column is followed by a storing unit for the VGO stream and a stripping section for the FLS, FLL, and FLP cuts. The stripping is done with low pressure steam to remove the light components that might be trapped in the products and acts as a pre-treatment for the hydrofinishing section.

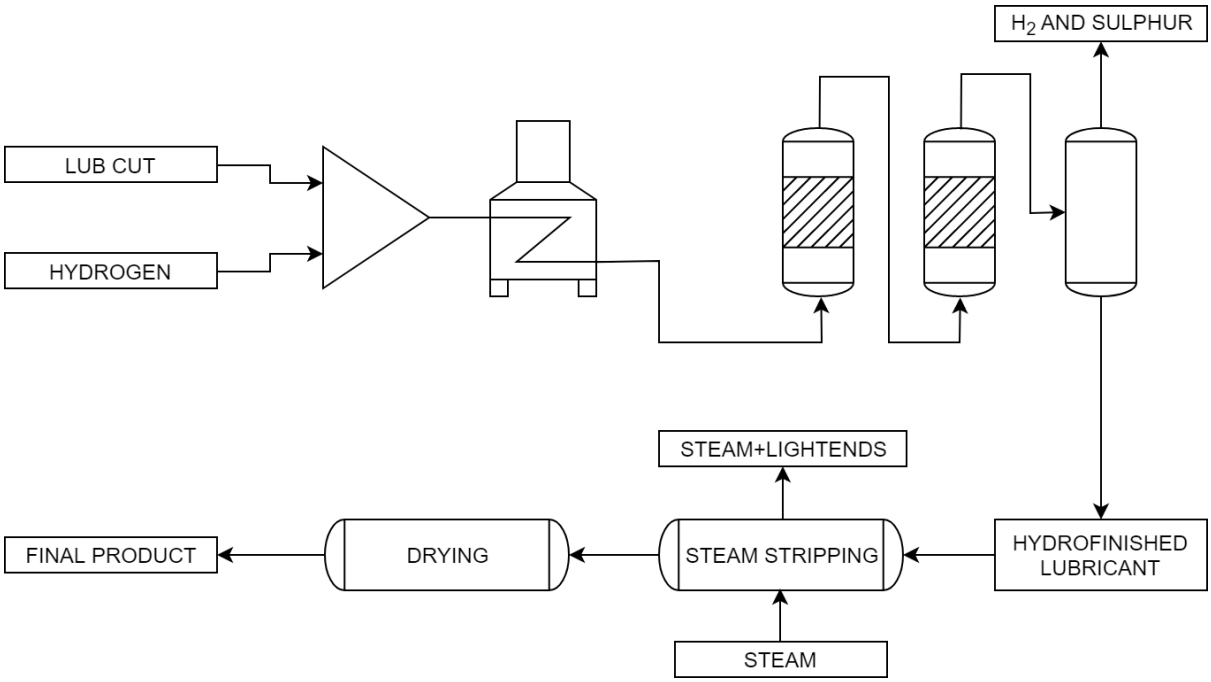

Figure 14: TDA downstream PFD

In the next step, each cut (VGO excluded) one by one is mixed with hydrogen and fed to a furnace where it is heated to about 300°C before entering the hydrofinishing reactors.

The result of the hydrofinishing step is a more stable, saturated lubricant from which residual sulfur is removed. It must be noted that since the feed is not crude oil the sulfur content is already low (hydrotreating is a standard refinery process applied to all products to remove sulfur) as well as the contents in unsaturated compounds (some will form during high-temperature operation). The resulting product will have sulfur contents lower than 0.5% w/w. Before being ready the last stripping step and subsequent drying are necessary to remove the light components formed during the hydrofinishing. This step is done with low pressure steam in two subsequent units.

1.4.3. Degrees of Freedom

As explained above the cyclone is considered as a simple equilibrium stage in this analysis. Each individual stage is considered in equilibrium conditions and working adiabatically. Outside of the column 3 exchangers and 10 splitting nodes are present.

The variables are:

- Flow rates (NF) two for each tray plus one feed stream: [2NP+1]
- Number of molar fractions (NC) for each stream: [(2NP+1)·(NC - 1)]
- Temperature of each stage, the temperature of the feed and outlet temperatures of each heat exchanger: [NP + NE + 1]
- Duty of each heat exchanger: [NE]
- Pressure of each stage and pressure of the feed: [NP + 1]
- Split factor and flowrate for each node: 2NN

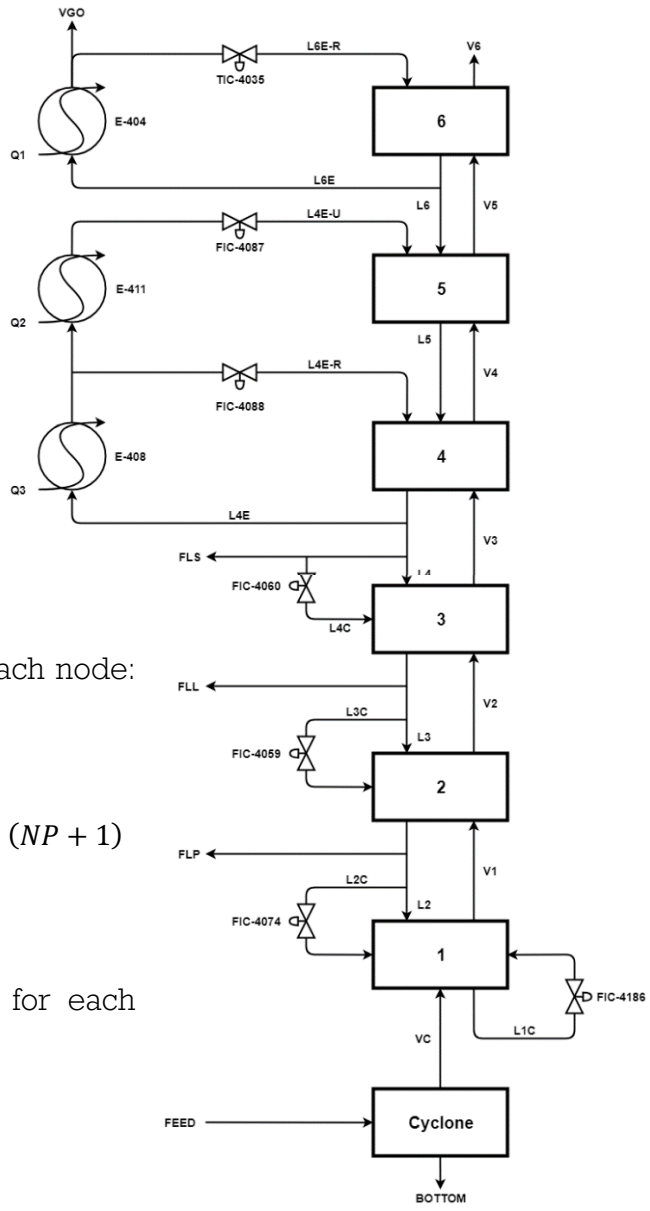

Figure 15: TDA column flowsheet

The resulting number of variables is:

$$V = NC \cdot (2NP + 1) + 2NE + 2NN + 2 \cdot (NP + 1)$$

The equations are:

- NP global mass balances
- (NC – 1)·NP mass balances for each species
- NC·NP equilibrium equations
- NP energy balances
- NP momentum balances
- NN global mass balances
- NE energy balances

The total number of equations is: $E = NP \cdot (2NC + 2) + NN + NE$

The degrees of freedom are: $DoF = V - E = NC + 2 + NE + NN$

1.5. Work Purposes

New simulation software and improved computational power can solve complicated problems in fractions of the time it takes to solve them by hand, easily predict unit performances under different working conditions, simulate risky situations, maximize the profits, rise the overall plant efficiency, and do so with great precision and accuracy. Such tools can greatly improve the quality and quantity of work by avoiding calculus or programming mistakes and minimizing the time expense.

Another aspect which is not to be underestimated is the huge databases which these simulators have at their disposal. Thermodynamics, kinetics, and transport properties are on hand and, whenever they are not known, they can be calculated using a wide range of specific algorithms and methods.

Steady-state and dynamic process simulators serve different purposes. The former help, for example, choosing the best design for an operative unit, while the latter can help the optimization of transients.

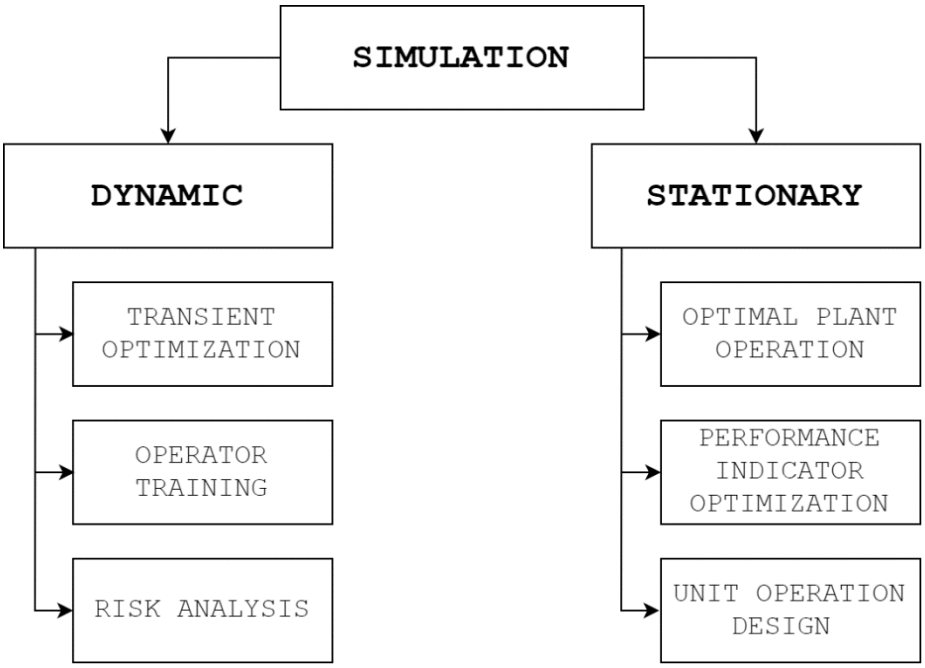

Figure 16: Advantages of simulations

1.5.1. TDA steady-state simulation benefits

While the Thermo deasphalting column is set within a context of continuous operation, its operative conditions change quite frequently. The column feed's flow rate changes every day depending on the availability of such. This requires modulating the controlled variables in order to keep the column in steady-state conditions. Also, customers may request for different product quantities and properties.

As things stand, on-field operators need to reach such specifications by changing controlled variables, but without the support of accurate predictions. The mathematical evaluation of optimal conditions is very time consuming, so the control operations are mainly driven by the experience of operators. This may occasionally lead to operative errors that end up being economical losses on the long-term.

A stationary model can help field operators to identify optimal steady-state conditions to recover as much in-spec product as possible. Unusual scenarios which have never occurred may be evaluated, as an example, it could be possible to evaluate whether by decreasing the duty of a condenser the product would be in-spec and this would happen without any actual loss of products in the plant.

Measurement costs for both column cuts' physical properties and plant's conditions can also be saved since the model can accurately predict them. Other uses can be pointed out, which are steady-state economic optimization and on-line data reconciliation. Such possibilities will be discussed in chapter 2.9.

1.5.2. TDA dynamic simulation benefits

While a stationary model permits the optimization of TDA's operative conditions, considering economic and technical aspects, a dynamic model may help in developing strategies to handle transients, which commonly occur on the field, such as events that follow the feed flow rate change.

Operations that can speed up those temporary phases can be evaluated and if such procedures are not considered safe, discarded. Accidents can, in fact, happen during such transients even if the final steady-state condition is deemed safe. The time that a scenario takes to become dangerous is also a critical aspect. Dynamic models can be an excellent tool for operator training, indicating when and how to act in critical situations. Moreover, the model can also help facing up and to optimize unordinary procedures, such as start-up and shutdowns, which are generally strictly followed without changes due to the high complexity of the economic, technologic and safety implications. Economic dynamic optimization and model predictive control, which will be discussed in chapter 3.12, are among other uses that can be offered by the software.

2. Stationary Model

The first part of this thesis describes the development of a stationary model for the TDA column. The model is developed on Aspen HYSYS Simulator. The program is well known in the refining industry and it has high potential in predicting steady-state conditions [5] for a high number of basic unit operations (e.g. distillation columns) and is meant to optimally characterize petroleum cuts [6]. However, it presents intrinsic limitations which will be discussed in the next paragraphs.

2.1. Input data for the stationary model

Input data to build and validate the model are furnished by the Pieve Fissiraga's plant. These data contribute to the available analysis performed on the lubricants, operative conditions and plant design. In particular, the data supplied are:

- ASTM D1160 curves for the furnace feed and the column's products, exception made for the lighter gases to the ejector group, incondensable, and the viscoflex exiting from the bottom, mainly solid at the test's temperature. These curves are the characterizing technique for blends. This especially regards the furnace's feed, for which more detailed analysis, such as gas chromatography, would be extremely expensive and are not practical since it is a semi-solid residue at atmospheric conditions. For this blend, Conradson carbon analysis, quantification of sulfur, olefin, and aromatic content is usually performed;
- Metal content in the viscoflex;
- Density and viscosity for a batch of produced lubricants and VGO;
- Detailed P&ID of TDA column, pre-flash unit, and furnace;
- Detailed technical sheets of valves, pumps and heat exchangers;
- Pressure and temperature profiles of the column from DCS, with corresponding feed and reflux flow rates. These data will be especially useful for the model and its validation;
- Water and solvent content in the pre-flash feed;
- Mean mass distribution of the feed among FLS, FLL, FLP, VGO and bituminous residual (Viscoflex) which are respectively 20%, 44,5 %, 7,8 %, 10,8 %, and 16,9%, while they constitute 100 % of the feed, vapor flow rate fraction to the vacuum group is negligible.

2.2. Limits

The model has several limits, both intrinsic of Aspen HYSYS and consequent to lack of data information:

- HYSYS presents few algorithms which are suitable for the program column solver, and all of them exhibit difficulties in solving systems with a high number of recycles. This makes the problem solving intricate and time-consuming. According to the users' manual [5], for systems with a high number of components and refluxes the best solver is the modified HYSYS inside-out;
- Polluting agents (as chlorides, sulfur, metals) cannot be evaluated due to their high number and variance from every plant's feedstock, for which specific analysis are not provided;
- HYSYS's column model considers each stage at equilibrium. While mass diffusion limitations cannot be directly proven from the DCS's survey, non-equilibrium is evident from temperature indicators (TI). In fact, two indicators are present on the liquid collector trays, one measuring liquid temperature and the other the vapor. While the temperature difference is about 2-3 °C for FLP, FLL and FLS trays, VGO presents a difference higher than 20 °C. This is due to high reflux flow rate at 20 °C that contacts hot rising vapor at a temperature of about 120 °C. This leads to the fact that the stage performs like a contact condenser. This feature can't be represented by HYSYS, so an external ad hoc model should be built and integrated into the program;

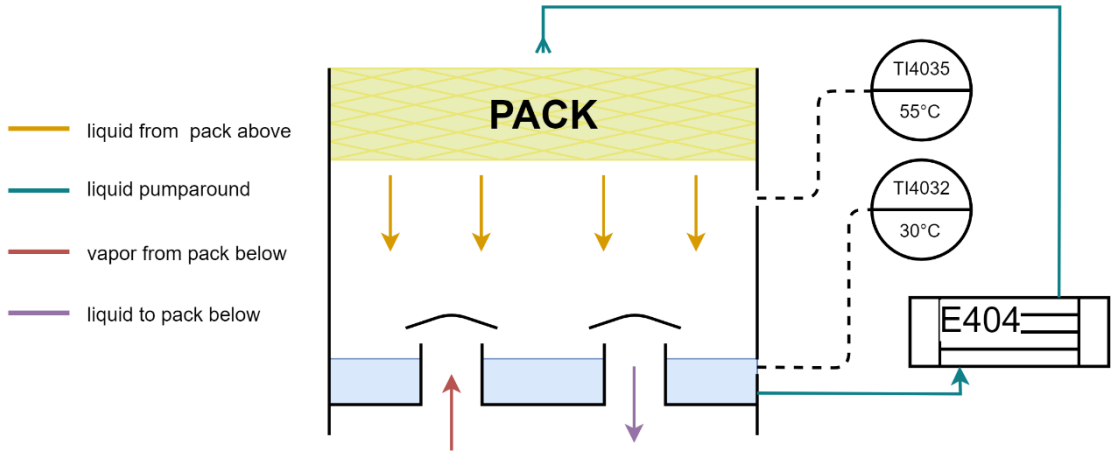

Figure 17: Sixth pack with corresponding pump-around

- TDA's structured packings are subjected to fouling, which varies from pack to pack. This aspect and its dynamics cannot be accurately implemented. A simplification was made not considering the fouling dynamics, but pressure drops, which are the main consequence of this phenomenon, can be modelled keeping a dirty factor into account;
- The cyclone separates feed which is a gas-slurry stream. Such a unit is not present in HYSYS. Moreover, fluid-dynamics are extremely complex and

aggregated asphaltene particles diameter distribution in the feed cannot be accurately described, nor have ever been analysed. Knowing this, even an external model is considered too complex for the purpose of this work, highly impacting on computational time without an important improvement of results. In light of high efficiency in the separation of heavy residuals from the gaseous phase, the cyclone can be represented by a flash. Such a solution will be discussed more in detail in chapter 2.5.4;

- Furnace regulates the column feed inlet temperature. Aspen HYSYS does not present a feature that can represent the furnace complex geometry, this approach was chosen. From the model's performance point of view, a normal heat exchanger can be an acceptable simplification. However, this limits the model potential regarding the prediction and optimization of the unit performance. Moreover, evidence of cracking is present, which cannot be represented in the exchangers feature. The lack of a kinetic model in the system prevents from evaluating directly the effect of temperature and feed composition on the cracking entity, which influences the column feed and consequently the simulation results. These aspects will be discussed more in detail in chapter 1.5;
- Ejector unit is not present in HYSYS, so the vacuum group cannot be implemented. However, this is not an issue since pressure profile in the simulator columns is specified by the user and is not dependent from boundary conditions.

2.3. Blends characterization

The topic of this chapter will be the thermodynamic characterization of the column feedstock. It is of fundamental importance for all the results reported due to its complexity and the topography of the data.

2.3.1. Blends implementation using ASTM curves

The first step for the model construction is the implementation of the involved components and, whenever the products quality is measured by its macroscopic properties, a robust characterisation of the involved process flows properties. In the case of lubricants and petrochemical cuts in general, the hydrocarbon species involved are so many and they are so difficult to identify that it is impossible to know a blend true composition. Even if this was done, the computational effort to manage all of the components would make the model useless from an industrial point of view. In such cases, a limited number of components representing all the species involved must be used.

In the case of exhausted lubricant oil, two feasible paths can be taken into consideration, which are:

- Detailed research on exhausted lubricants or gas chromatography analysis of the involved blends, to identify the more present compounds and group them in lumped species;
- Build a set of hypothetical pseudo components from the boiling point curves.

The choice of the method also depends on the hydrocarbon stream data provided. Since Itelyum could provide an ASTM D1160 curve analysis at 10 torr on most of the streams, the second option was chosen as a first approach, which was revealed to be appropriate for our purpose. The curve was used to build a set of pseudo components to characterise them. ASTM D1160 curves are built measuring the change of the boiling temperature with the relative evaporated volume of heavy hydrocarbon mixtures, until approximately 400 °C, using a single stage batch distillation under vacuum with no reflux [7].

HYSYS has robust algorithms for the analysis of such curves [8]. ASTM D1160 are converted to TBP curves, which are graphically subdivided into several intervals equal to the number of pseudo components involved. Each pseudo component has a normal boiling point (NBP) equal to the mean temperature of each corresponding interval. The number of pseudo components can be optimally calculated by HYSYS, as it was chosen to do, or given by the user. Being these curves the only provided data, the only possible validation that can be done at the moment is about the reliability of the output blend curve evaluated by HYSYS and Itelyum's input. The graph for the plant feed ASTM curves and pseudo components distribution is represented, showing that the program can well reconstruct this information. The same procedure is followed for the products curves.

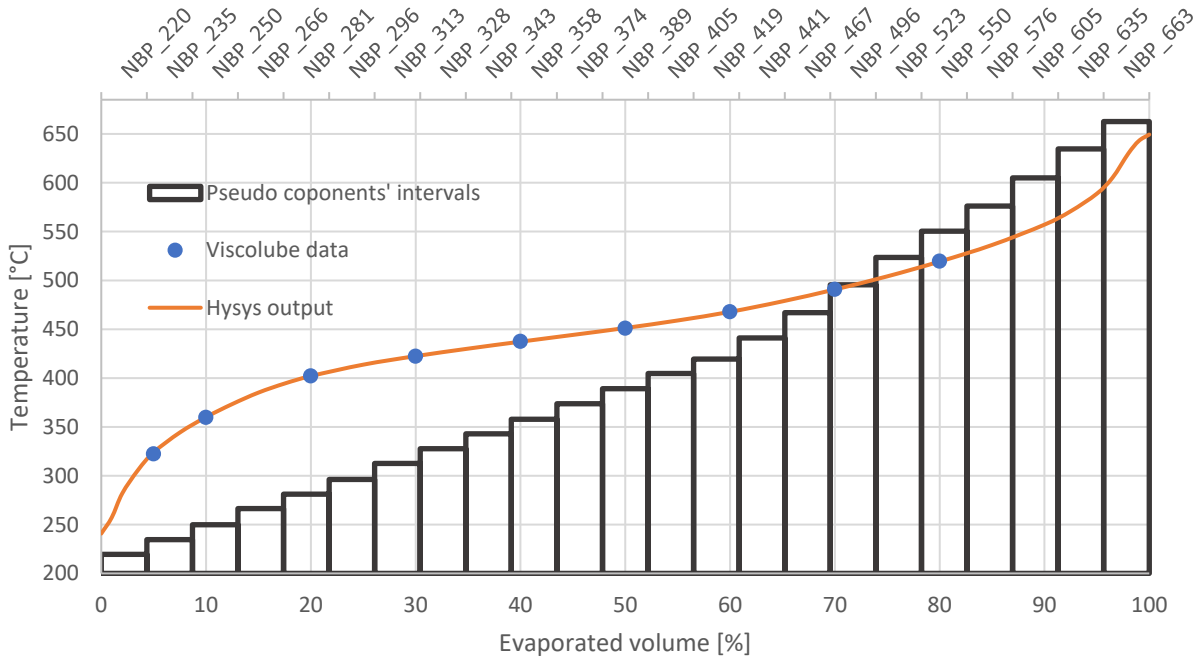

Figure 18: Plant feed ASTM D1160 atmospheric equivalent temperature (AET) and pseudo components distribution graph

2.3.2. Methods for blends properties description

There is no general approach for the prediction of hydrocarbon blends properties. This strongly depends on the nature of such. In literature, a high number of correlations have been proposed to better describe these properties in different situations. HYSYS has a high number of methods to describe petrochemical blends. To have a more compact sheet where to display results, its methods are used whenever possible.

According to literature, the Twu method for the prediction of critical properties and acentric factor is optimal for hydrocarbon mixtures [9]. The implicit extended Twu method for the molecular weight evaluation developed from HYSYS is instead used, since it is recommended for heavy oil fractions [8]. Ideal gas enthalpy is evaluated using the Lee-Kesler method, due to its high accordance with API data book [10]. Other important properties such as boiling point temperatures and pressures and residual enthalpies are evaluated from the corresponding equation of state, which will be discussed on the thermodynamic validation chapter. Unfortunately, there is a lack in such experimental data, so a validation could not be performed. However, a set of data on product densities at 15 °C and viscosities at 40 °C and at 100 °C is provided.

The density evaluation of hydrocarbon blends in HYSYS depends on the SG and on the dependent density evaluation methods. Default methods are COSTALD [11] for density evaluation and Constant Watson K method for the specific gravity. This last considers the characterization factor K as constant, calculated from the ASTM curves, and evaluates SG as:

$$SG = \frac{T_b^{\frac{1}{3}}}{K_{blend}} [-]$$

However, a high discordance with the experimental data is present. Rackett equation is a good candidate for saturated liquid densities [12]. Also, Hariu-Sage [13] correlation can be used to evaluate SG knowing the molecular weight, which in this case is calculated by HYSYS. Such correlation, which is usually used to evaluate the molecular weight, can be combined with the SG definition written above to re-evaluate K_{blend}:

$$Log_{10}(MW) = \sum_i \sum_j a_{ij} * T_{b,i} * K_j$$

where a_{ij} are binomial coefficients for the components evaluated from the program. The results compared with the experimental values and relative errors over the corresponding experimental values are reported below.

Industrial [kg/m³]	874	862	863	849
Rackett Constant Watson K [kg/m³]	913	898	882	830
Relative Error [%]	4.5	4.2	2.2	2.3
Rackett Hariu Sage [kg/m³]	888,1	869	857	828
Relative Error [%]	1.6	0.9	0.6	2.5
Costald Hariu Sage [kg/m³]	909,5	899	895	885
Relative Error [%]	4	4.3	3.7	4.3
Costald Constant Watson k [kg/m³]	937	928	924	924
Relative Error [%]	7	7.7	7.1	8.9

Table 3: HYSYS products density compared to industrial values

As shown, Rackett and Hariu-Sage are the best correlations in this case study.

Dynamic viscosities can be calculated in the program only using the standard HYSYS method. The calculation involves the basic physical properties and parameters that are estimated by the Twu correlation. Such correlation, however, resulted to be unsatisfying. Some external methods for petrochemical cuts are studied and implemented in Excel. The more promising methods are Bingham's mixing rule [14], that uses as inputs the single components viscosities, which are calculated by HYSYS:

$$\mu_{mix} = \frac{1}{\sum \frac{VolFrac_i}{\mu_i}}$$

and the Bergmann-Sutton dead oil correlation [15], which needs to be integrated by a bubble point and an undersaturated oil correlation, since undersaturation is the condition at which the experimental viscosity is measured by Itelyum. No Bergmann-Sutton correlations for bubble point and undersaturated oil exists, so Kartoatmodjo's [14] correlations for heavy oils are used. No dissolved gas is considered, and HYSYS's SG is used for calculations:

$$Tb = 540.39 - 1776.8 * SG + 2744.7 * SG^2$$

$$\tau = 0.533272 + 1.91017 * 10^{-4} * Tb + 7.79681 * 10^{-8} * Tb^2 - 2.84376 * 10^{-11} * Tb^{13} + 9.59468 * 10^{27} * Tb^{-13}$$

$$\alpha = 1 - \tau$$

$$SG_0 = 0.843593 - 0.128624 * \alpha - 3.36159 * \alpha^3 - 13749.5 * \alpha^{12}$$

$$\Delta SG = SG - SG_0$$

$$\varepsilon = \left|2.68316 - \frac{62.0863}{\sqrt{Tb}}\right|$$

$$f1 = 0.980633 * \Delta SG * \varepsilon - 47.6033 * \frac{\Delta SG^2}{\sqrt{Tb}}$$

$$f2 = \Delta SG * \varepsilon - 47.6033 * \frac{\Delta SG^2}{\sqrt{Tb}}$$

$$v2 = e^{2.40129 - 9.59688 * \alpha + 3.45656 * \alpha^2 - 143.632 * \alpha^4} + 0.152995$$

$$v1 = e^{0.701254 + 1.38359 * \ln(v2) + [0.103604 * \ln(v2)]^2}$$

$$v210 = e^{\ln\left(v2 + \frac{232.442}{Tb}\right) * \left(\frac{1+2*f2}{1-2*f2}\right)^2} - \frac{243.442}{Tb}$$

$$v100 = e^{\ln\left(v1 + \frac{232.442}{Tb}\right) * \left(\frac{1+2*f1}{1-2*f1}\right)^2} - \frac{243.442}{Tb}$$

$$Z210 = v210 + 0.7 + e^{-1.47 - 1.84 * v210 - 0.51 * v210^2}$$

$$Z100 = v100 + 0.7 + e^{-1.47 - 1.84 * v100 - 0.51 * v100^2}$$

$$Z100 = v100 + 0.7 + e^{-1.47 - 1.84 * v100 - 0.51 * v100^2}$$

$$B = \frac{ln[\ln(Z210)] - ln[\ln(Z100)]}{\ln(669.67) - \ln(559.67)}$$

$$Tabs = T + 459.67$$

$$H = ln[\ln(Z100)] + B * [\ln(Tabs) - \ln(559.67)]$$

$$\Gamma = e^{\mathrm{H}}$$

$$\mathrm{Zt} = e^{\Gamma}$$

$$\varphi = \mathrm{Zt} - 0.7$$

$$\chi = -0.7487 - 3.295 * \varphi + 0.6119 * \varphi^2 - 0.3193 * \varphi^3$$

$$\mathrm{vt} = \varphi - e^{\chi}$$

$$\Delta T = T - 60$$

$$\alpha 60 = \frac{2.5042 * 10^{-4} + 8.302 * 10^{-5} * SG}{SG^2}$$

$$VCFt = e^{-\alpha 60 * \Delta T * (1 + 0.8 * \alpha 60 * \Delta T)}$$

$$SGt_0 = 0.999012 * SG * VCFt$$

$$\mu_{dead\ oil} = SGt_0 * vt\ [cp]$$

$$F = 0.8592 * \mu_{dead\ oil}{}^{0.9889}$$

$$\mu_{bubble\ point} = -0.6311 + 1.078 * F - 0.003653 * F^2\ [cp]$$

$$\mu_{bubble\ point} = 0.9886 * \mu_{bubble\ point}\ [cp]$$

The experimental values, absolute relative errors, and results are reported below for kinetic viscosities at 40 °C and 100 °C. Used densities are extrapolated from HYSYS, to quantify the real error in case of a prediction. As for Bergmann-Sutton, Kartoatmodjo's correlations for bubble point and undersaturated oil are used if a method has none.

	FLP		FLL		FLS		VGO	
40 °C	*Value [cst]*	*Error [%]*	*Value [cst]*	*Error [%]*	*Value [cst]*	*Error [%]*	*Value [cst]*	*Error [%]*
Industrial	68.76	0	32.39	0	14.17	0	3.38	0
Bergmann	81.68	19	39.02	20	20.43	44	4.45	32
Kartoatmodjo	72.59	5.6	44.21	36	28.52	101	1.47	56
Bergmann-Sutton	72.86	6	32.1	0.9	16.29	15	3.24	4
Egbogah	74.71	8.7	38.74	20	21.81	54	4.77	41
Beal	56.85	17	30.7	5	18.89	33	5.88	74
Beggs-Robinson	61.66	10.3	35.71	10.2	22.58	59.3	6.36	88.4
Arrhenius	121.07	76	37.8	17	16.45	16	3.05	9.6
Bingham	74.47	8.3	28.15	13.1	13.41	5.3	2.41	28.7
Cragoe	111.91	62.8	35.89	10.8	15.96	12.6	2.92	13.4
HYSYS	89.2	29.7	31	4.3	14.34	1.1	2.67	2.1

Table 4: Industrial and modelled viscosity values at 40 °C

As it can be noted in Table 4 and Table 5, both Bergmann-Sutton's and Bingham's methods provide good results at 40 °C, but at 100 °C Bingham is in far better accordance with experimental values. Relative errors are just indicatives and whereas they are very high for FLS and VGO at 40 °C, and for all blends at 100 °C, it must be noticed that the absolute error is generally in the order of the measurement error, of 1-2 cst.

Concluding, HYSYS can describe quite well all the blends properties except for viscosity, for which external correlations need to be used.

	FLP		FLL		FLS		VGO	
100 °C	*Value [cst]*	*Error [%]*	*Value [cst]*	*Error [%]*	*Value [cst]*	*Error [%]*	*Value [cst]*	*Error [%]*
Industrial	9.3	0	5.75	0	3.76	0	unmeasured	
Bergmann	20.92	124.9	10.58	83.9	6.4	70.2	2.26	-
Kartoatmodjo	16.66	17.9	9.17	59.5	5.78	53.7	1.55	-
Bergmann-Sutton	16.86	81.3	8.2	42.6	4.8	27.7	1.72	-
Egbogah	14.84	59.6	8.4	46.2	5.4	43.7	2.06	-
Beal	19.65	11.3	10.51	82.7	6.55	74.2	2.53	-
Beggs-Robinson	2.88	69	1.96	65.9	1.4	62.9	1.08	-
Arrhenius	10.83	16.4	5.67	1.4	3.48	7.4	1.2	-
Bingham	9.17	1.4	5.08	11.7	3.22	14.5	1.07	-
Cragoe	10.54	13.4	5.57	3.2	3.44	8.4	1.17	-
HYSYS	10.12	8.8	6	4.3	3.32	11.7	1.11	-

Table 5: Industrial and modelled viscosity values at 100 °C

2.3.3. VBA implementation

Considering the computation of viscosity involves several steps and knowledge about the correct data to be picked, it was decided to automate the process. Since this function will be mostly used by Itelyum once the simulation is later put to use it was decided to use an easy and intuitive Excel interface, keeping the VBA code in the backwound, so that no coding knowledge is needed.

If desired the code can be used as a basis for automated sensitivity analysis, but the implementation of this feature was not carried out due to technical problems and time constraints. The biggest of these problems was that despite the fact that VBA can change input data in the simulation and run it, i.e. outlet temperature of the top condenser, the complex stationary model will rarely converge in a predictable way. The implementation of procedures to handle these unconverged cases and to define a robust procedure to obtain convergence without rebuilding the column from scratch reflux after reflux was not feasible within the timeframe of this work.

The code is however built in such a way to allow an easy implementation of what discussed above once the automated convergence of the column is dealt with.

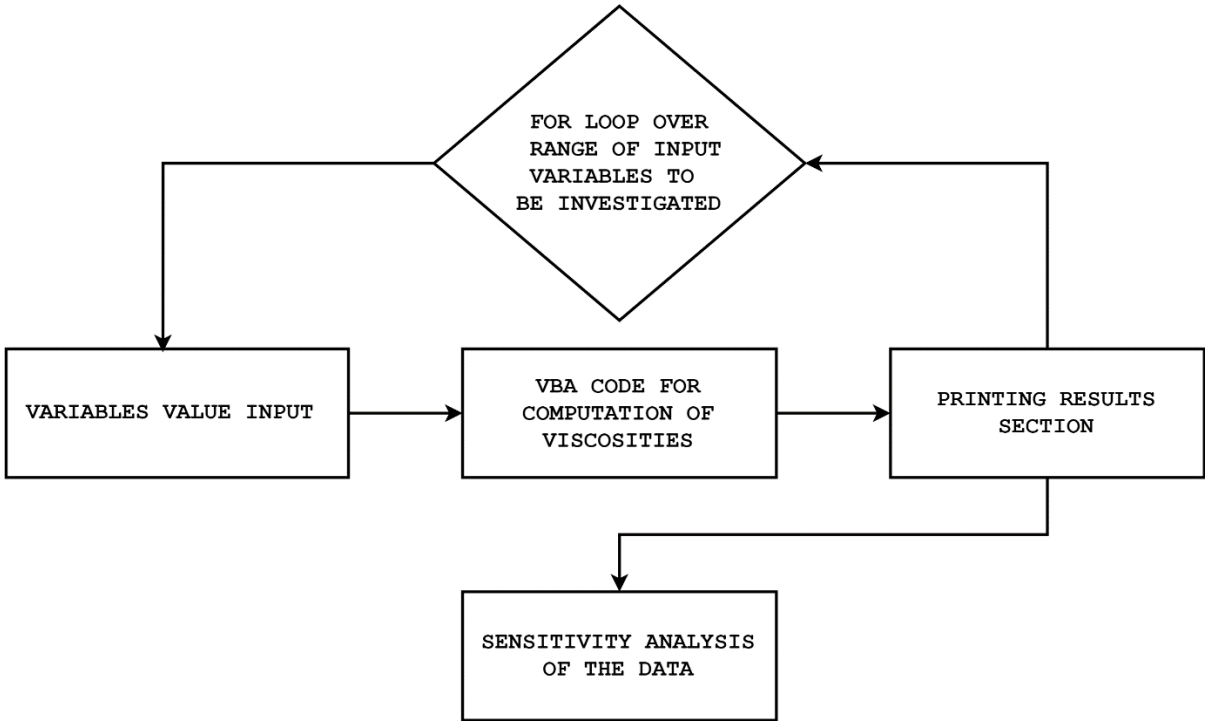

Figure 19: Automated sensitivity analysis code structure

OBJECT	VALUE	INSTRUCTIONS
Simulation path	C:\Users\USERNAME\Desktop\Aspen\Colonna\21_ColonnaFinale_Flash.hsc	Directory of the simulation with the simulation name
Blend Name	all	Name of the blend used in the simulation from *"Properties"*
VGO product stream name	VGO_prod	Name of the VGO output stream in the simulation
FLS product stream name	fll_prod	Name of the FLS output stream in the simulation
FLL product stream name	flp_prod	Name of the FLL output stream in the simulation
FLP product stream name	fls_prod	Name of the FLP output stream in the simulation
Number of real components	3	Number of real components with the blend
	RUN	

Before running for the first time:

- Activate developer by clicking File > Options > Customize Ribbon, here check the Developer Box
- Go to Developer > Visual Basic > Tools > References… , here look for and check "HYSYS 10 type library "
- Click RUN, ASPEN will open, ask for some "Yes"s and then in the "Output" sheet the results will be displayed

Figure 20: Input interface of the VBA script

As for now the code, exploiting *"HYSYS 10 type library"*, will compute the viscosities at 40 and 100 °C following the Bingham and the Sutton rules alongside the density at 15, 40 and 100 °C as computed by HYSYS. The results will then be printed in another sheet.

Viscosity [cSt] Bingham	40C	100C
VGO	1.756078435	0.841269731
FLS	10.02184428	2.68244309
FLL	36.53781944	5.877227968
FLP	78.53715458	9.659770344

Figure 21: Printed results

2.4. Thermodynamic validation in HYSYS environment

Since the separation of products is achieved exploiting thermodynamic equilibrium the choice of the right equation of state (EoS) is a very important aspect to take into consideration, together with blends characterization. It is important to be conscious that choosing one EoS instead of another may dramatically change the predicted results. For example, Dohrn and Pfohl [16] show how similar models, like Redlich-Kwong-Soave and Peng-Robinson, may yield different designs even for binary non-polar hydrocarbon mixtures. In this step, the nature of the involved mixture and the operative conditions need to be taken into consideration.

The pseudo components that need to be considered are a set of heavy, non-polar hydrocarbons. Such streams are processed in units which operate under vacuum, up to 3 torr, and in a range of temperatures between 365 °C and 20 °C or less.

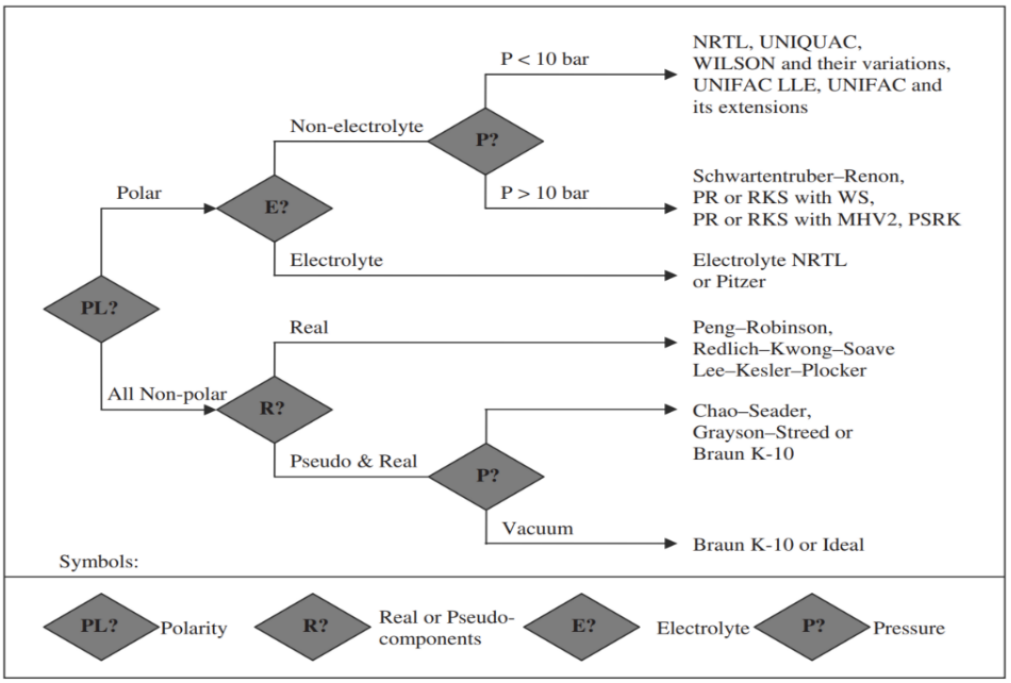

Figure 22: Decision three for thermodynamic models depending on operating conditions and blend [17]

Kontogeorgis in his "Thermodynamic Models" [17] makes a clear distinction between which model is more indicated in certain conditions (Figure 22).

The indicated EoS in the specified conditions is Braun K-10 which, as will be discussed, requires a small number of coefficients and so it is of easy use when pseudo components are involved. However, since HYSYS has a complete set of EoS parameters also for pseudo components [5], Peng-Robinson and Redlich-Kwong-Soave are also considered. Lee-Kesler-Plocker is discarded since it is not indicated for vacuum

conditions [5] [17]. Also, according to "HYSYS operation guide" [5], Redlich-Kwong-Soave model is much less enhanced in the simulator than Peng-Robinson concerning pseudo components, so it was decided not to test it.

The remaining two candidates are:

- Peng-Robinson, one of the most popular equations of state in the petrochemical industry [18]. It can rigorously predict the behaviour of single and multiphase systems in a wide range of temperatures and pressures. In HYSYS, it generates a wide range of binary coefficients for both real and pseudo components. It has also been enhanced to better predict activity coefficients and interactions with water [5]. Peng-Robinson-Stryjek-Vera was also considered, but it showed very little differences with respect to Peng-Robinson and a much higher computational demand, so it was discarded;
- Braun BK-10 is very specific for heavy hydrocarbon systems in vacuum conditions. It defines the equilibrium constant K as:

  $$K_i = \frac{y_i}{x_i}$$

  at 10 psi from the components NBP using Braun convergence pressure method charts. Those K values are then adapted to every pressure using the modified Antoine equation [5]. This approach is however semi-ideal since it does not consider molecular interaction changes with pressure. However, it has the advantage of having few parameters to be evaluated, which are the modified Antoine's ones.

The two selected methods need to be confronted and validated. The TDA itself presents a high number of refluxes, stages, and other issues which are not related to thermodynamic equilibrium and make a comparison between the models in this unit impossible. The pre-flash unit upstream to the column is much simpler and was used for this purpose.

2.4.1. Introduction to the preflash

The pre-flash unit is located upstream to the column, to remove solvents and water from the lubricant stream. A simple scheme of this section is represented in Figure 23. The feed stream is preheated up to 140 °C by two heat exchangers, using steam at two different pressures. The separation takes place in vessel C-311. Flash liquid product is sent to tank TK-401 while vapor outlet is cooled to roughly 50 °C using water. This stream is finally sent to V-312, a 2-liquid separator, which recovers water and light gas oil (mainly made up of organic solvents and light ends). Off gases are sent to the flare. The pressure in the pre-flash is kept at 380 torr, by sending the vapor product at the vessel kept at 180 torr with the help of an ejector (not represented).

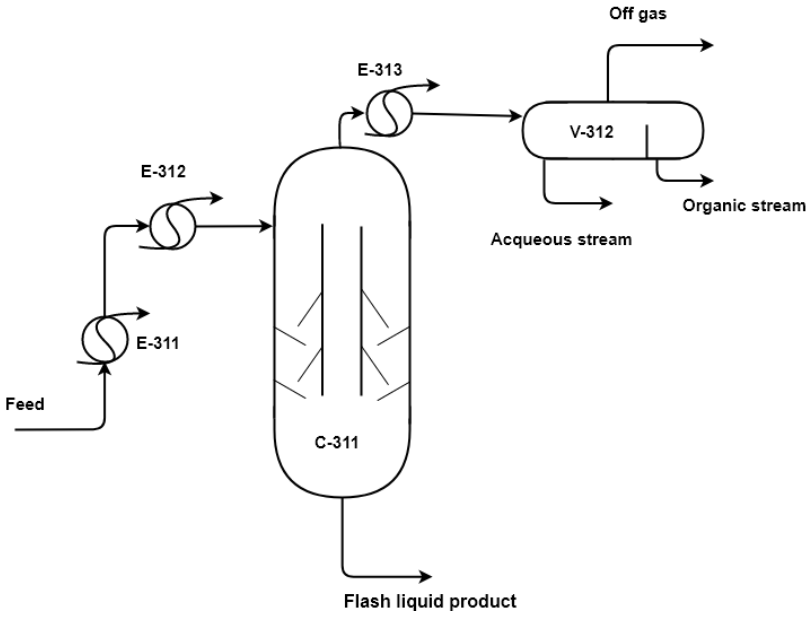

Figure 23: Pre-flash P&I

The pre-flash feed is built summing up the products in the right quantity: flash liquid product, which is the column's feed, constitutes 89% in weight, while recovered water and organic phase constitute 8% and 3% in weight, respectively. It is assured by the plant's operators that the organic light-ends and solvents are mainly made up by simple aromatic components, which can be approximatively represented by styrene.

The scheme built up in HYSYS is shown in Figure 24. The conditions are set to 140 °C, setting the outlet temperature of the heat exchanger which is not rigorous, and 380 torr. Vessel's temperature is set at 50 °C by the exchanger E-313, while its pressure is set at 180 torr by the lamination valve PIC-3013. Lastly, the pre-flash inlet is built by feeding used lubricants, water, and styrene in the quantity described above.

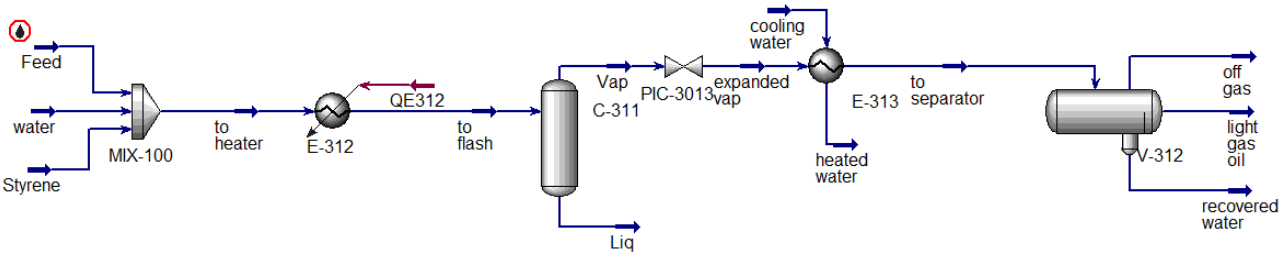

Figure 24: Pre-flash section scheme in HYSYS

2.4.2. Results and discussion

Validation is done using two different feeds. Since no experimental data is available except the flash liquid outlet ASTM D1160 curve at 10 torr and the liquid flow rate, only those are considered. Regarding both feeds, PR and BK10 predict a mass fraction of the liquid products around 88,95 % and 89,3%, respectively. The liquids' composition shows that BK10 tends to volatilize more the organic phase and to keep more water in the liquid phase. The ASTM curves are analysed by means of absolute errors in °C and parity plots, both with respect to the experimental values.

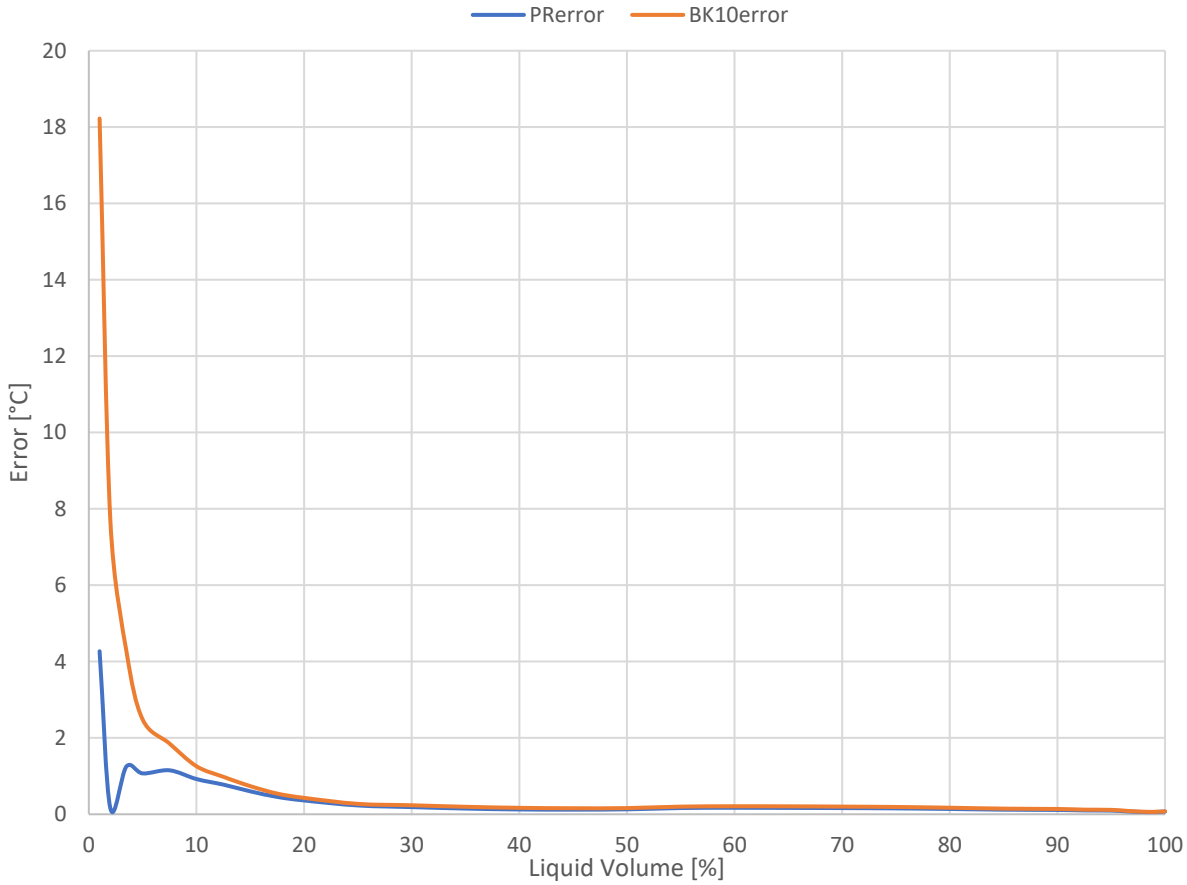

Figure 25: EoS ASTM D1160 absolute error with respect to feed 1

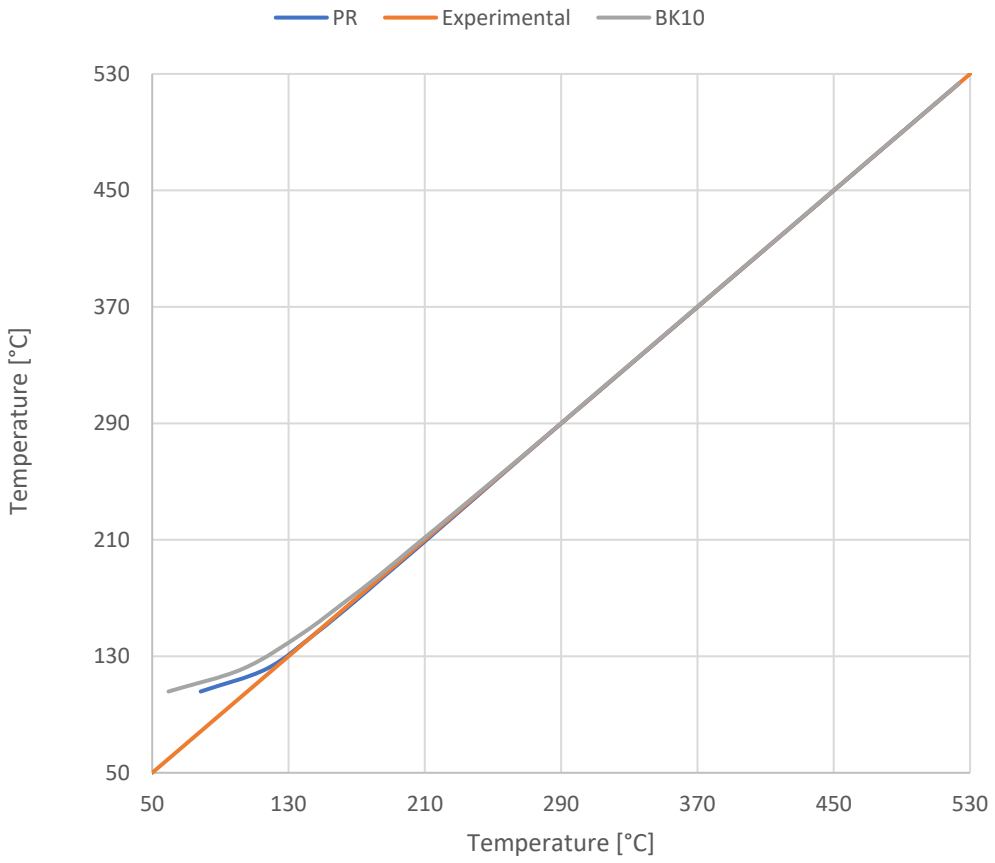

Figure 26: Parity plot of feed 1 prediction error

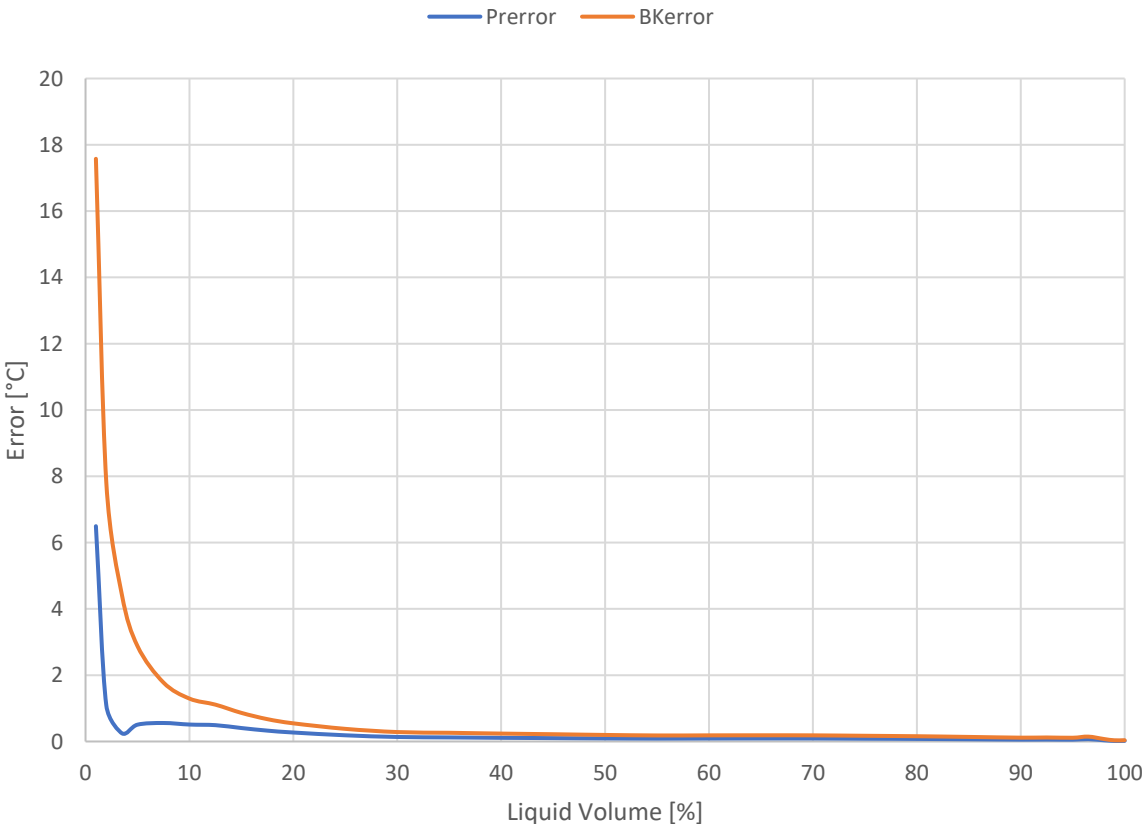

Figure 27: EoS ASTM D1160 absolute error prediction with respect to feed 2

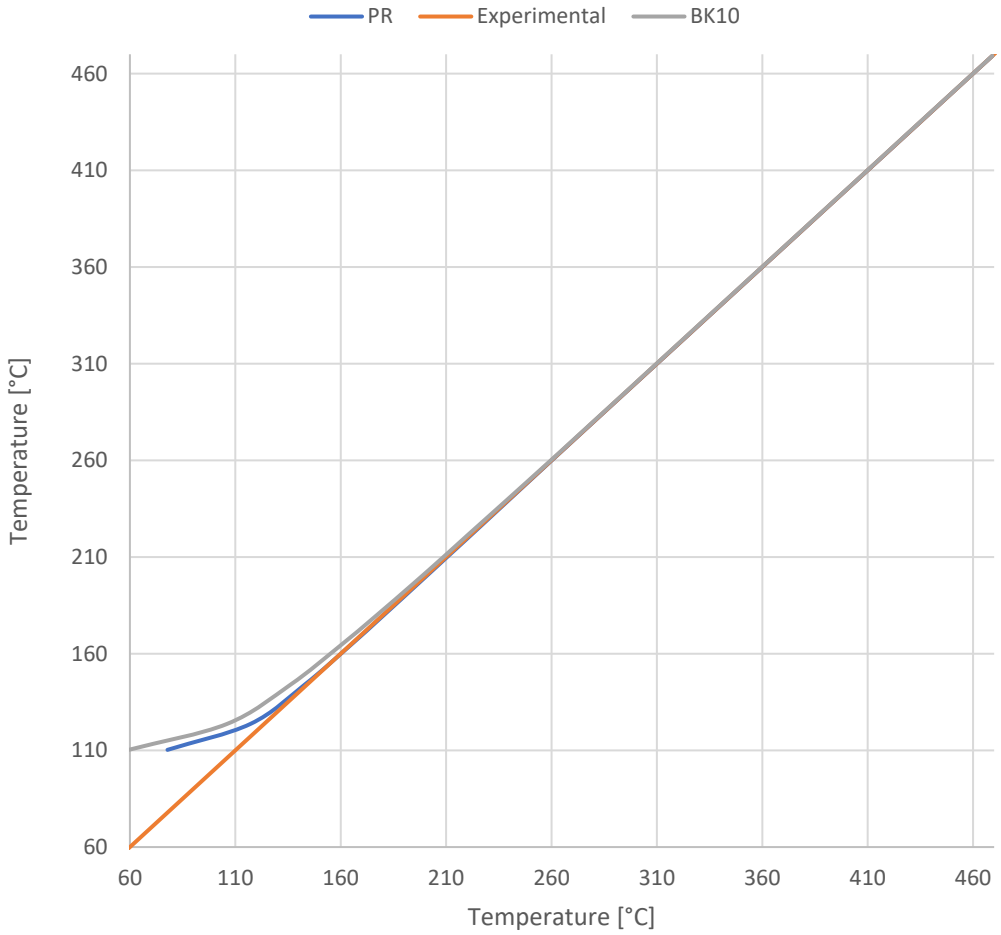

Figure 28: Parity plot of feed 2 prediction error

Braun BK10 exhibits a larger error along the whole ASTM curve compared to Peng-Robinson EoS. The latter model shows deviations with the lightest part of the blend. Such problems can be considered negligible and PR EoS is considered more reliable and accurate.

Lastly, the V-312's results show that the organic phase is completely separated from water, as reported by Itelyum. The predicted water mass fraction in such product is less than 0.02 %.

2.5. Equipment

In the following chapter the equipment upstream and downstream of the column will be described in detail alongside the column.

2.5.1. Convective furnace

The convective furnace covers the function, traditionally carried out by the reboiler, to provide the heating duty necessary for the operation of the column.

The feed is preheated by a process-process heat exchanger with the asphaltenes feedstock acting as utility, then furnace duty is adjusted in order to provide the correct outlet temperature of about 360°C.

The contact time in the furnace is about 10 minutes and this combined with relatively high temperature leads to significant cracking taking place.

The presence of cracking was verified when the experimental data on the boiling point curves of the products and feed were compared. A significant quantity of light components not included in the feed are extracted on top of the TDA column (Figure 29).

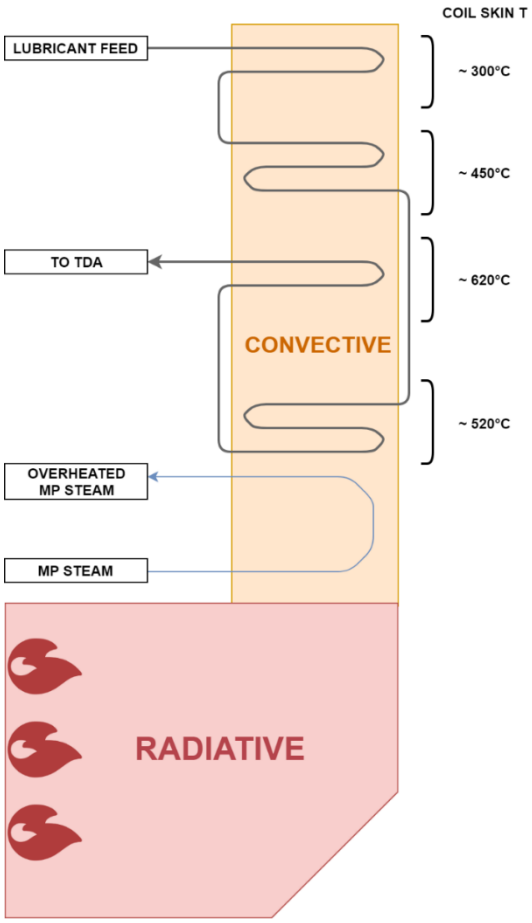

Figure 29: Convective furnace structure

The development of a rate model for the feedstock in the furnace was considered as a modelling possibility, but discarded as it was unfeasible for the following reasons:

- A proper chemical characterization of the feedstock is not available (contents of aromatics, paraffins and olefins, etc.) and a simulation of this kind requires a pseudo-component cut set customized for a reacting system;
- During use lubricants are commonly contaminated by metals present in their working environment. By a recent detailed chemical analysis (dated May 2018) it was possible to verify a significant presence of metal contaminants in the feedstock (Boron, Iron, Copper, and Phosphorous among them). Quantifying how much of them are present in the furnace feedstock and their catalytic properties was not possible [19];
- The biphasic mixture in the furnace further complicates the modelling introducing the necessity of a fluid dynamic model.

For these reasons the idea of a furnace simulation had to be dropped and postponed as a possible future development of the plant modelling. The implementation in HYSYS must be a simple heat exchanger provided with an external utility stream.

2.5.2. Cracking

The examination of input output experimental data on a control volume containing the furnace and the column confirmed the suspicion held by Itelyum that relevant cracking phenomena were taking place in the furnace.

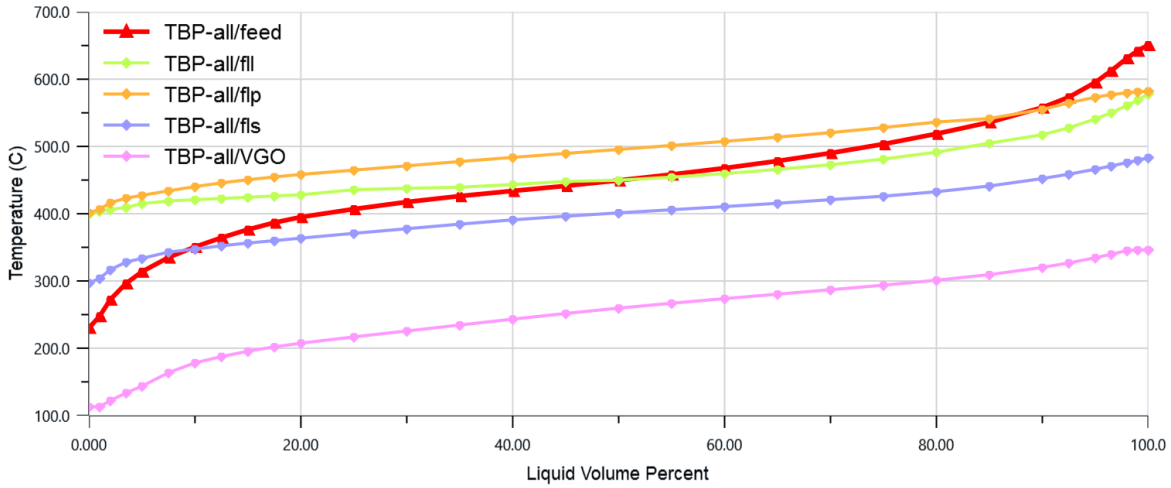

Figure 30: Normal boiling point curves of products and feed of the column

From the boiling point curves, it is evident that among the products there are compounds lighter than the ones introduced as feed to the furnace. This phenomenon is mostly expected when heating heavy hydrocarbons, but due to the topography of the data, several problems come from it. Due to unknown composition of stream FEED, ASP and VAC (Figure 31) the column is undetermined and cannot be solved. The possibility to disregard cracking was soon dropped since the phenomenon has important consequences on the process yield and a different approach was used to characterize the column feed.

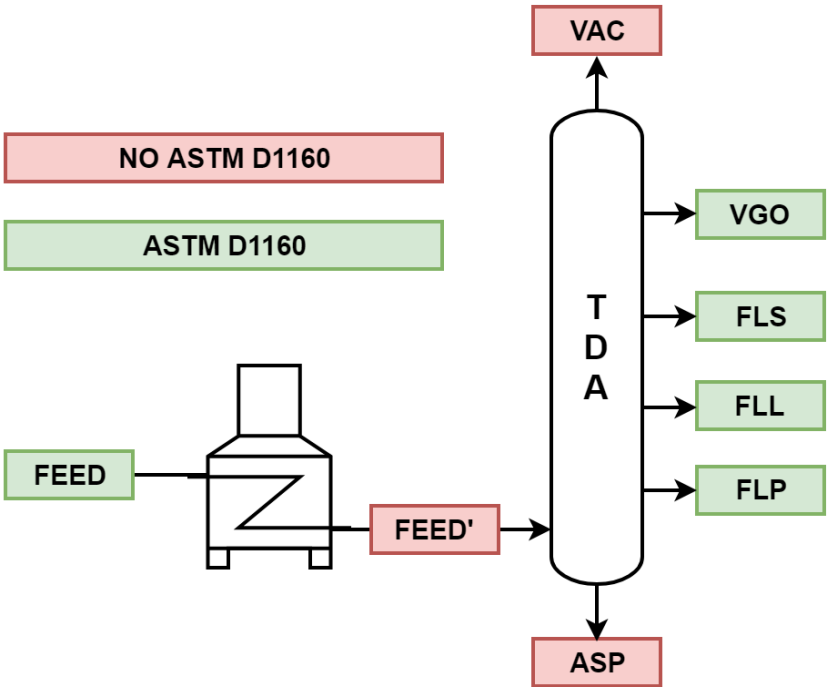

Figure 31: Data topography

2.5.3. Reconciliation

Detaching the TDA from the furnace and downstream 7 streams are left (ASP, FEED, VAC, VGO, FLS, FLL, FLP) of which 4 have a known composition (the ASTM D1160 curve has the meaning of 'composition' for a petrochemical stream). A single node, intended as a control volume to which a global mass balance can be applied, is present (the TDA column itself) so the redundancy of the system is:

$$R = N_{MeasuredFlow} + N_{nodes} - N_{TotalFlow} = -2$$

making the system impossible to reconcile. The first hypothesis introduced is that the vacuum stream is negligible. This information was provided by Itelyum and further confirmed by the simulation later. By removing an unknown stream, the redundancy of the system is still negative and coaptation impossible so a different control volume must be used.

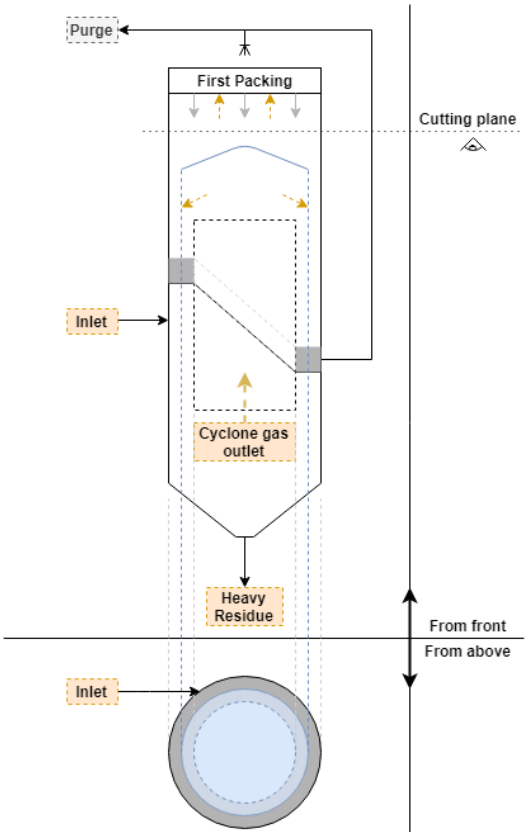

Figure 32: Column inlet structure

By examining the detailed flowsheet of the column, it was noticed that the cyclone interacts with the upper part of the column through a single unidirectional vapor stream. Considering only the lower part of the column and defining a new feed stream it is now possible to obtain a control volume with redundancy equal to 0 and thus determined.

This approach has some drawbacks:

- Information about the asphaltenes stream (Viscoflex) is lost and its composition cannot be verified;
- The cyclone is an undetermined unit;
- The extent of cracking in the furnace is unknown;
- The model is awkward for practical applications, since it is usually desired to predict the products from the feedstock rather than the opposite. It must be noted however that the information lost about cracking will impact more the very heavy asphaltenes (the ones more susceptible to low T cracking) and the very light ones (light-ends formed by the cracking) which are not the main products of the column.

In order to have a complete model however both the furnace and the cyclone are necessary. This is truer for the dynamic model than the stationary one, but nonetheless it is necessary to work back the reconciled feed to the furnace feed.

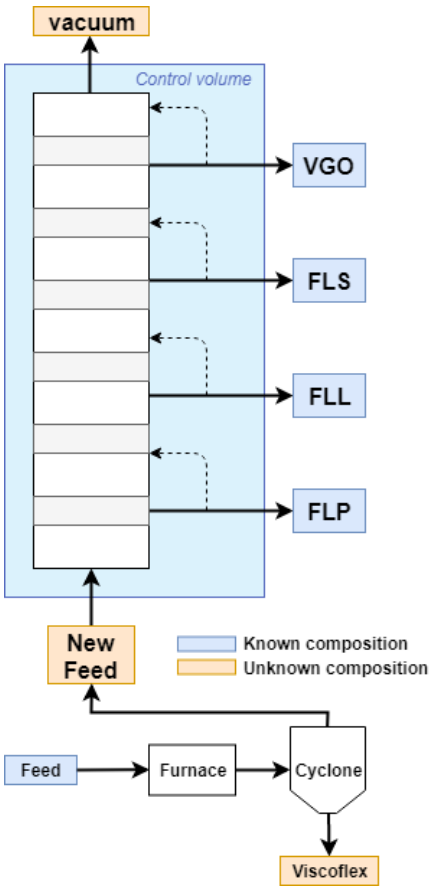

Figure 33: New control volume breakdown

2.5.4. Cyclone

The inlet of the column is shaped as a cyclone and located at the very bottom of the unit. The triphasic mixture coming from the furnace is fed tangentially to the outer shell of the column as it would be done in a conventional cyclone. However, the mixture is a slurry-vapor one and not solid-gas, meaning the conventional model for a cyclone can't be applied.

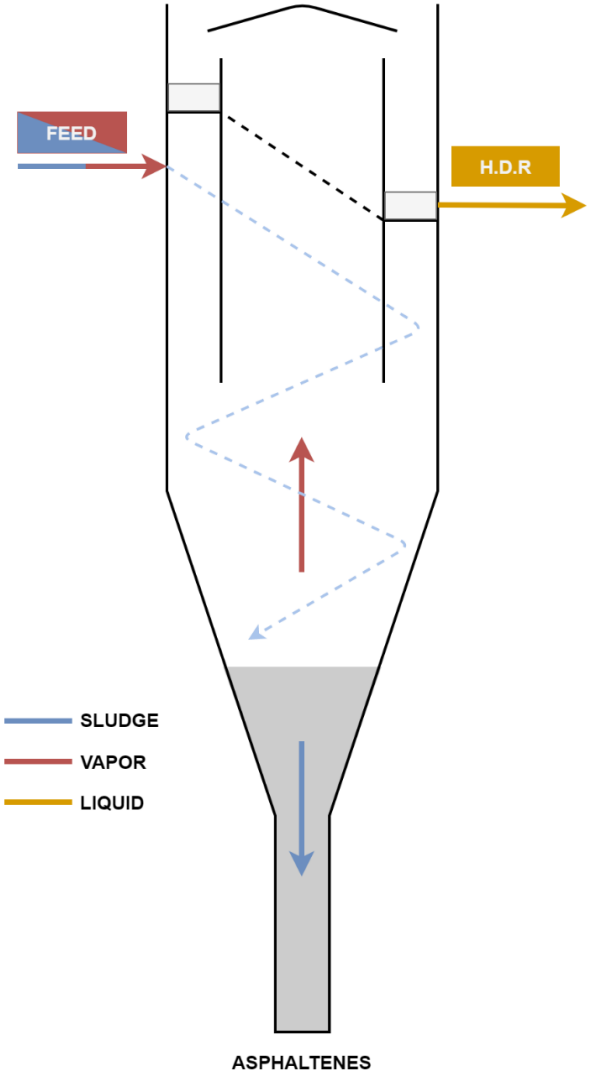

Figure 34: Cyclone detailed structure

Depending on the inlet speed of feed the slurry phase will be pushed to the outer shell with different intensity and time. The higher the speed the higher the turbulence and exchange rate at the interface. Higher speed means also higher flowrate since the geometry is fixed and this means that the contact time in the cyclone will be lower and so will be also the amount of exchanged mass. It could be the case the vapor phase might not have the time to disengage from the liquid phase before leaving the unit and the stage would not be an equilibrium one. This eventuality is considered unlikely for mainly two reasons:

- Furnace and column are not next to each another and so extra time to disengage in the pipeline will be available;
- The rate at which the vapor phase will disengage from the slurry will depend as by Fick law by the diffusivity, the concentration gradient and the area of exchange. Since the liquid flow enters tangentially to the column it will be pushed to the border by centrifugal forces that will spread the liquid on the lateral surface of the column cylinder rising both the turbulence and exchange area.

Due to cracking in the furnace the inlet feed of the cyclone is unknown and asphaltenes are too heavy to be analysed through ASTM D1160, so their composition is unknown too. The vapor outlet can be derived by reconciliation of the packed section of the column, but since both the inlet feed and liquid outlet have unknown composition the unit is undetermined.

It is possible to derive a reasonable approximation of the cyclone feed by knowing the extent of vaporization (the mass flowrates are known for all the involved streams) and the composition of the vapor outlet. Aspen HYSYS can solve the flash to get back the composition of the feed knowing this data, but:

- Information on pseudo-components that are too heavy to be present in the vapor phase are lost;
- The cyclone-flash equivalence cannot be verified;
- All the error is dropped on asphaltenes, which is an acceptable result considering their marginal role in the TDA.

By approximating the cyclone to a flash unit, the plant assumes a more conventional design in which the distillation column is preceded by a pre-flash unit to separate compounds lighter or heavier than a certain threshold, even if usually it's the liquid phase that is fed to the column and light-ends that are removed.

Assuming thermodynamic equilibrium between the liquid and the vapor, the cyclone was considered as an adiabatic unit operating at the temperature of the cyclone. The input data are:

- Flash temperature of 330 °C;
- The composition of the vapor outlet obtained by a reconciliation;
- The mass flow rate of feed, vapor, and bottom.

With this information, considering the pseudocomponents present in furnace feed, it is possible to solve the flash unit to derive the feed of the column.

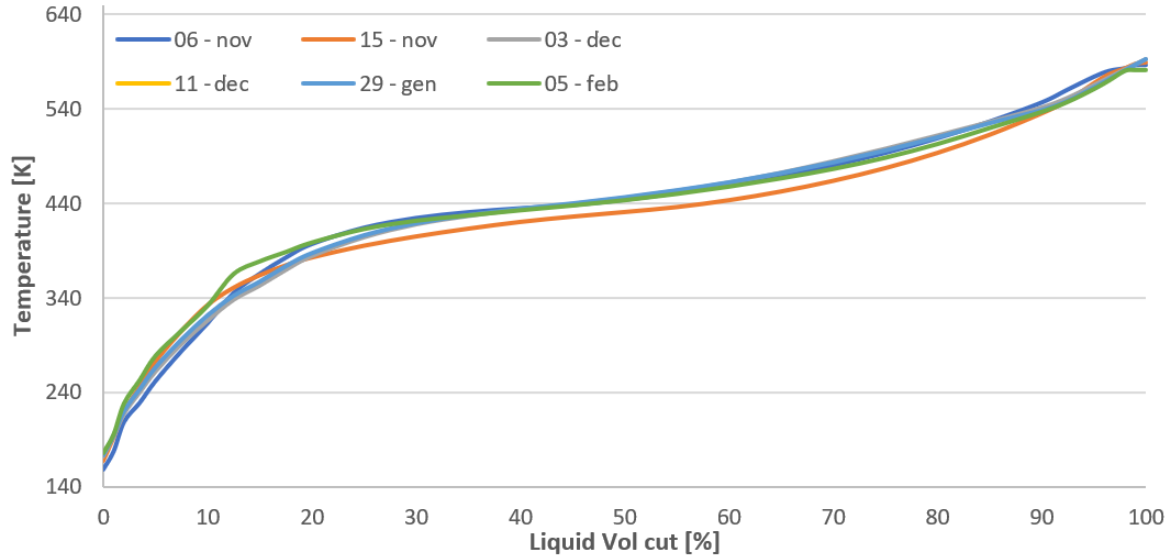

Figure 35 ASTM curves as calculated by ASPEN by solving the flash backward

Carrying out the simulation for several reconciled feedstocks, the furnace feed was derived in different moments of winter season 2018/19 (Figure 35). The resulting ASTM boiling point curves are very similar over the season, this could be due to either a constant behavior of the furnace (meaning cracking is not changing in time sufficiently

to affect the product distribution significantly) or the fact that the plant is fed with a very similar raw material every time.

As a future development it is suggested to validate this hypothesis by carrying out an ASTM D1160 of the cyclone feed. This measurement is further suggested because it is the most straightforward way to verify the extent and consequences of cracking in the furnace and could serve as a basis to build a model of it. Once this measure is obtained a flash simulation with this feedstock is to be carried out and the experimental vaporization extent must be compared with the simulated one. Higher vaporization extent is impossible, lower one suggests a non-equilibrium stage, in the which case a Murphree efficiency could be introduced.

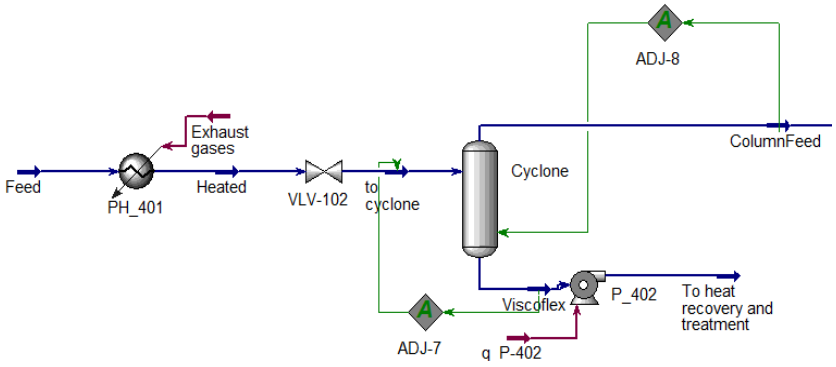

Figure 36: ASPEN HYSYS V10 cyclone flowsheet

The implementation of the flash unit in HYSYS makes two adjust operators necessary. ADJ-7 operator acts on the feed pressure to regulate the outlet temperature of viscoflex (the asphaltenes), this operator has the purpose of simulating the pressure drops from the furnace to the cyclone. It also has the indirect desired effect of dropping the temperature from the one of at furnace's outlet to the one at the cyclone's inlet. This effect is achieved by valve VLV-102 that laminates the flow simulating both the pressure drops between the furnace and column and the consequent temperature loss of about 20°C. ADJ-8 acts on the operating pressure of the flash to control the mass flow rate to the column, and thus the extent of vaporization, to the proper value.

2.6. HYSYS column

A column in HYSYS is a unit operation made up of several theoretical stages at equilibrium, whose number in this case is evaluated using pack height equivalent of a theoretical plate (HETP), as explained in chapter 2.6.2. Also, pressure drops are not calculated by default from the column but need to be inserted by the user. Therefore, the choice of the kind of stage (e.g. plates) do not affect the solution. Pressure drops can be calculated from HYSYS for very specific pack and tray types, however, since the program does not consider fouling and some of the packing types are not available, this option was abandoned and a separate model for pressure drops was used. Lastly, different inlets and outlets for each stage can be set, from which refluxes can be made up.

Aspen HYSYS solves the column when all degrees of freedom are provided from the users. Their number has been discussed in chapter 1.4.3. The adopted specifications for the simulation coincide with the column controlled variables, excluding LIC since holdups are not considered in steady state calculations. Such variables are:

- Feed temperature, flow-rate and composition;
- Product flowrate;
- Refluxes flowrate;
- Temperatures of exiting heat exchangers streams.

Additionally, since no momentum balances to calculate pressure drops is performed by HYSYS, also stages pressures are inserted as inputs, as discussed in chapter 2.6.1.

2.6.1. Column pressure profile

The need to predict the column real pressure profile is crucial, since it is needed for the correct evaluation of the column's performances accordingly to the operating conditions, especially fouling. A reliable model is the best choice, so that measurements from DCS are not necessary. The model can be chosen to be:

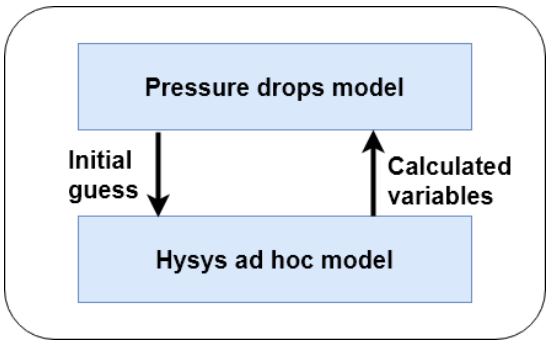

Figure 37: Dependent model iterative cycle

- dependent from stream and pack properties. Density, viscosity and flow rates are considered for each stage but also stages' structure, fouling and liquid levels. This model can be very rigorous but also very complex to implement, due to the lack of data. However, the most challenging aspect of it is the pressures evaluation from case to case, since fluid's transport properties depends from the separation efficiency which also depend on the pressure drops, making necessary an iterative routine involving both the simulator and the model (Figure 37);

- Independent from internal streams properties. Such a model can be a simple equation representing the pressure profile as a function of the most important parameters, which have proven to be fouling and feed flow rate. Refluxes flow rates have been neglected since no relationships seem to be present;

The independent model is far simpler and can offer results comparable to the independent model, after a proper regression of the parameters, so this approach was chosen. To build it up, 4 different sets have been provided by the plant's operators. They consist in series of measurements over a time span of several hours in which operating conditions are constants. The mean values of pressures are taken in consideration. Standard deviation is also an important factor to take care of, since a high value may compromise data's reliability. However, as shown in Table 6, this is not the case.

	Pack 6	Pack 6	Pack 5	Pack 4	Pack 3	Pack 1
Position	Above	Below	Below	Below	Below	Below
Standard deviation [torr]	0,21	0,19	0,18	0,19	0,21	0,2

Table 6: Pressure measurement standard deviations

In this case a reliable pressure model is even more urgent, since the pressure indicators showed various pressure reversals in the column, which would indicate vapor flow descending the stages. Such a behaviour is unfeasible, since the flow driving force is determined from the higher pressure downstream and by the ejector group on

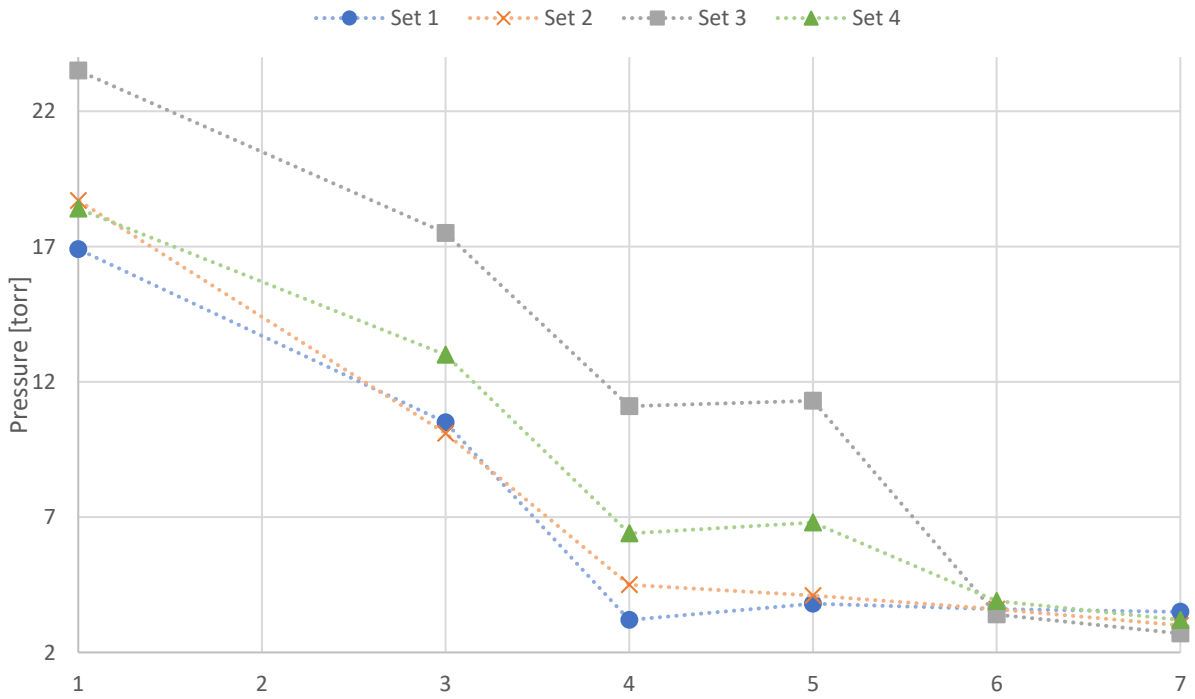

Figure 38: Column pressure profile

top of the column. Moreover, the upper part of the column would be at a much lower temperature due to the absence of hot vapor rising. These values could depend on malfunctioning of the indicators, which could be due to fouling, wrong placement or others. Pressure values for the different data set are plotted in Figure 38, where values are reported starting from position 1, corresponding to the column bottom, to position 7, corresponding to the column top.

Set number 3 corresponds to the column less than 1 month before its cleaning, while the other profiles are after it. Feed flow rate is set at 15000 kg/hr for sets 2 and 4, while it is set at 13500 kg/hr for sets 1 and 3.
Before choosing the right model to implement, the data were evaluated. Some observations can be made:

- The pressure on the top of the column and the pack below is constant and equal to 3.2+-0.4 torr;
- The pressure lecture of the flow entering the column, not reported in Figure 38, varies from a value of -550 to 900 absolute torr, thus was considered unreliable and couldn't be used;
- Fouling is the dominant factor, changing the column pressure profile from exponential (clean column) to quasi linear (dirty column).

Two different models are taken in consideration, which are a polynomial one and a exponential one:

$$P[torr] = a + b * (6 - x) + c * (6 - x)^2$$
$$P[torr] = \frac{F}{15000} * (\frac{c}{D} * (7 - x) + \frac{D}{a} * e^{b*(7-x)})$$

where *a*, *b* and *c* are the adaptive parameters, *D* is the dirtiness factor, F in kg/hr is the feed flow rate and x are the relative position in the column, counted bottom-up. Both functions are evaluated using Matlab' s toolbox. F and D are not used in the polynomial model since no improvements could be noticed, probably due to some difficulties in the parameters' regression. The parameters are obtained minimizing the following objective function, considering data set 1, 2 and 3:

$$f = \sum(P_{model} - P_{exp})^2_{i=1}^{N} + 1e^8 * \max(0, P_{model}^{upper\ stage} - P_{model}^{lower\ stage})$$

Value of parameters a, b, and c are 2.6, 1.2336 and 0.5953 for the polynomial model and 0.3850, 0.3313 and $4.4502*10^{-4}$ for the linear-exponential one. The Dirtiness factor is 1 for clean column and 10^{-4} for dirty column. Results are plotted below in Figure 39, Figure 40, Figure 41 and Figure 42.

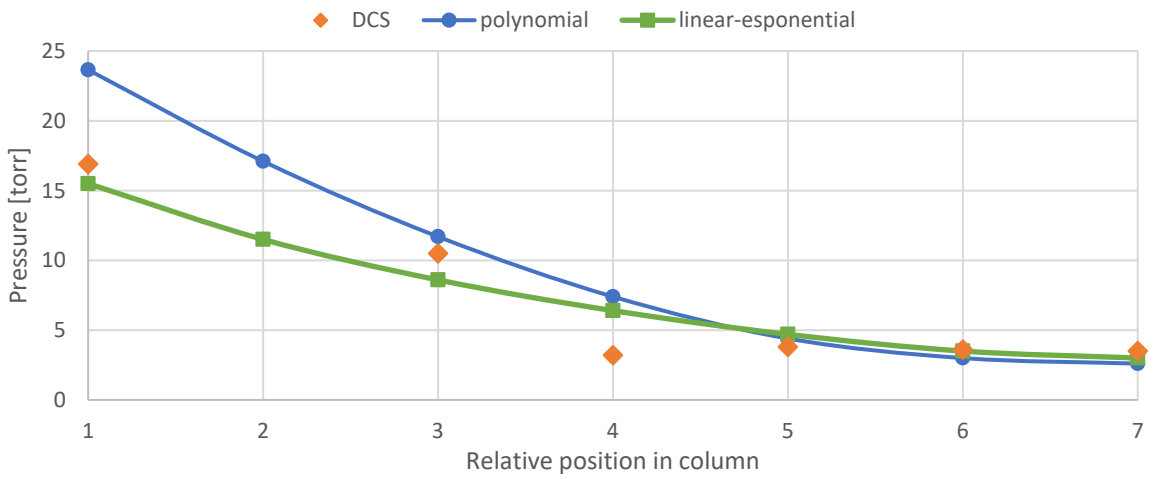

Figure 39: Pressure models results for dataset 1

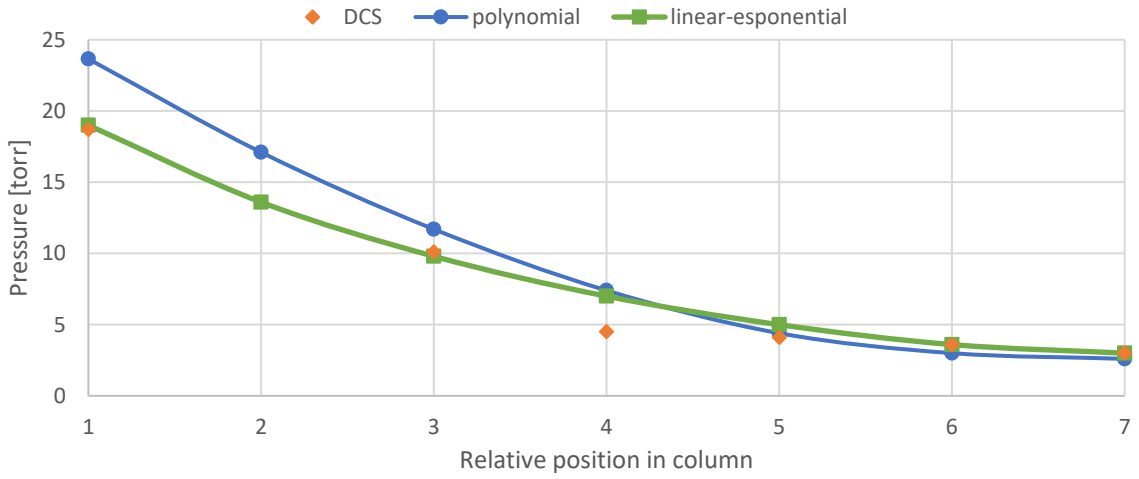

Figure 40:Pressure models results for dataset 2

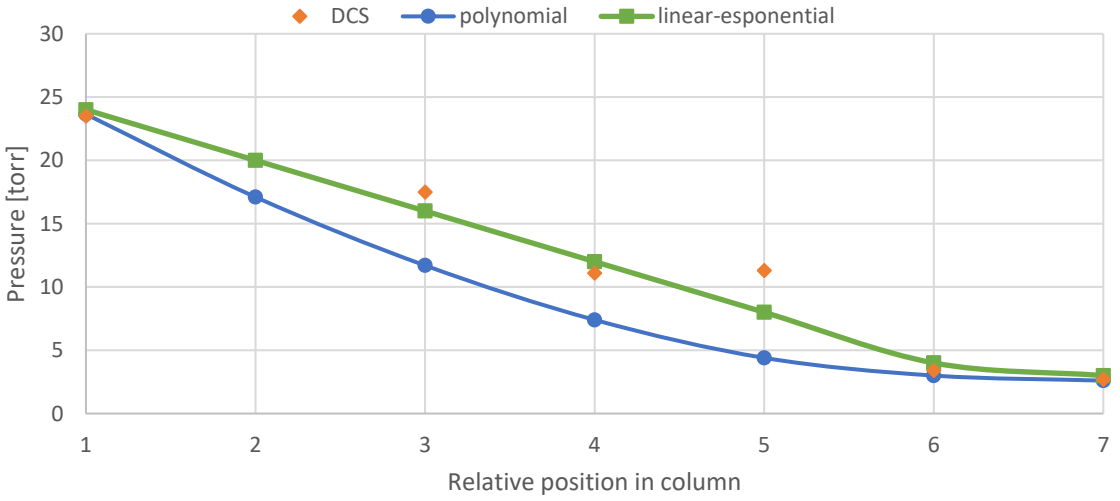

Figure 41: Pressure models results for dataset 3

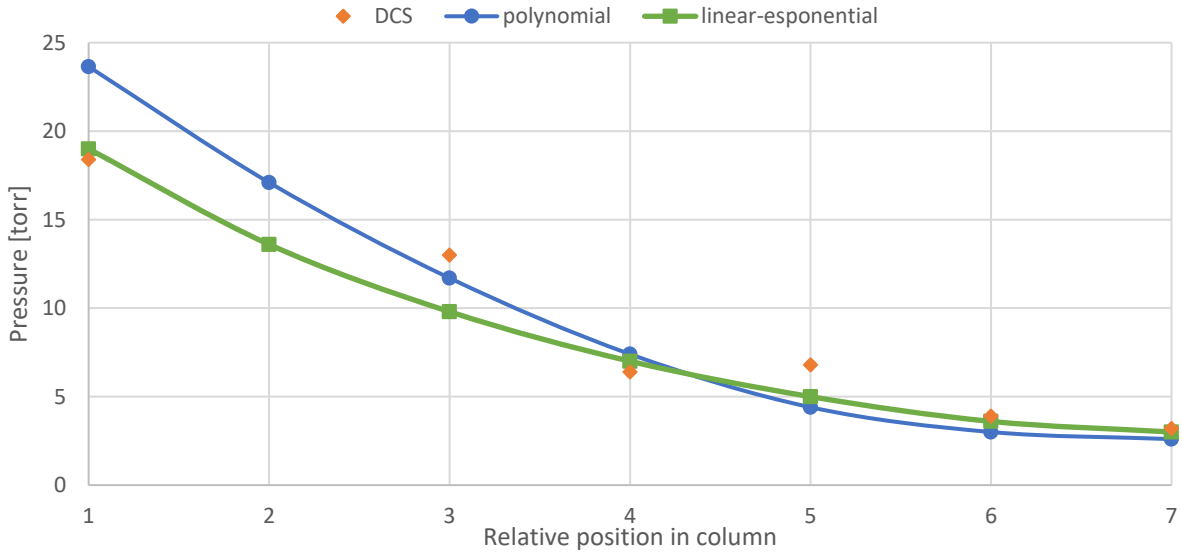

Figure 42: Pressure models results comparison for dataset 4

It is evident that the linear-exponential fits the pressure far better than the polynomial one which significantly overestimates the pression of the clean column bottom.
In order to have a quantitative measure of the model deviations, the R^2 test is adopted on the 4 different data sets. The test's results are reported below:

Model	R^2_1	R^2_2	R^2_3	R^2_4
polynomial	0.5549	0.5828	0.8073	0.7402
linear-exponential	0.9068	0.9434	0.9028	0.9018

Table 7: R^2 test results

Table 7 shows that the linear-exponential model offers better results in accordance to experimental values, but in both cases R^2 value do not approach 1. This issue is due to the pressure reversals in position 4 but may also be affected from other parameters, like the temperature influence which is indirectly controlled by refluxes. Model results are considered satisfactory and no additional features are added.

2.6.2. Column equilibrium stages

Number of theoretical equilibrium stage needs to be estimated since TDA column mainly performs separations through packed beds. Alternatively, a column can operate using trays, but this leads to a much higher column height and so a much higher capital cost. Generally, in these cases the equivalent height of a theoretical plate (HETP) is needed for each pack. These values are a function of the packing's type and operating pressures [20] [21] (Figure 44), whose dependences are explained in chapter 2.6.1.

Also, reflux inlets flow rates and products outlet positions are important. Outlets are positioned on the first equilibrium stage representing the pack (counting bottom up), while inlets are set one stage below the last one. This choice is taken after seeing the beneficial effect it has on the model's accuracy and can be justified observing that the

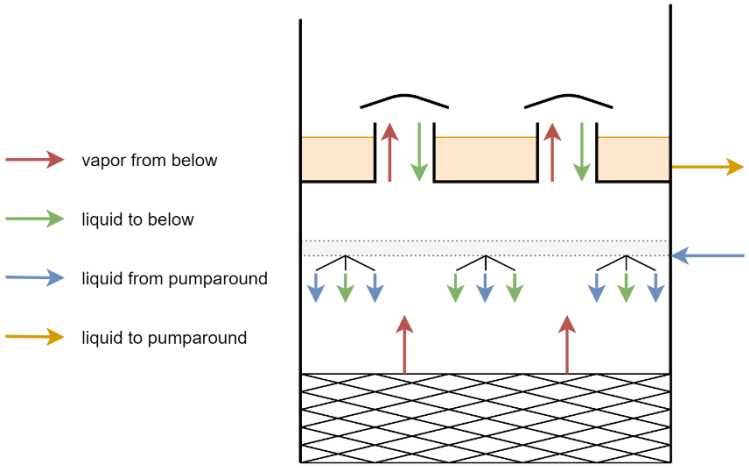

Figure 43: Sprinklers scheme

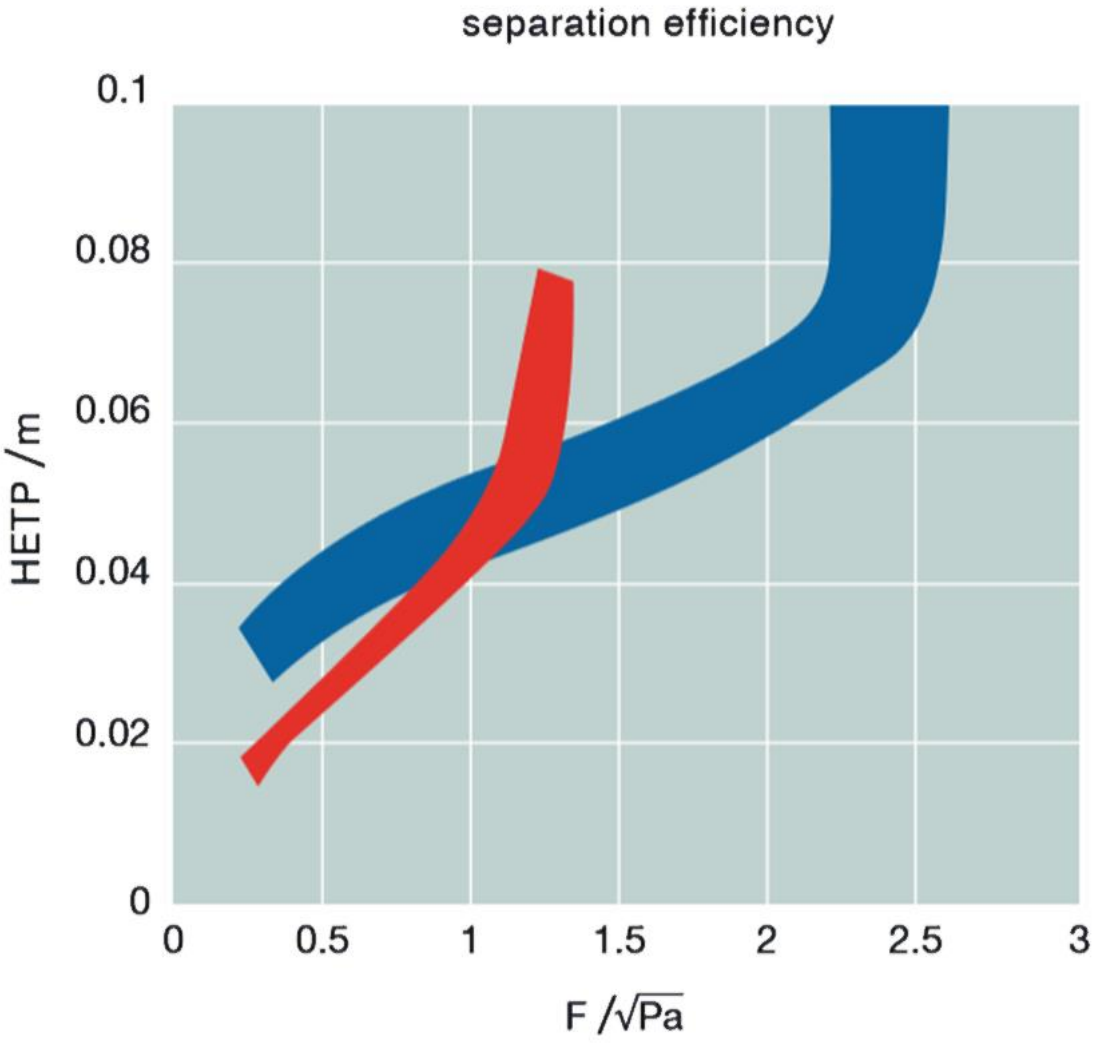

Figure 44: Example of dependence between HETP, feed, and pressure

sprinklers are set middle height above the pack, they are diffusing the reflux on (Figure 43). This may cause a stripping like effect on the liquid descending from the tray above, as well as on the atomized liquid.

To respect industrial secrecy, packs type and their HETP are not reported. The numbers of theoretical stages (Nt) used in HYSYS's column are calculated using the formula:

$$Nt = \frac{Pack\ height}{HETP}$$

Murphree efficiency is used to round the number of stages to the Nt value whenever its value is not an integer. The results are indicated in the tables below.

Pack	Ntrays	Efficiency
1	3	1
2	3	0.33
3	4	1 for all except the last one being 0.78
4	4	0.78
5	3	1
6	4	1

Table 8: Number of stages and efficiency for each pack

Last stage of pack 3 is set to 0.78 due to sensibly better results this brings. Stage number of pack number 2 is set to 3 with an efficiency of 0.33 and not to 1 with a unitary efficiency to have a stage for the FLP's withdrawn, a stage for the reflux and a stage between the reflux and the following pack first stage. The resulting column structure in HYSYS is represented in Figure 45.

2.6.3. Refluxes scheme

Refluxes are a branch of the column outlets, which are indicated in Figure 45 as VGO, FLS, FLL, FLP and heavy reflux and level control. Each of them splits in nodes as indicated in chapter 1.4.3, generating the refluxes and the TDA products. These nodes are implemented in HYSYS as splitters, which divide material streams according to a splitting ratio given by the user. Since refluxes are recycles, HYSYS requires an operator named R. It iteratively converges its outlet stream, whose first guess is given by the user, making it equal to its inlet, which coincides with the nodes branch representing the reflux.

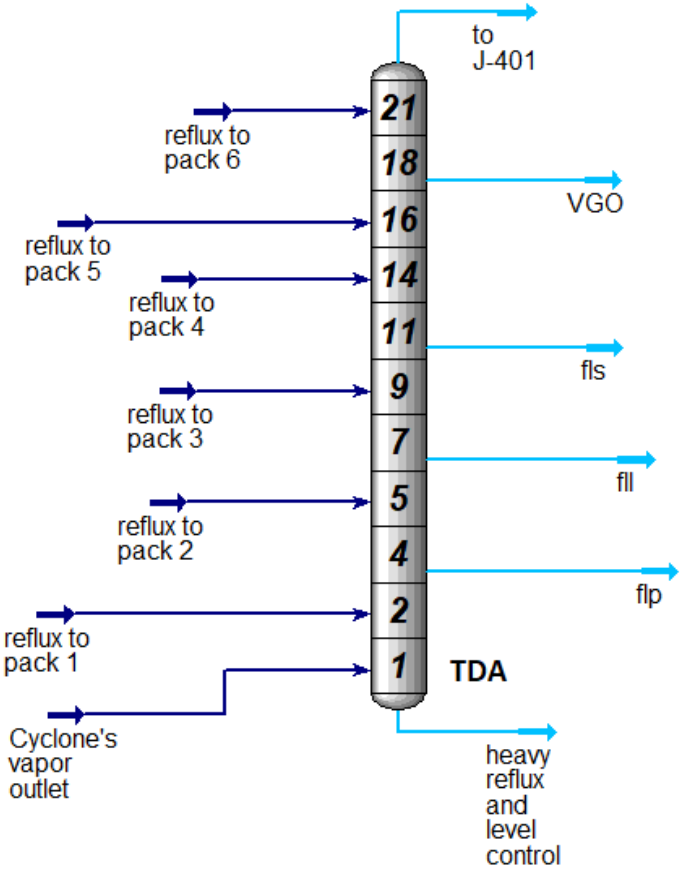

Figure 45: Column input-output flow scheme

Heat exchangers are implemented as a HYSYS's feature named cooler, which, once provided the inlet stream, only needs a specification to solve the energy balance. In this case such specifications are the outlet temperatures, as said in chapter 2.6.

Lastly, also pumps, valves and heat exchanger pressure drops are included in the model. However, these aspects are discussed in chapter 3.6 since they do not affect the column solution in HYSYS, while they are of primary important in the dynamic simulation. They are present also in the steady state simulation since it has been used to dimension various parameters as explained in chapter 3.6.

2.6.4. Model representation in HYSYS

The complete scheme of the model in HYSYS is shown in Figure 46 and Figure 47.

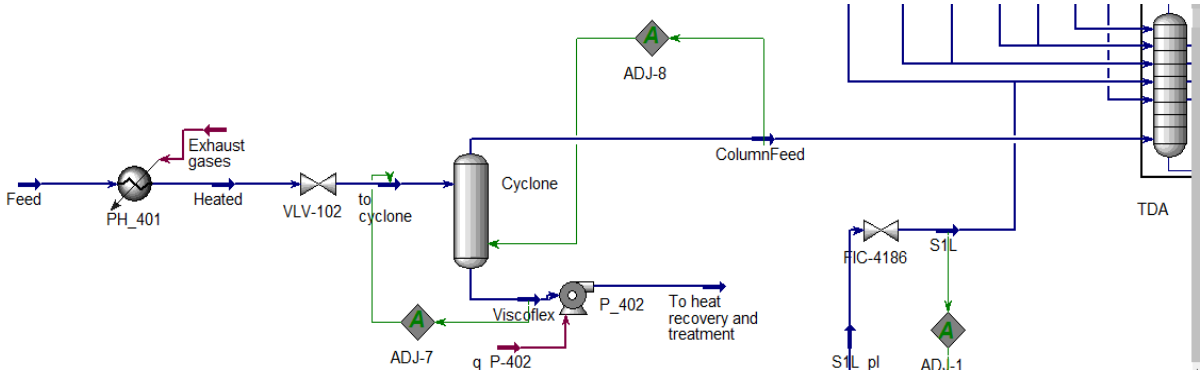

Figure 46: TDA inlet section with furnace

It is notable that the refluxes scheme is not trivial. This mostly leads to resolution problems. At first, recycles first guesses need to be as accurate as possible to fasten the solution. Old products ASTM can be used, tough they can change considerably depending on the required specifications. HYSYS has a feature which is the recycles simultaneous solver, but it proved to be worthless in this application. Consequently, recycles need to be solved one by one, taking several minutes. A good idea is searching an initial solution using a higher tolerated error for global energy balance, defined as heat flow imbalance over the total heat flux through column, in order to have a reliable first guess in much less time, and consequently diminishing it to HYSYS default value, which is $5*10^{-4}$.

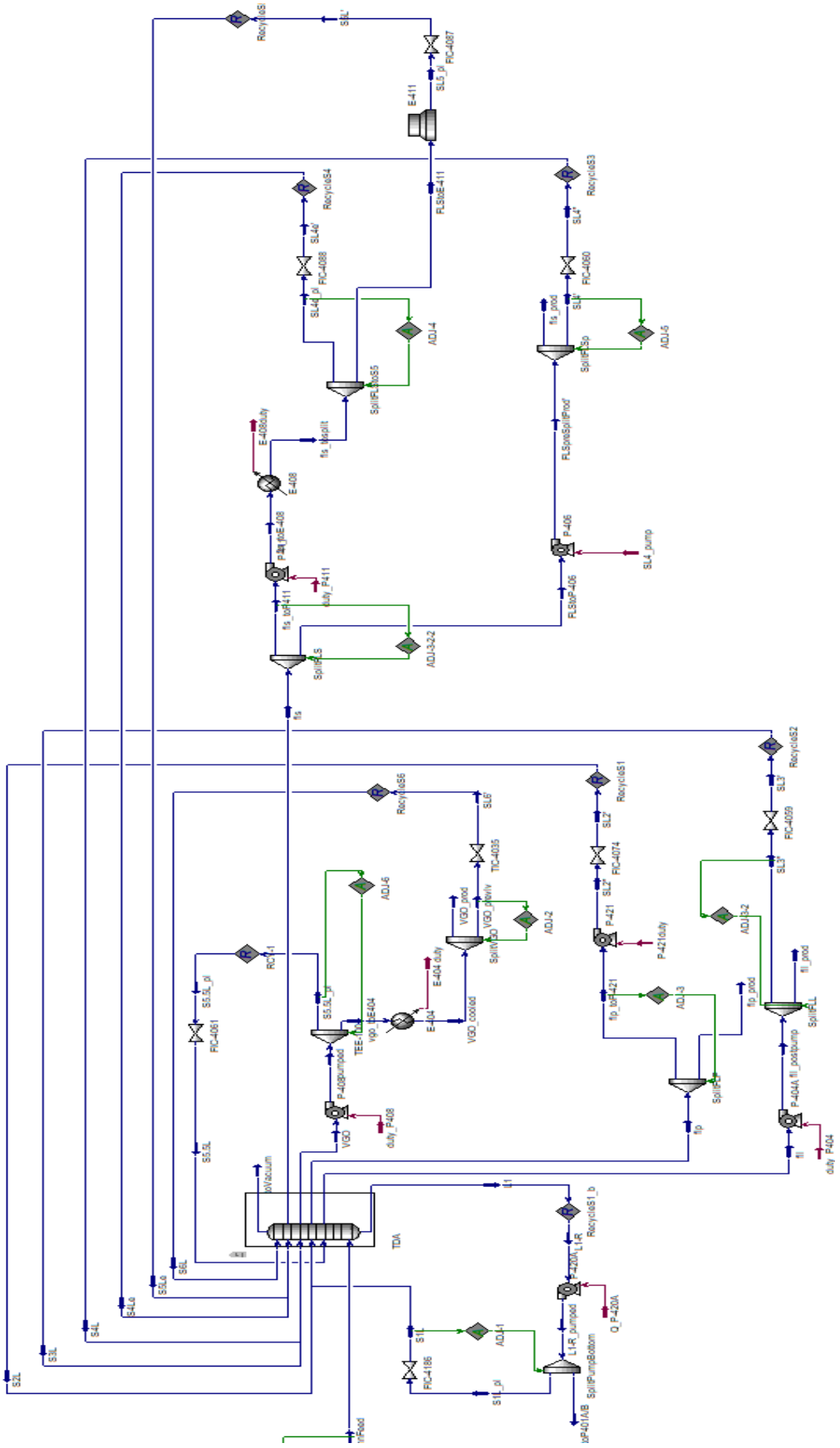

Figure 47: HYSYS TDA flowsheet

2.7. Model performance evaluation

A reliable model has to accurately predict column performance as a function of controlled variables. The latter are of primary importance in order to achieve different product properties, which also need to be accurately predicted by HYSYS TDA model. Two different data set are used to perform validation operating with different flow rate reflux and outlet heat exchanger temperatures. Column temperatures and pressures, together with product densities, viscosities and ASTM D1160 curves are confronted with the experimental data.

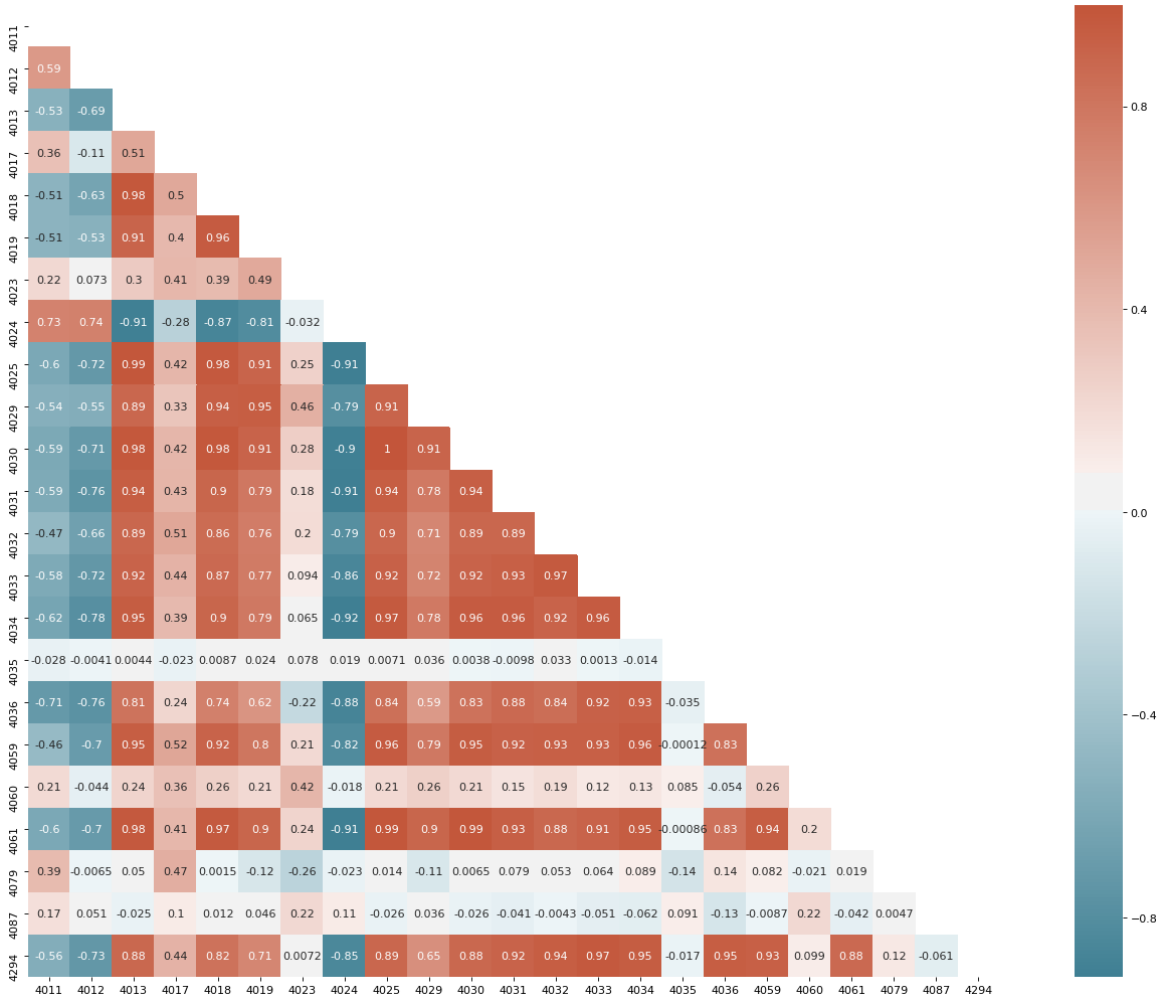

Figure 48: Temperature indicators correlogram

All pressure indicators present into the column are considered since their small number while temperature indicators are more numerous, they are placed: above and below each pack, two below them, one used to measure the liquid temperature and the other for the vapor, on each product stream and on the top of the column. In order to select the right indicators to be considered and not to miss important information, a correlogram is used (Figure 48) considering all furnished temperatures measurements from the DCS, which are taken along 7 months.

The correlogram is built linking the deviations of two parameters or measures (Y and M) as a function of a variable (i), according to the following formula:

$$Correlation_{Y,M} = \frac{\sum_i^{time}(Y_i - Y^{mean}) * (M_i - M^{mean})}{\sum_i^{time}(Y_i - Y^{mean})^2}$$

In this case, temperature indicators, which are reported along axes, are evaluated over time. Strongly correlated measures, with an absolute value of the correlation index of 0.96 and above, are grouped in patterns and only one of the indicators each are considered. The indicators with less disturbances are used, which proved to be always the ones measuring the temperature of the liquid phase in the liquid collectors. Those indicator's standard deviations are reported in Table 9.

Pack	6	6	5	4	3	2	1
Position	Above	Below	Above	Below	Below	Below	Below
Standard deviation [°C]	0,37	0,12	0,17	0,21	0,18	0,15	0,24

Table 9: Temperature measurements standard deviation

2.7.1. Results and discussion

Temperature (Figure 49 and Figure 51) and pressure (Figure 50 and Figure 52) profiles are analysed. The values reported match the stages in which the indicators are located, starting from position 1, corresponding to the column bottom, to position 21, corresponding to the column top.

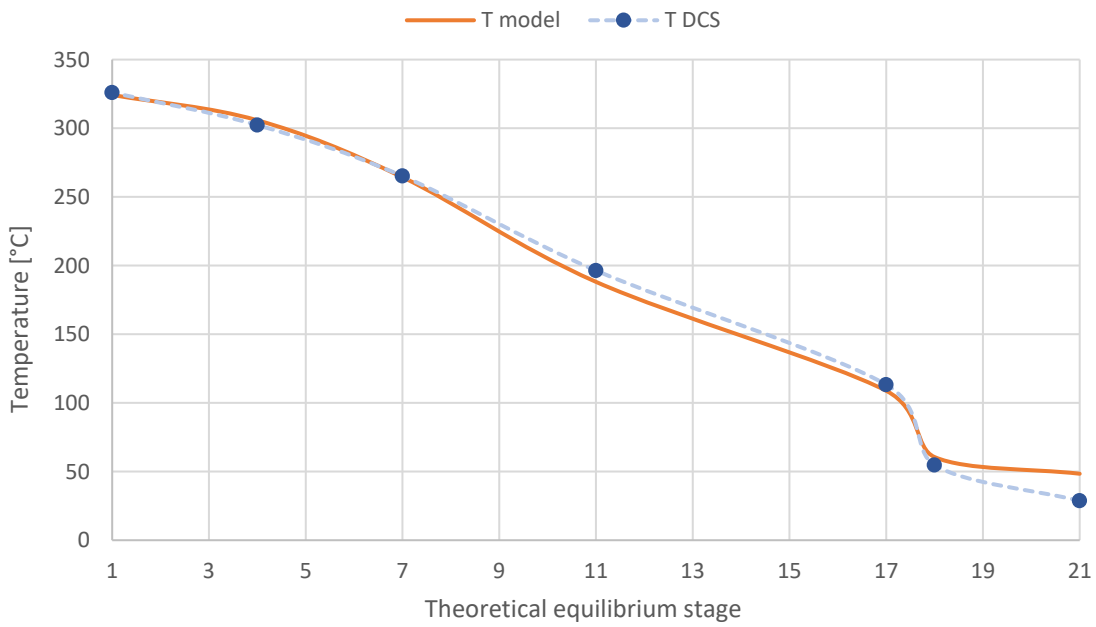

Figure 49: Temperature profile in the first case study

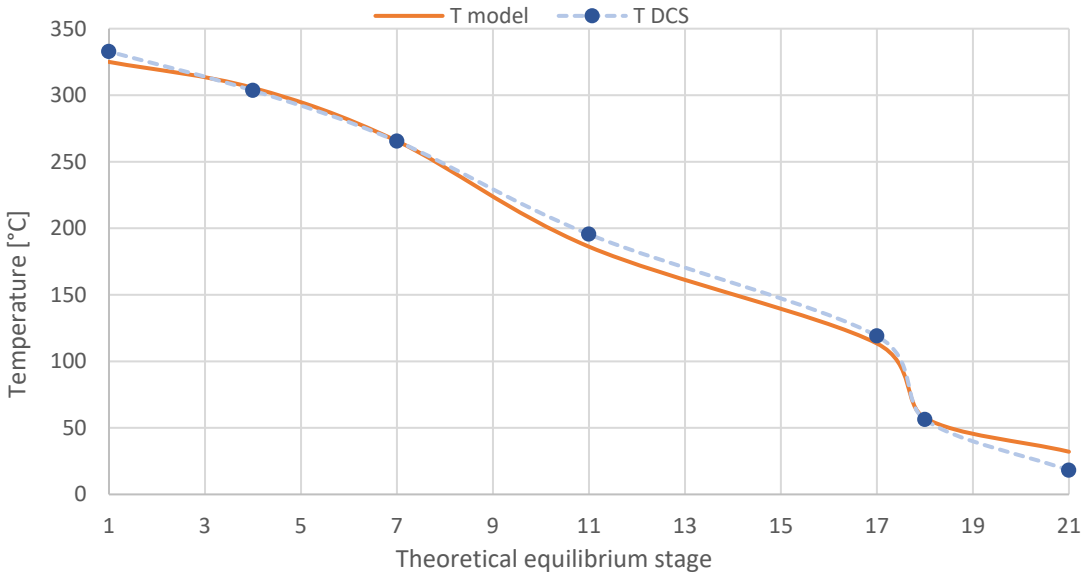

Figure 51: Temperature profile in the second case study

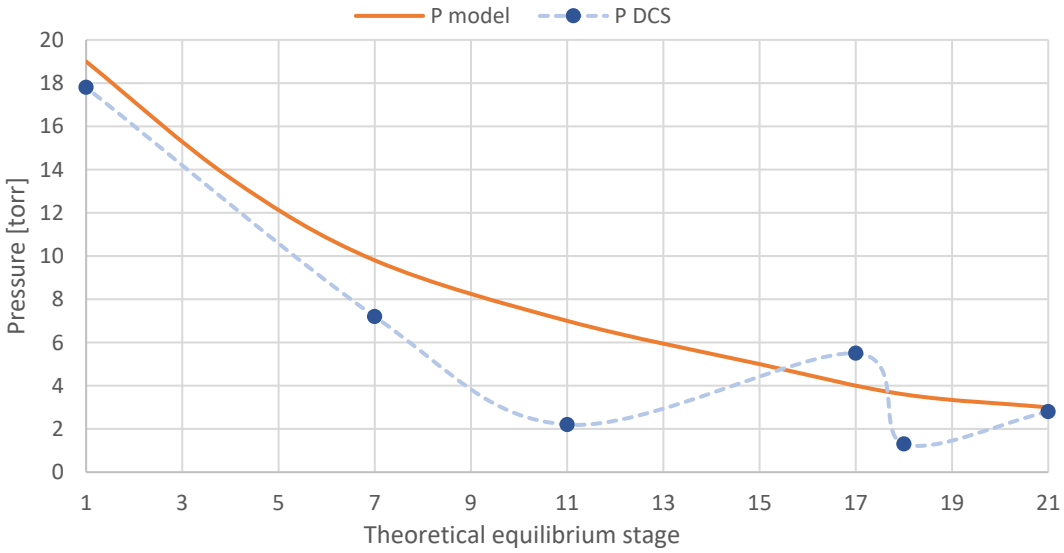

Figure 50: Pressure profile in the first case study

As shown, temperature profiles agree well, with discordances of 2-3,5°C and 7-9 °C in positions 4 and 11, corresponding to the FLP and the FLS draws respectively, and on the column top, corresponding to position 21. This last measurement shows greater incompatibility with the model prediction, much probably because of the high non equilibrium behaviour of such stage and the loss of information on the lightest vapor flow rate to the ejector group. Pressure trends show the same behaviour as from the data sets used to build the column pressure profile's model. The mean errors ε, defined as:

$$\varepsilon = \frac{\sum \sqrt{(V(i)^{model} - V(i)^{dcs})^2}}{Nmeasures}$$

are 1,5 torr for the pressure and 6,1 °C for the temperature. If column top is not considered as not producing any kind of product, the temperature's error is 3,6 °C.

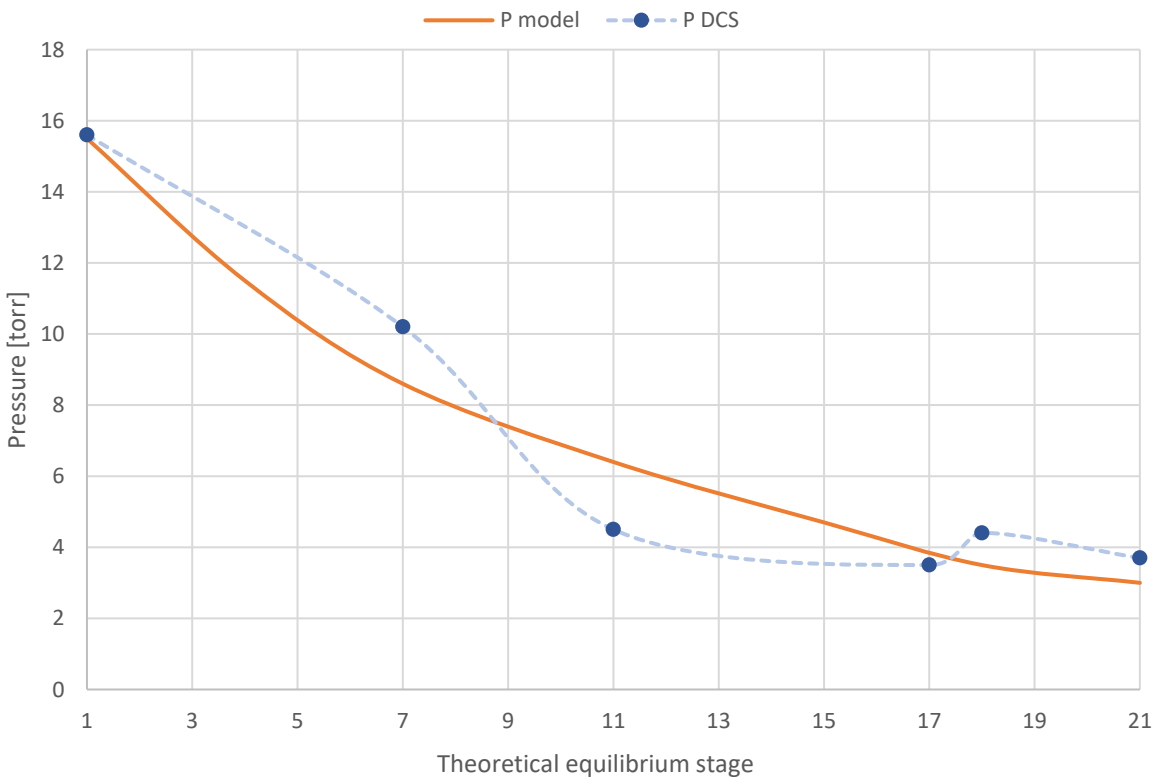

Figure 52: Pressure profile in the second case study

Products ASTM D1160 at the atmospheric equivalent temperature are reported in the following figures.

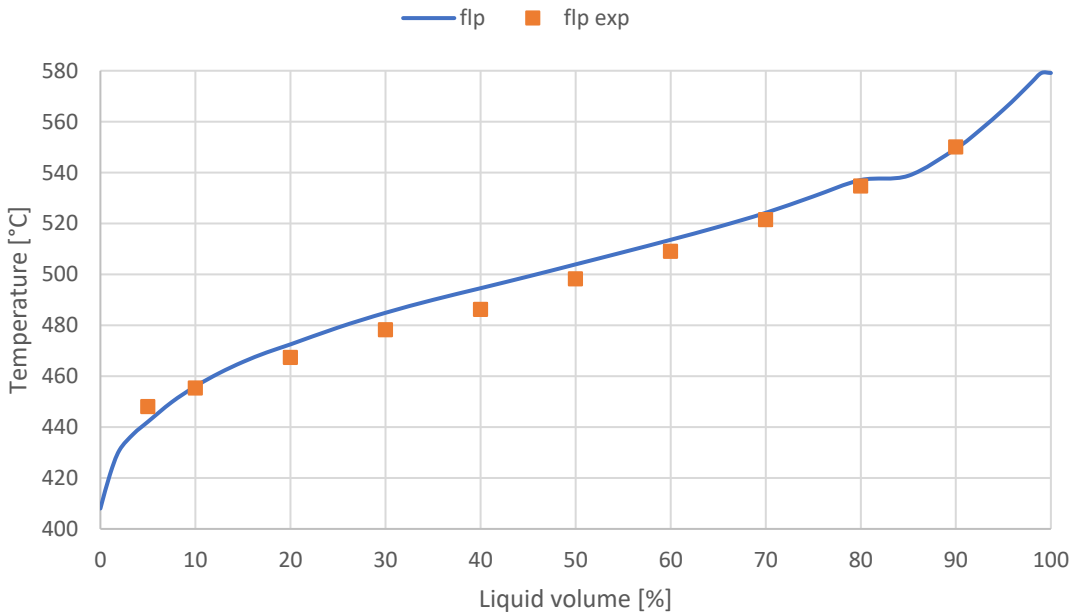

Figure 53: FLP's ASTM curves for case 1

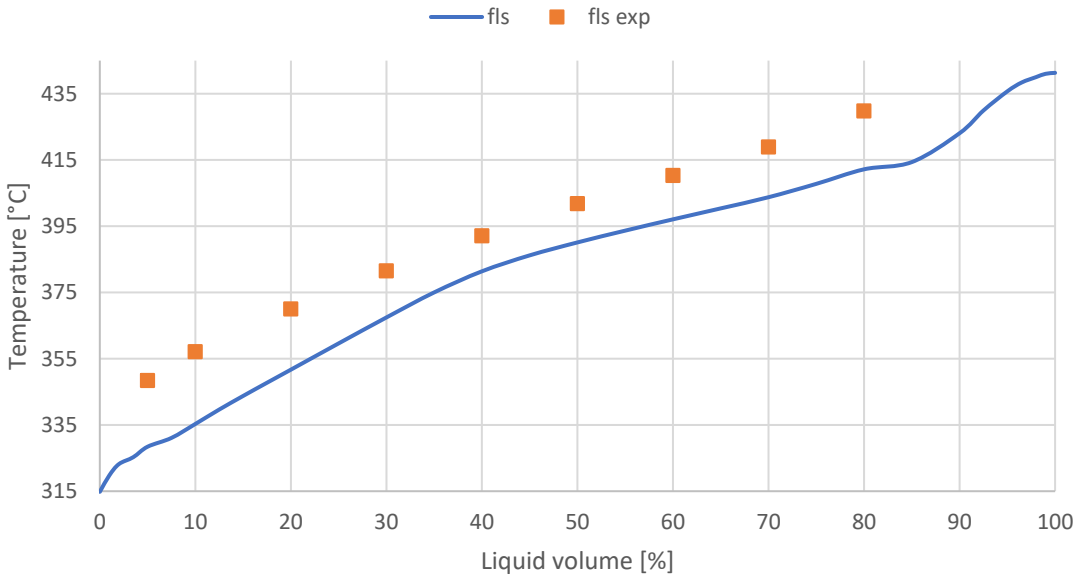

Figure 54: FLS's ASTM curves for case 1

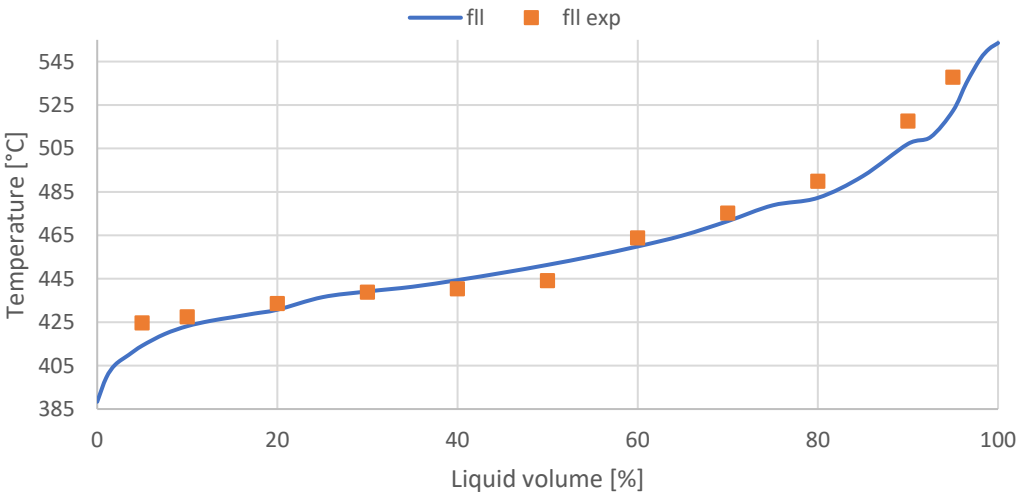

Figure 55: FLL's ASTM curves for case 1

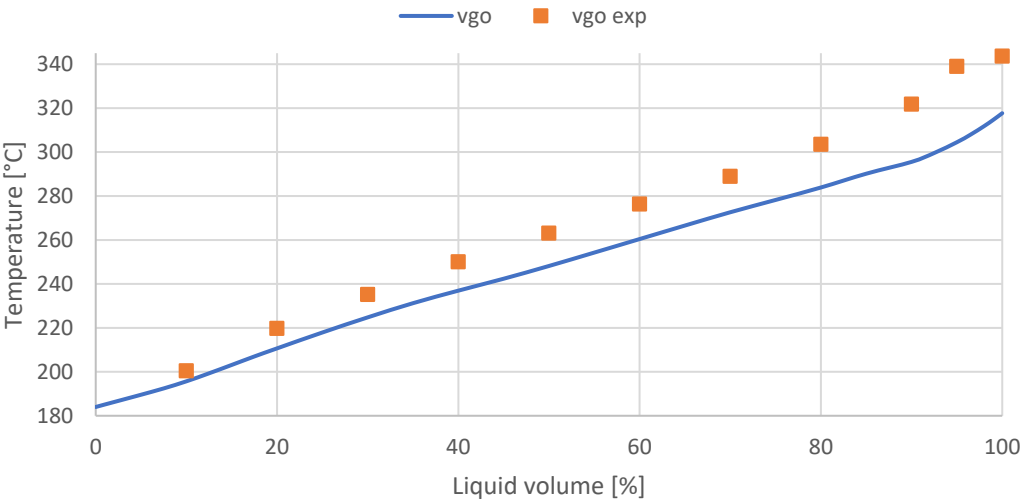

Figure 56: VGO's ASTM curves for case 1

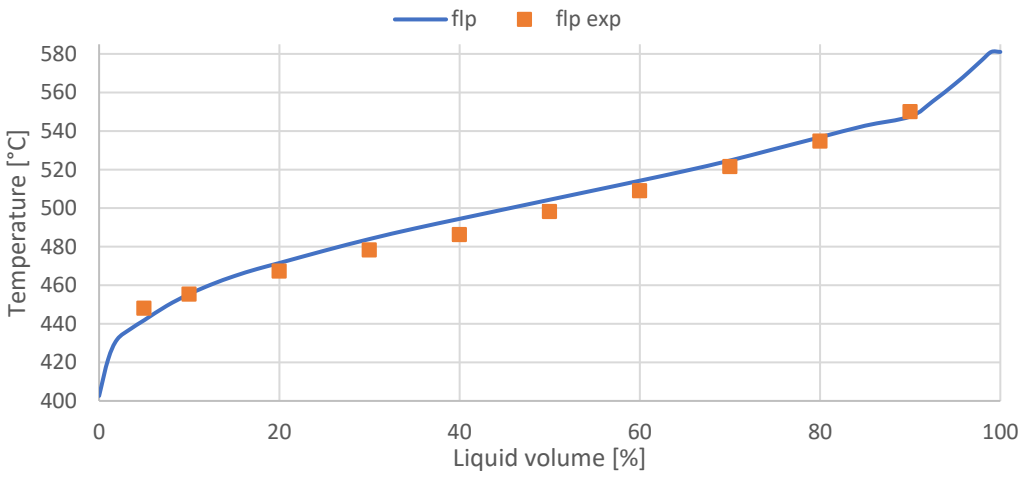

Figure 57: FLP's ASTM curve for case 2

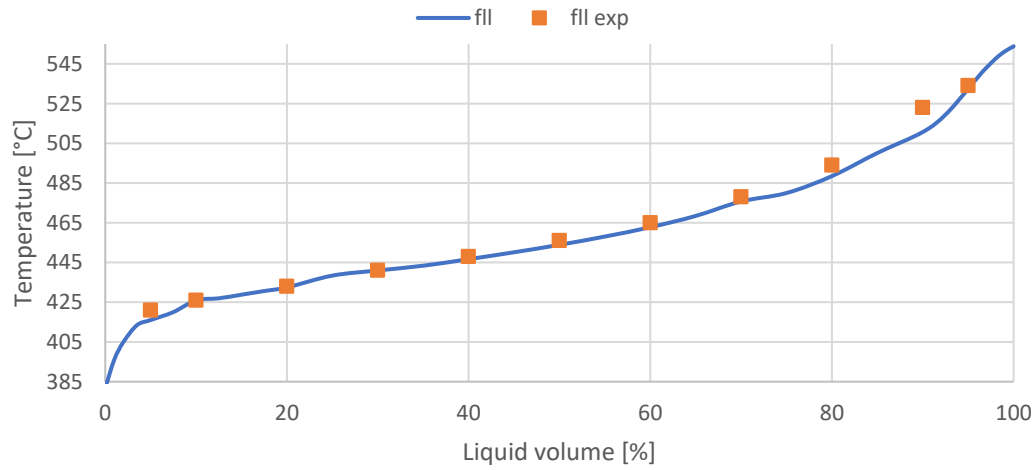

Figure 58: FLL's ASTM curve for case 2

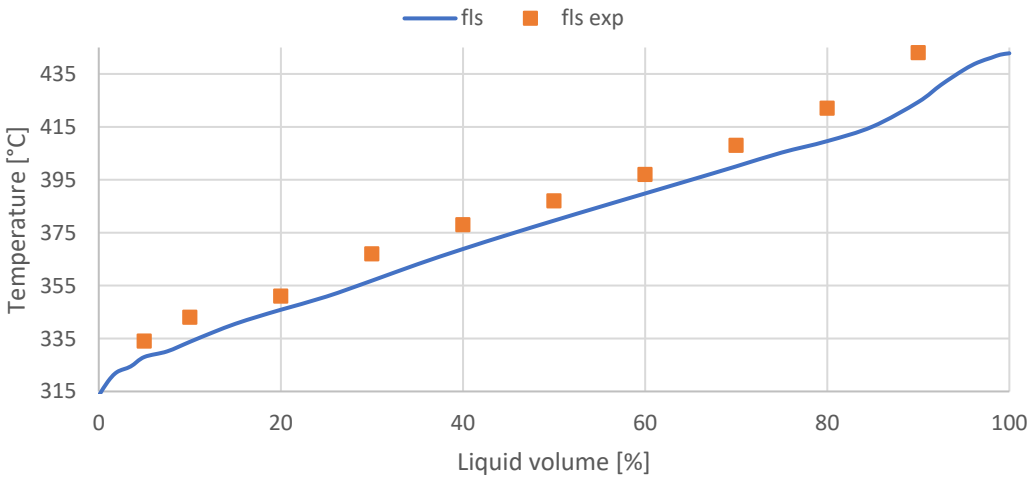

Figure 59: FLS's ASTM curve for case 2

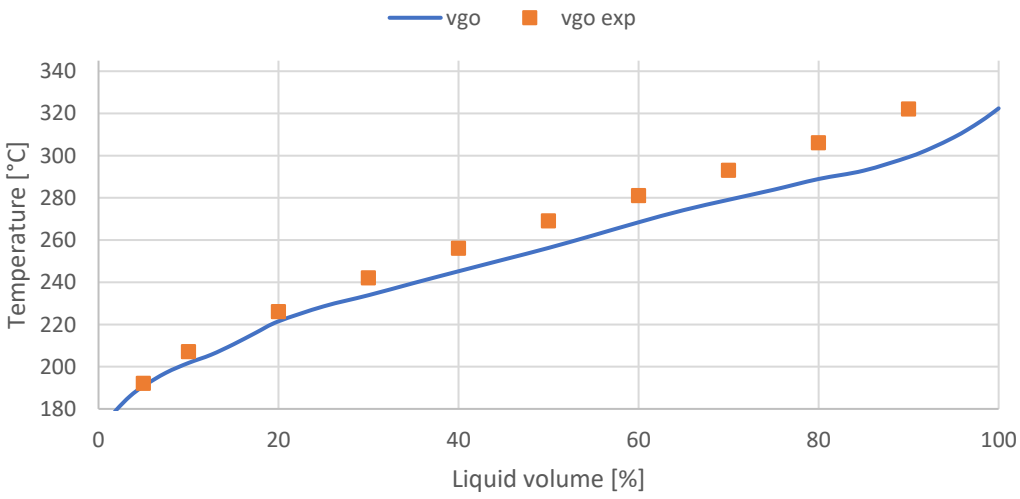

Figure 60: VGO's ASTM curve for case 2

As graphed, FLP and FLL curves are excellently predicted from the steady state model, while FLS and VGO show that the model predicts lighter products with respect to reality. Still, they are very similar to the real values thus are considered acceptable. Lastly, products transport properties are reported in Table 10, Table 11, Table 12, and Table 13. Experimental values were not furnished, so HYSYS's viscosities evaluated from the experimental ASTM curves are used.

Viscosity [cSt] at 40°C CASE 1	Industrial blend Bingham	Simulated Product Bingham	Industrial blend Sutton	Simulated Product Sutton
VGO	*1.7*	*1.8*	*3.3*	*3.5*
FLS	*13*	*10*	*17.2*	*13.5*
FLL	*40.3*	*36.5*	*41.6*	*39.5*
FLP	*72*	*78.4*	*71.8*	*74.7*

Table 10: Viscosities at 40°C of the products in the first case

Viscosity [cSt] at 100°C CASE 1	Industrial blend Bingham	Simulated Product Bingham	Industrial blend Sutton	Simulated Product Sutton
VGO	*0.8*	*0.8*	*1.7*	*1.8*
FLS	*3.2*	*2.7*	*5*	*4.1*
FLL	*6.2*	*5.9*	*10*	*9.7*
FLP	*9.1*	*9.6*	*16.1*	*17.3*

Table 11: Viscosities at 100°C of the products in the first case

Specific gravity at 15°C CASE 1	Industrial blend	Simulated Product
VGO	*0.805*	*0.808*
FLS	*0.863*	*0.856*
FLL	*0.884*	*0.883*
FLP	*0.898*	*0.899*

Table 12: Specific gravity of products at 15°C

Viscosity [cSt] at 40°C CASE 2	Industrial blend Bingham	Simulated Product Bingham	Industrial blend Sutton	Simulated Product Sutton
VGO	*2.2*	*2.0*	*4.0*	*3.7*
FLS	*11.5*	*9.9*	*15.1*	*13.1*
FLL	*42.6*	*39.8*	*45.5*	*43.3*
FLP	*69.9*	*84.5*	*71.1*	*75.4*

Table 13: Viscosities at 40°C of the products in the second case

Viscosity [cSt] at 100°C CASE 2	Industrial blend Bingham	Simulated Product Bingham	Industrial blend Sutton	Simulated Product Sutton
VGO	*1.0*	*0.9*	*2.0*	*1.9*
FLS	*3.0*	*2.7*	*4.6*	*4.1*
FLL	*6.5*	*6.3*	*11.0*	*10.6*
FLP	*9.2*	*10.1*	*16.6*	*17.8*

Table 14: Viscosities at 100°C of the products in the second case

Specific gravity at 15°C CASE 2	Industrial blend	Simulated Product
VGO	*0.813*	*0.81*
FLS	*0.86*	*0.856*
FLL	*0.887*	*0.885*
FLP	*0.9*	*0.9*

Table 15: Specific gravity of products at 15 °C

Transport properties are also well predicted from the model, due to the high resemblance with the experimental blend ones. Specific gravity presents a nearly null error for all cases, while viscosity showed some oddities. As introduced in chapter 2.3.2, Bergmann-Sutton's model is much less accurate than Bingham's at 100 °C. However, in this case, the viscosity of FLP at low temperature present high discordance with respect to the experimental values at 40 °C. This is due to the fact that heavy pseudo-components, which make most of the FLP composition, present a far bigger absolute value in viscosity than all other components (Figure 61 and Figure 62). Therefore, a very small variation in composition causes very big relative errors in the viscosity predictions. For instance, the composition difference in the first case study of the FLP cut, which has a sum square residual of:

$$SSR = \sum_{k=0}^{n} \left(x_{exp.blend,k} - x_{model,k}\right)^2 = 3.17E-3$$

results in a relative error in the viscosity prediction of about 20%. This error, while less accentuated, is still present also at high temperatures. However, here the performance of the Bingham is much better than the one of Sutton at high temperatures when compared to the industrial expected values of viscosity provided by Viscolube. As a general guideline, the Sutton correlation should be preferred at low temperatures, while the Bingham should be the go-to at high ones, with a general relative error of around 2-7 %.

2.7.2. VGO reflux sensitivity analysis

The top stage of the column is a key, yet problematic, topic. The model feasibility relies on the fact that the vacuum stream is negligible with respect to the packed column feed flowrate. In the plant this is accomplished by operating the top stage somehow more like a contact condenser than a packed bed, but this is not possible in Aspen HYSYS. Ideally, a custom model of this stage should be devised and implemented, but data to

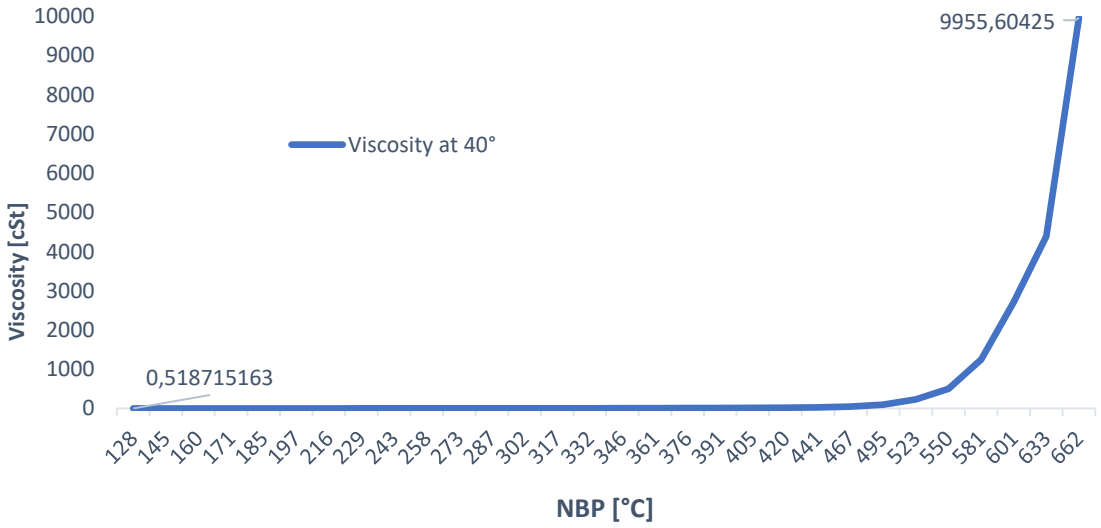

Figure 61: Viscosity [cSt] of pseudocomponents at 40 °C

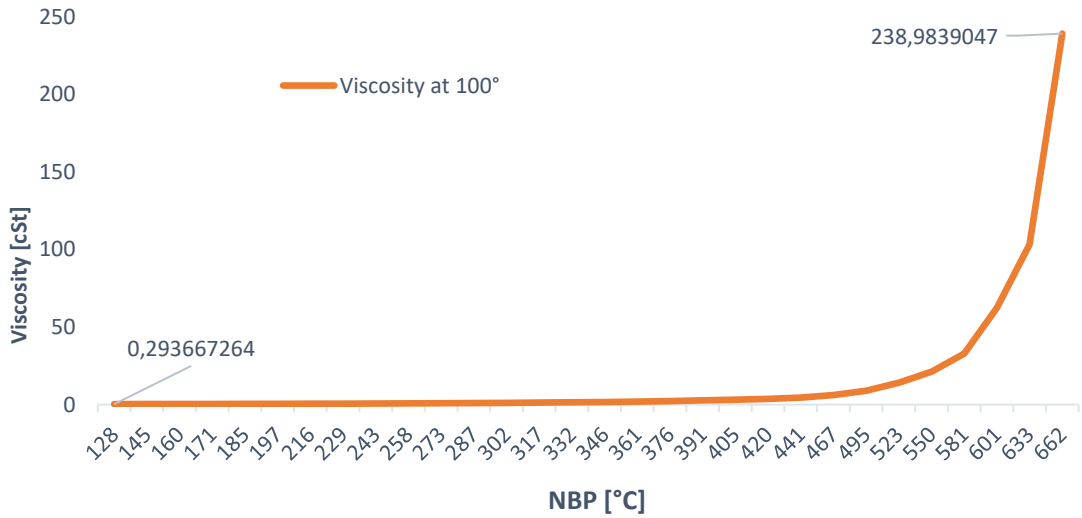

Figure 62: Viscosity [cSt] of pseudo-components at 100 °C

do so

were not available. Moreover, considering than VGO is a side product for the TDA column, unless the lubricant cuts were to be negatively influenced by the bad performance of this section an accurate prediction here has low priority.

Nonetheless it is necessary to verify if the model is respecting the hypothesis made and behaving properly without having negative effects on the other stages. For this purpose, a sensitivity analysis on the VGO reflux rate was carried out.

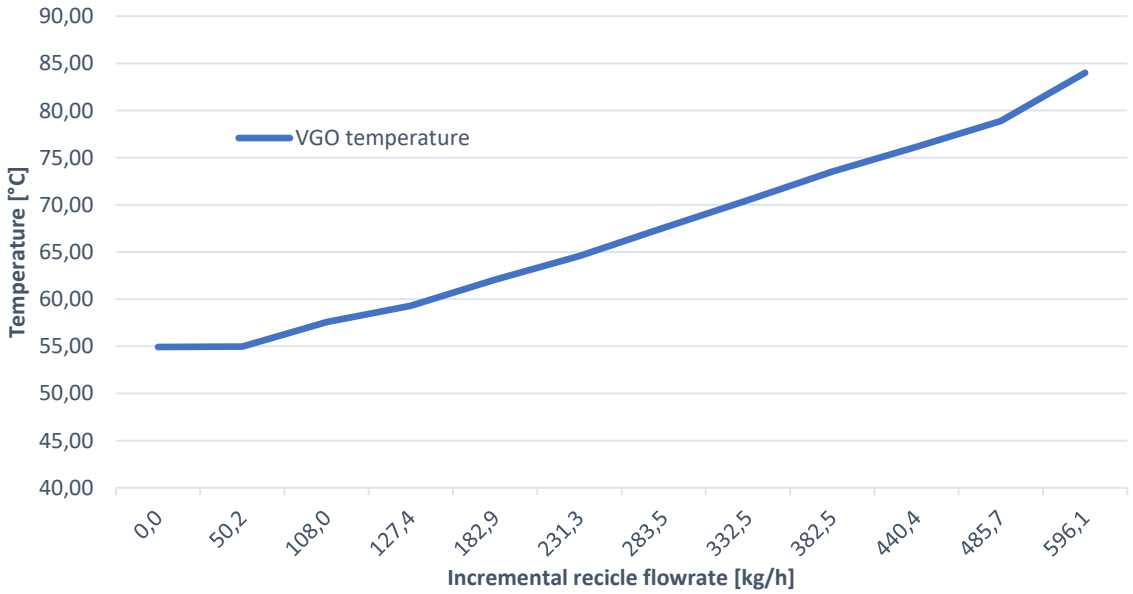

Figure 63: Temperature of the VGO change once the reflux rate is increased by x

The reflux flowrate was raised with respect to the stationary value by decreasing the amount of withdrawn VGO product.

By rising the reflux flowrate, the cooling duty of the column is raised and therefore the compounds on top of the column will become heavier. This will result in a rising temperature on the VGO withdrawal stage and the ones above it. The situation is different for the stages below, the incremented reflux will lead to a higher presence of light compounds with a normal boiling point similar to VGO in the column. For the stages below the VGO one these are lighter compounds and thus the temperature in those stages will decrease. The effects will be more and more mitigated in lower stages.

Since less VGO is now withdrawn the quantity of light components in the column will rise and, since these components cannot condense, they will leave passing through the vacuum group and this will rise the mass flow rate of the vacuum group. As it can be seen in stationary conditions the flow rate to the vacuum group is negligible (7.75 kg/h over 12 470 kg/h making for less than 0.06% of the feed), but as the reflux rises so does the flowrate to the vacuum. By incrementing the reflux by about 600 kg/h what was considered the threshold above which the hypothesis of negligible flowrate is no more valid is reached (274 kg/h, about 2% of the feed).

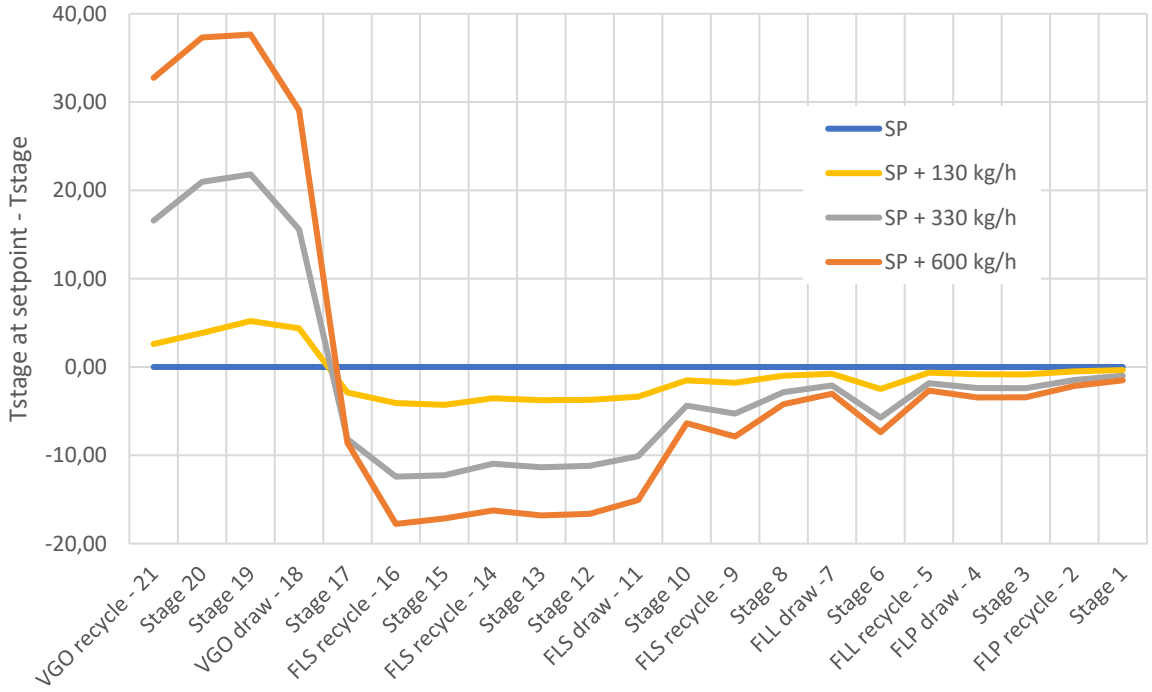

Figure 64: Temperature variation of each stage due to different increments of reflux

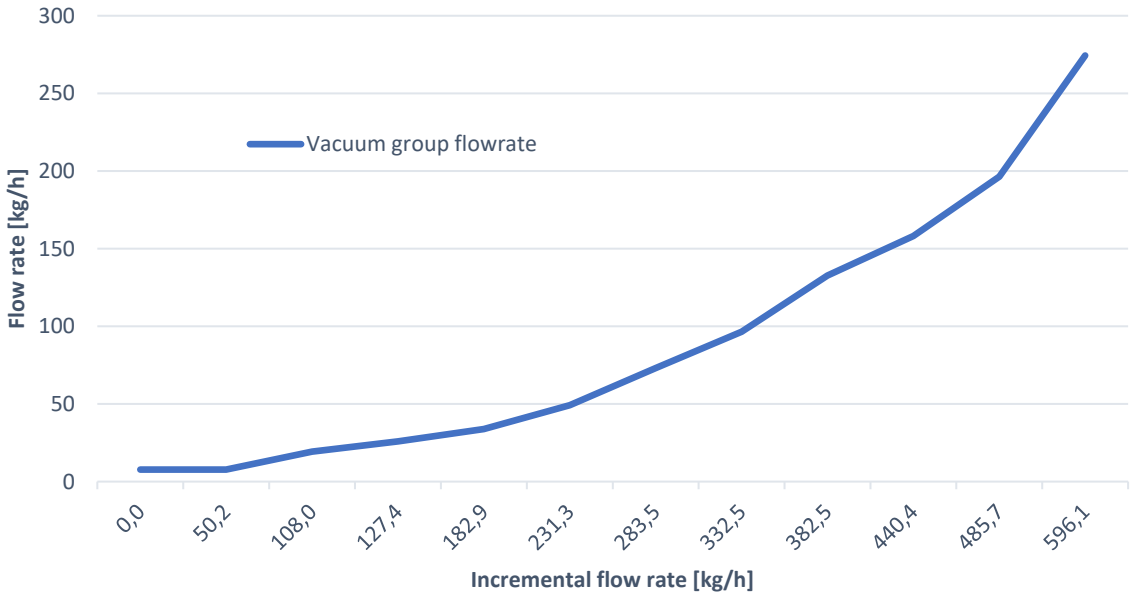

Figure 65: Flowrate to vacuum after step variations in the reflux rate

Despite the limitations the model has in dealing with the top of the column the behaviour of the VGO stage is in accordance with the physics of the system, being able to reasonably predict the composition of vacuum gasoil, while keeping true to the hypothesis of negligible vacuum flowrate within a relatively wide range of reflux rates.

2.8. Conclusions

A stationary model for a vacuum distillation column is built using HYSYS's steady state simulator and successively validated. Initially, lubricant blends properties are characterised using HYSYS's and external correlations for viscosity. Such correlations are implemented in VBA for Excel to have a more direct method to evaluate the products viscosities.

Using the preflash experimental operative conditions, a proper thermodynamic model is selected from a shortlist compiled after an accurate bibliographic research. Validation is carried out by confronting the experimental and simulated TBP curves.

The presence of cracking in the furnace was noticed due to extremely low boiling temperatures profiles in ASTM curves, with respect to the furnace inlet. This required a proper estimation of the column's cracked feed. For this purpose:

- The cyclone is approximated to a flash and the furnace outlet is reconstructed, starting from the available cyclone's vapor outlet. Unfortunately, a proper validation is not possible, due to lack of information regarding the furnace outlet stream data;
- The stream is reconciled using the cyclone vapor outlet, reconstructed considering a combination of the outlet products. Such operative unit is treated as a flash and, knowing the extent of vaporization, temperature and vapor stream composition, the feed is reconstructed.

The reconciled feed is used to carry out a simulation, which is self-consistent with the cyclone and the column product.

Pressure profile of the column also needed to be acquired to build an external model which can keep into account the feed flow rate and column fouling. This is even more necessary since the DCS showed pressure's unphysical behavior. The industrial data from several operating conditions are considered and used to customize two models, one of which accounted also for the dirtiness of the packings. The models are compared and the best one is implemented in the simulation.

Two case study are presented, one of them was mainly used to model the column while the other for validation. Both show good accordance with the on-field plant, regarding predicted operative conditions and products characteristics. Unfortunately, modelled the column top pack does not exhibit good accordance with experimental values. This precludes studies about its behaviour and, possibly, on the ejector group.

Finally, the column top behaviour is analysed by means of a sensitivity analysis on the reflux flow rate of VGO.

2.9. Future developments

The static model is proved to be valid and it can be used for several purposes, though some improvements are possible. Such enhancements are:

- A custom-made simulation of the furnace to better analyse its behaviour. This, together with an accurate chemical kinetic scheme involving the blend species, may be used to better characterise the column feed and build an external model for the cyclone as well. If a kinetic scheme could not be built, a sampling of the furnace outlet and its deep characterisation would permit the prediction of the exact column feed;
- The development of a standalone model of the top stage to properly predict its behavior, which requires a rigorous non-equilibrium ad hoc description;
- The development of the ejector group by means of an external model.

The model potentials are also listed. To better identify products quantities and viscosities by changing operative conditions, a sensitivity analysis on the refluxes mass flow rate and temperatures can be performed. This may help on field operators to identify the right values of controllers set point for different sets of demanded products.

A steady state economic optimization can also be done. This feature can be both performed using HYSYS's optimization tool, or by means of an external optimizer which can take into account also the products physical properties, maximizing the following objective function:

$$f_{profit} = \sum reveneus - \sum costs + \sum w * (property^{model} - property^{required})^2$$

Lastly, on-line data reconciliation can be performed. This may allow to check measures, evaluates non-measured data and identify unfeasible values. In this case, an external model communicating with HYSYS is needed, which receives the DCS's measures as input. These data are inputs for an optimizer, which provides the results as initial guess for HYSYS, which re-evaluates the variables and provides them to the optimizer again, until the differences between the last two calculation cycle reconciled data are small enough, as set by the user. The optimizer should minimize the following objective function f:

$$f = \sum \left(variable^{model} - variable^{measured}\right)^2 + \sum z * g(variables) + \sum l * h(variables)$$

where g are penalty functions, which are steady state mass, momentum and energy balances as a function of the variables, h are also penalty functions that instead keep into account variables physical limits, for example Temperature(K)>0, while l and z are penalty coefficients.

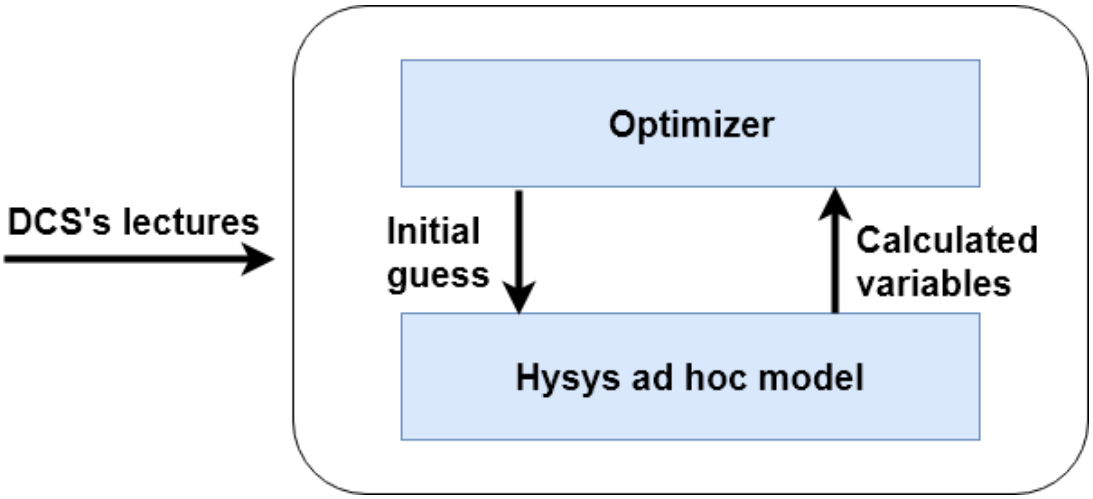

Figure 66: Scheme of data reconciliation process

3. Dynamic Model

The second part of this thesis concerns the development of a dynamic model for the TDA column and its apparatuses. Though it would have been functional to develop such a model on HYSYS, to have both the stationary and the dynamic aspect of the column on the same program, inefficiencies in it forced us to adopt a different solution. In fact, as the dynamic simulation on HYSYS started, the pressure on the last stage of the column reaches values in the order of 10^8 torr in a few seconds, with no apparent reason and despite the fact that the feed enters the column at a pressure of indicatively 20 torr. This causes the simulator to crash. Since the problem could not be solved even by Aspentech assistance, it was decided to develop the model on the dynamic simulator DynSim.

3.1. Input data for the dynamic model

The dynamic model of the TDA column requires two different typologies of input data:

- The data concerning the thermodynamic aspects, which include all the information in the stationary model. It applies to components and flows characterisation, number and arrangement of equilibrium stages and column stage efficiencies. Such data were imported from HYSYS and implemented on DynSim, then a thermodynamic validation was performed using HYSYS as a reference;
- The data concerning geometrics, controllers parameters, battery limits conditions and equipment features which include pumps characteristic curves and valves CV. Such data are provided by Itelyum. Unfortunately, not all data was available. In such cases, necessary piece of information is extrapolated from HYSYS. Geometric data are not reported in this thesis, respecting data protection and industrial secrecy of Itelyum.

3.2. Hypothesis on the equipment

Even regarding the dynamic model, some hypotheses are included:

- All column stages are at equilibrium. A kinetic parameters approach could not be developed since it is not a feature included in DynSim's column equipment;
- Pieve Fissiraga plant includes two furnaces, a convective and a radiative one. It was asked to implement only the convective one since the radiative is about to be removed. This furnace is implemented as a simple process-process heat exchanger, whose heat duty is supplied by hot air at a temperature of 760 °C and 1 atm, assumed as a mean value of the combustion chamber one. Such a model is an approximation, since a detailed one should have followed a strict

geometric scheme and simulated a temperature gradient inside the furnace chamber.

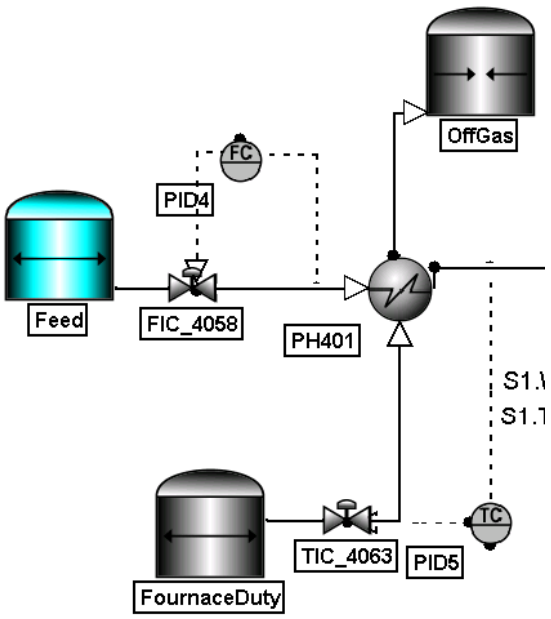

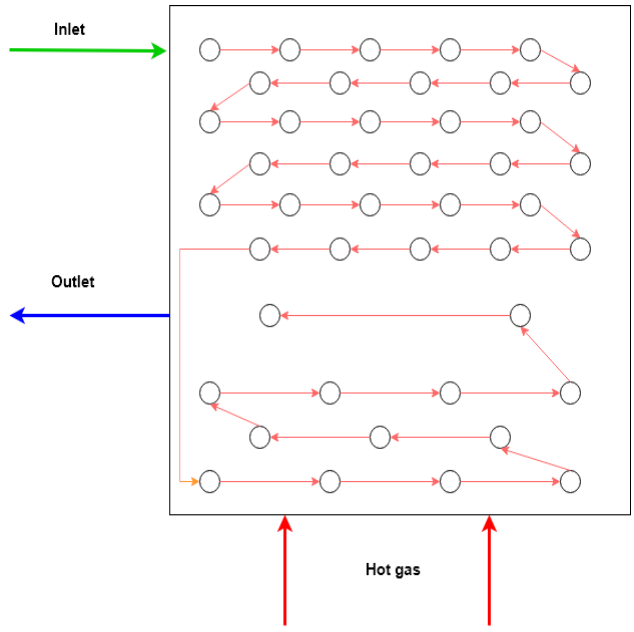

Figure 67: Furnace in the DynSim model *Figure 68: Real convective furnace scheme*

Such a simplification does not penalize the TDA's model, since the only parameter which this furnace influences is the outlet temperature, which is a controlled variable;

- The vacuum group is not fully implemented. Instead, a sink preceded by a fictitious valve, with a CV of 1000, is displaced. The sink pressure value is set at the column top pressure of 3 torr, as in the static model. A different approach was tested, implementing the first part of the vacuum group, constituted by an ejector and a 2-liquid separator. However, this detail did not improve the quality of the prediction and slowed down the program calculations considerably. It was decided to keep the simplest vacuum scheme;

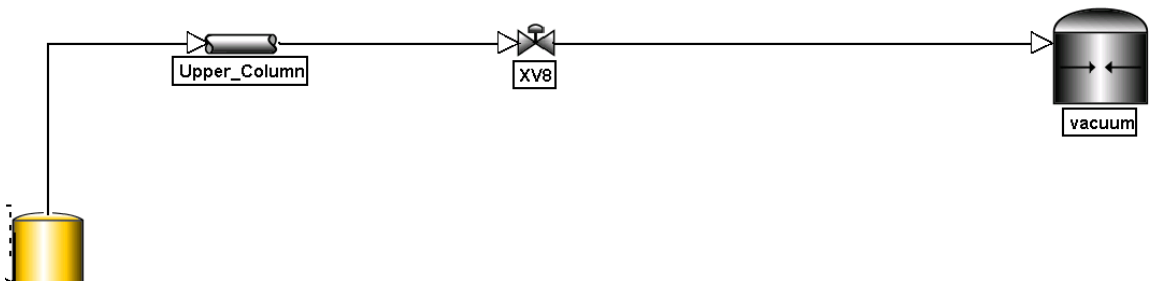

Figure 69: Vacuum group simplified implementation

- The controllers parameters furnished by Itelyum lack of units of measurements. In fact, inserting them in various controllers in the model, they oscillated or did not react, depending on the units of measurements that were chosen. Finally, it was decided to divide the proportional gain (Kc) value by 100. This provided

good accordance with the plant controllers responses, as shown in the dynamic validation;

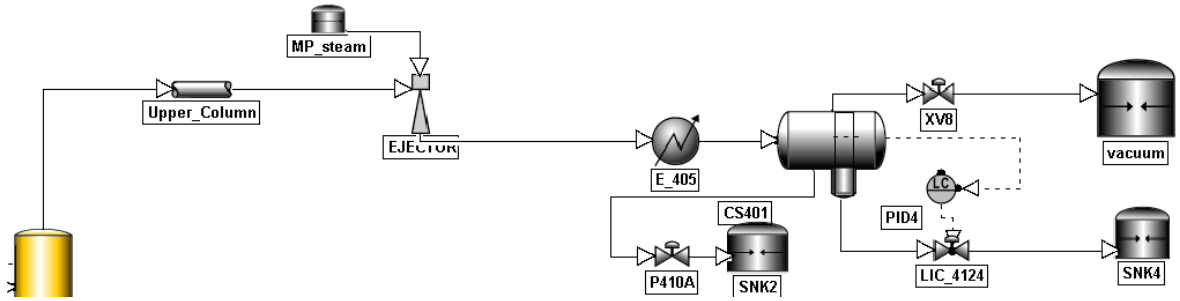

Figure 70: Vacuum group detailed implementation

- The cyclone is implemented as a flash;
- Pumps are implemented as centrifugal, connected to a motor. Though the cyclone LIC is regulated by a volumetric pump, whose feature is not present in DynSim, it was decided to implement it as a centrifugal pump followed by a fictitious valve, which regulates the liquid flow rate. The valve CV is assumed to be 100. Ramps of motors are left untouched, with a time to ramp of 3 seconds. Shaft speeds were left at 3600 rpm;

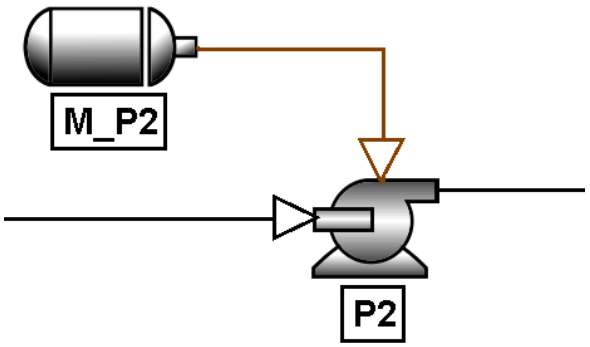

Figure 71: Basic pump implementation

- Column P&I is not strictly followed. Bypasses, units in parallel and lines which are not operative during operative and planned transient operations are not implemented.

3.3. Limits

The dynamic simulator DynSim focuses on the prediction of plant's unit operations in standard transient conditions but lacks information about the interaction with the external ambient and mechanical properties of the equipment itself. Moreover, modelled units and boundaries intrinsic limitations together with the simplifying hypothesis introduced may weaken the reliability of the results and the simulation potential. Details and possible consequences are reported:

- Since thermal and mechanical stress are not accounted in DynSim, damages that can be caused by extremely fast transient cannot be simulated. This constriction forces the users to investigate catastrophic scenarios such as the column collapse to depressurization or the furnace overheating separately.

Trusting blindly the simulation results may be harmful to the plant and the personal involved;

- Peculiar aspects during plant operations cannot be observed. The most important are air leakages, water accumulation during the column cleaning which can remain stagnant before the Startup and accumulation of solid particles. All these issues need to be investigated separately;
- Column dirty factor cannot be intrinsically represented as a time varying parameter in the model. However, vapor flow conductance and specific surface per unit volume of the packing can be modified, as discussed in the chapter dimensioning;
- DynSim requires battery limits conditions. These conditions, such as temperature, pressure or flow composition, are however static. The influence of units upstream and downstream the column is considerably limited due to their dynamic behaviour which may cause unforeseen, unpredictable consequences;
- DynSim has a feature which permits to simulate simple malfunctions, for example valves fail or pumps shut downs. The lack of bypasses and lines operative in such cases do not permit to analyse consequences and responses in such scenarios;
- Furnace simple design does not permit to analyse its real behaviour. Consequently, utility costs optimization and safety analysis cannot be performed. Moreover, as in the static model, a kinetic model for the crack is not developed. Though this may not influence the column performances during normal conditions, the column feed may not be reliable during furnace's transients;
- The flash which substitute the cyclone posed at the column base proved to be in good accordance with the plant results during standard operative conditions. However, the cyclone separation's efficiency strictly depends from the entering feed velocity which may drop dramatically with low feed's volumetric flow rate Q. Efficiency regards heaviest asphaltenes, which can be represented as particles with diameter D_p:

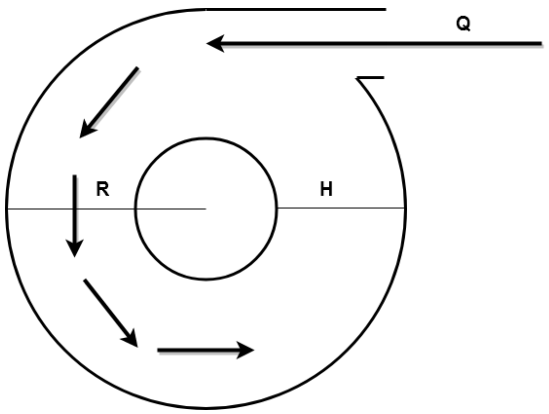

Figure 72: Cyclone entrance as seen from above

$$\varepsilon_{cyclone} = \frac{N\ particles\ collected\ on\ the\ bottom}{N\ particles\ entering}$$

$$D_{p\ minimum} = \sqrt{\frac{9 * \mu_g * B * H^2 * R}{\rho_{solid} * \pi * N_{rounds} * Q * (R - H)}}$$

but also regards evaporations, since the mass transfer coefficient is influenced by velocity. This may cause inconsistencies during the first steps of Startups and the last steps of Shutdowns;

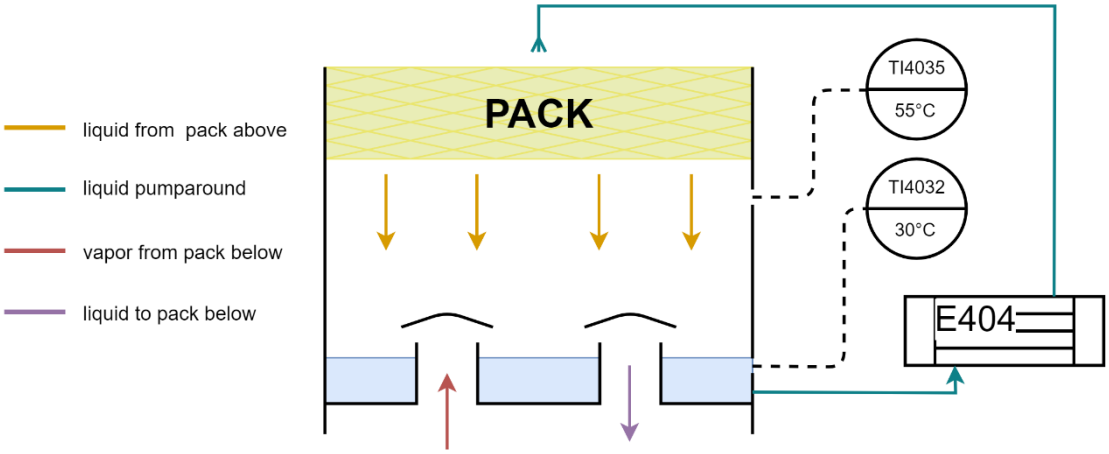

Figure 73: Sixth pack with its pumparound

- Since all column stage are at equilibrium, vapor and liquid temperatures are identical. This, as already discussed, is not true in practice, especially on column top stage. This significant difference, which comports all the consequences that were discussed for the steady state and may be even more critical for the dynamic simulation. In fact, a liquid temperature equal to the stage's one may influence the exchanger efficiency, which may not be able to properly cool down the reflux. However, this is not the case, since E-404 is designed for higher flow rates and temperatures than the plant usually adopts;
- Since the ejector group is not fully implemented, considerations about it cannot be done. For example, the maximum flow rate to the ejector and its efficiency cannot be discussed;
- As will be properly discussed chapter Dynamic model thermodynamics, DynSim could not properly predict blends viscosities and specific gravity (SG). This issue makes the program unreliable in predicting those properties which are of primary importance under the products quality point of view.

3.4. Thermodynamics

Blends which are implemented and used in HYSYS need to be re-implemented in DynSim. Since their reconstruction from ASTM curves provided good results in Aspen's simulator, the same method is adopted using DynSim. Also, all thermodynamic packages used in HYSYS are re-adopted, which are the Peng-Robinson as the equation of state, the Rackett method to calculate liquid density, the extended Twu method for the evaluation of MW and the Twu method for critical temperature and pressure and acentric factor. However, characterisation is not a straightforward procedure, since differences between the two programs are present in this sense. While the equation of states and transport properties packages are the same, pseudo components in DynSim, which are used to build up the blends, are different from the ones present in HYSYS. Moreover, the dynamic simulator does not present the Hariu-Sage method for the SG characterisation. To compensate such lack, SG from HYSYS has been used in DynSim to better characterise the blends. Nevertheless, it will be shown that this lack still strongly influences the density prediction and consequently the viscosity value estimated by the Bergmann-Sutton. Moreover, since DynSim's pseudo components do not present their own viscosity value, the Bingham method cannot be used.

DynSim's resemblance with reality will be clarified by comparing the simulation results with HYSYS. For this meaning, the preflash unit model of the plant is once again used. Thermodynamic data inputs are still the ASTM D1160 curves provided by Viscolube and already used in HYSYS's thermodynamic validation. However, new elements needed to be added, which are the controllers, the heat exchangers utility and conductances, valves CV, flash and the vessel with weir's geometrics. The preflash unit's results are taken only when steady state conditions are reached.

Lastly, since DynSim requires a higher computational effort with respect to HYSYS, several proves have been done changing the number of cuts constituting the blends. The idea is to use the less pseudo components as possible, without penalizing numerical results.

3.4.1. Preflash

The preflash in DynSim presents the same conditions as in HYSYS. The inlet, as indicated by Viscolube, is once again composed by 89% in weight of the flash's outlet, 8% in weight from water and 3 % in weight by styrene as general component representing the solvent. Such streams are generated by three different sources at 110 °C and 2 bars, which represent the outlet conditions from the heat exchanger E-311 set before E-312 in the plant.

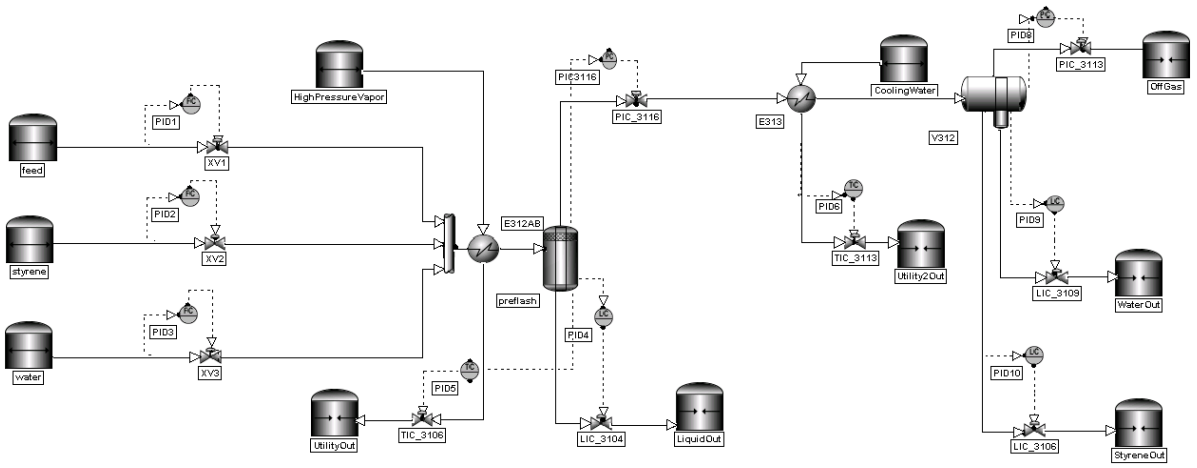

Figure 74: Preflash flowsheet in DynSim

The exchangers geometrical parameters have been inserted, and the total heat transfer coefficients and conduction coefficient have been calculated and implemented in the model. Concerning the heat transfer coefficients U, the following simple relation has been used, using HYSYS as a reference for the heat flow value:

$$U = \frac{Heat\ Flow}{Surface * \Delta T_{ln}}\ [\frac{W}{m^2 K}]$$

The E-312's utility is constituted by condensing high pressure vapor at 14 bars, at about 200 °C, so the utility side temperature is considered constant. The resulting U coefficient is equal to 23.2 W/m^2/K. The E-313's utility is instead constituted by water which heats up from 25 °C to 37 °C, cooling the vapor out of the flash vessel down to around 50 °C. The resulting heat transfer coefficient is 141.6 W/m^2/K.

The flow conductance K_J is calculated as:

$$K_J = \frac{Flow}{\sqrt{\Delta P * \rho_{fluid}}}\ [\frac{\mathrm{kg}}{\mathrm{s} * \mathrm{sqrt(kPa * kg/m3)}}]$$

The pressure drops DP are calculated using the geometrical data from Viscolube and the fluid data from HYSYS's simulation. The data from the currents are reported in the table below. The mean values of density and viscosity have been taken in consideration.

Exchanger	ρ [kg/m3]	μ [Pa*s]	Velocity [m/s]	Reynolds
E-312	3.3	1.03E-5	19.62	119809.3
E-313	468.7	42.22E-5	0.14	3011.8

Table 16: Flow rate transport properties through heat exchangers at nominal conditions

The data provided by Viscolube are listed in Table 17.

	Symbol	E-312	E-313
N tubes [-]	Nt	254	245
Length [m]	L	4.88	4.88
Tube Diameter [m]	Dt	0.01905	0.01905
N passes [-]	Np	3	2
Utility type	-	Steam	Water
Process fluid side	-	Tube	Tube

Table 17: Heat exchanger data

Process fluids are tube side, so the following correlation has been considered:

$$Dp = Np * \left(\rho * \frac{v^2}{2} * 4 * f^* * \frac{L}{Dt} + 2.5 * \rho * \frac{v^2}{2} \right) [Pa]$$

Where f^* is the friction factor, calculated as:

$$f^* = 1.2 * 0.048 * Re^{-0.2}$$

The results are 15.597 kPa for E-312 and 0.138 kPa for E-313, which lead to tube side K_J values of 4.83 [kg/s/sqrt(kPa*kg/m^3)] and 4.75 [kg/s/sqrt(kPa*kg/m^3)], respectively. Shell side K_J values are set to 100 [kg/s/sqrt(kPa*kg/m^3)], due to the lack of data concerning utility flow rates.

Some of preflash valve CV are provided. Between those which are not, process side valves are dimensioned using HYSYS, while utility flow valves' CV using DynSim.

Valve	CV	Provided
TIC-3106	0.3	No
TIC-3113	28.5	No
PIC-3113	86.2	Yes
PIC-3116	306.5	No
LIC-3104	500	No
LIC-3106	2.1	Yes
LIC-3109	5.3	No

Table 18: CV of the valves

Fictitious feed valves are also needed to be dimensioned. Their CV are 80, 7 and 110 for the lubricant, the styrene and the water flow respectively.

Finally, the controllers parameters are inserted. As for the column, K_c values provided by Viscolube are divided by 100.

Controller	Controlled variable	Manipulated variable	Kc	τi [s]
TIC-3106	Flash temperature	Actuator position	0.8	20
TIC-3113	V-312 temperature	Actuator position	1	20
PIC-3113	Flash pressure	Actuator position	1	20
PIC-3116	V-312 pressure	Actuator position	0.5	10
LIC-3104	Flash liquid level	Actuator position	1	200
LIC-3106	V-312 organic liquid level	Actuator position	0.6	70
LIC-3109	V-312 water liquid level	Actuator position	0.5	50

Table 19: Controller characteristic parameters

3.4.2. Results and discussion

Different cut sets are used and validated, for two different feeds, blend 1 and blend 2. The first test is done using the same number of pseudo-components as HYSYS' preflash simulation, which are 31, and the same pseudo component distribution in terms of normal boiling points of the components. Since small discordances was noted in the outlets' compositions, the pseudo component distribution was changed. More components in the normal boiling point range where the molar fraction is higher were used. The reason behind this approach is attributed to the fugacity balance. Since those are linked through components fractions as:

$$\Phi(T,P,y)_i^v * y_i = x_{i*}P(T)_i^0 * \Phi(T,P(T)_i^0)_i^v * \gamma(T,P,x)_i^l$$

it is likely that increasing the blends characterisation where, quantitatively, most of the components are, the results improve. The cuts component distribution is done as follows, for three cut sets constituted by 11, 15 and 21 components, using the molar fraction of components calculated by HYSYS:

$$Ncomponents = Molar\ Fraction\ in\ NBP\ range * Total\ components$$

The results are listed in Table 20.

NBP range	**200-425 °C**	**425-600 °C**	**600-750°C**
Molar fraction of components from HYSYS	0.386	0.545	0.069
HYSYS's cut	15	6	4
Constructed cut, 11 components	3	6	2
Constructed cut, 15 components	5	8	2
Constructed cut, 21 components	8	11	2

Table 20: Pseudo-componenents for each range of temperature

Observing Table 20, this approach improved the simulations results slightly. The results for feed blend 1 and feed blend 2 are listed in Tables 21 and 22, together with the used cuts that are HYSYS' s 31 components and the constructed 11, 15 and 21 components cut sets.

	HYSYS results	HYSYS's cut	11 components	15 components	21 components
Flash T [°C]	140	140.1	140.3	140.3	140.1
Flash P [torr]	380	380	380	380	380
x^{l}_{h2o}	0.0031	0.0043	0.0035	0.0035	0.0035
$x^{l}_{styrene}$	0.0182	0.026	0.0204	0.0204	0.0204
MW [g/mol]	445	445	446	445	445
API	27.3	25.3	25.3	25.3	25.3
Recovered liquid [%]	88.9	89.2	89.1	89.2	89.1

Table 21: Results for blend 1

As shown in Table 23 and Table 24, adopting the constructed cuts, flash liquid outlet composition's results slightly improve, while decreasing the total number of components the results show almost no changes. Other values like molecular weight (MW), instead, are almost constant for every cut set. However, great discordances are present concerning the API gravity, and consequently the SG value. The error which DynSim introduces is of the order of 7% in density predictions at 15 °C. This value tends to 0 for temperatures above 140 °C. Since the Bergmann-Sutton method for viscosity predictions uses as input the specific gravity, an error is expected. The values of viscosity for the preflash liquid have been calculated.

	HYSYS results	HYSYS's cut	11 components	15 components	21 components
Flash T [°C]	140	140.1	140.2	140.3	140.3
Flash P [torr]	380	380	380	380	380
x^{l}_{h2o}	0.0031	0.0041	0.0036	0.0036	0.0036
$x^{l}_{styrene}$	0.0185	0.021	0.0198	0.0199	0.0199
MW [g/mol]	423	424	425	424	424
API	28.4	27.3	27.3	27.3	27.3
Recovered liquid [%]	88.9	89.4	89.2	89.2	89.2

Table 22: Results for blend 2

	Blend 1 viscosity [cP]	Blend 2 viscosity [cP]
HYSYS, 40 [°C]	54.7	41.8
DynSim, 40 [°C]	80.9	54.8
Error, 40 °C [%]	48	30
HYSYS, 100 [°C]	12.9	10.3
DynSim, 100 [°C]	19.9	12.9
Error, 100 °C [%]	49	25

Table 23: Viscosity values for HYSYS and DynSim according to Bergmann-Sutton equation

The error introduced by DynSim has great influence on viscosity. Unfortunately, this makes DynSim not suitable to determine the products quality, being viscosity one of the most important indicator used in the lubricants production sector.

Lastly, ASTM D1160 curves between the simulated lubricant inlet, which is built from the experimental preflash outlet, and the simulated preflash outlet are compared. Since curves remain identical changing the cut sets, only one DynSim curve for each blend will be reported in the graphs, which are ASTM plots and their parity plots. Note that both curves are generated by DynSim.

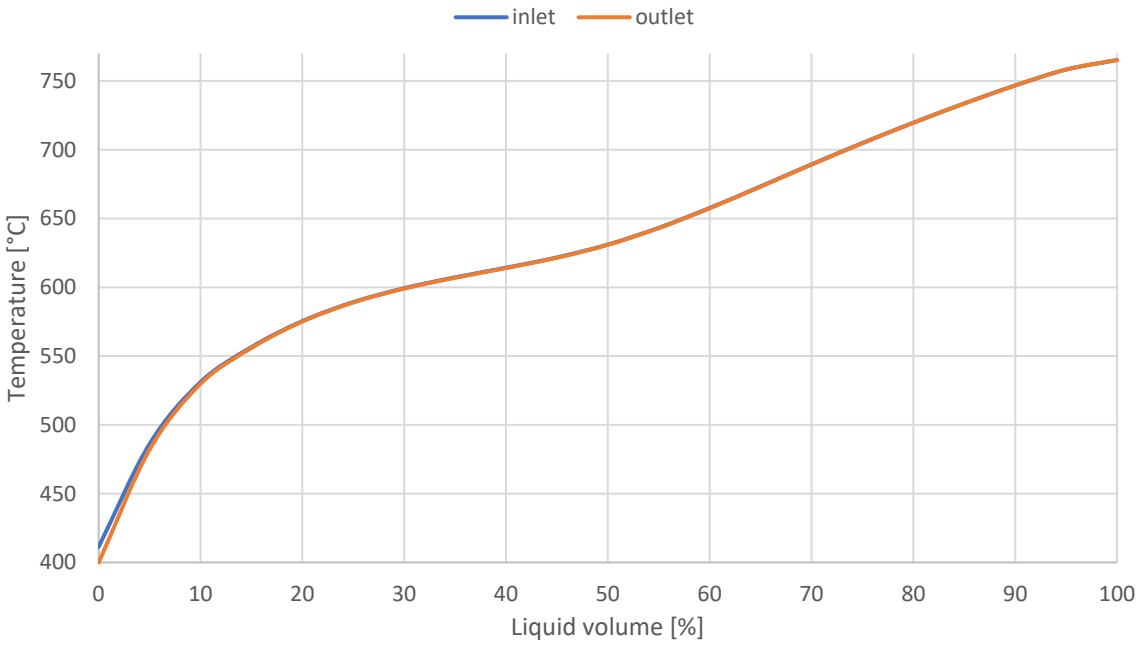

Figure 75: Blend 1 flash inlet and outlet ASTM plot

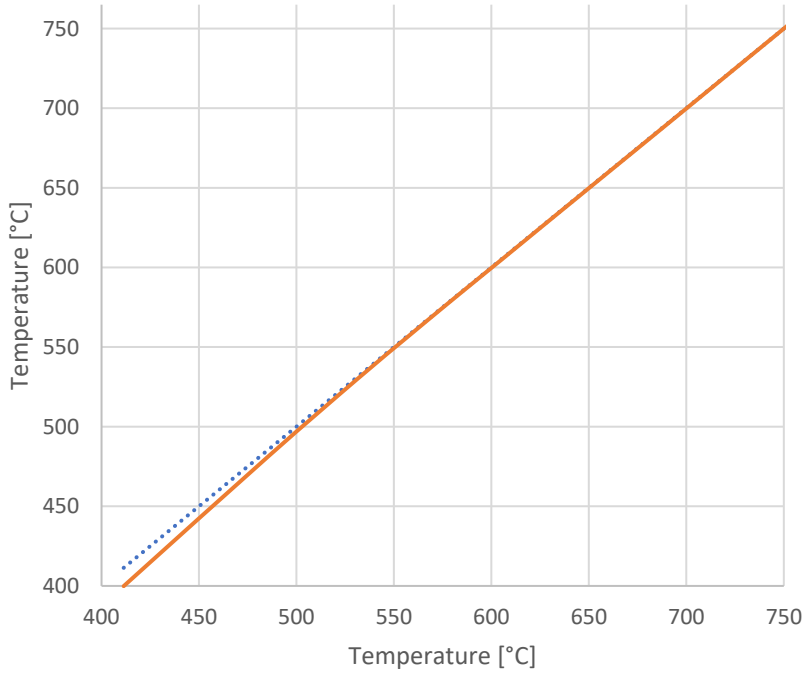

Figure 76: Blend 1 flash inlet and outlet ASTM parity plot

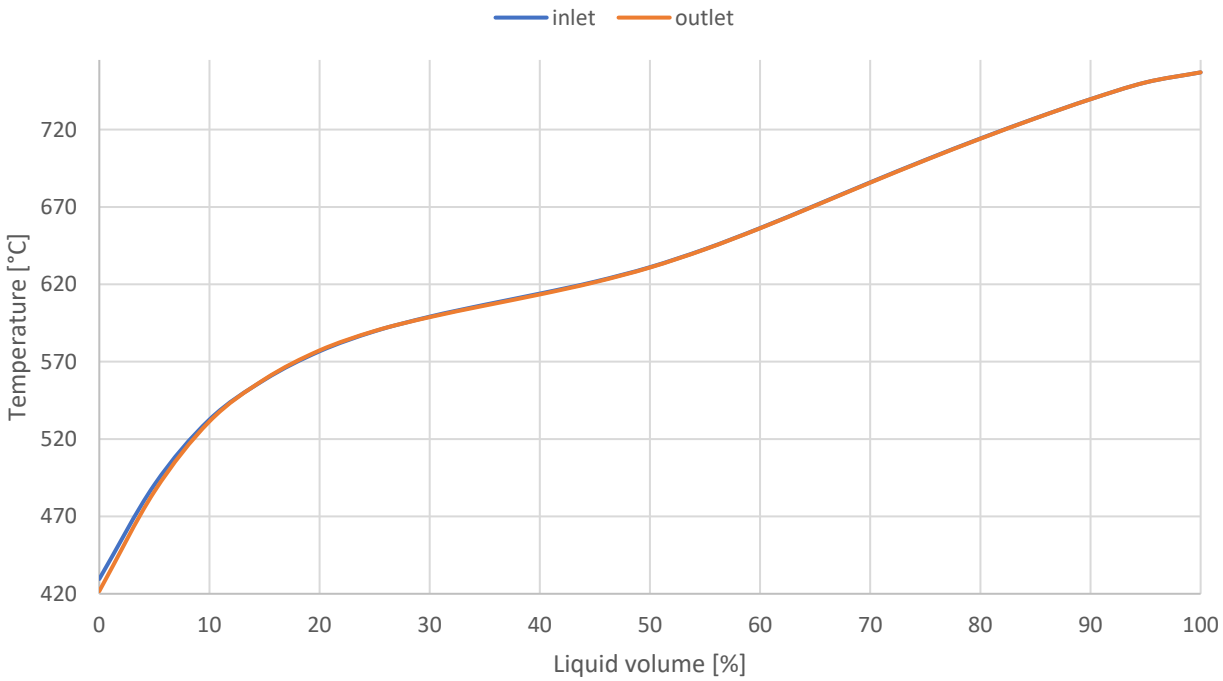

Figure 78: Blend 2 flash inlet and outlet ASTM plot

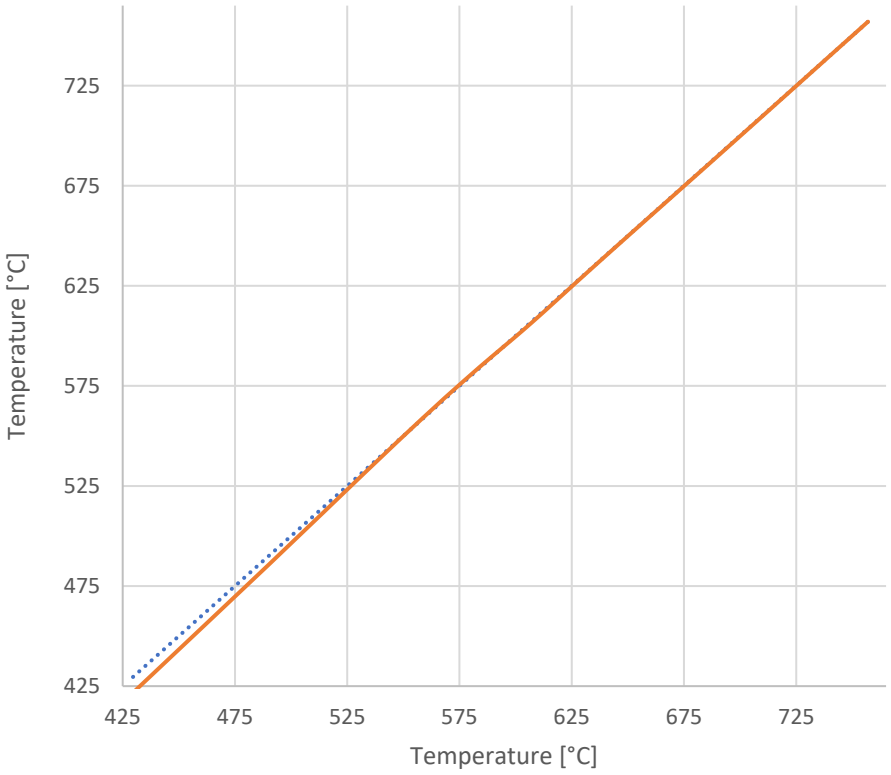

Figure 77: Blend 2 flash inlet and outlet ASTM parity plot

It is clear from the outlets compositions reported and the graphs that the thermodynamic equilibrium works well DynSim. In fact, the liquid outlet composition, using the constructed cut set, is very similar to HYSYS's validated one, and the ASTM curves coincide except for the initial parts of the curves, as in HYSYS. However, the D1160 curves generated from DynSim are very different from HYSYS's ones, as graphed below (Figures from 79 to 82).

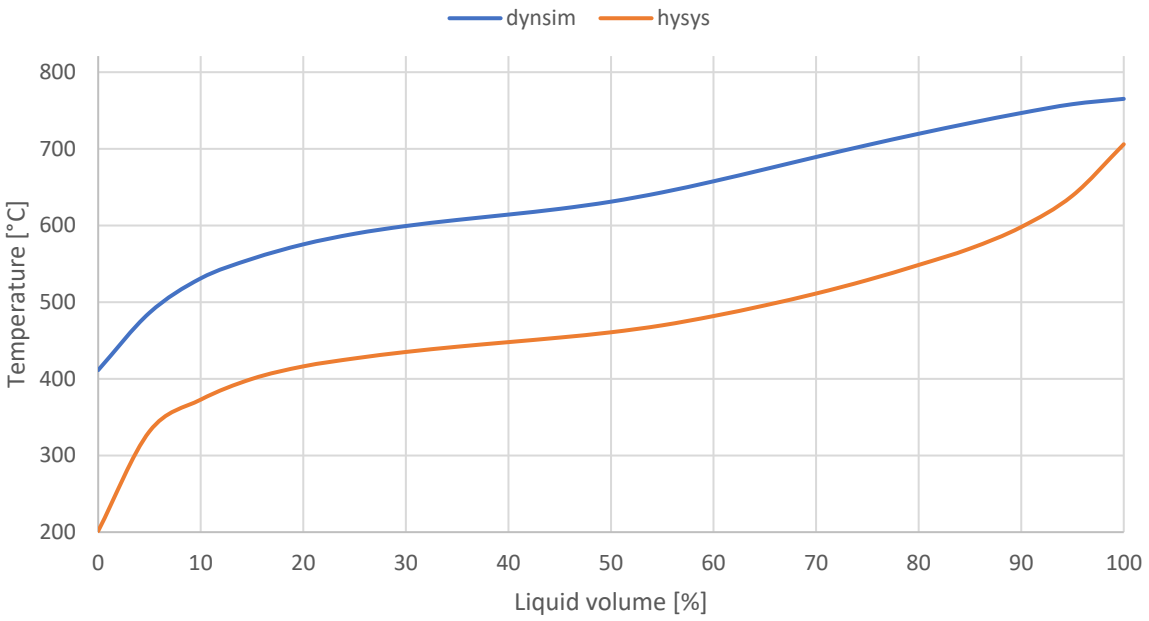

Figure 79: Blend 1 outlet ASTM DynSim comparison with HYSYS

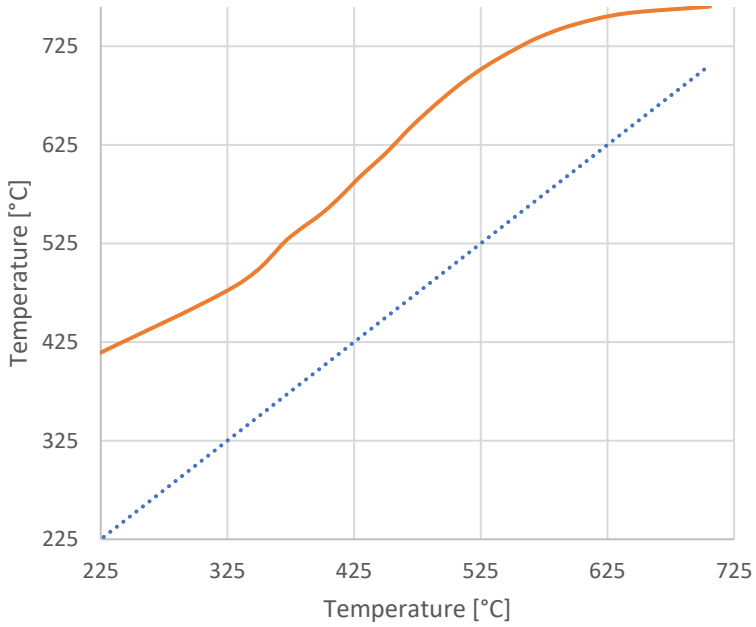

Figure 80: Blend 1 outlet ASTM DynSim/HYSYS parity plot

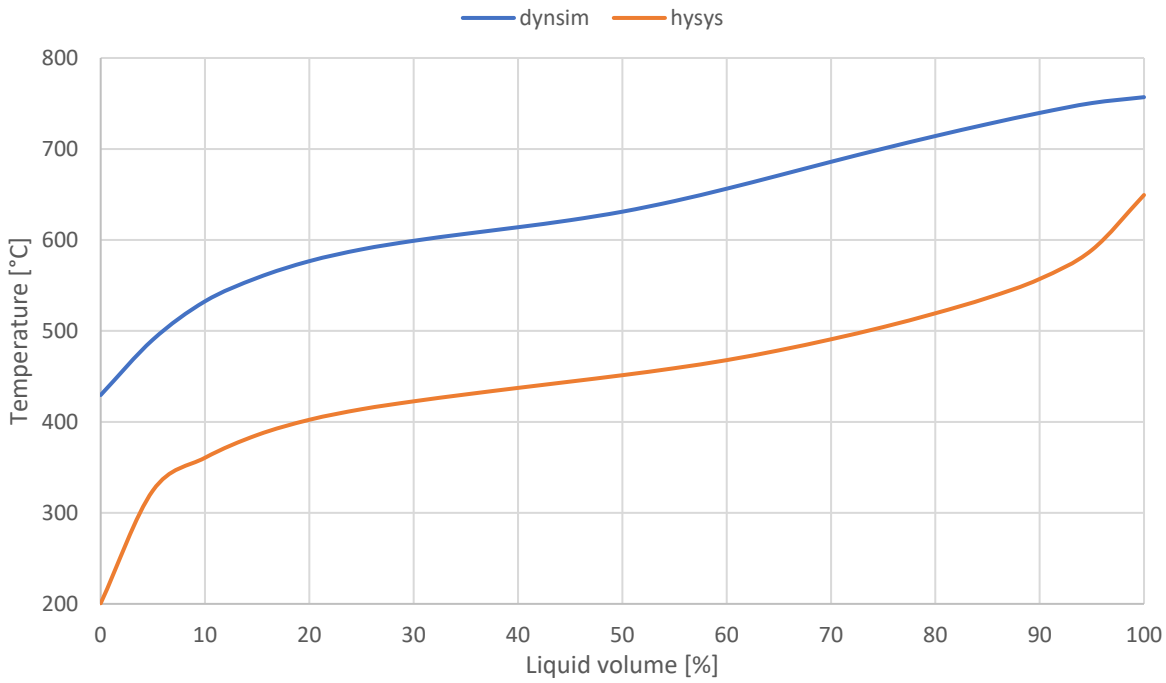

Figure 81: Blend 2 ASTM DynSim comparison with HYSYS

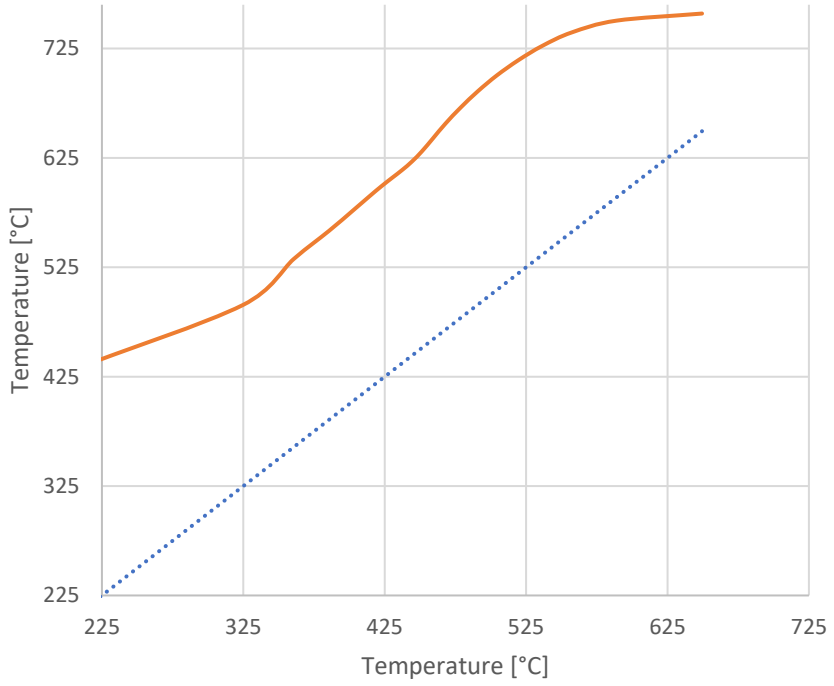

Figure 82: Blend 2 outlet ASTM DynSim/HYSYS parity plot

As shown, DynSim's curves are in high discordance with HYSYS's, which are proven in the chapter about HYSYS's thermodynamic validation to be equal to the experimental ones. Such difference is another limitation to DynSim's accuracy in describing the lubricant products. It is not even possible to import the products ASTM curves in HYSYS to better characterise them, since they are too different from reality.

Beside this inconvenient, the thermodynamic equilibria described in the dynamic simulator is considered reliable. The constructed cut set constituted by 15 components is used to perform the column simulation, since little difference in computational effort with the 11 components one is observed.

Lastly, the two liquids separation vessel V-312 is analysed. As said in the stationary part, no experimental data are available about the streams leaving the vessel, so HYSYS is considered for the validation, since it is in good accordance with the other furnished data. The two blends simulations bring back identical results, probably due to the very similar preflash vapor outlet. Considering this, only one result is reported and compared with HYSYS's one. For this purpose, aqueous and organic outlets are listed in Table 24.

	HYSYS aqueous	HYSYS organic	DynSim aqueous	DynSim organic
x^{l}_{h2o}	1	0.0002	1	0.006
$x^{l}_{styrene}$	0	0.8434	0	0.9939
$x^{l}_{light\ gas\ oil}$	0	0.1564	0	0.0004
Flowrate [kg/hr]	1346	524	1345	469

Table 24: Vessel V-312 results

The off-gas outlet is not reported, since both in HYSYS and in DynSim its flow rate is equal to 0. This may be because the outlet is only posed for security reasons, or more likely since no information about the flow are given and so its contribution has not been added to the preflash's entry flow rate in the model as for the lubricant, the water, and the styrene. No component in the blend is light enough to be drawn as off-gas. The reason behind the different results may be attributed to mainly two points:

- DynSim's resultant temperature and pressure in the vessel are 55.8 °C and 159 torr, while HYSYS's ones are 50 °C and 179 torr;
- The flash's vapor outlet is different both in flow rate and in composition, as reported in Table 25;
- Discordances showed in Table 25 may affect the vessel operative conditions.

These measurements have no further consequences in the model since no liquid-liquid equilibria is present in the column. Considering this and the little importance of the light gas oil recovered from the vessel, the results can be considered acceptable from utility on field point of view and unimportant for the TDA's model.

	HYSYS	DynSim
x^{l}_{h2o}	0.9412	0.9435
$x^{l}_{styrene}$	0.0534	0.0564
$x^{l}_{light\ gas\ oil}$	0.0054	0.0001
Flow rate [kg/hr]	1870	1813.6

Table 25: Flash vapor outlet characteristics

3.5. TDA tower

In this chapter the tower features in the dynamic simulator and the approaches used to build it up are described. This necessity arises since new features are present with respect to the stationary model. These features are linked to mass and energy holdups, flows conductions, pressure drops intended as driving forces for vapor flows, and metal's thermal inertia.

DynSim's tower is generally constituted by a series of equilibrium stages, which can be sieve trays, chimney trays, baffle trays or packings. For each of them, geometric parameters and efficiencies can be inserted as inputs. Liquid and vapor flow rates are calculated accordingly to the stage type, geometrical parameters, fluid's transport properties, vapor and liquid holdups, and conductances. Every tower model in DynSim requires a base that can be represented from the tower sump's feature, an equilibrium stage in which only some geometrical parameters are accounted for. Another option can be using another equilibrium model like a separator or a flash drum.

3.5.1. Two modeling approaches: one-piece vs split

DynSim's model has its starting point in HYSYS implemented deasphlating column model, from which it took the equilibrium stage features, which are their number, efficiencies, refluxes and outlet stages location. Such stages correspond to the structured packs from TDA's plant, which are represented in DynSim with the pack feature. Their characterisation is better described in chapter *3.6*. Liquid collectors must also be modelled, together with the column empty zones above each packing. To implement these last features in the simulator, two different approaches are developed to model the column: the representation of the column as tower in one piece or as a tower split it in several sections.

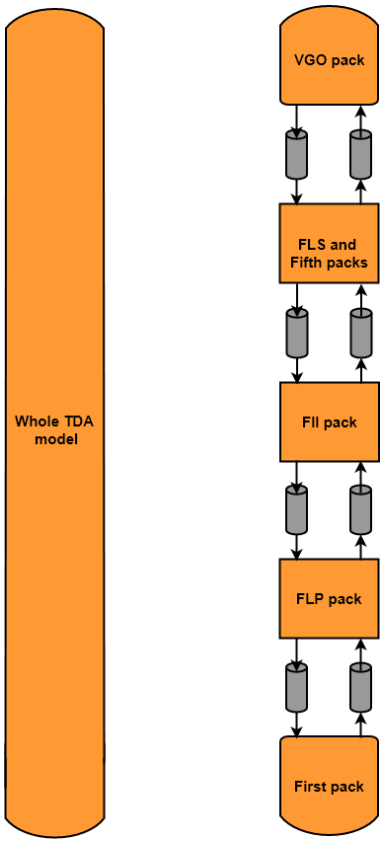

Figure 83: The two different model approaches

The one-piece model design tried to be as loyal as possible to the actual design of the column and was thus made of:

- 6 packed beds with geometrical characteristics as seen in the technical sheets, and flow properties calculated used the results from HYSYS as a basis;
- A single tower with 5 side draws and 6 refluxes in the proper position;

- A single sump at the bottom. Being an equilibrium stage, this required for a reduction in equilibrium stages of the first pack.

The main concern with this model was how to approach the representation of the basins at the bottom of each pack. The most reasonable solution seemed to be a chimney tray with very high weir height and low efficiency of exchange. However, once this model was implemented and run, it was impossible to keep it numerically stable. The target level of the chimney tray was ranging from 200mm to 400mm, but the model became unstable and diverged at much lower values making it impossible for the column to run.

The chimney trays were removed and only a structure with a sump, six packs and a single tower was left. In this configuration the level control on the product withdrawal was not representative of the real situation. Moreover, the liquid was now taken directly from the pack, affecting the material exchange by changing the amount of liquid in the packing and not being accurate on the geometrical position of the withdrawal pipe. Considering that also the total liquid holdup in the column was incorrect due to the lack of the basins below the packs, this model was deemed inadequate to simulate a start-up of the column.

The split column is constituted by 4 sections, which are the first pack, the FLP, the FLL, the FLS-Fifth pack and the VGO pack section. Each section is constituted by:

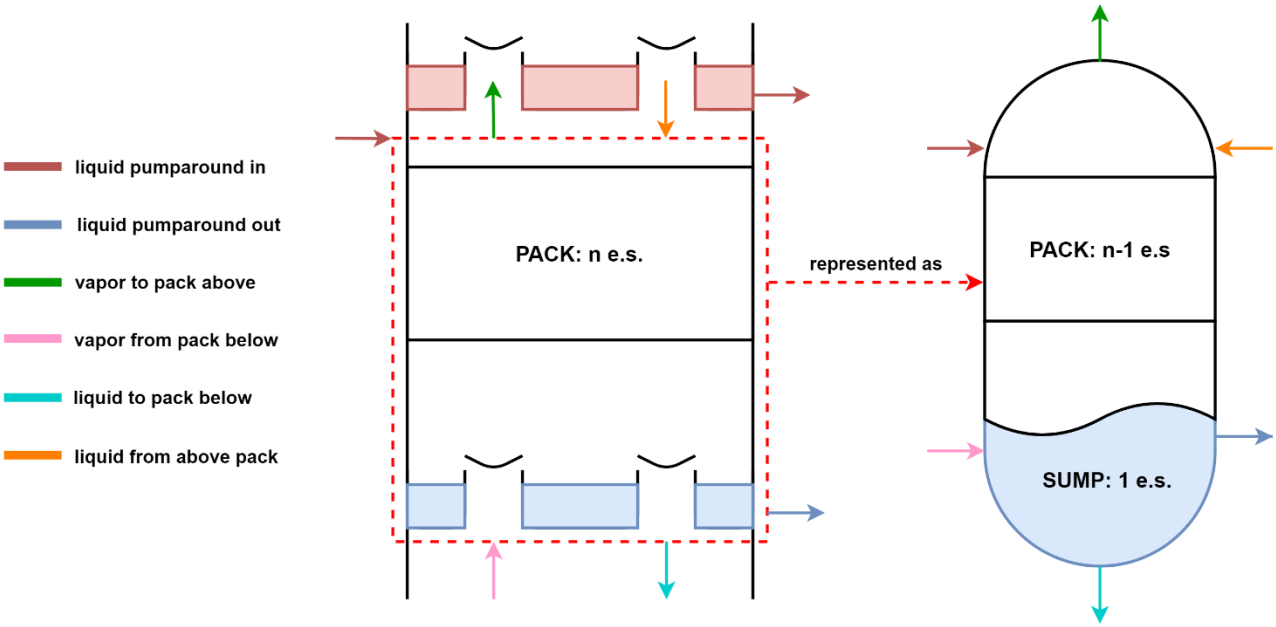

Figure 84: Section of the split column

- A sump, which acts as the liquid collector;
- Pack equilibrium stages;
- A pair of vertical tubes located above the pack. Such tubes represent the empty zones between the structured packings and the collector trays, so that the local vapor holdups and correct tray elevations can be kept in consideration. A single

tube cannot be considered since flows in DynSim's pipe can course only in a single direction, while in a distillation column both rising and descending flows are present simultaneously. Usually, such flows are the vapor leaving the pack and the liquid overflowing the trays.

FLS's pack and the fifth pack are in the same section, since no collector tray is located between the two. The empty space among the two packs is represented as a baffle tray where the empty downcomer fraction is set to 1. Lastly, the column's top empty zone is represented as a single tube for the vapor rising to the ejector group.

3.5.2. Choice of the split model

After dimensioning and characterising both the tower models, the steady state conditions for both are analysed. While the split model shows good accordance with the plant TDA conditions, as will be represented in the validation chapter, the one-piece model presents a colder column, up to 25 °C below the operative temperature in the first stage. The main reason is attributed to the higher quantity of liquid flow descending the column. In fact, since in the one-piece tower no chimney trays are present, such flow is free to descend the column without any impedance caused from the collector tray. On the contrary, sumps collect the liquid from above, which cannot flow below until it reaches the ports, whose heights can be located at the level of the plant tray chimneys top. Also, the conductance factors for the liquid flow tube can be implemented modelling the fluid flow resistance. Despite this major disagreement with reality, some other differences are needed to be pointed out:

- The vapor flow rising from the pack below a collector tray meets less resistances than in a pack. This particularity is not reported in the one-piece column. Moreover, even if the chimney and the baffle trays were present in there, the same vapor flow rate can be modelled in a more independent way in the split column. In fact, having the vapor flow tube as an independent channel for it, the conductance factor can be modelled without having any direct consequence on the descending liquid flow. In the simulator's chimney trays, the two flows are linked by the same geometrical parameters, which may be an issue since such trays in Itelyum's plant have custom designs that are not present in DynSim;
- Liquid levels cannot be accurately described in the one-piece column model since it has no collector trays. This is mainly because the liquid holdup in the pack is distributed all along its height, which does not correspond to the liquid level on a chimney tray. This causes discrepancies with the liquid level controlling of the plant;
- Vapor holdups in empty parts of the column are not described;
- The relative height of each part of the column cannot be well represented in the one-piece model, since no baffles nor chimneys, for which tray spacings can be accounted, are present. Increasing the pack height to fulfil such lack is not

practicable, since would penalize the description of the flows and the holdups in those parts of the tower which should be empty.

In conclusion, split model is chosen due to the higher flexibility of the model and to the higher resemblance with reality it can reach without incurring in numerical instabilities. All further considerations in this thesis refer to this modeling approach.

3.5.3. Model representation in DynSim

The TDA flowsheet in DynSim is reported below. The images represent the column from top to bottom.

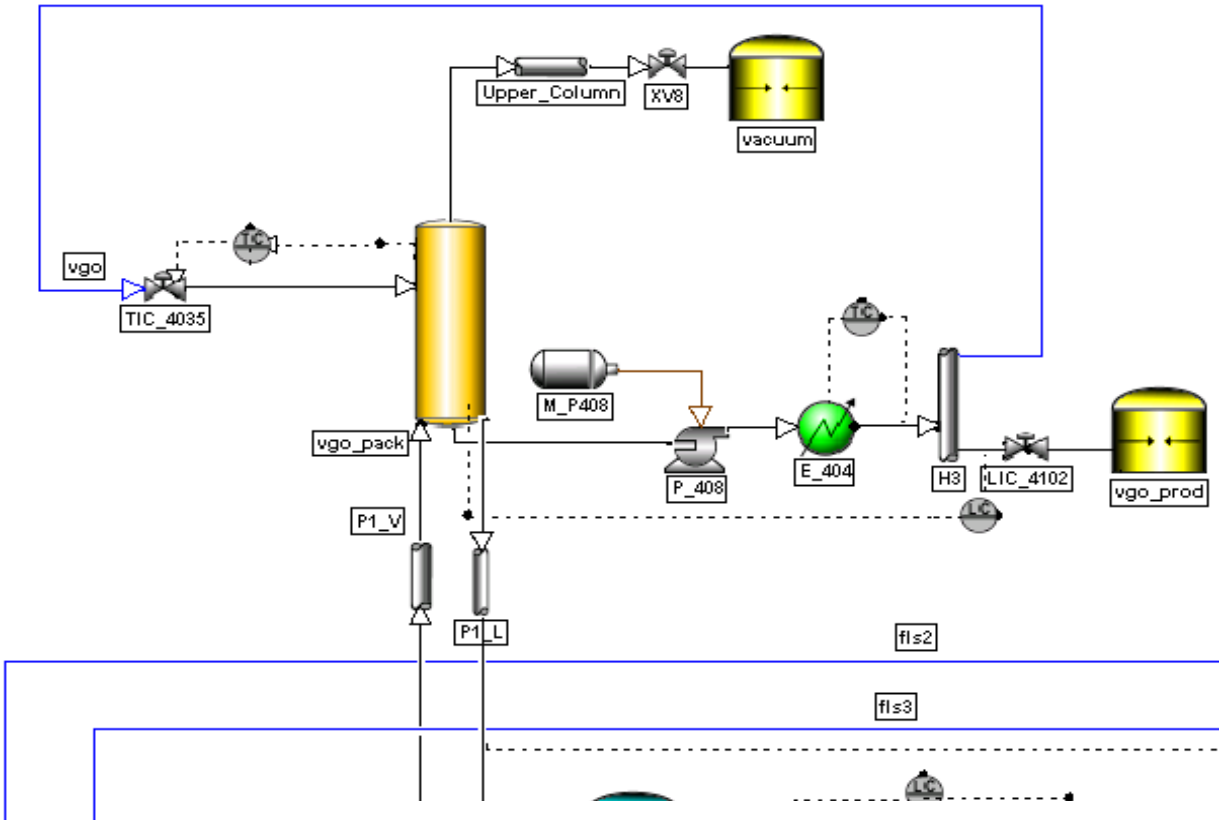

Figure 85: VGO group with pumparound

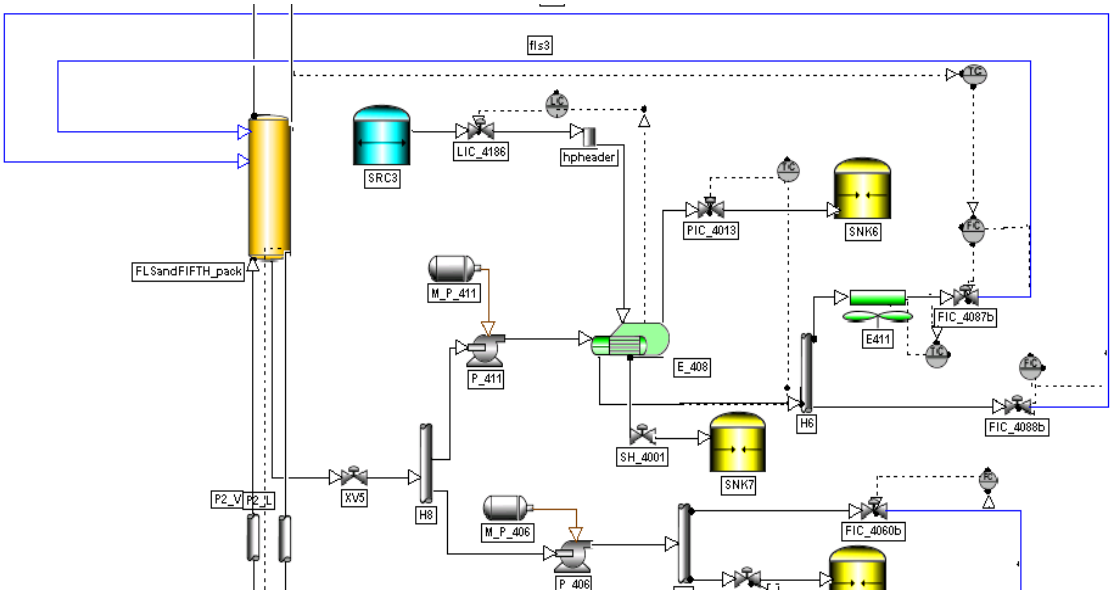

Figure 86: FLS and fifth group with pumparound

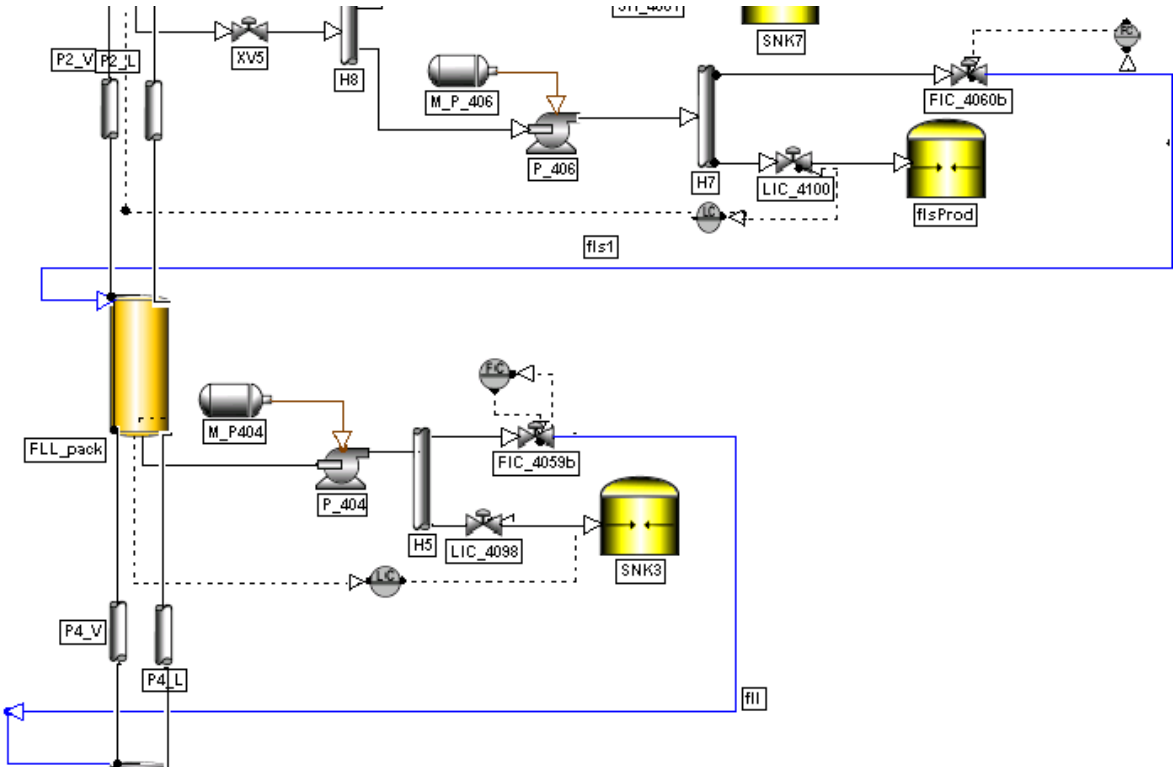

Figure 87: FLL group with pumparound

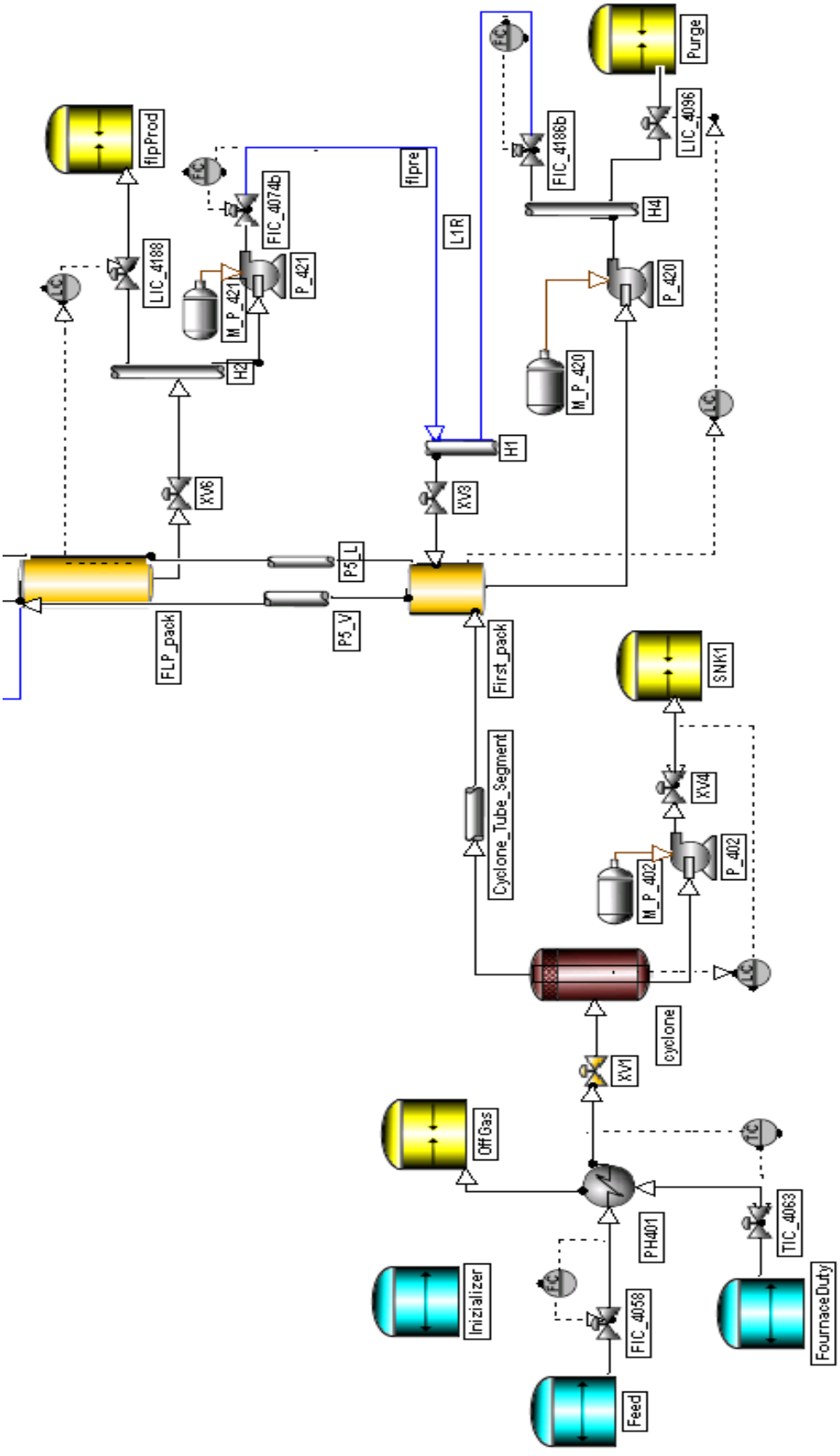

Figure 88: Inlet, first and FLP pack with pumparounds

3.6. Dimensioning

DynSim model equipment requiring a high number of parameters, which can be changed by the user. Such data include both geometrical features, which are provided from the plant P&ID, construction drawings, and transfer coefficients, which must be calculated. In order to fully implement the potential of the ad-hoc model, all these data must be collected, evaluated and included.

It must be pointed out that only the split version of the column will be discussed, since it is the chosen model, but the same approach has been used also for the other model during its evaluation.

3.6.1. Sections and cyclone dimensioning approach

In the TDA model, different data can be specified for each pack. Choosing this approach, the number of sections must firstly be specified. In the following table, the division in sections of the column is described. The number of equilibrium stages is inclusive of the sumps and the stage efficiencies. This is not true for sumps, which have efficiency equal to 1 by default and for section 6, in all other cases data is taken from HYSYS.

Section Number	Position	Number of equilibrium stages	Type	Efficiency (Vapor, Murphree)
1	First pack	3	Pack	1
2	FLP pack	3	Pack	0.3
3	FLL pack, below	3	Pack	1
4	FLL pack, above	1	Pack	0.78
5	FLS pack	4	Pack	0.78
6	Between FLS and fifth packs	1	Baffle	0.01
7	Fifth pack	3	Pack	1
8	VGO pack	4	Pack	1

Table 26: Section characterization

Since the baffle is not an equilibrium stage, the efficiency is set nearly to zero. For each section packs and sumps diameters, relative elevations and heights are specified. These data are not reported to respect industrial secrecy.

Ports height and diameters are also included. Feed, refluxes and products ports diameters are furnished by Viscolube. Since the column model is split, chimneys diameters, vapor outlets and liquid entrances from the section above are treated as fictitious feed and product ports, for each involved section. Unfortunately, these ports can only be considered as horizontal on the column sides in DynSim tower's model, so to avoid liquid entrance in the vapor outlets and inlets and vapor entrance in the liquid ones, the default diameter value is kept. Chimneys port positions are located at chimneys height, while vapor outlets are located at the top of each section.

Cyclone geometry could not be strictly followed, since the cyclone is substituted by a flash. The decision was to keep the column diameter and to calculate the flash's height by keeping the same volume of the plant cyclone. The vapor and liquid exit ports have been dimensioned according to the plant data and are positioned respectively at the top and at the bottom of the unit. The model flash entrance is set at a height proportional to the cyclone one:

$$Height\ Entrance_{\ flash} = Height\ Entrance_{\ cyclone} * \frac{Height_{\ flash}}{Height_{\ cyclone}}\ [m]$$

Tower metal mass is also included, distributed on each stage and on the cyclone. The column mass data provided by Viscolube included only the total column, the packing and the internals' mass. The value to be specified in the model for each section is evaluated as follows:

$$M_{shell} = M_{total} - M_{packing} - M_{internals}\ [kg]$$

$$M_{cyclone} = \frac{Surface_{cyclone\ shell}}{Surface_{total\ TDA\ shell}} * M_{shell}\ [kg]$$

$$Surface_{\ column\ shell} = Surface_{\ total\ TDA\ shell} - Surface_{\ cyclone\ shell}\ [m^2]$$

$$M_{\ section} = \frac{Surface_{section\quad pack}}{Surface_{total\ packing}} * M_{packing} + \frac{Surface_{section's\ shell}}{Surface_{\ column\ shell}} * (M_{shell} + M_{internals})\ [kg]$$

The heat transfer coefficients to the external ambient are evaluated, to improve the default values of 10 W/m^2/K and 100 W/m^2/K for the internal and the external coefficients, respectively. The natural convection coefficient from metal to ambient is calculated using the natural convection expression of the Nusselt number [22], for both the cyclone and the upper part of the column. The external and the internal wall temperatures are evaluated considering:

$$\sum Heat\ flows = 0$$

$$Heat\ flow_{to\ internal\ wall} = Heat\ flow_{from\ external\ wall}$$

Air properties are considered at an ambient temperature of 25 °C, while feed and vapor properties are evaluated using Aspen HYSYS.

$$k_{metal} = 62.05\ [\frac{W}{m * K}]$$

$$Rayleigh = \frac{(T_{wall,external} - T_{air}) * Height_{section}^3 * g * \rho_{air}^2 * Cp_{air}}{T_{air} * \mu_{air} * k_{air}} [-]$$

$$h_e = \frac{k_{air}}{Height_{section}} * 0.13 * Rayleigh^{\frac{1}{3}} [\frac{W}{m^2 * K}]$$

$$U_e = \frac{1}{\frac{1}{h_e} + \frac{\sigma_{metal}}{k_{metal}}} [\frac{W}{m^2 * K}]$$

The internal convection coefficient from fluid to metal is evaluated differently in the cyclone and in the upper part of the column. In the cyclone, the expression regarding a flow in a helical rectangular channel [22] is used, while for the rest of the column Carpenter-Colburn's [22] expression is used, which describes a forced vapor flow rate rising in counter current with a descending liquid film.

$$Nu_{cyclone} = 0.0265 * Re_{feed}^{0.8} * Pr_{feed}^{0.3} [-]$$

$$\frac{1}{\sqrt{f}} = 4 * log_{10}(\frac{roughness_{metal}}{3.7 * D_{cyclone}} + \frac{1.256}{Re_{feed} * \sqrt{f}})$$

$$hi_{column} = 0.065 * G_{vapor} \sqrt{f * \frac{Cp_{vapor} * k_{vapor}}{2 * \mu_{vapor} * velocity_{vapor}}} [\frac{W}{m^2 * K}]]$$

$$hi_{cyclone} = Nu * \frac{k_{feed}}{D_{cyclone}} * \left(1 + 3.5 * \frac{D_{eq}}{D_{cyclone}}\right) [\frac{W}{m^2 * K}]]$$

The first expression is chosen assuming that the feed enters the cyclone tangentially and keeps flowing against the wall with a shape which is equal to the cyclone's inlet, while the second one is considered assuming that a liquid film is formed on the wall, both due to the liquid that may spill on it from above and that the vapor condenses, since the wall is colder. Considering that the flash's area in the model is different from the area of the cyclone in the plant, not to compromise the real heat flux, the $h_{e/I}$ factor was re-scaled as:

$$h_{e/i,flash} = h_e * \frac{Surface_{cyclone}}{Surface_{flash}} [\frac{W}{m^2 * K}]$$

The values of the heat transfer coefficients are reported in Table 28.

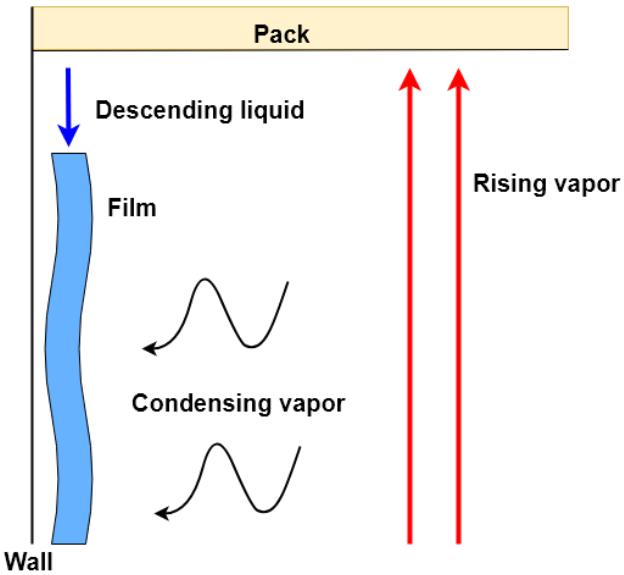

Figure 89: Liquid film model schematics

Section	hi $[\frac{W}{m^2K}]$	he $[\frac{W}{m^2K}]$
Cyclone	770.7	14.1
First pack	19.9	9.2
Empty zone (tube)	19.4	9.2
FLP pack	24.1	9.1
Empty zone (tube)	24.8	9.1
FLL pack	28.7	8.7
Empty zone (tube)	27.7	8.4
FLS and Fifth pack	23.9	7.4
Empty zone (tube)	16.1	6.3
VGO pack	14.8	4.6
Top column (tube)	14.5	4.3

Table 27: Heat transfer coefficients

Finally, the pack flow rate conductance is evaluated. The liquid flow rates are only dependent from the packs height, specific surface a and void fraction ε, which have been provided to the model from the plant data. The gas flow rates are dependent from a conductance K_J which is provided by the user. Those values are evaluated starting from the functions used by DynSim, and using the packs and HYSYS transport data, for both clean and dirty column. Liquid holdup's fraction is evaluated iteratively simulating in DynSim.

$$c = [5 \;\; 3 \;\; 0.45]\;[-]$$

$$D_{eq} = 6 * \frac{1-\varepsilon}{a}\;[m]$$

$$Sez = \pi * \frac{D_{column}^2}{4} * \;\varepsilon\;[m^2]$$

$$G_v = \frac{Gas\ Flow\ rate}{Sez}\;[\frac{kg}{m^2 * s}]$$

$$Re_v = \frac{G_v * D_{eq}}{\mu_v}\;\;[-]$$

$$f0 = \frac{c_1}{Re_v} + \frac{c_2}{Re_v^{0.5}} + c_3\;\;[-]$$

$$C = -\frac{\frac{c_1}{Re_v} + \frac{c_2}{2 * Re_v^{0.5}}}{f0}\;\;[-]$$

$$\Delta P_d = (1 - \frac{\text{Holdup}}{\varepsilon})^{4.65} * \frac{\Delta P}{(1 - \;\varepsilon * \frac{1 - \frac{\text{Holdup}}{\varepsilon}}{1-\varepsilon})^{\frac{2+C}{3}}}\;\;[kPa]$$

$$K_J = velocity_v * \sqrt{\frac{3}{4} * \frac{f0 * \frac{1-\varepsilon}{\varepsilon^{4.65}} * \rho_v * Height_{pack}}{1000 * \Delta P_d * D_{eq}}} \quad [-]$$

The resulting values are reported in Table 28. The K_J parameter for the baffle is set to 10, not to have flow resistance in this stage.

	K_J, clean	K_J, dirty
First pack	0.2632	0.2412
FLP pack	0.8532	0.7682
FLL pack	1.8844	0.9924
FLS pack	2.8229	1.2466
Baffle	10	10
Fifth pack	1.9401	1.0833
VGO pack	3.1358	1.6617

Table 28: Conduction coefficients

3.6.2. Pumps

Pumps data provided by Viscolube at nominal conditions are; differential pressure, head, volumetric flow rate and power absorbed. Unfortunately, not all pumps were provided, so their data are estimated, starting from the available pumps information.

Data to be included in DynSim are; head, volumetric flow rate, rpm and efficiency at nominal conditions. Efficiency is estimated from the available data at nominal conditions, rounded up:

$$Power_{to\ fluid} = \Delta P * Q \quad [W]$$

$$Efficiency = \frac{Power_{to\ fluid}}{Power_{to\ pump}} \quad [-]$$

Since rpm are not provided, the default value of 3600 rpm is kept. It is important to point out that downstream every pump there is a valve which act as a flow rate controller, so errors introduced by estimating data are minimized.

The data included in DynSim are reported in Table 29 differentiating from provided and not provided data. SinceP-402 is a volumetric pump implemented as a centrifugal one, data are estimated.

Pump	Head [m]	Flow rate [m^3/hr]	Efficiency [%]	Provided
P-402	70	3.5	75	no
P-404	70	16.2	80	yes
P-406	80	20.6	75	yes
P-408	92	263	80	yes
P-411	20	55	80	no
P-420	100	5.5	75	no
P-421	85	16	80	no

Table 29: Pumps data

3.6.3. Heat exchangers

While in the stationary model the typology and characteristics of heat exchangers could be ignored, the dynamic model requires this information to simulate appropriately efficiency and response.

Three heat exchangers are involved in the column operations. E-404 is the top column shell and tube heat exchanger and, cooling the VGO reflux rate (about 40.000 kg/hr) down to 15-20 °C, is the main cooler. E-408 is a kettle type shell and tube utility heat exchanger, which generates low pressure steam and acts as a cooler of the reflux to the FLS pack and a pre-cooler to the following exchanger E-411. This last exchanger is an air heat exchanger, constituted by two fans which lay below 8 tube passes, that cool the reflux to the fifth pack down to 90°C.

The data provided by Viscolube are listed in Table 30.

	Symbol	E-411	E-408	E-404
N tubes [-]	Nt	23	498	1160
Length [m]	L	5.1	6.074	6.096
Tube Diameter [m]	Dt	0.021	0.016	0.01905
N passes [-]	Np	8	2	1
Tube pitch [m]	Tp	-	-	0.0254
N baffles [-]	Nb	-	-	19
Shell diameter [m]	Ds	-	-	1.067
Utility type	-	Air	Water	Water
Max utility rate	-	-	Floods the tubes	-
Process fluid side	-	Tube	Tube	Shell

Table 30: Exchangers data

The maximum utility flow rate of E-404 is estimated as the nominal value provided by Viscolube, which is 5 times the operative reflux flow rate, increased by 10%, resulting in 216 ton/hr. A different approach is used for E-411. The exchanger is implemented in HYSYS using the rigorous air cooler feature. By inserting the available technical data, a rigorous model is implemented by the program, which also choses from its database the exchanger which more respects the users' input. Consequently, the maximum flow rate of E-411 is evaluated from the nominal value calculated from HYSYS and assuming that the fans' operative curves "*Air flow rate vs rpm*" are quasi-linear, with a maximum number of fans rotations equal to 420 rpm. Since the flow rate of air is 485.8 ton/hr at 170 rpm, the maximum air flow rate is calculated as 1200 ton/hr.

Some other data is required, which are the overall heat transfer coefficients and the flow conductance.

The flow conductance K_h links pressure drops and flow rates as follows:

$$Flow = K_h * \sqrt{\Delta P * \rho_{fluid}} \ [\frac{kg}{s}]$$

In order to evaluate it, the pressure drops ΔP at a certain flow need to be estimated. Their evaluations have been carried out using the technical data from Viscolube and the fluid data from HYSYS's simulation. Stream data are reported in the Table 31. Note that the mean values of density and viscosity have been taken in consideration.

Exchanger	ρ [kg/m3]	μ [Pa*s]	Velocity [m/s]	Reynolds
E-411	786.03	0.001824	0.445	4032.4
E-408	755.3	0.000568	0.15	3186.5
E-404	792.2	0.001721	0.025	69

Table 31: Flow rates transport properties through heat exchangers at nominal conditions

For tube side process fluids, the following correlation has been considered:

$$Dp = Np * \left(\rho * \frac{v^2}{2} * 4 * f^* * \frac{L}{Dt} + 2.5 * \rho * \frac{v^2}{2}\right) [Pa]$$

Where f^* is the friction factor, calculated as:

$$f^* = 1.2 * 0.048 * Re^{-0.2}$$

The results are 8194.3 Pa for E-411 and 354.6 Pa for E-408.

For shell side process fluid, the equivalent Diameter of the section must be considered, where for square pitch tubes distribution:

$$WettedSection = Tp^2 - \pi * \frac{Dt^2}{4} \ [m^2]$$

$$WettedPerimeter = \pi * Dt\ [m]$$

The Reynolds number is calculated according to the equivalent diameter. In this case, the friction factor has been calculated as:

$$f = \frac{24}{Re}$$

The resulting pressure drop, calculated as:

$$Dp = f * \rho * \frac{v^2}{2} * \frac{Ds}{Deq} * (\mathrm{Nb} + 1)\ [Pa]$$

is equivalent to 302.9 Pa.

The resultant conductance factors are reported in Table 32. Utility side conductance factor is not calculated due to the lack of data, so a reasonable value is considered when needed.

*Conductance factor [kg/s/sqrt(kPa*kg/m³)]*	E-404	E-408	E-411
Process side	2714	2598	134
Utility side	Not needed	3000	Not needed

Table 32: Heat exchangers conductance factor

The overall heat transfer coefficient for E-404 and E-408, which are counter current and 1:2, is evaluated from HYSYS's calculated cooling duty using the following simple equation:

$$U = \frac{Cooling\ duty}{F * Exchange\ Area * \Delta T_{ln}}\ [\frac{W}{m^2 * K}]$$

Since DynSim does not consider the number of passes for utility heat exchangers, a doubled number of tubes is implemented in the model and the F factor is kept equal to 1. The U values for E-404 and E-408 are 122.6 W/m²/K and 67.5 W/m²/K respectively. The U value of E-411, for which the number of passes is considered, is calculated from HYSYS's rigorous air cooler model. The result is equal to 10.3 W/m²/K.

3.6.4. Furnace

As reported in the introduction, the furnace is implemented as a process-process heat exchanger. In this case, the methodology to calculate the process side conductance factor and the overall heat transfer coefficient is the same adopted for E-408 and E-404.

The trend of the pressure drops provided from Itelyum's DCS shows that it changes depending from the dirtiness factor, but since DynSim cannot account for it, the pressure drop of the clean furnace is considered, equal to approximatively 4.2 bar. The

resulting process side conductance factor is of 26.84 $\frac{kg}{s} \cdot \sqrt{\frac{m^3}{kPa \cdot kg}}$ while the utility process side one is considered of 50 $\frac{kg}{s} \cdot \sqrt{\frac{m^3}{kPa \cdot kg}}$

The heat transfer coefficient is also evaluated from Viscolube's trends, considering the utility heat flow inlet and exit temperatures of respectively 750 °C and 400 °C and a heat flow calculated as:

$$Heat\ flow = Feed\ flow\ rate * Cp_{feed} * \Delta T$$

equal to 2450 kW. The resulting U coefficient is equal to 8 W/m^2/K at nominal conditions.

The utility heat flow rate can also be calculated from the equation above, using its mean thermodynamic properties. As a simplistic approach, air is considered. The resulting flow rate is of 25.2 ton/hr.

3.6.5. Pipes and headers

In the simulation, pipes have been used to include the empty section of the column, to consider the gas holdup and the column height increase. A tube has also been used for the section which connects the flash vapor outlet to the column bottom to consider the tube segment that permits the vapor to exit the cyclone, without entraining a high quantity of solid particles.

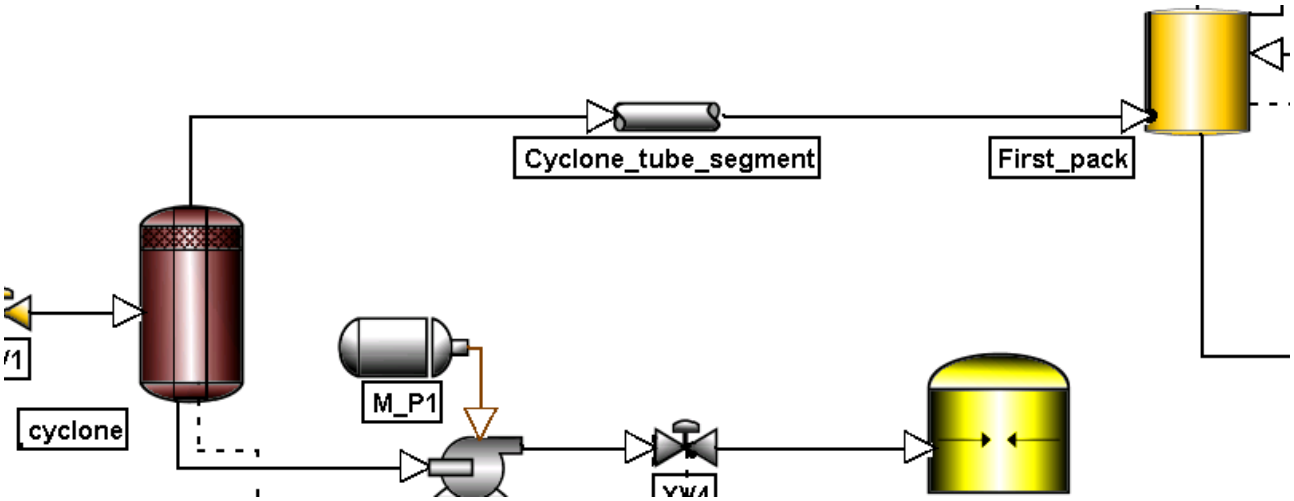

Figure 90: Implementation of the flash outlet

The cyclone tube segment diameter and length are implemented in the model, and the conductance is override, which means that DynSim evaluates it from the tube geometrical characteristics. Since the tube segment is inside the cyclone shell, its heat transfer coefficients are set equal to 0 not to have heat loss to the ambient.

Inlet and outlet flow pipes from the column sections are treated differently. Inlet flow pipes have the same diameter of the column, with a heat transfer coefficient different from zero, already discussed in table 2 of chapter 1.2. The conductance is override as for the cyclone tube segment and the mass holdup is considered. Outlet flow pipes

have the same diameter of the column, but it does not influence the flow crossing it since:

- The heat transfer coefficient is set equal to 0. This choice was taken since these tubes mainly represent the liquid flows exiting the chimney trays, which are prevalently not in contact with the column wall, so do not exchange heat;
- No holdup is considered, since liquid does not accumulate in the empty zones of the column;
- Flow conductance is calculated externally, to consider the higher flowing resistance induced by the chimneys. The relation between flow and pressure drops is the same as in heat exchangers. Pressure drops are evaluated considering both the pressure difference between sections and the liquid head:

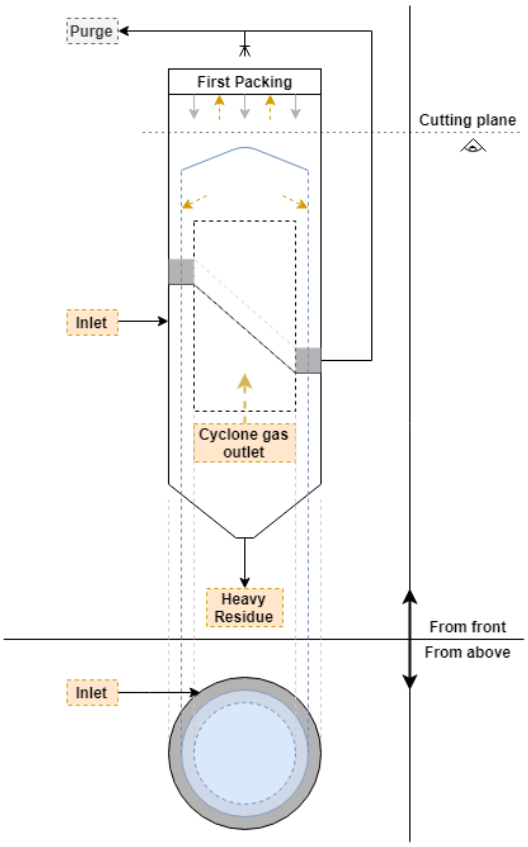

Figure 91: Cyclone structure

$$\Delta P_{outlet\ tubes} = \Delta P_{trays} + g * \rho_{liquid} * (Tube\ Length + 0.05)\ [Pa]$$

The factor 0.05 is introduced as the liquid height above chimneys entrance.

Headers are only introduced where a flow split is necessary. Splitters are not used since, not considering hold up, they produce an equal-composition outlet stream as soon as the stream starts flowing. This condition is momentary but takes a transient of several minutes. Headers, considering holdup, do not have this issue. Due to the lack of data concerning the pipeline, headers' volume is kept at the default value of 1 m^3 and the heat transfer coefficients are set to 0.

3.6.6. Valves

Though a high number of valves are present in the plant, it was decided to include only the ones which act during normal operation, startup and shutdown. Bypass and security valves are omitted, simplifying fluid controllers configurations. This approach limits the model potential in predicting valves' malfunctioning and some specific incidents. However, such equipment can be easily implemented in future models.

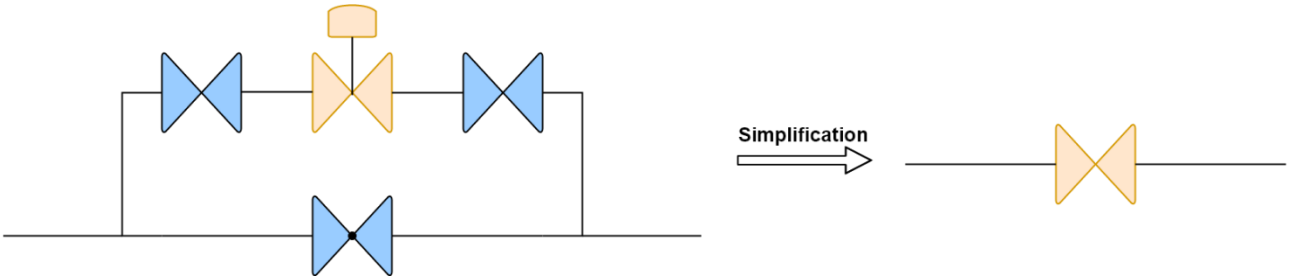

Figure 92: Flow controller structure simplification

The data acquired from the plant consisted in some of the valves CV. Due to lack of data, an opening and closing time of 30 seconds, linear trim types and diaphragm actuators are selected for all the valves. Missing valves CV are estimated using HYSYS's sizing tool, considering an opening percentage of 50 % during operative conditions. No reverse flow is permitted. Below, valves CV are reported in Table 33.

Valve	CV	Provided
TIC-4035	107	Yes
FIC-4087	18	Yes
FIC-4088	110	Yes
FIC-4060	31	No
FIC-4059	50	Yes
FIC-4074	7	Yes
FIC-4186	10.4	Yes
FIC-4058	72.7	No
PIC-4013	138	Yes
SH-4001	100	No
LIC-4186	100	No
LIC-4096	20	Yes
LIC-4188	135	Yes
LIC-4098	50	Yes
LIC-4100	30	Yes
LIC-4102	3.5	No

Table 33: valves CV

Since DynSim does not permit the direct connection between two pieces of equipment with holdup, some fictitious valves have been added, whose CV have been chosen equal to 100000 and are always completely open, not to have flow interferences. Moreover, such valves have an opening and closing time of 0.1 seconds, exception

made for the valve to the vacuum sink, whose CV is 1000 and opening time is 1800 seconds since a lower opening time causes severe numerical instabilities. These valves are located before or after headers which are located upstream or downstream other pieces of equipment with holdup, sinks or sources, if other valves are not present.

Another fake valve is included before the flash representing the pressure drop of cyclone, as in HYSYS. The valve is included to consider lamination in the sector between the furnace and the column, which causes a temperature drop of approximatively 15-20 °C. Such valve has a CV of 5607 and a fixed opening fraction of 25%.

3.6.7. Battery limits

Battery limits in DynSim are represented as sources, which require compositions, temperature, pressure and elevation, or sinks, which require pressure and elevation. Sources are three in total:

- Column feed source to the furnace, whose temperature of 140 °C and composition is assumed as the ones exiting the preflash, while the pressure is equal to 4.2 bar, which is the pressure downstream of pump P-401 alimenting the furnace when it is clean. While the pressure approximation has already been discussed, also the temperature presents an approximation. In fact, upstream of P-401 there is a buffer tank, which collects the preflash liquid outlet and preheats it using the viscoflex exiting the cyclone bottom. The extent of preheating is dependent on the temperature at which the viscoflex is demanded from the customer and can bring the feed's temperature entering the furnace to temperatures in the range of 110°C and 180°C. Such an assumption does not affect the column performance, since the stream temperature exiting the furnace is controlled efficiently;
- E-408 cooling water source is set at 25 °C. Such water is used as the liquid level controller acting on the shell side. Such level is regulated by the water inlet;
- Furnace heating stream source has a temperature of 750°C and a pressure of 1 atm, as discussed in the dynamic model's introduction.

All sources are assumed to be at ground level.

Column downstream conditions, vacuum group excluded, were not provided by Viscolube, so some assumptions are needed, depending on the sinks typologies:

- Sink downstream the cyclone, collects the viscoflex. It follows P-402 which is a volumetric pump and so does not provide a pressure increase. A pressure of 200 torr, corresponding to the liquid head plus the pressure inside the cyclone is adopted. It is assumed to be at ground level;
- Sink downstream LIC-4096 is located after P-420, whose real characteristics are not known. A pressure of 365 torr is adopted, which is higher than the liquid head's contribution;

- Product sinks represent the vapor strippers located downstream the column, except for the VGO product which is sent to the storage tank. Though their pressures and elevations are not known, lube oil deasphalter strippers operate usually under vacuum conditions down to 250 torr [20]. Their elevations are considered as the same as the products outlets.

Lastly, vacuum sink is set at 3 torr and located at top column height.

3.6.8. Controllers

All the column controllers are PI. As anticipated in the dynamic model chapter, the column controller parameters were provided by Viscolube and Kc values were divided by 100. The values are reported in Table 34.

Controller	Controlled variable	Manipulated variable	Kc	τi [s]
FIC-4058	Feed flow rate	Actuator position	0.11	50
FIC-4186	Heavy reflux flow rate	Actuator position	1	50
FIC-4074	Reflux to first pack flow rate	Actuator position	1.5	100
FIC-4059	Reflux to second pack flow rate	Actuator position	0.55	50
FIC-4060	Reflux to third pack flow rate	Actuator position	1.2	80
FIC-4088	Reflux to fourth pack flow rate	Actuator position	2.5	200
FIC-4087	Reflux to fifth pack flow rate	Actuator position	2.5	100
TIC-4035	Temperature below sixth pack	Actuator position	0.7	50
TIC-4034	Temperature above fifth pack	FIC-4087 set point	3	100
TIC-4013	Reflux to fourth pack temperature	Actuator position	0.7	50
LIC-4102	VGO tray liquid level	Actuator position	5	50
LIC-4100	FLS tray liquid level	Actuator position	1	15
LIC-4098	FLL tray liquid level	Actuator position	0.5	50
LIC-4188	FLP tray liquid level	Actuator position	1	15
LIC-4096	First tray liquid level	Actuator position	2	50

Table 34: Characteristics of the controller

3.7. Dynamic Validation

The validation of a dynamic model focuses both on the analysis of steady state conditions and on transient trends. Consequently, the appropriate choice of a case study depends on the magnitude and the duration of the transient. In fact, these characteristics must be appreciably intense, to recover enough valuable data.

One of the most influential parameters on the column behaviour is the feed flow rate. Viscolube managed to provide the transient data historian of an important step change, in which the cited variable increased from 11000 kg/hr to 13000 kg/hr. At the same time, refluxes were also manipulated from the plant operators, in attempt to maintain the column almost at steady state. An appreciable transient was anyway present.

The column DynSim model was brought to the initial steady state and the manipulated variables (feed and refluxes) were changed as was done on field. The initial, final steady state and the transient could finally be evaluated.

3.7.1. Results and discussion

In the first step of this discussion, the steady state conditions were evaluated. Temperature and pressure profiles are analysed. The values reported match the stages in which the indicators are located, starting from position 1, corresponding to the column bottom, to position 21, corresponding to the column top.

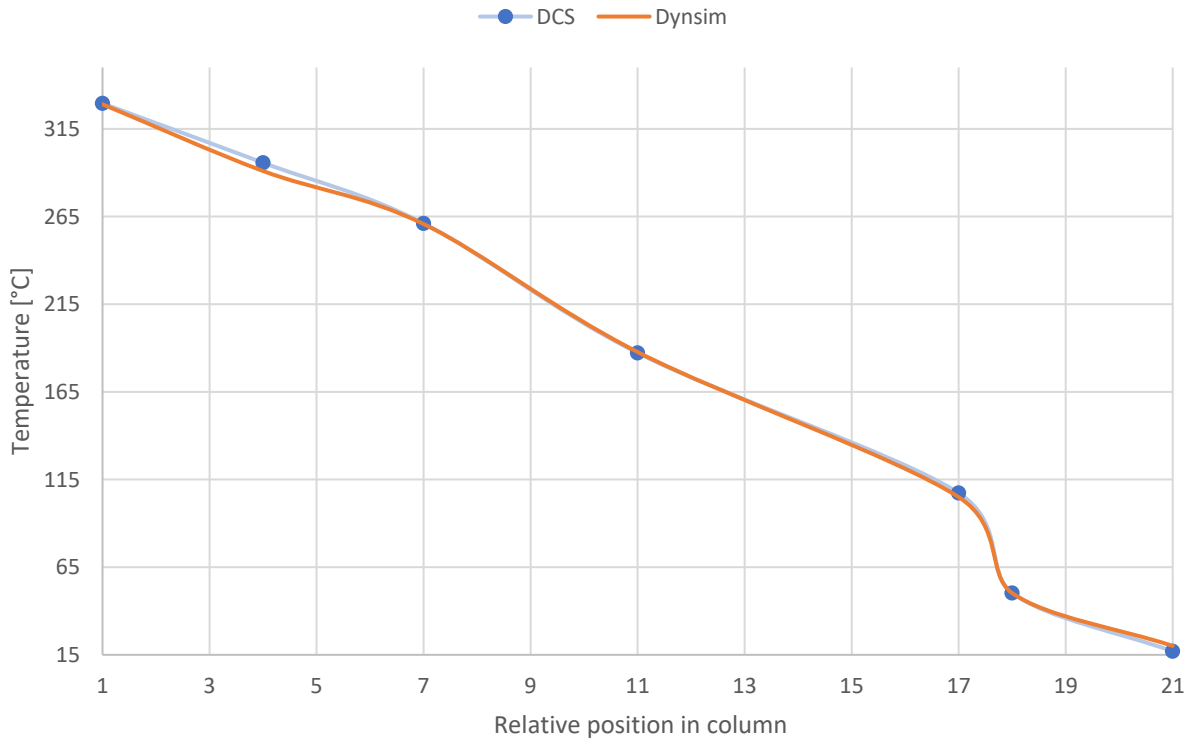

Figure 93: Column temperature profile at initial steady state

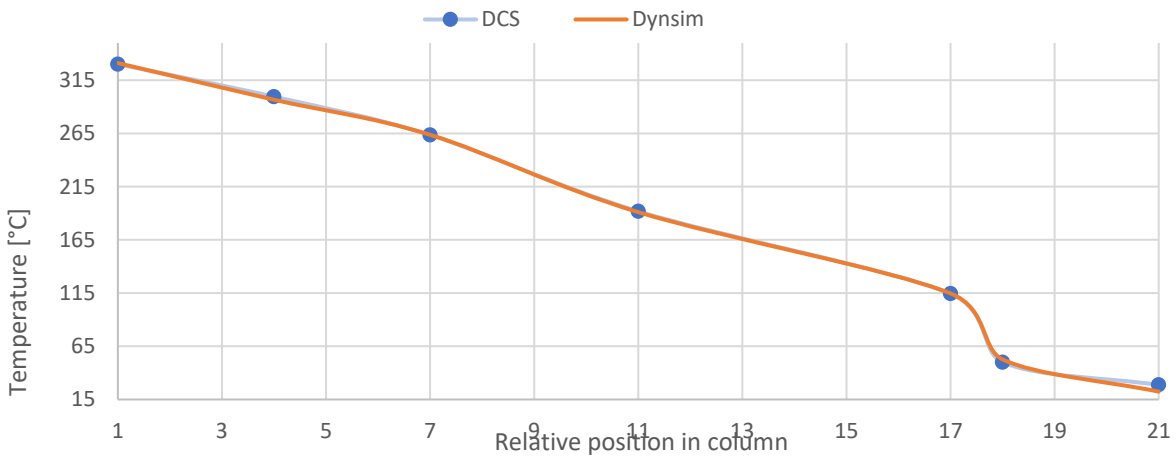

Figure 94: Column temperature profile at final steady state

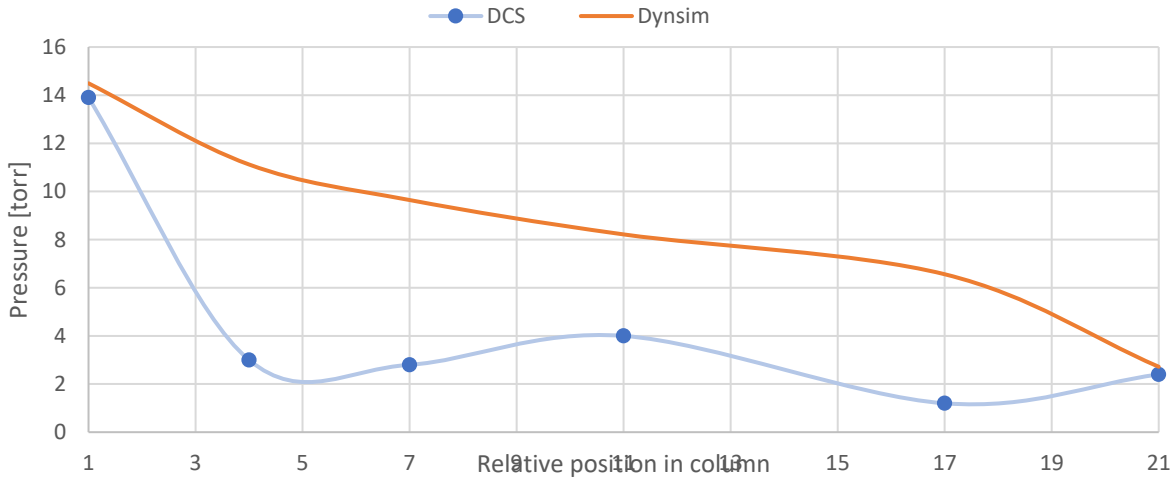

Figure 95: Column pressure profile at initial steady state

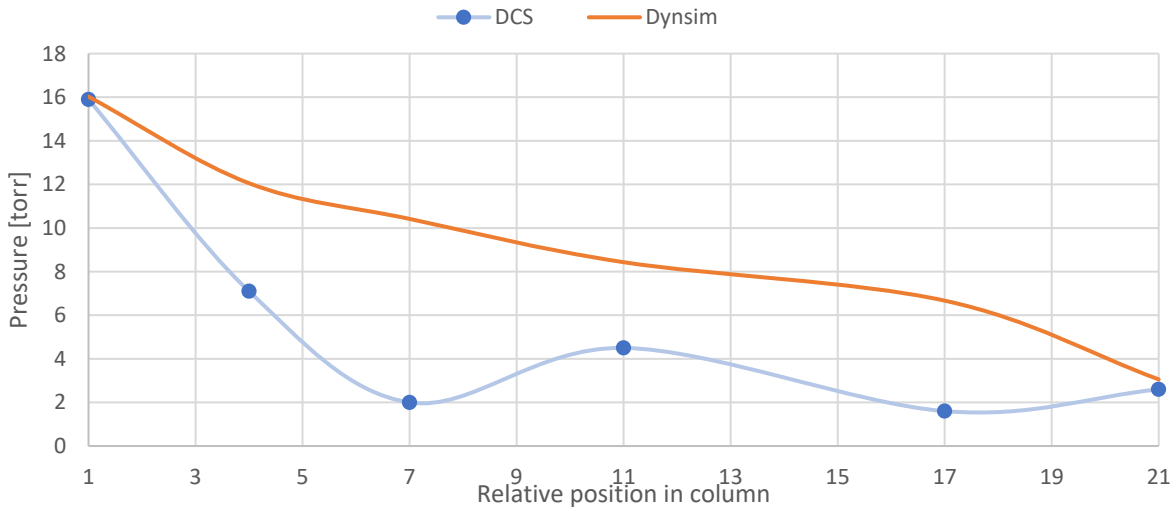

Figure 96: Column pressure profile at final steady state

	ε_T[°C]	ε_P[torr]
Initial	1.41	4.24
Final	1.31	4.16

Table 35: mean errors defined as $\varepsilon = \frac{\sqrt{\left(V_{(i)}^{model} - V_{(i)}^{dcs}\right)^2}}{N_{measures}}$

As expressed by the graphs 94 and 95 and by the table, the model temperature profile fits very well with the data reported by the DCS. The major issue regards the temperature on the FLP and the VGO trays, for which the discordances ranges from 2.5 to 4.5 and from 0.8 to 2.6 Celsius degrees respectively. Such discordances were already noticed in HYSYS and may be due to non-equilibrium stages in the real column. Regarding the pressure profile indicated from the DCS, it is notable that the measures are not reliable as already discussed in the steady state part. Unfortunately, this means that pressures cannot be directly compared, though the top and the bottom pressures seem to be in good accordance with a mismatch of 0.45 to 0.35 and 0.6 to 0.15 torr respectively.

The dynamic transient is now to be evaluated. Temperatures and pressures from the DCS and the model were plotted and compared in a time span of 4 hours and a half. To better analyse the trend, the following quantity was introduced for every evaluated variable V, with respect to their value at initial time t_0:

$$\delta = \frac{V(t)}{V(t_0)} - 1$$

Before this, the manipulated variables were evaluated in the same way to analyse the controllers responses.

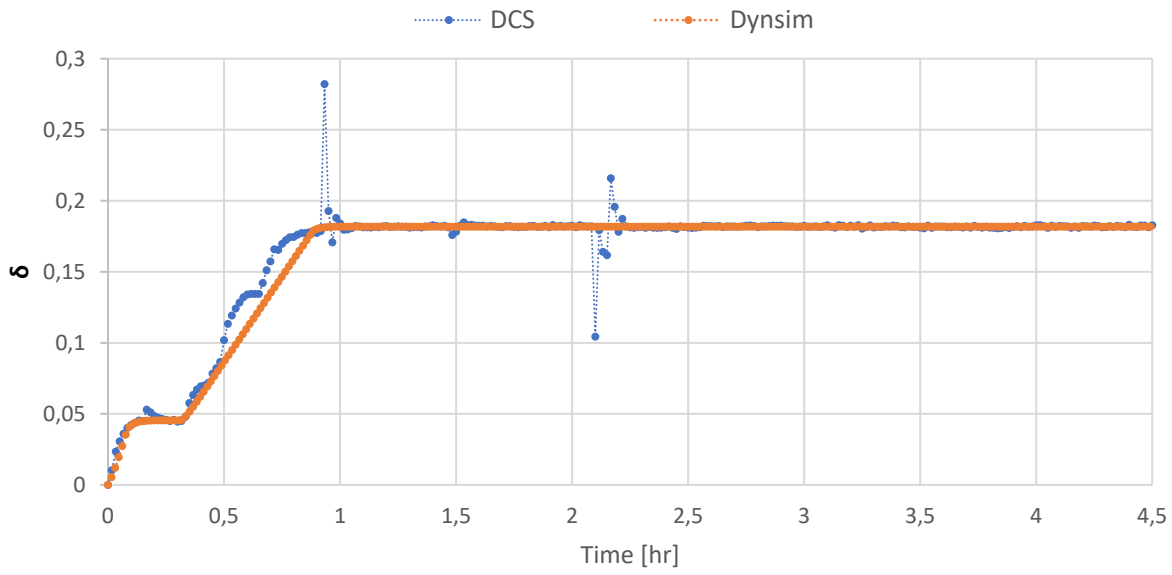

Figure 97: Feed flow rate in time

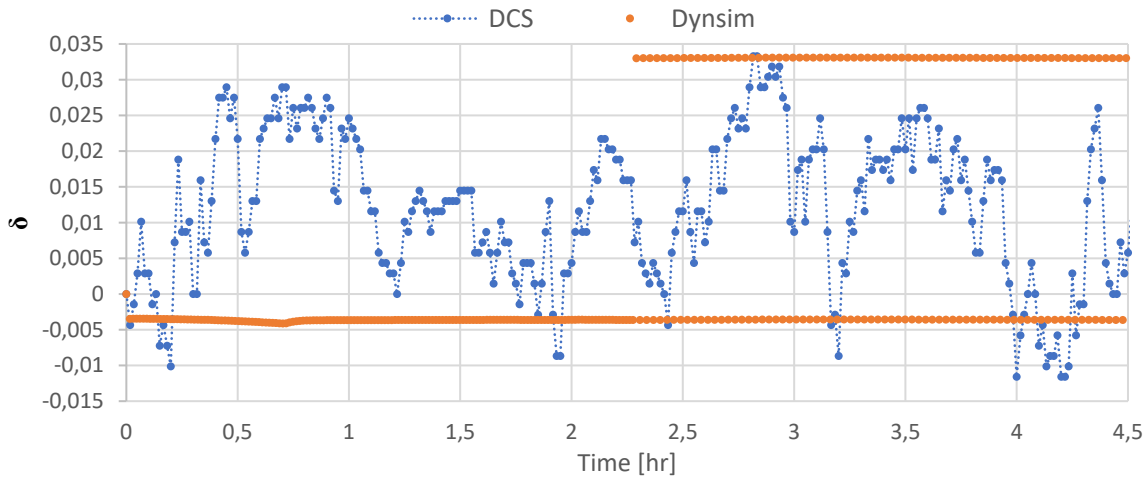

Figure 98: FLP reflux flow rate in time

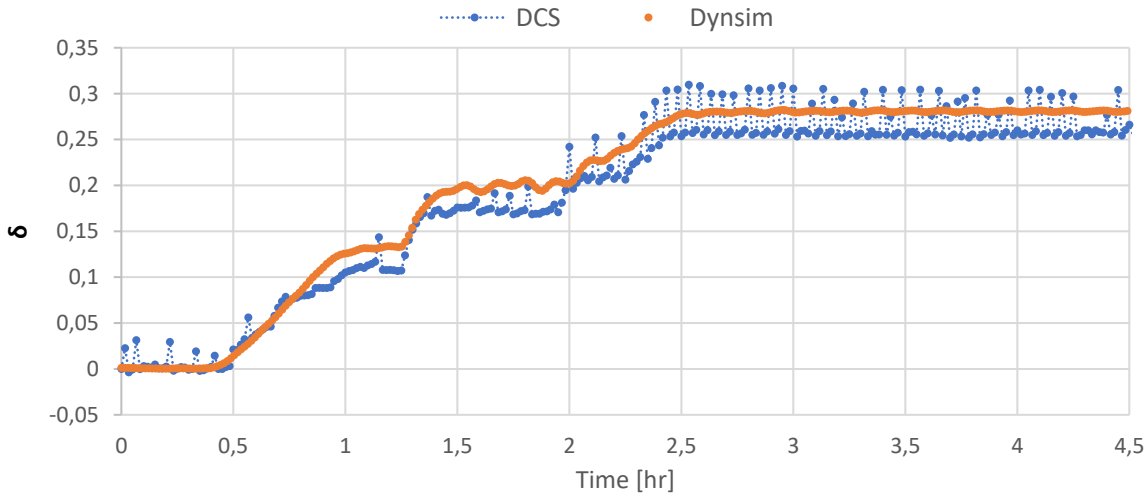

Figure 99: FLL reflux flow rate in time

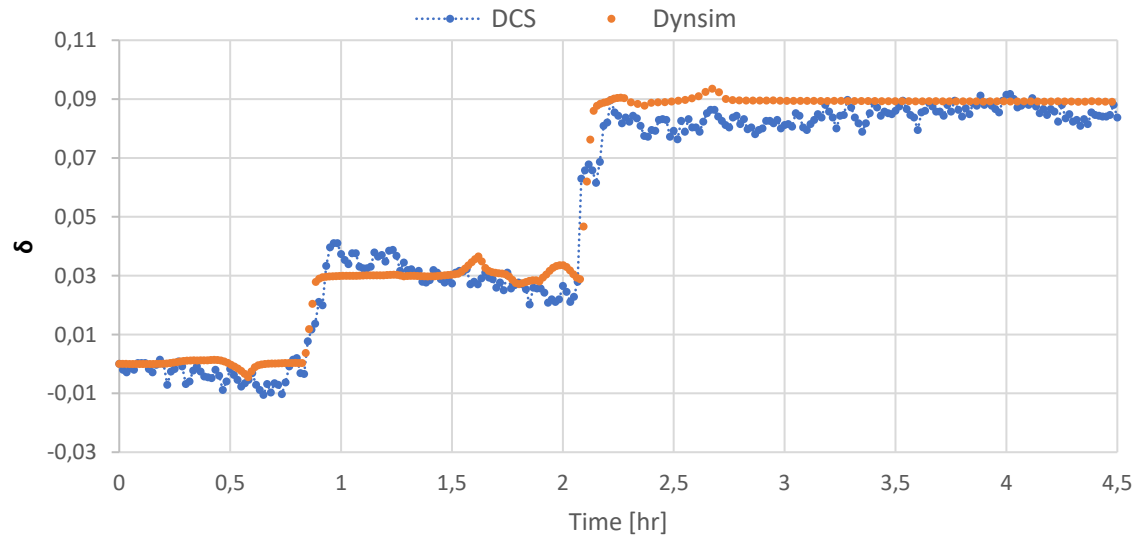

Figure 100: FLS reflux flow rate to third pack in time

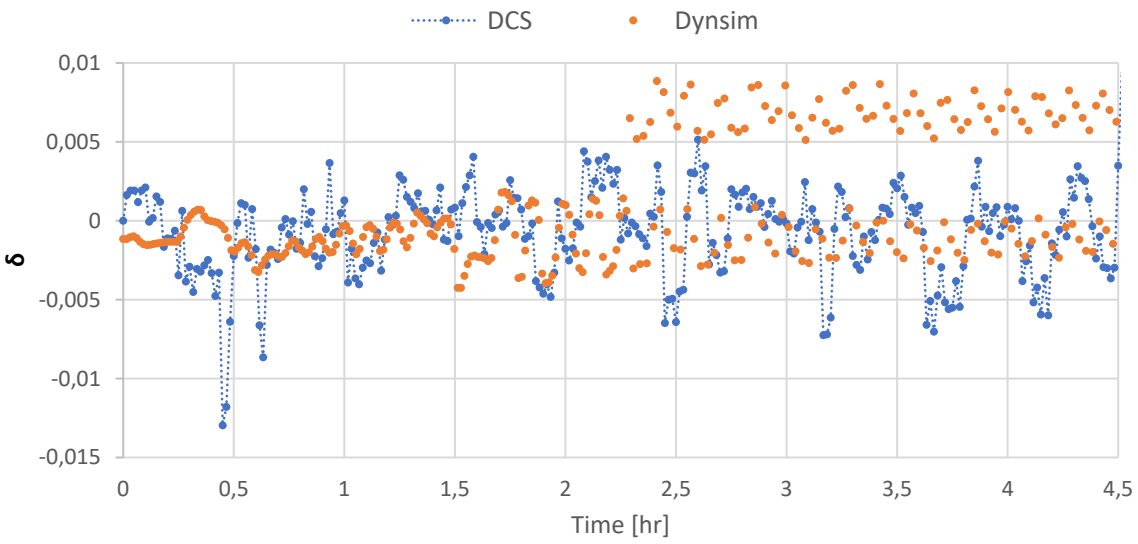

Figure 101: FLS reflux flow rate to forth pack in time

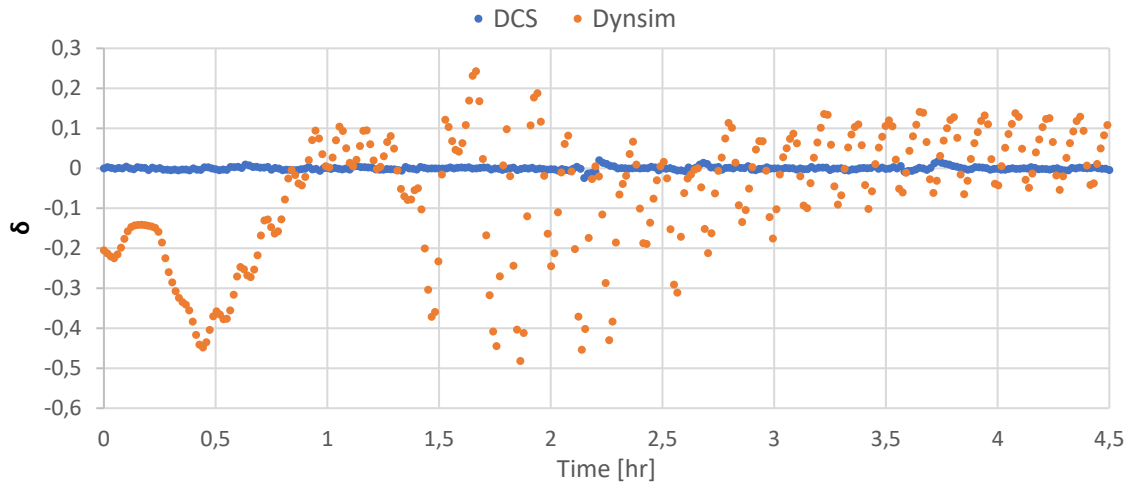

Figure 102: FLS reflux flow rate to fifth pack in time

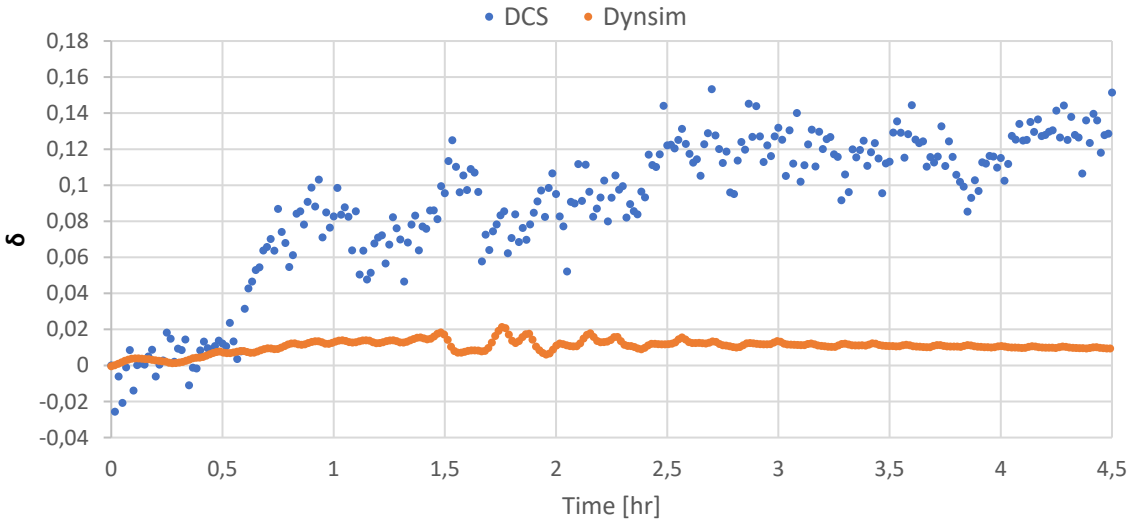

Figure 103: VGO reflux flow rate in time

The manipulated variables on the model represent well the ones reported by the DCS. However, some differences must be pointed out. Trends in FLP reflux is quite different, though the range is approximatively always between 680 kg/hr and 705 kg/hr. Major dissimilarities are present in the VGO's and the last FLS's refluxes. Concerning the model, flow rate of VGO reflux is already at the maximum value allowed by the model; 47200 kg/hr. Though the exact motivations of this behaviour are not clear, it appears that the top stage may not be adequately represented by a thermodynamic model, as pointed out in the stationary case. The last FLS reflux may be also influenced from this, since the flow rate set point is controlled remotely by a temperature controller. In fact, the excess of heat removed from VGO reflux may relapse on the stage below, decreasing the necessary FLS's flow rate.

Finally, temperatures and pressures trends can be compared in from Figure 104 to Figure 107.

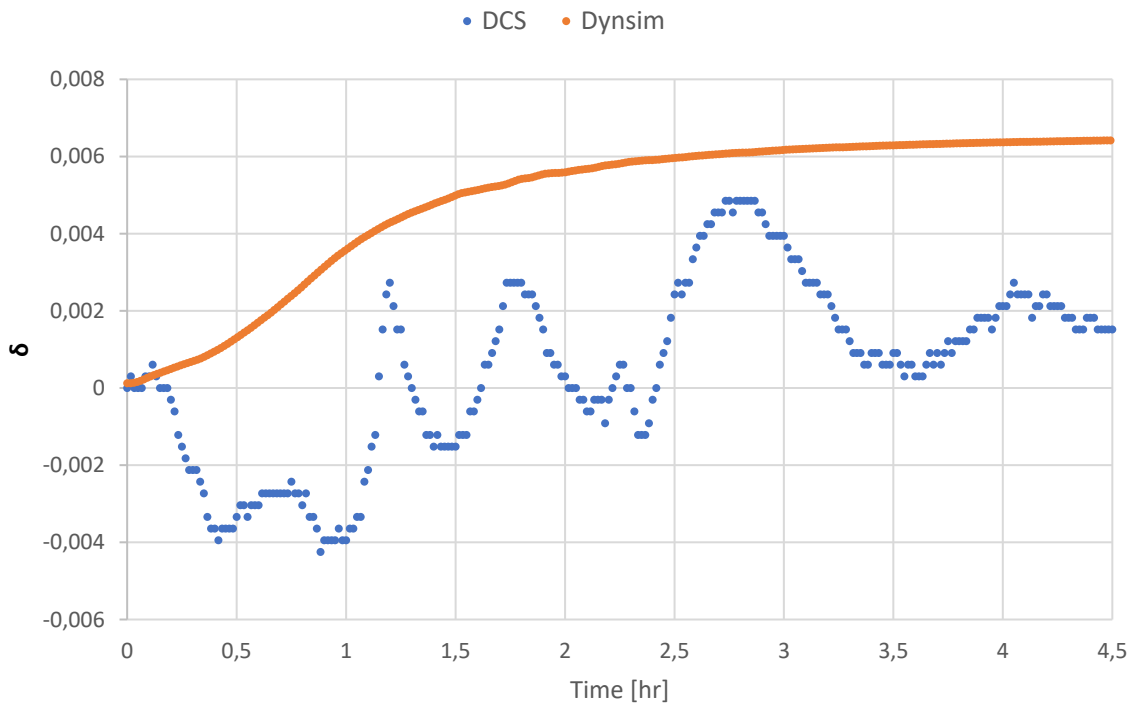

Figure 104: First pack temperature in time

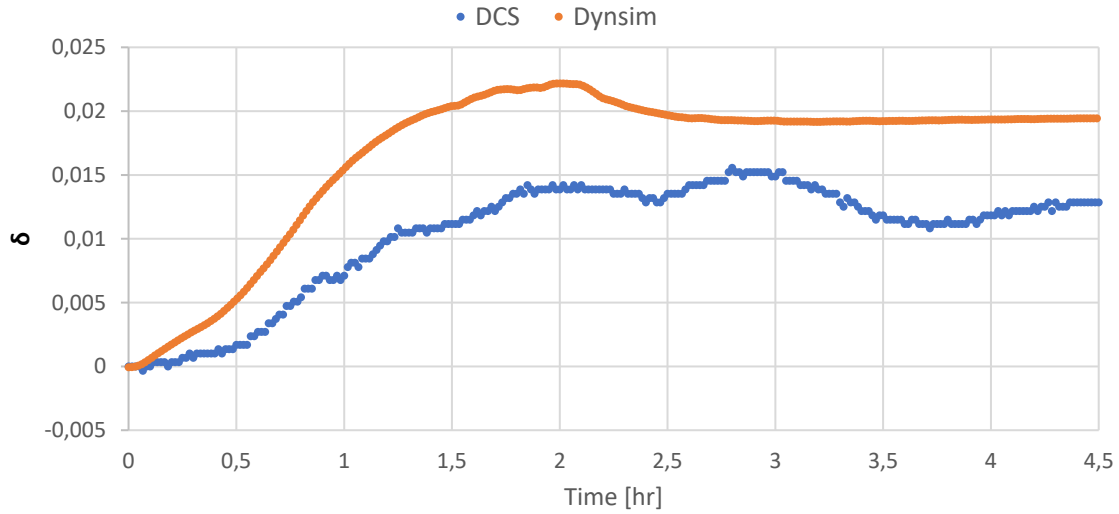

Figure 105: FLP tray temperature in time

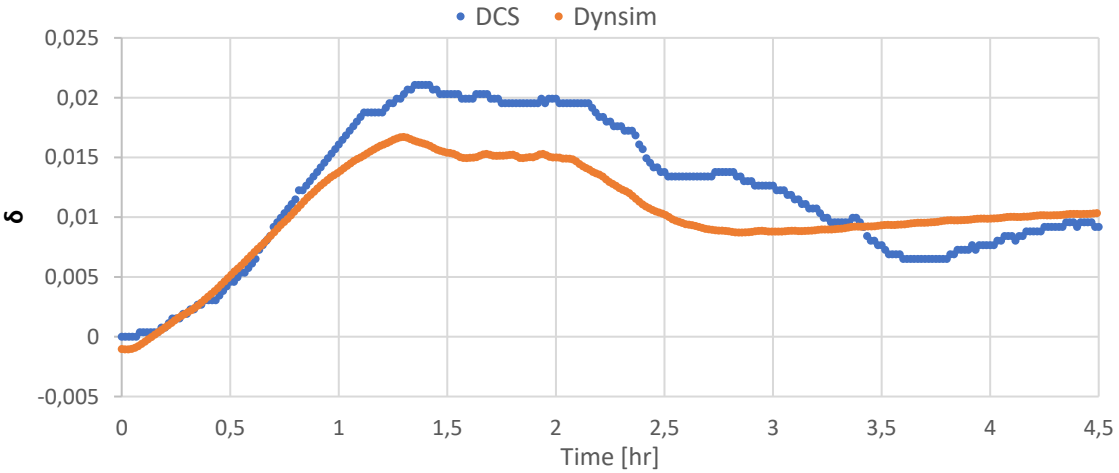

Figure 106: FLL tray temperature in time

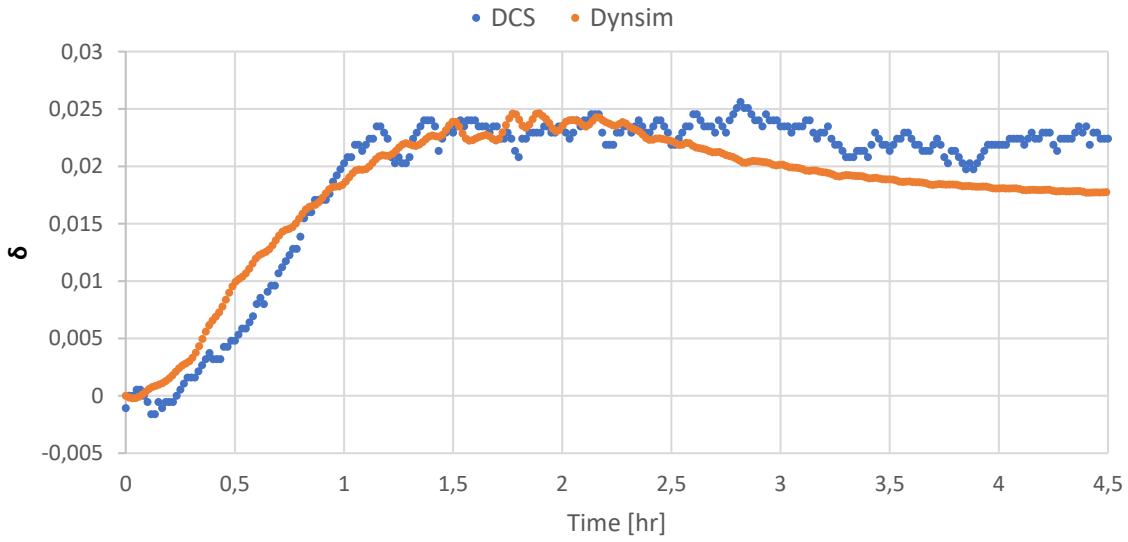

Figure 107: FLS tray temperature in time

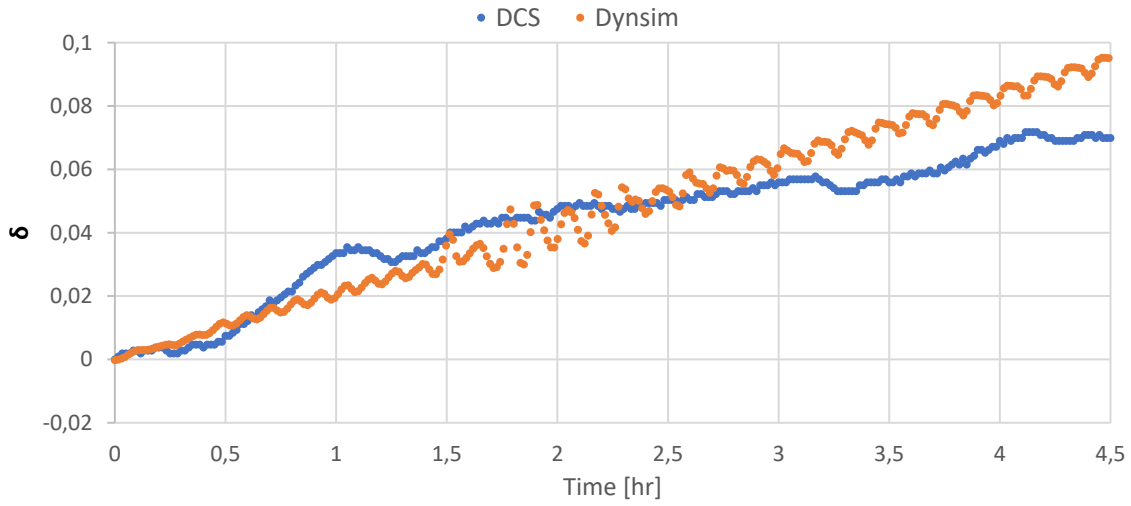

Figure 108: Fifth tray temperature in time

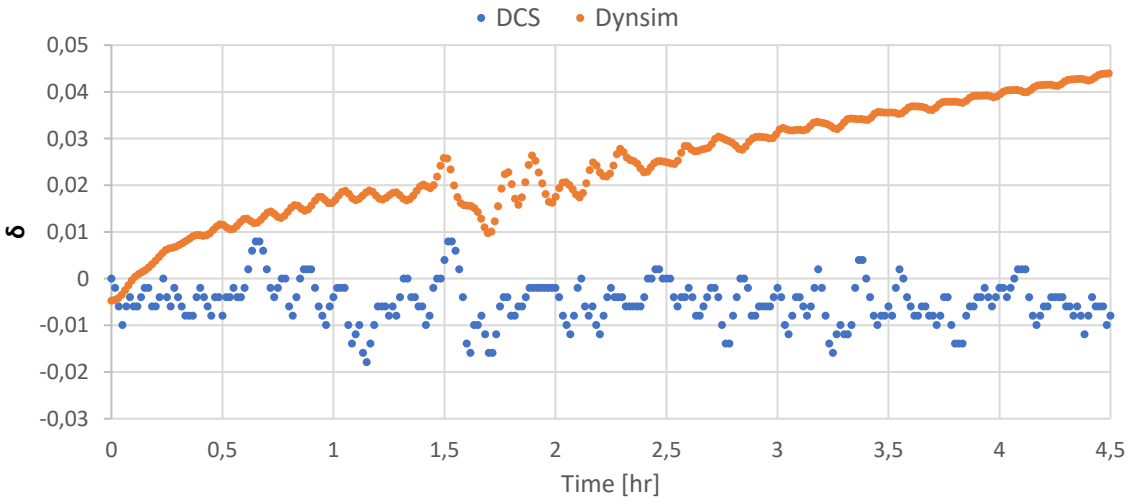

Figure 109: VGO tray temperature in time

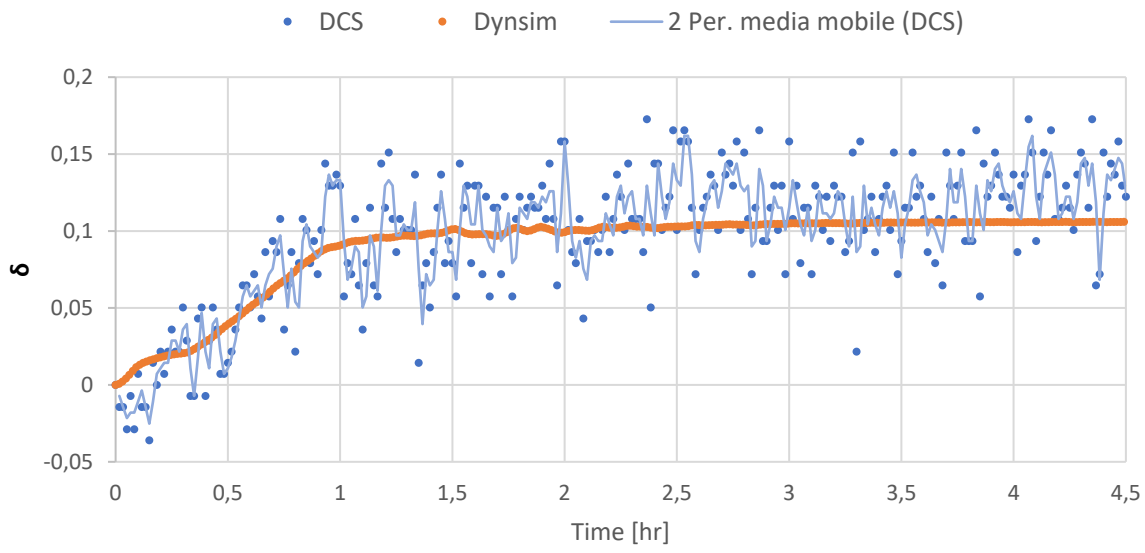

Figure 110:Pressure below first pack in time

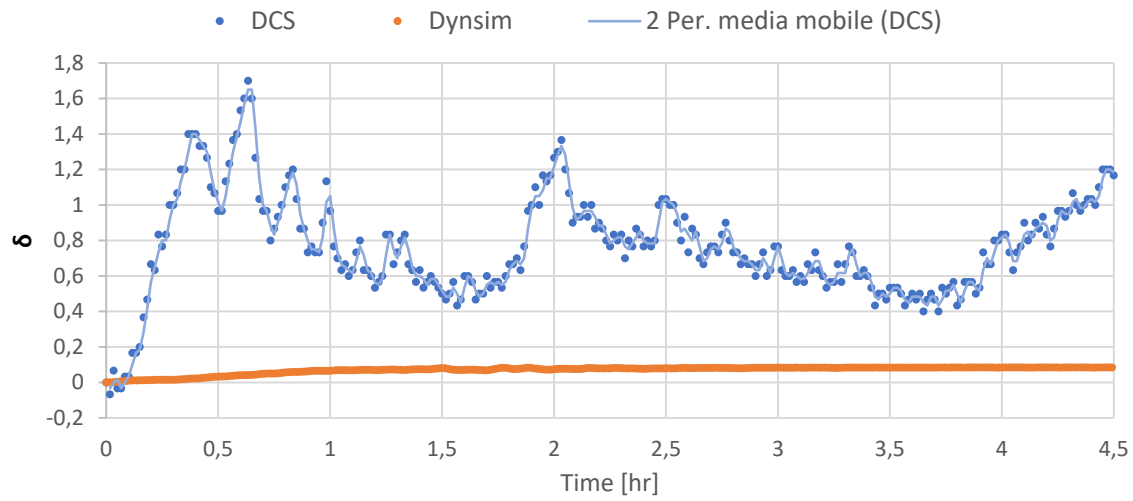

Figure 111: Pressure below third pack in time

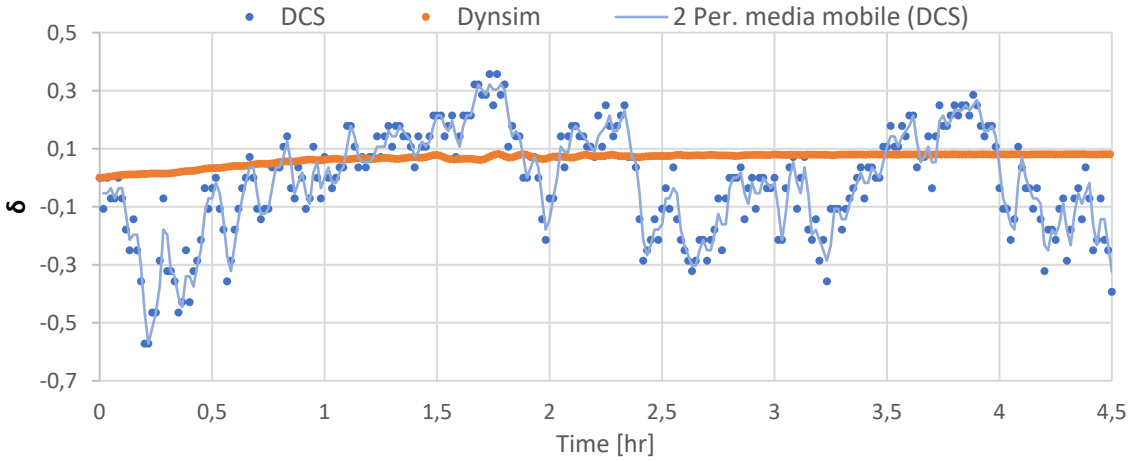

Figure 112: Pressure below fourth pack in time

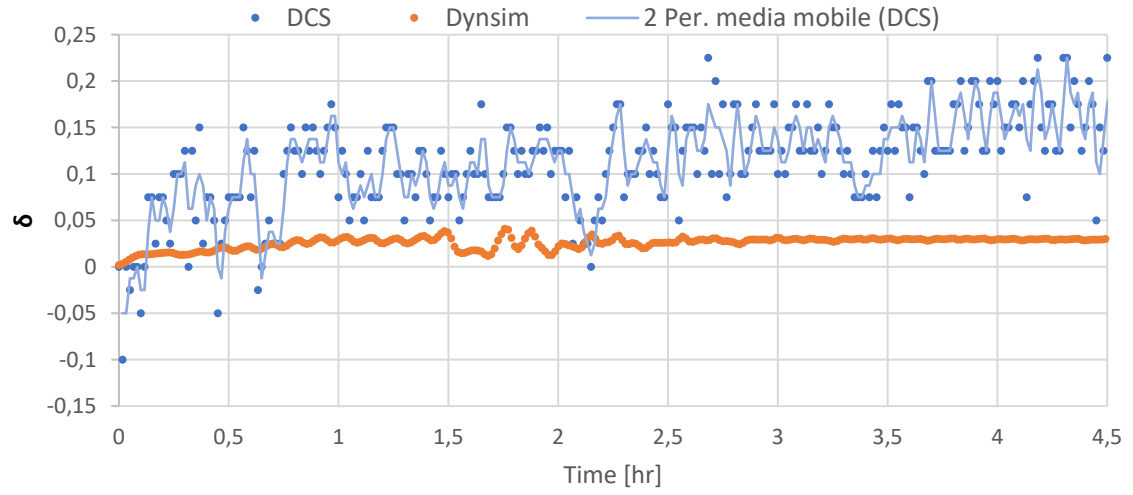

Figure 113: Pressure below fifth pack in time

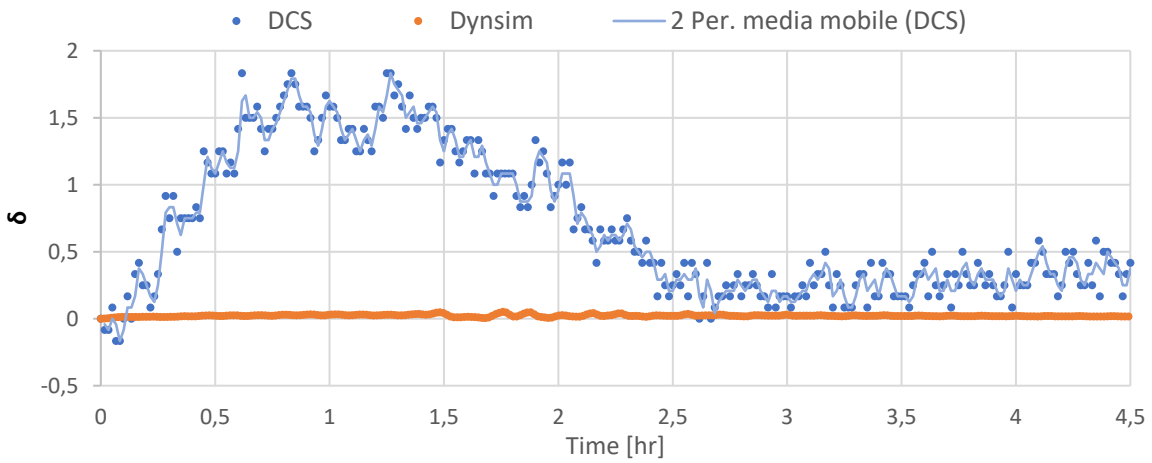

Figure 114: Pressure below sixth pack in time

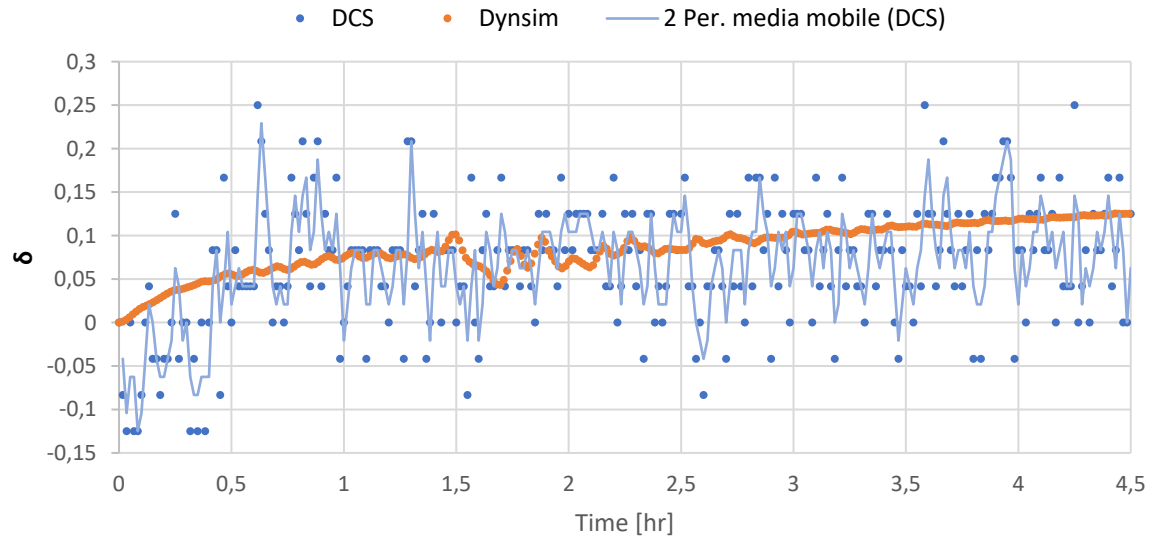

Figure 115: Top column pressure in time

	ε_T [-]
T_{first}	$4.4*10^{-3}$
T_{flp}	$7.1*10^{-3}$
T_{fll}	$3*10^{-3}$
T_{fls}	$3.3*10^{-3}$
T_{fifth}	$7.2*10^{-3}$
T_{sixth}	$2.5*10^{-2}$

	ε_P [-]
P_{first}	$3.1*10^{-2}$
P_{third}	$6.7*10^{-1}$
P_{fourth}	$1.7*10^{-1}$
P_{fifth}	$9.4*10^{-2}$
P_{sixth}	$6.2*10^{-1}$
$P_{top\ column}$	$6*10^{-2}$

Table 36: mean errors defined as $\varepsilon = \sqrt{\frac{(\delta(i)^{mod} - \delta(i)^{dcs})^2}{N\ of\ time\ steps}}$

Though pressures indicated from DCS present an extremely high variance in time and its values are not reliable, as shown in figures 3 and 4, they present similar trends to the one proposed by the models. Exceptions are present, which are in the third and below the sixth pack. The third pack pressure shows a wrong behaviour difficult to comprehend, the model could not predict the increase of pressure below the sixth pack. This may be due to the lack of change of the VGO reflux, which may cause evaporation of part of the reflux.

Temperature profiles look to be in good accordance, but some differences are present. VGO and fifth pack temperatures present discrepancies since the VGO reflux in the model could not increase. This fact leads to a temperature increase in the VGO tray and on the fifth stage. Temperature on FLP tray increases more in the model with respect to the experimental data. Lastly, the temperature trends in the first pack are different, even if the mean error is quite low. This is explained looking at the position of the temperature transmitter connected to the indicator TI-4017. In fact, it is the only one considered which is not below the liquid level, so it may be influenced from the contact intervals between hotter gas from below and colder liquid from above.

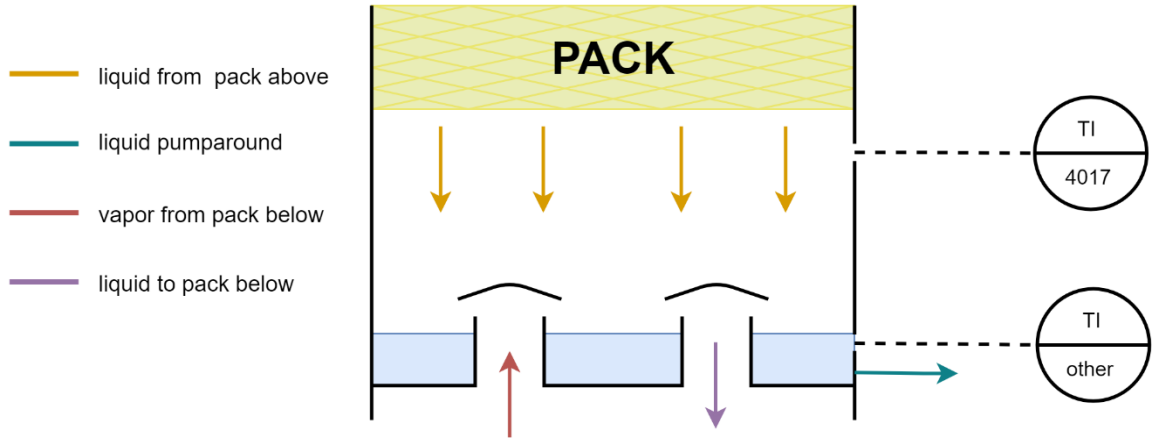

Figure 116: Temperature controller locations

In order to evaluate the real differences in temperatures predictions, since they are the reference variables through which the column performance is evaluated on field, graphs of the real variables are shown.

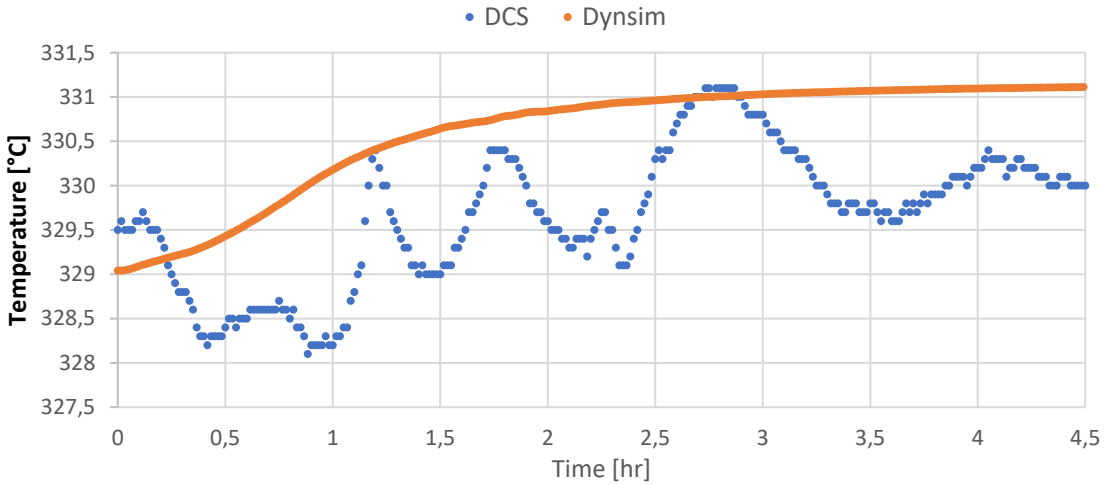

Figure 117: First tray temperature in time

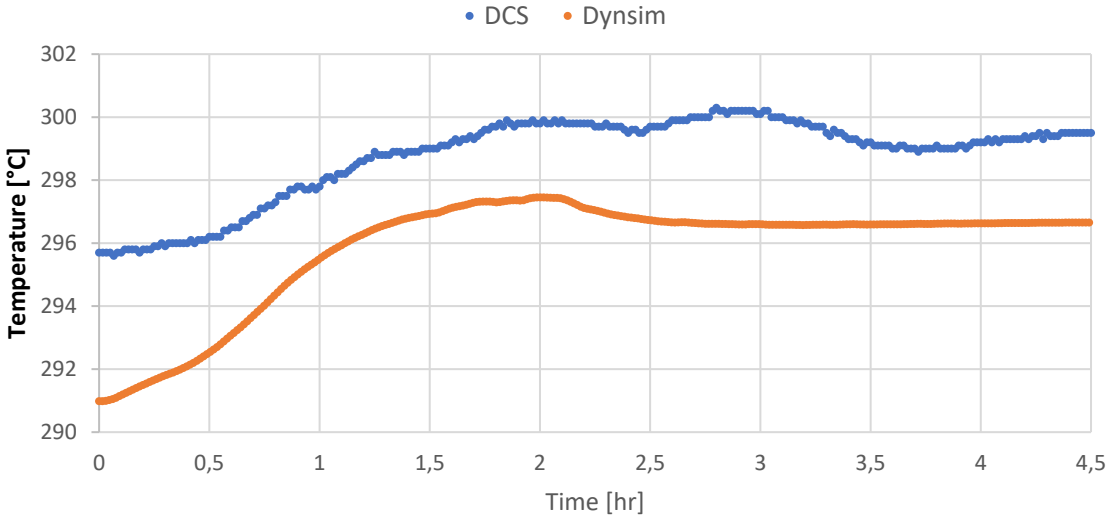

Figure 118: FLP tray temperature in time

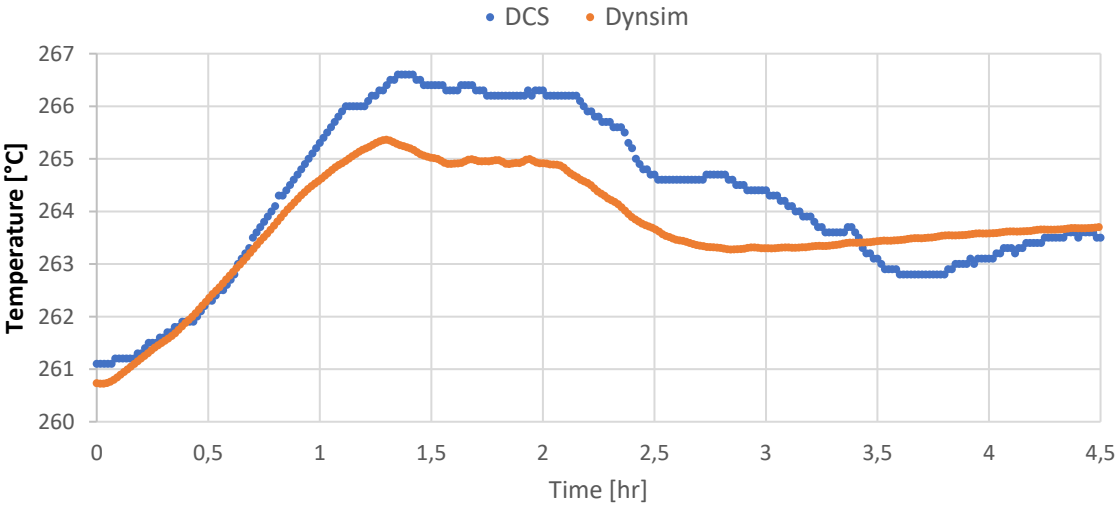

Figure 119: FLL tray temperature in time

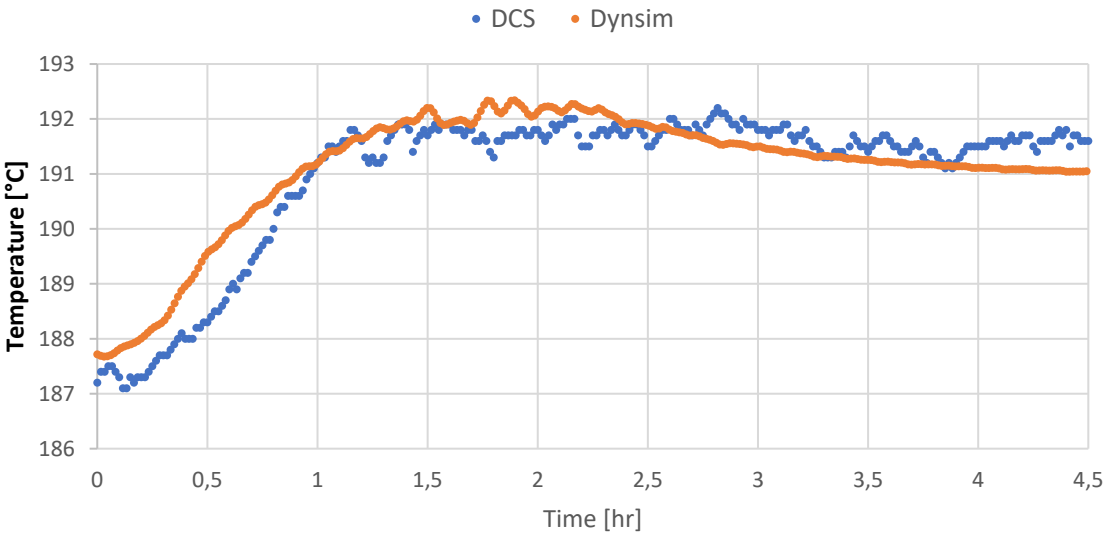

Figure 120: FLS tray temperature in time

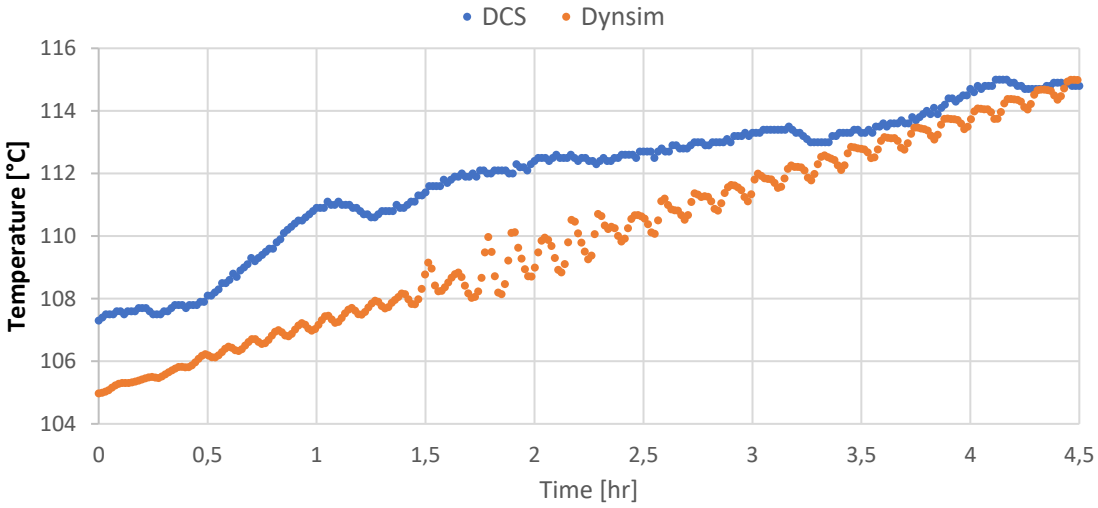

Figure 121: Fifth tray temperature in time

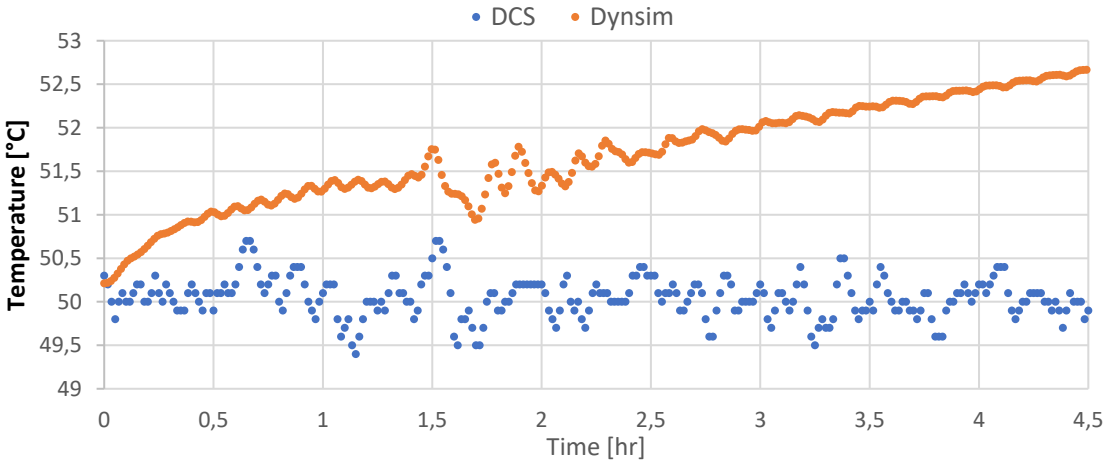

Figure 122: VGO tray temperature in time

As shown, temperature differences are not that high, even for FLP the differences are less than 0.8%. It may be noted that differences in FLP decreases increasing its temperature, probably because the modeling of the column was done only with case studies in which the tray temperature was around 305 °C, which may have penalized the model's accuracy at lower temperatures.

In conclusion, it has been showed that the model agrees well with reality. Even if pressures from DCS are not reliable, so an accurate confrontation cannot be done, it can be considered the following hypothesis. Liquid and gas flow rates can be considered reliable, since the enthalpic fluxes cause the temperature profiles through the column, which were shown to be in good accordance with experimental data. Given that gas flow rates are determined from pressure drops using the following equation:

$$\Delta P \approx F^2$$

it can be asserted that the pressure profile predicted by the column model should be accurate.

3.8. Column Startup

The dynamic model of the column has the potential to investigate new, better and safer dynamic procedures, together with transients which have never been actuated in practice. The development of such delicate operations, with the help of this model, can be done at nearly zero risk and with little expenditure.

In this thesis, it was decided to investigate a new Startup operation. The main goal of this analysis is to accelerate the procedure and increase the operative hours. This way, it can be verified if the procedure is worth implementing, considering that the saved costs have to justify the training of the operators for the new procedure, the approval route of the operation and the preparation of the additional pieces of equipment which can be involved.

Moreover, it can be checked the safety of the operation. According to the Major Accident Reporting System (MARS), 6% of major accidents in petrochemical industry can be ascribed to Startup operations [23]. Likely, this risk may be higher for new procedures, while some minor inconvenient can also occur, like flooding or cavitation of a pump. Of course, the limits of a dynamic model, which is not meant to describe accidents, must be considered. Air leakages, water retainment and freezing, mechanical and thermal stresses must be analysed separately.

3.8.1. Limits

Besides the limits regarding the security of the operation, some other issues have to be analysed. In particular:

- The column's feed considered for the Startup is the one cracked by the furnace during steady state operation. Much probably this is not the real case, since its temperature rises in a ramp of 6 hours due to technical reasons linked to the furnace itself. This compromise was necessary since a kinetic model was not implemented, so it is impossible to consider a more and more present cracking in time;
- Column battery limits are static, since sources and sinks cannot modify their composition, pressure and temperature conditions, so the steady state values were kept. Pressure influences the mass flow of streams directly and indirectly linked to those limits and unfortunately its influence can't be quantitatively defined. The source temperature which is more relevant is the feed one, which comes before the furnace. This was kept at 140 °C, which is anyway a reasonable value, since it is the preflash operational temperature and it is likely to be reached before the column Startup to remove water and solvents. The other temperatures are linked to the vapor stream utility sources, which are likely to be constant. Lastly, what happens in practice is that the flow exiting the cyclone is sent to the feed tank before the column, during the starting phase of the Startup. The influence on the feed composition cannot be considered;

- Since it was decided not to implement a rigorous model of the vacuum group, a solution was needed to simulate the conditions in which the ejectors are not operating. The choice was to split the vapor outlet, locating an additional sink with a different value of the pressure (Figure 123).

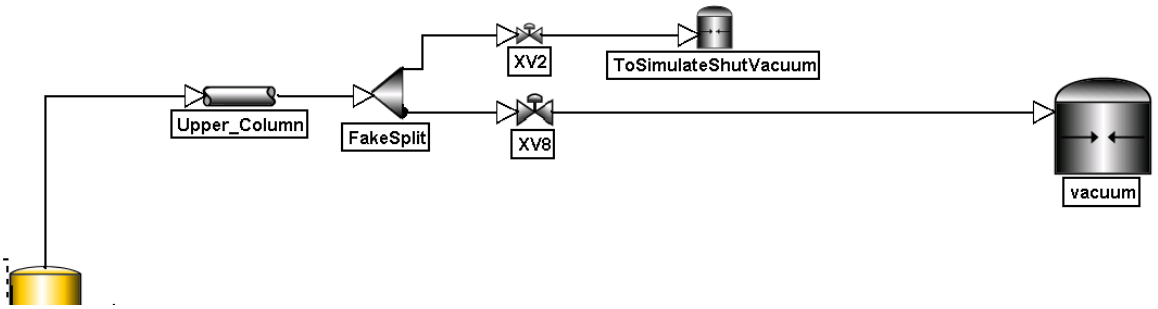

Figure 123: Top sink split

The main limit of this approach is the impossibility to evaluate the behaviour of the Ejector group;

- Water draining and inerting of the column cannot be simulated properly, since the model considers only equilibrium stages and cannot keep into account stagnation or blanking.

3.8.2. New Startup procedure

As said, a new procedure may be appetible if it permits to save costs, so if it is quicker than the actual operation, without or with little investments and additional operative costs.

The limiting time step of this operation is the column heating up, especially of the packs 4 and 5, which need to reach temperatures in the range of 180 °C to 200 °C, that can only be reached after packs 1, 2 and 3 are heated. For this purpose, it was considered to use kettle E-408, heated with the high-pressure steam line which during steady state is mixed with the low-pressure steam generated by the kettle reboiler. Thought that line is linked only to the heat exchanger steam effluent, it was confirmed that it may be possible to connect it to the kettle and use it as a heater. Such steam is produced at 15 bars and 205 °C.

Before starting with the procedure, the initial conditions have to be discussed. The column is set under vacuum, at the pressure of about 10 torr. Starting the column under vacuum helps avoiding liquid accumulation in the bottom, favours the column heat up due to the feed evaporation and permits to check the vacuum endurance itself. A wet Startup was chosen, since it permits safer operations, avoiding blanking and pump cavitation, and a quicker adjustment of the column to the steady state. For this purpose, the lube oils and the VGO are fed to the respective product trays of the column, which was previously filled with nitrogen. Clogging is not likely to occur since the products

pour point does not exceed -9°C. Liquid levels of each tray are set above the product outlet, in order not to have cavitation when the pumps are turned on. Moreover, liquid levels of the FLS and the VGO trays are kept as high as possible, since the flow demand to the exchangers may dry such trays. The exchangers are also filled with liquid. The starting temperature of the column is set at 25 °C.

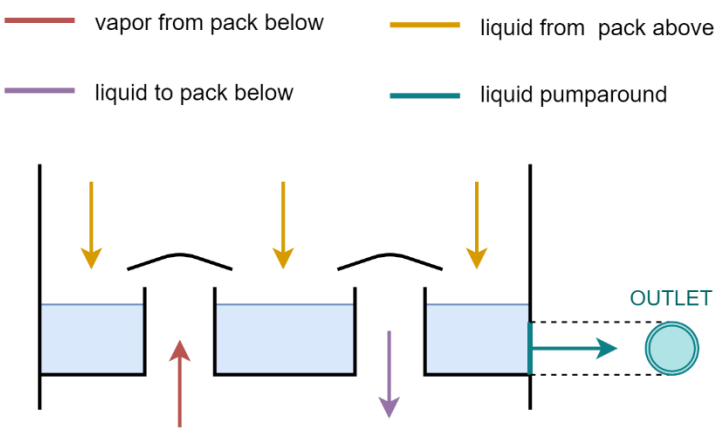

Figure 124: Liquid in trays in pre-startup conditions

The procedure itself is now discussed in Table 37. The outline was built analysing the column response to each operation and using the procedure followed by Viscolube as a reference, especially whenever technical issues has to be considered.

Time [hr]	**ACTION**
IC	ALL CONTROLLERS ON MANUAL
	ALL VALVES ARE SHUT
0:00	SET LIC-4095.SP = 0 %. Keeping the level of the cyclone as low as possible minimizes the thermal inertia
	SET FIC-4058.SP = 4000 kg/hr
1:00	RAMP FIC-4058.SP = 12000 kg/hr and TIC-4079.SP = 365 °C in 6 hr. Thought this is the main heat provider to the column, it can't be accelerated due to technical issues linked to the furnace
	TURN ON PUMP P-420 and SET LIC-4096.SP = 20% not to flood the column base
4:00	Once TI-4017 indicates a temperature of 130 °C, TURN ON P-421 and SET FIC-4074.SP = 1400 kg/hr to heat up the liquid below the second pack. This can't be done before because the tray would have dried

4:30	It can be started heating packs 4 and 5 using steam. Starting earlier would bring the packs on temperature too soon, wasting steam for no reason. The approach used was to heat up the packs as soon as the FLL product tray reaches the temperature of 85 °C, **TURN ON P-411, SET TIC-4060 in manual, total open**, to recover the steam and make it flow and **SET FIC_4088.SP = 30000 kg/hr**. Successively, the liquid on the FLS tray can be refluxed to the pack below to heat it up
5:00	As soon as the temperature of the second pack is above 105°C, **TURN ON PUMP P-404** and **SET FIC-4059.SP = 1440 kg/hr** to heat up the liquid on the FLL tray
	As soon as the temperature on the FLS tray reaches 150 °C, **TURN ON PUMP P-406** and **SET FIC-4060.SP = 1800 kg/hr**
5:15	As pack 6 reaches the temperature of 50 °C, **TURN ON PUMP P-408** and **SET TIC-4033 AND TIC-4035 on AUTO**, to maintain the vacuum;
	As the column feed reaches the temperature of 300 °C, **TURN ON VACUUM GROUP** (Main Ejector). In our simulation, this correspond to close valve XV2 and open valve XV8 (Figure 126)
	SET LIC-4102 and SET LIC-4188 on AUTO to avoid flooding
5:30	As TI-4017 indicates a temperature of 180 °C, **SET FIC_4186.SP =1420 kg/hr** to wash the vapor that rises from the cyclone
	SET FIC-4059.SP = 2000 kg/hr, increasing the reflux
	SET LIC-4095.SP = 25%
6:30	**SET LIC_4098 on AUTO** to prevent flooding
	As soon as the FLL tray reaches the temperature of 180 °C, **STOP HP FLOW and CLOSE TIC_4060**, since the vapor from below can heat the pack 4 and 5
7:00	**SET LIC_4100 on AUTO** to prevent flooding
7:15	As soon as the FLL tray reaches the temperature of 250 °C, SET **FIC_4060.SP = 7500 kg/hr** to heat the liquid on the FLS tray
7:40	Once TI-4017 indicates a temperature of 300 °C, **SET FIC_4074.SP = 700 kg/hr**, taking the reflux to standard values

8:00	Once FLS tray has reached the temperature of 190 °C, **RAMP LIC_4186 at SP in 30 min** to cool pack 4 and 5 gradually
8:30	Once FLP tray has reached the temperature of 290 °C, **SET FIC_4059.SP = 0.972**, increasing the reflux
	SET TIC_4034 AND TIC_4087 on AUTO
	SET TIC_4066 on AUTO, producing low pressure steam

Table 37: Startup procedure

3.8.3. Results and comments

Below are discussed the column profiles and some other aspects regarding its behaviour. A comparison between this procedure and the other from Viscolube was also made.

Cavitation of the pumps was checked. To avoid this issue, it is sufficient that no vapor enters the involved lines and that $NPSH_a > NPSH_r$. The vapor fraction of the flow entering the pumps was kept at 0 by controlling the liquid levels, as indicated in the procedure. The available Net Positive Suction Head was certainly always above the required one for pumps connected to the trays, since the volumetric flows during this procedure never exceeded the steady state operative ones. A separate comment is dedicated to pump P-402. Considering that the maximum volumetric flow (Q) reached was about 6.5 m^3/hr, and that the liquid draw from the cyclone is set at a height 25% higher than the required Net Positive Suction Head, we can verify the absence of cavitation:

$$NPSH_r = 1\ [-]\ \ Fictitious\ value, since\ the\ real\ value\ can't\ be\ reported\ in\ this\ thesis$$

$$L_{tube} = NPSH_r * 3\ [-]\ \ Inclusive\ of\ tube\ length, filters\ and\ elbows$$

$$Height = -NPSH_r * 1.25\ [-]\ Minimum\ liquid\ free\ surface\ level$$

$$Re = 60.000[-]\ Turbulent$$

$$f = 0.03[-]\ Asymptotic\ value\ of\ the\ friction\ coefficient$$

$$NPSH_a = -Height - \ 4 * f * L_{tube} * \frac{v^2}{D * 2 * g} = 1.24\ [-] > \ NPSH_r$$

The steam sent to the kettle in this procedure was set to 38.5 ton/hr for two hours. According to the simulation, 38 ton/hr of steam at 14.6 bar and 198 °C, which is approximatively 98.7% of the used steam, nearly at the boiling point. Such steam can be re used, significantly reducing its net cost.

Below, the graphs reporting the most significant temperature and pressure profiles are reported.

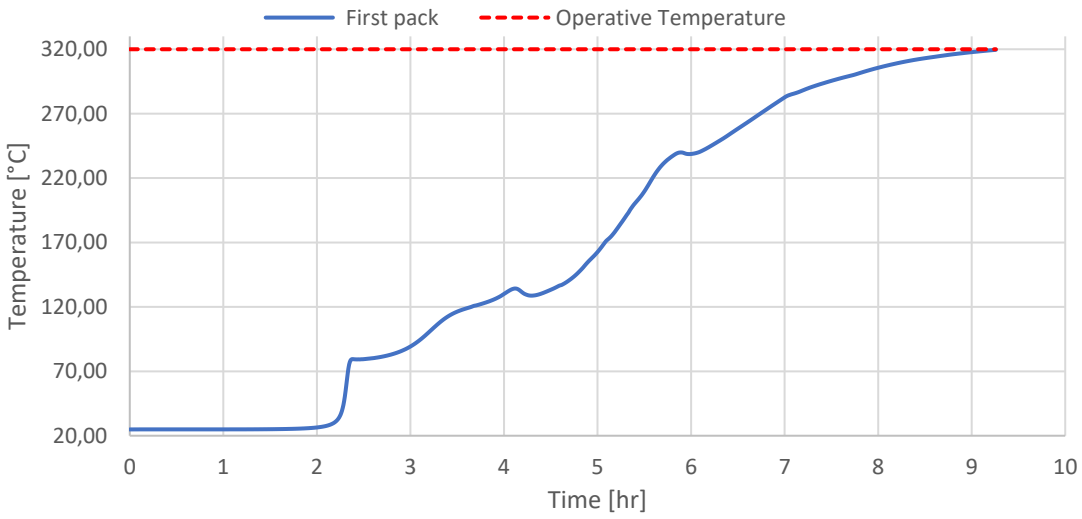

Figure 125: First tray temperature

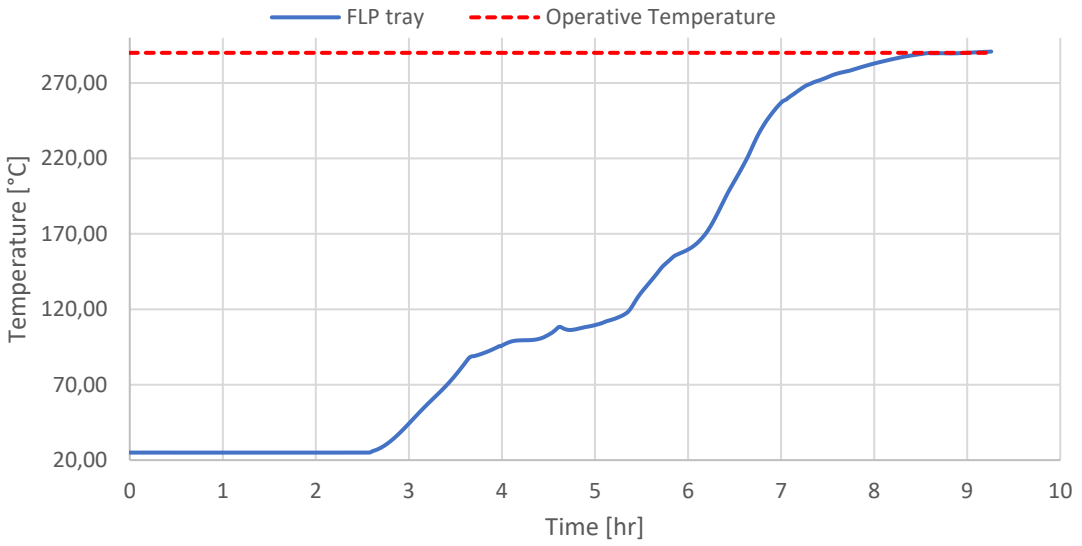

Figure 126: FLP tray temperature

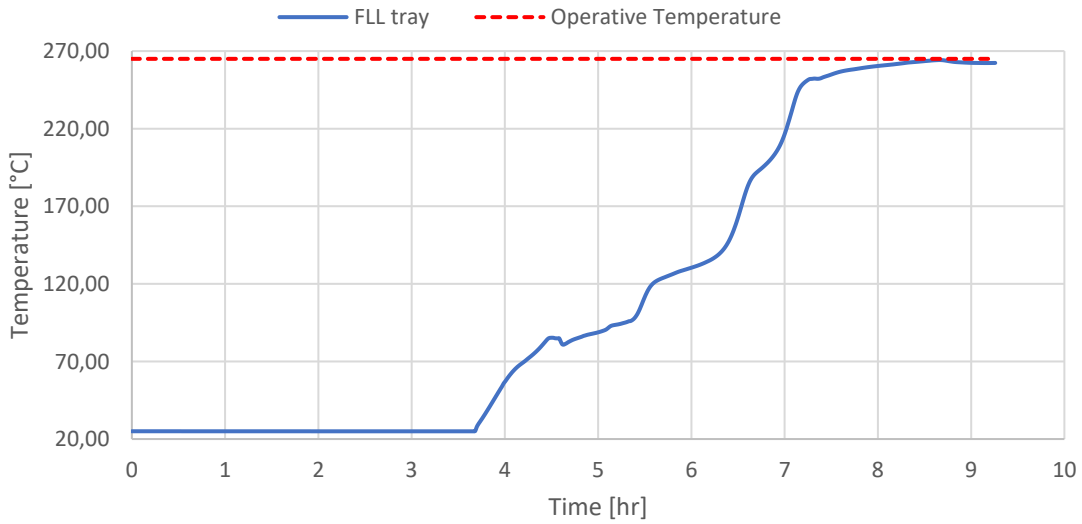

Figure 127: FLL tray temperature

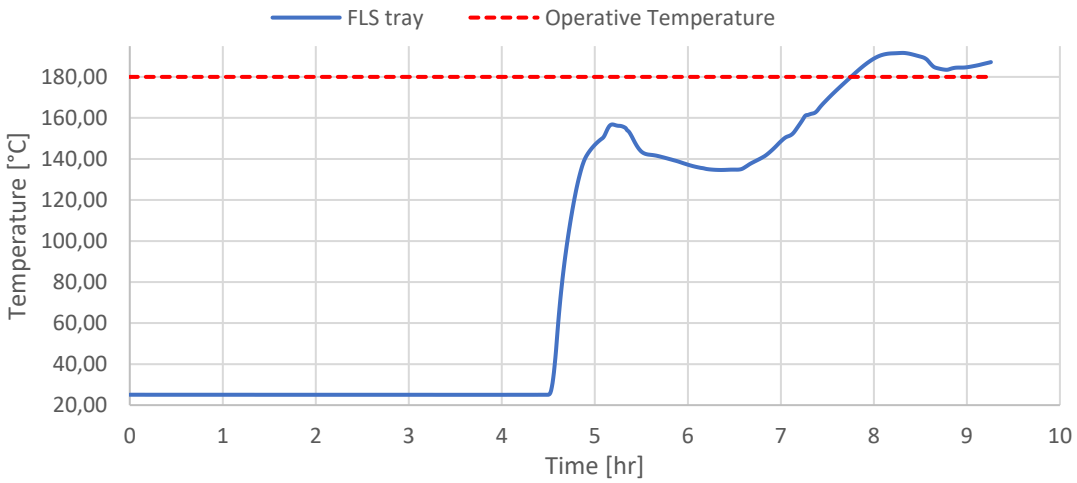

Figure 128: FLS tray temperature

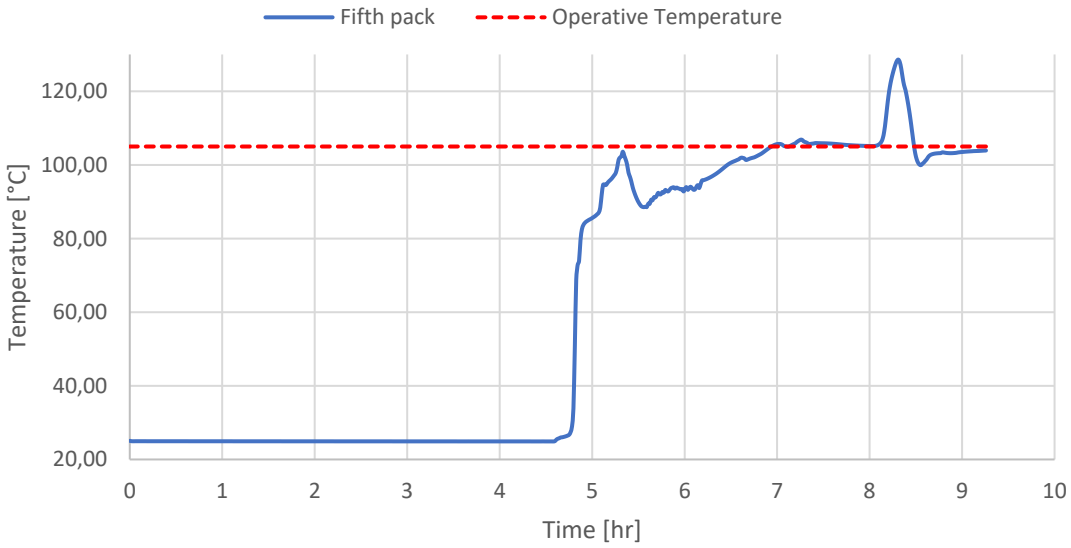

Figure 129: Fifth pack temperature

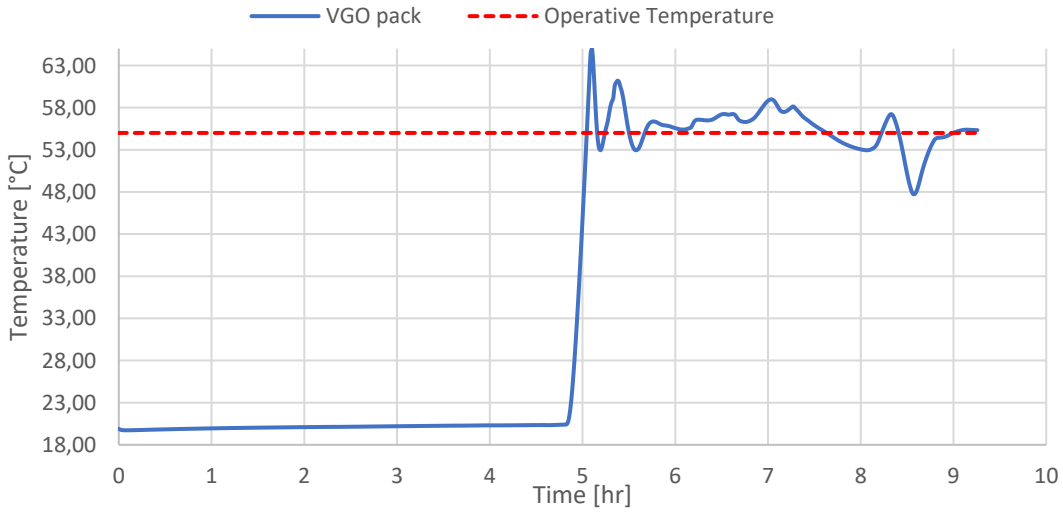

Figure 130: VGO tray temperature

It is clearly noticeable that using this procedure the column reaches operative conditions in 8-9 hours. Profiles for the lower packs are almost monotonically increasing, exception made for some decreases caused from the increase of cold refluxes from above. Profiles of the upper section of the column, starting from the FLS tray, are nearly fixed until the high pressure vapor is provided. This proves how much it can be beneficial. Besides, the hot reflux from the FLS tray to the FLL pack seems to give little contribution to its heating. No alarming temperature increase, or picks, have been reported.

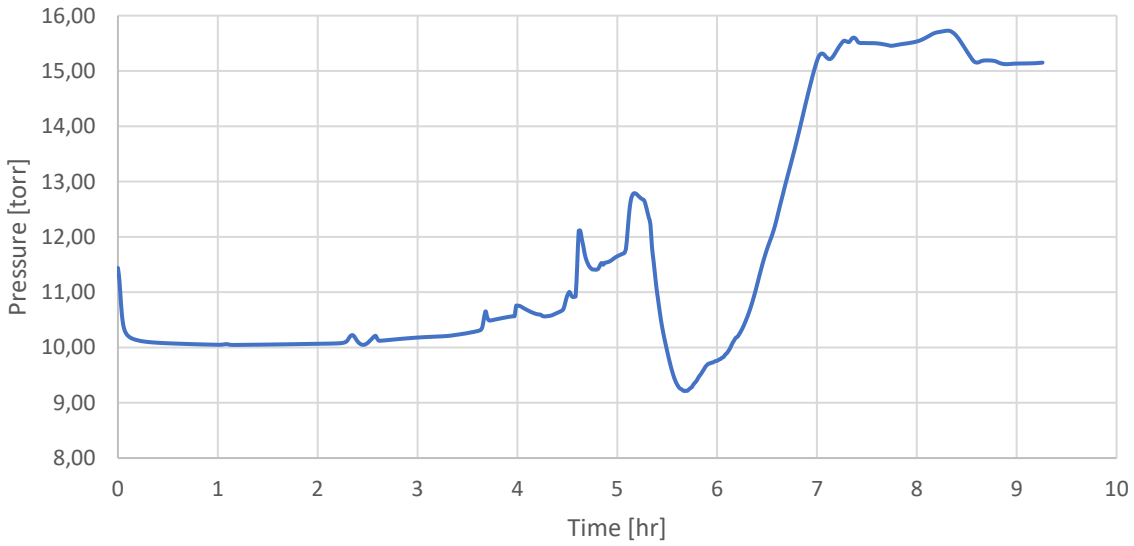

Figure 131: Pressure first pack

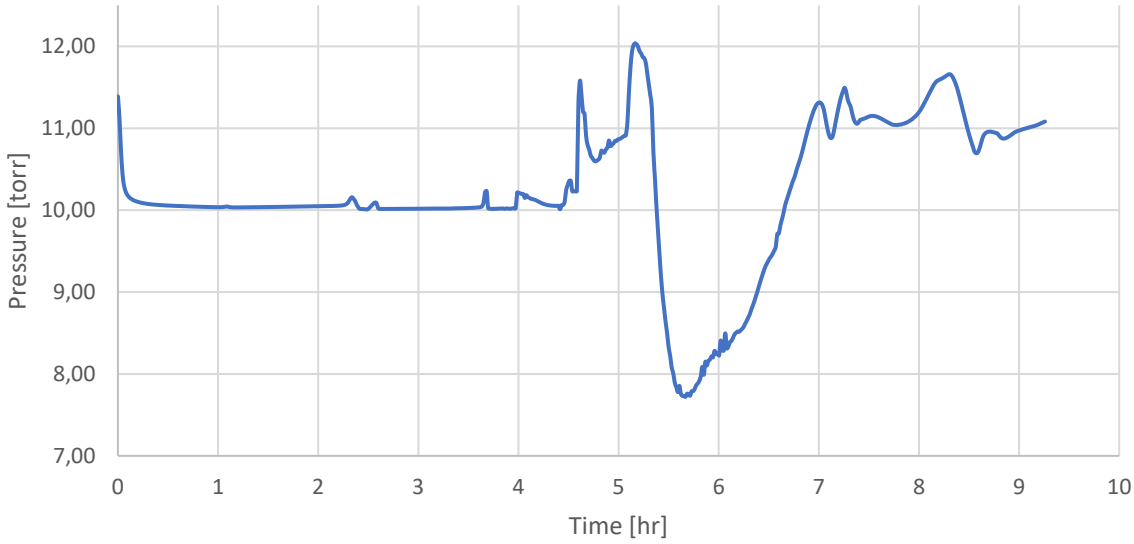

Figure 132: Pressure FLL tray

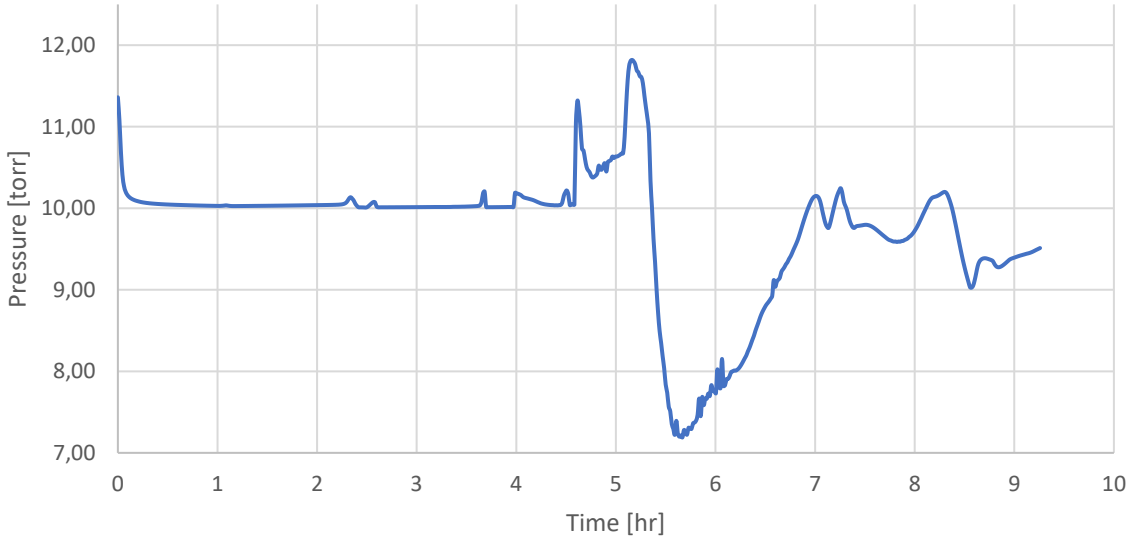

Figure 133: Pressure FLS tray

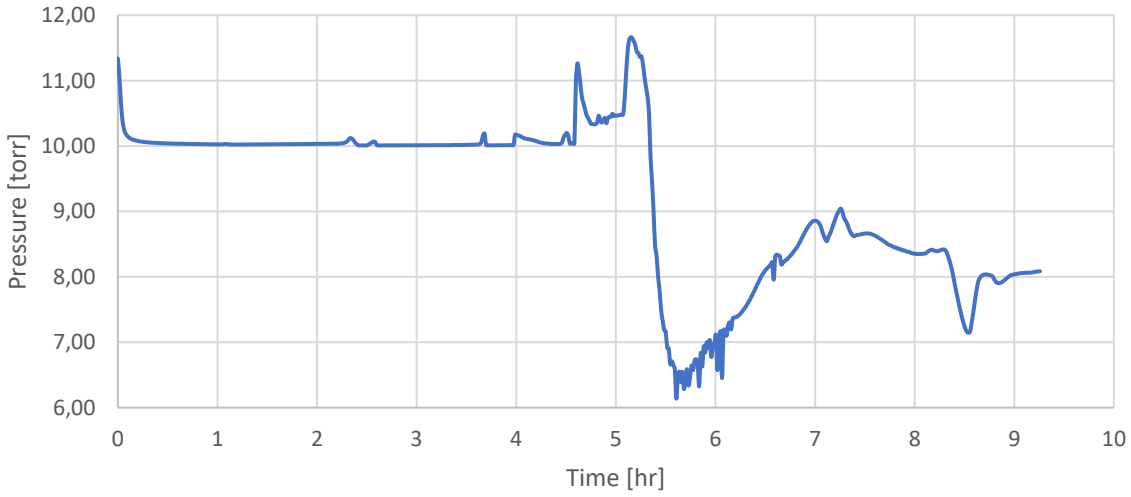

Figure 134: Pressure fifth pack

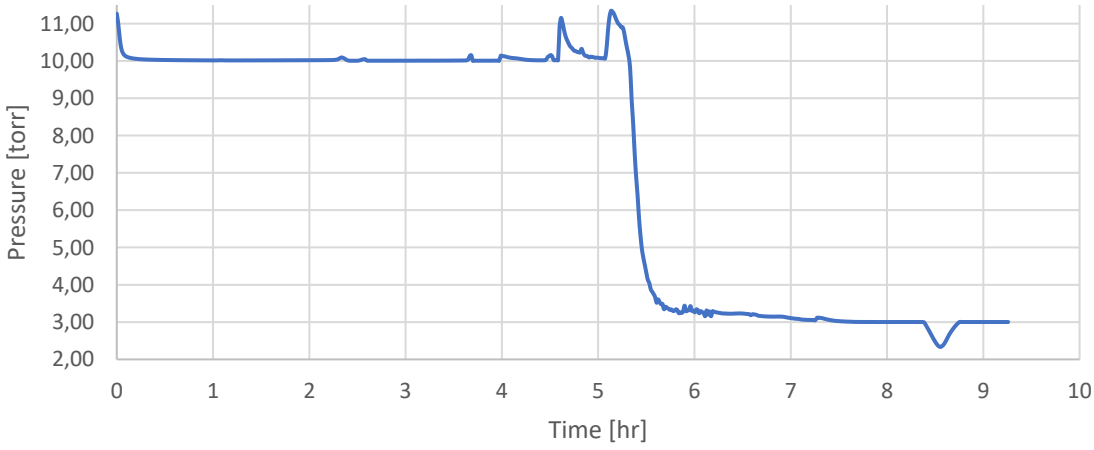

Figure 135: Pressure top column

The pressure profile in the column is almost identical for every stage. The initial, slow increase which is less and less notable going up through the column is caused from the increasing vapor flow in time. Once the main ejector is turned on, the column suffers a slight depressurization but not severe, the magnitude is in the order of 5 torr.

Finally, a comparison between our column profiles during Startup and Viscolube's was done. Unfortunately, only a partial startup was available from their data historian, where the column was not cooled to ambient temperature. To compare the behaviour, it was decided to start from the condition at which the real column was colder and the simulation time when the temperatures of the first pack, of the simulated and the real column, matched.

The feed in the real case study followed a ramp of 4 hours, starting from a temperature of 200 °C to 365°C and a flow of 4300 kg/hr to 13000kg/hr.

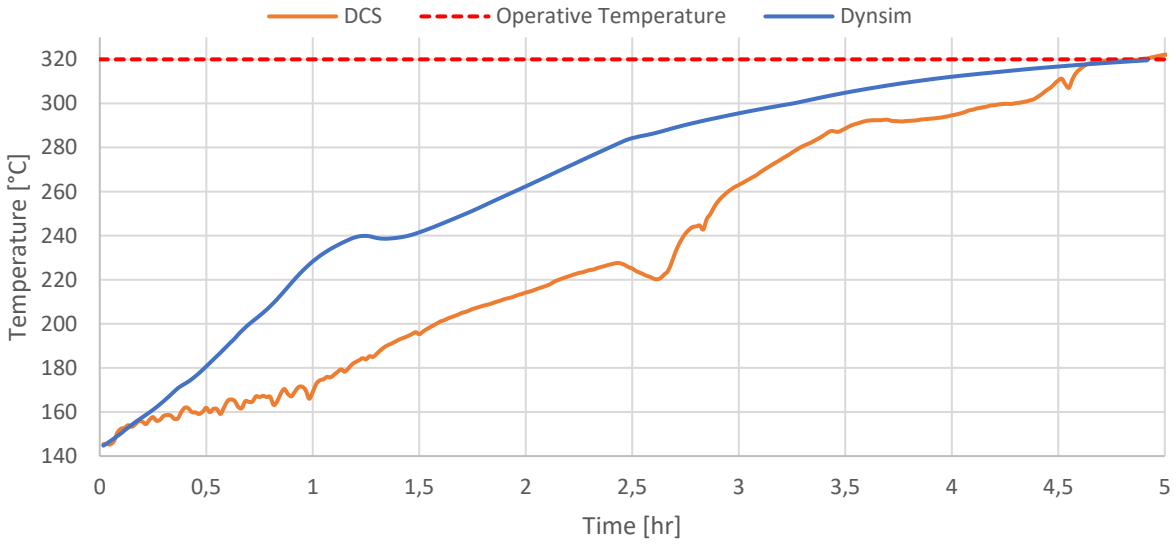

Figure 136: Temperature first tray

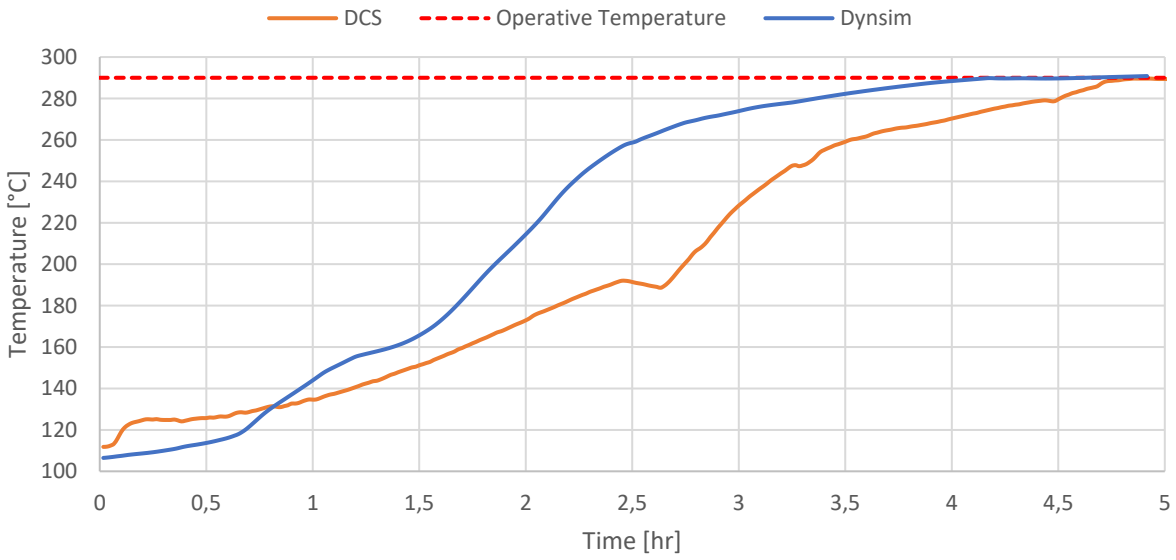

Figure 137: Temperature FLP tray

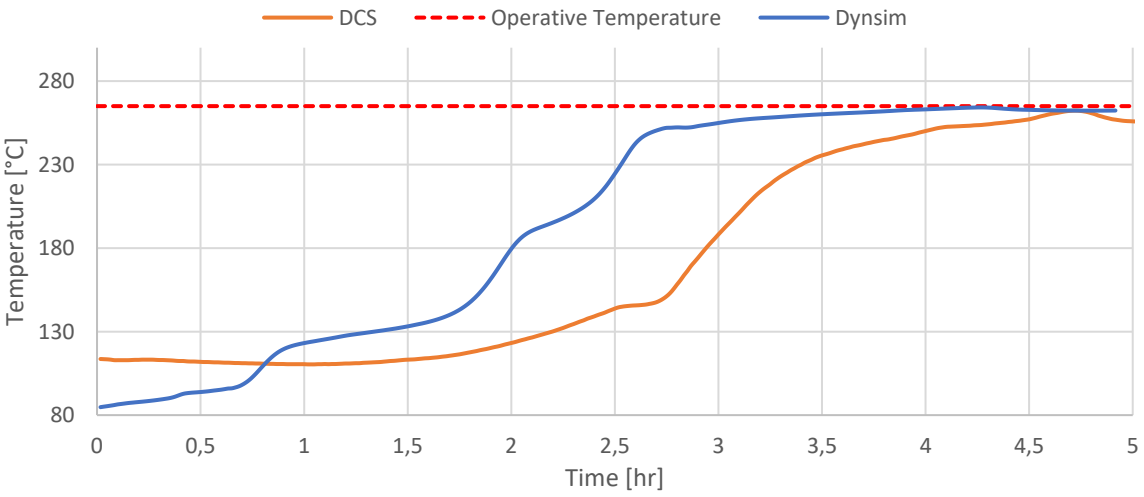

Figure 138: Temperature FLL tray

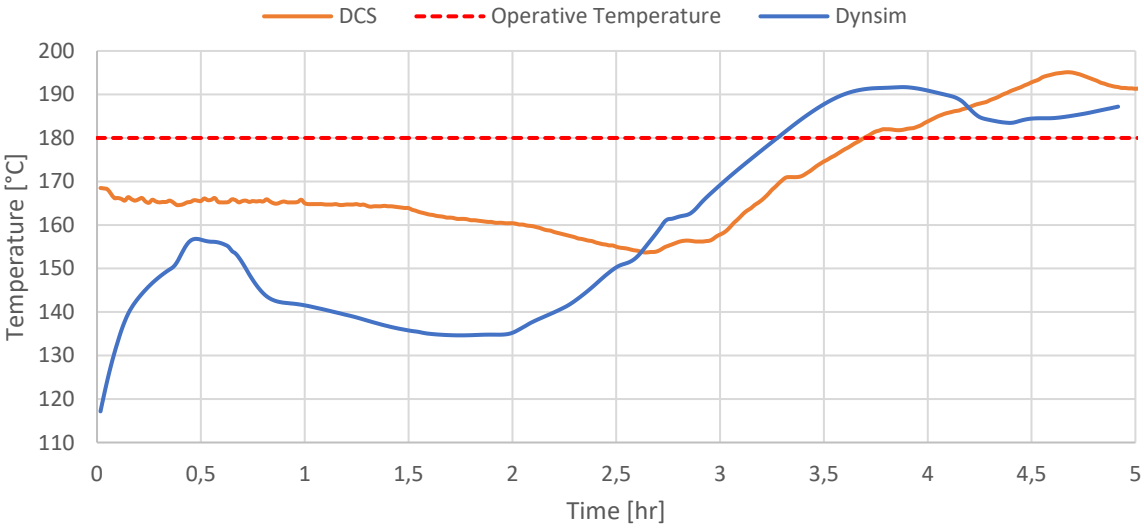

Figure 139: Temperature FLS tray

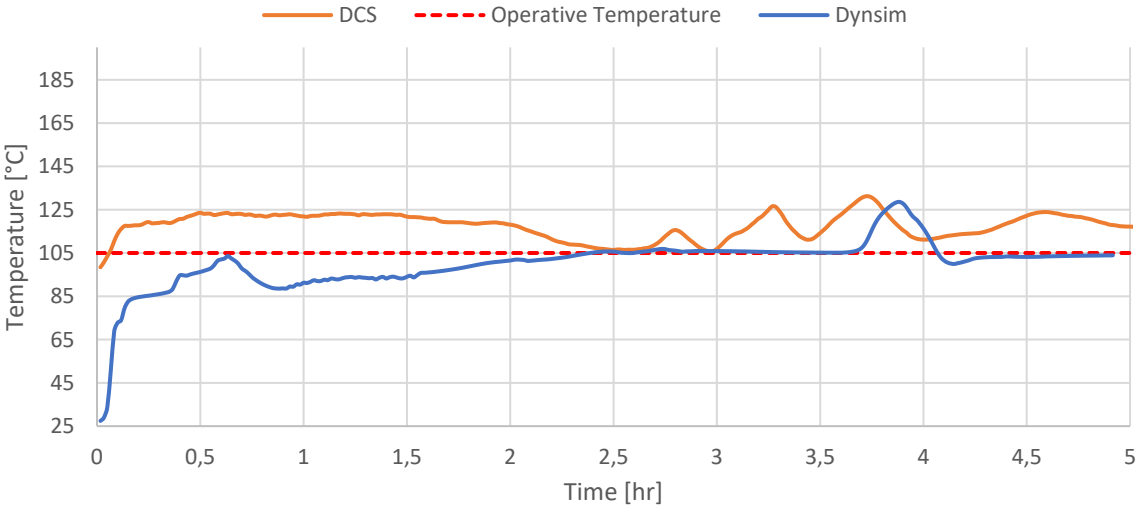

Figure 140: Temperature fifth pack

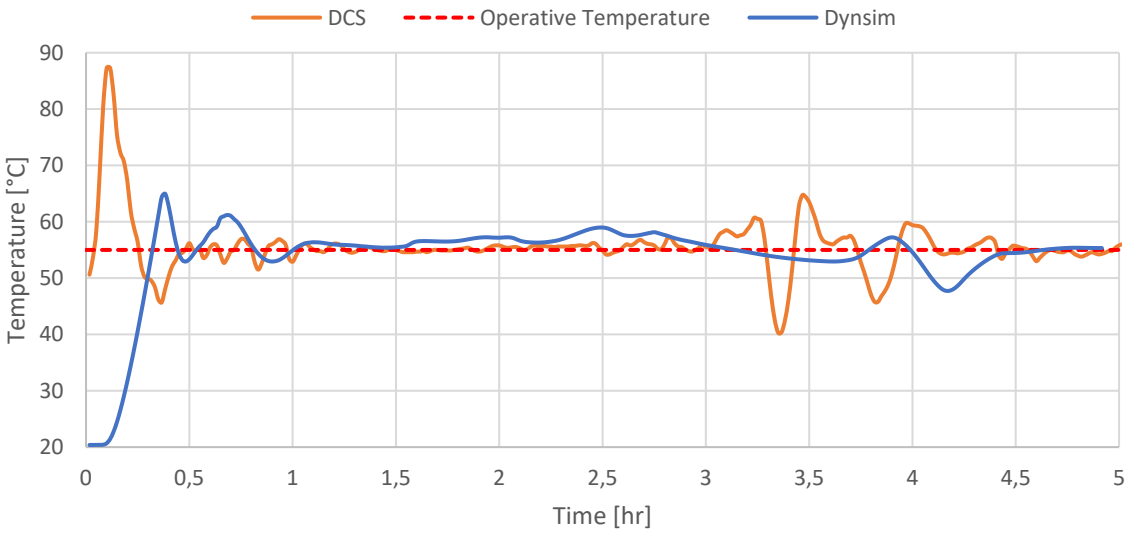

Figure 141: Temperature VGO tray

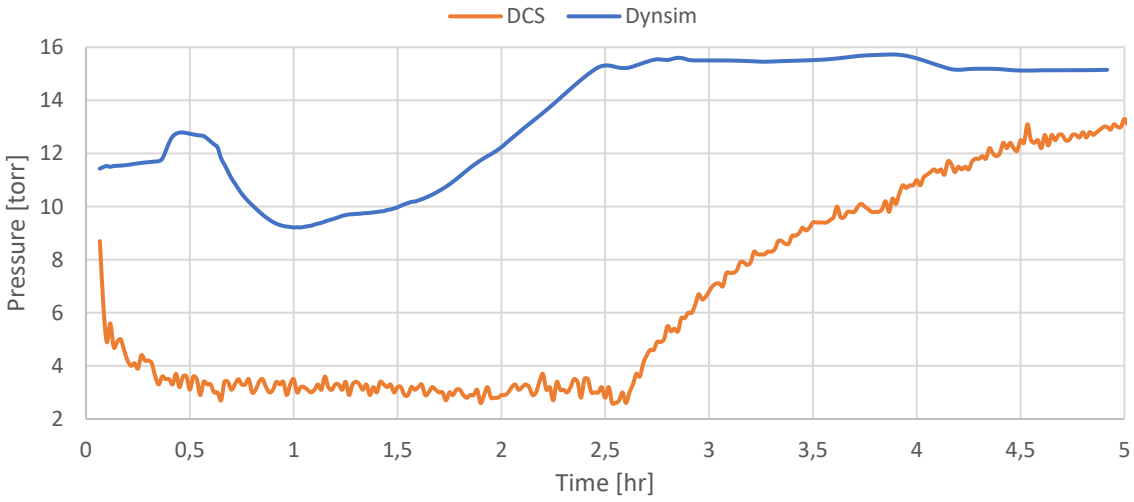

Figure 142: Pressure first pack

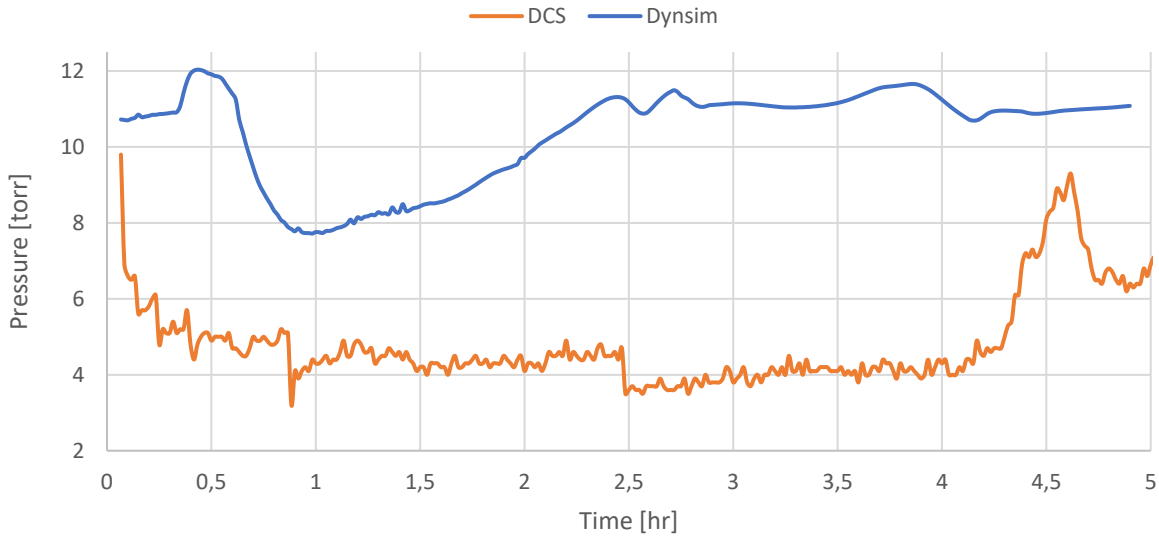

Figure 143: Pressure FLL tray

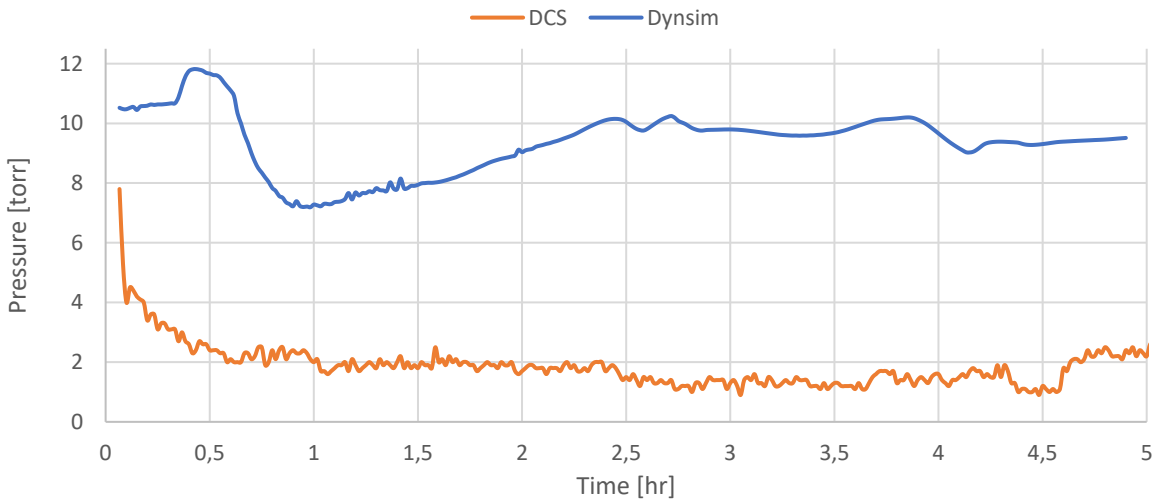

Figure 144: Pressure FLS tray

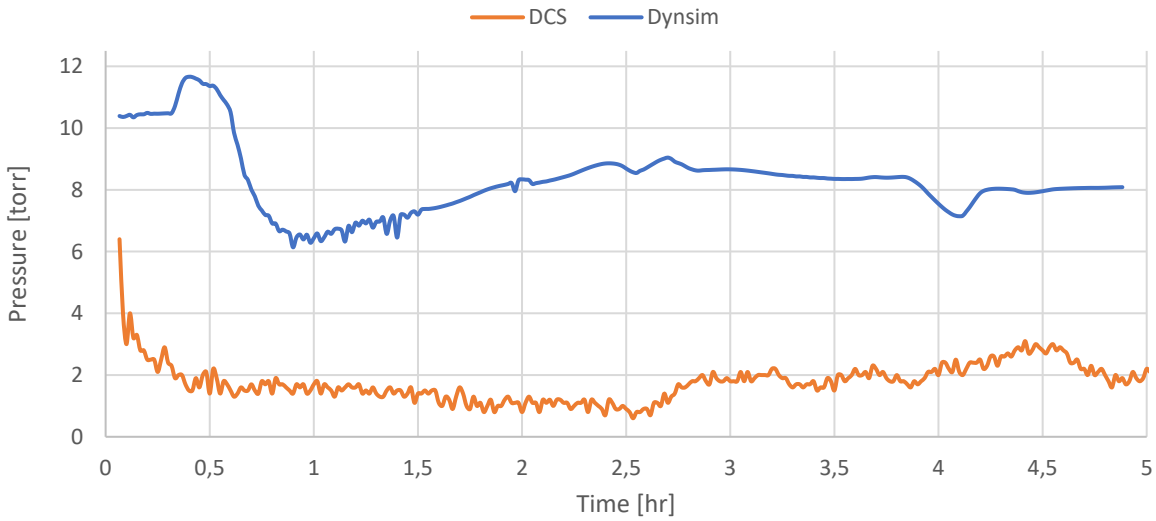

Figure 145: Pressure fifth pack

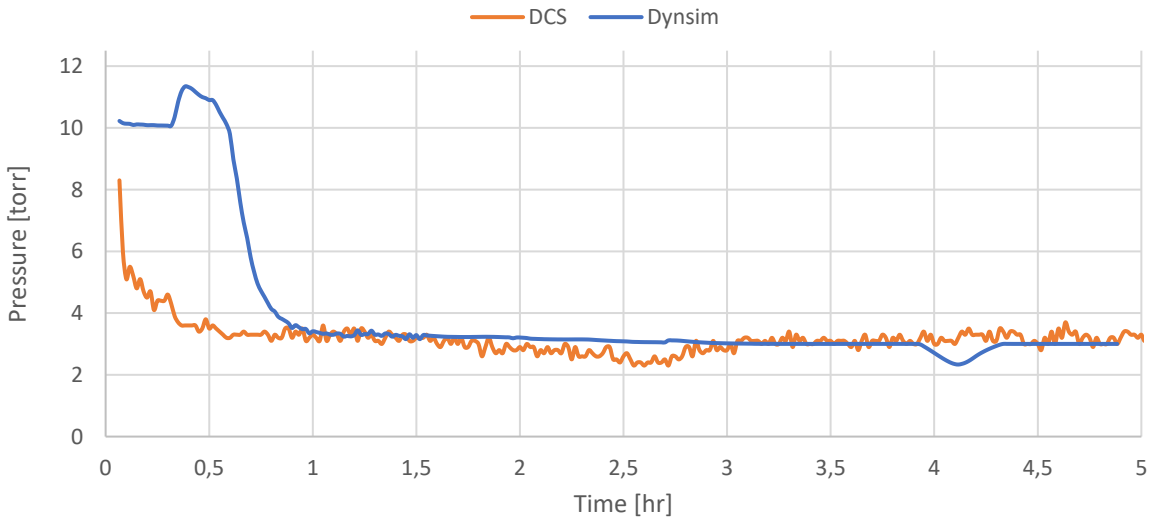

Figure 146: Pressure top column

Even if in the DCS initial conditions the column was hotter, in the new procedure the column reaches the operative conditions quicker. Unfortunately, since at DCS the FLS and fifth pack were already hot, the difference from using high pressure steam cannot be noticed properly. As usual, pressure odds are present, due to the discordances in the feed flow rates and temperatures, but also to the unreliability of some measurements from the DCS. It is noticeable in fact that pressures from the FLL tray to the fifth pack are lower than the pressure at the top of the column.

3.9. An accident simulation

One of the most important applications of DynSim is operator training to face uncommon and dangerous situations which cannot be experimentally reproduced in a safe way.

One such occasion could be a malfunctioning of the main condenser of the column. In steady state during normal operating conditions the E404 condenser covers more than 50% of the total cooling duty. It is cooling water and it was imagined that the water supply line suffered from damage making the utility unavailable. The problem is imagined detached from the unit operation, because if something like a leak was taking place, modelling the exact extent of contamination and consequences would have been unfeasible within the simulator limits.

As it was stressed in the introduction the model of the column is a limited representation of the interactions that can take place between boundary limits and the column and, lacking a kinetic model, it is unable to predict combustion due to air-hydrocarbon contact or mechanical failure of the equipment. Under these considerations the response procedure and the behavior of the column once E404 is shut down is to be interpreted as a general approach in conditions of relative safety of the column, meaning:

- The mechanical integrity of the column is not under question;
- No leakages are present in E404 (no contact between water and HC);
- The boundary conditions around the column are unchanged (no fire in proximity of the column);
- The plant environment is safe for plant operators and personnel to work.

Under such hypothesis the plant can still be operated and does not necessarily require an emergency shutdown. An emergency respecting these constraints could be a rupture of the pipes bringing water to E404 or a failure of the pumps destined to this task.

Once E404 is lost in order to avoid excessive heating of the column the two remaining exchangers will be ramped up at maximal capacity and operated this way until a new stationary is reached.

While all of this is taking place, several things have to be kept in mind:

- The column is going out of specification and is filling the storage tanks with this product. Considering the dimensions of the tank and the window range of viscosity the product can be sold in a limited amount of off-spec operation time can be tolerated;
- The source of the accident can be acted upon; a pump or pipe might be changed or fixed if the time allows it;
- The time the plant takes to get back in spec must be accounted for as off-spec time.

The column model can be used to evaluate both the time necessary to reach the new stationary and the time to come back from it.

3.9.1. Accident

The accident scenario involves the following steps:

1. TIC of top stage, TIC and FIC of E411 (these two controllers are in cascade) and FIC of E408 are set to manual
2. The FIC of the top column responsible for the reflux that passes through E404 is ramped down linearly to closed position in 15 min simulating a gradual loss in cooling duty at the top
3. 10 min are left without any action taking place to account for decision making and planning in the DCS
4. In 5 minutes, the flowrates passing through E411 and E408 are linearly ramped up to maximum
5. The situation is monitored for the following 6 hours and 50 minutes

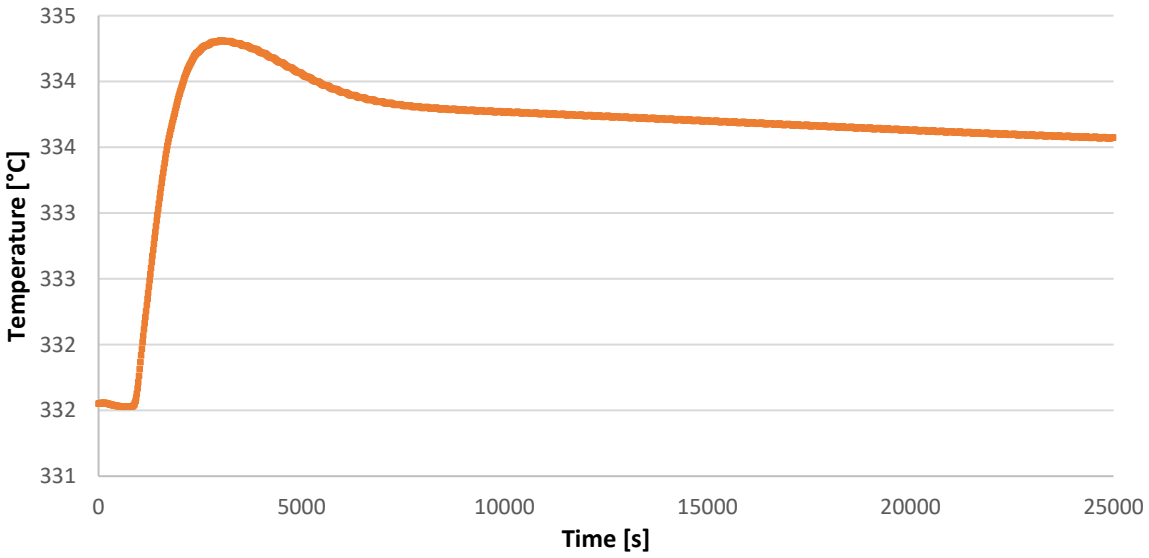

Figure 147: First pack sump temperature

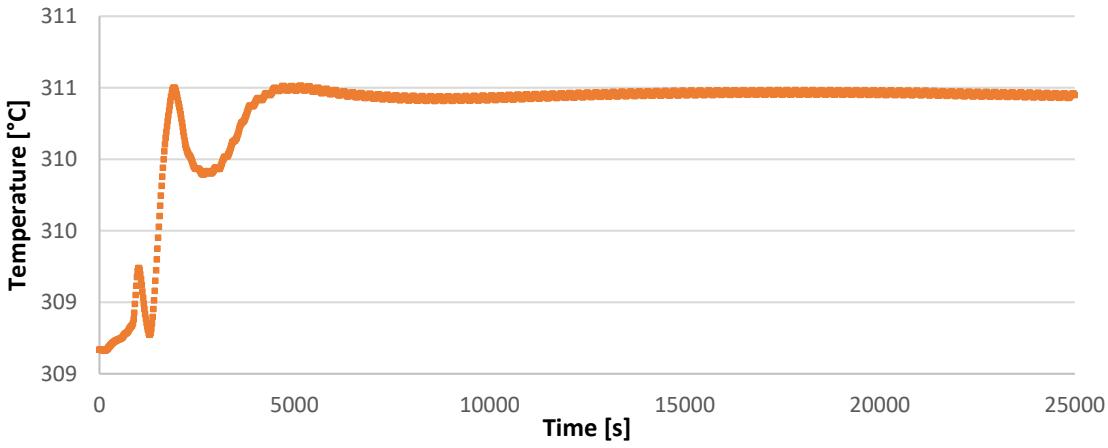

Figure 148: FLP pack sump temperature

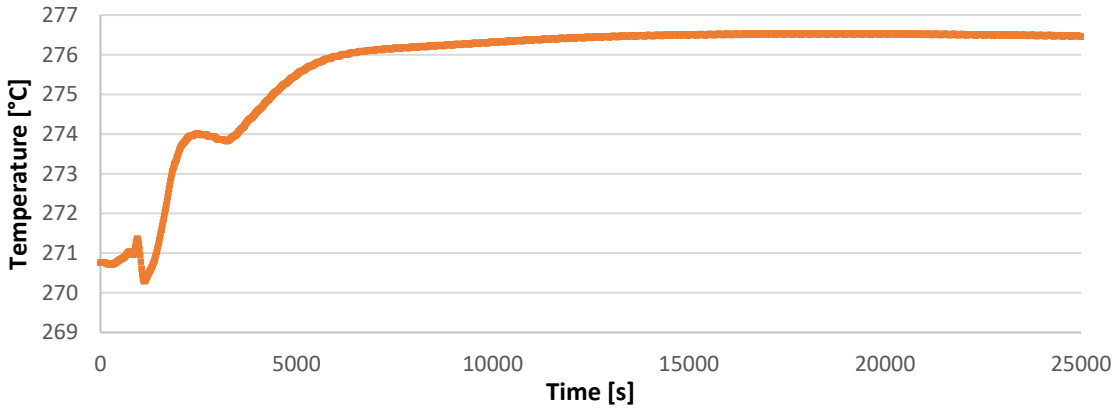

Figure 149: FLL pack sump temperature

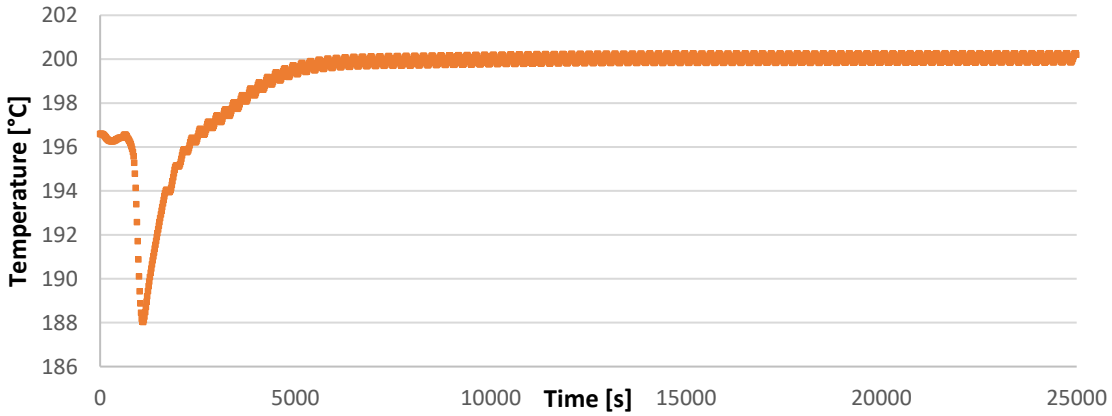

Figure 150: FLS pack sump temperature

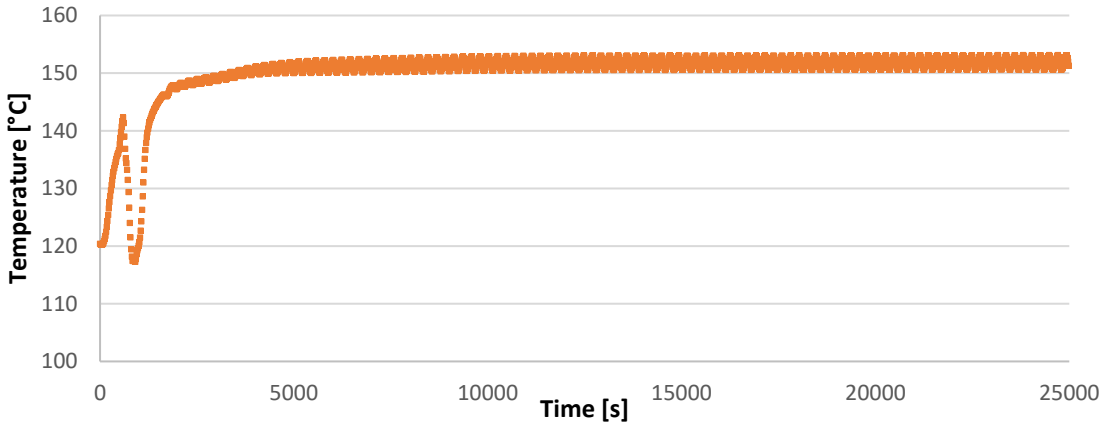

Figure 151: Fifth pack top stage temperature

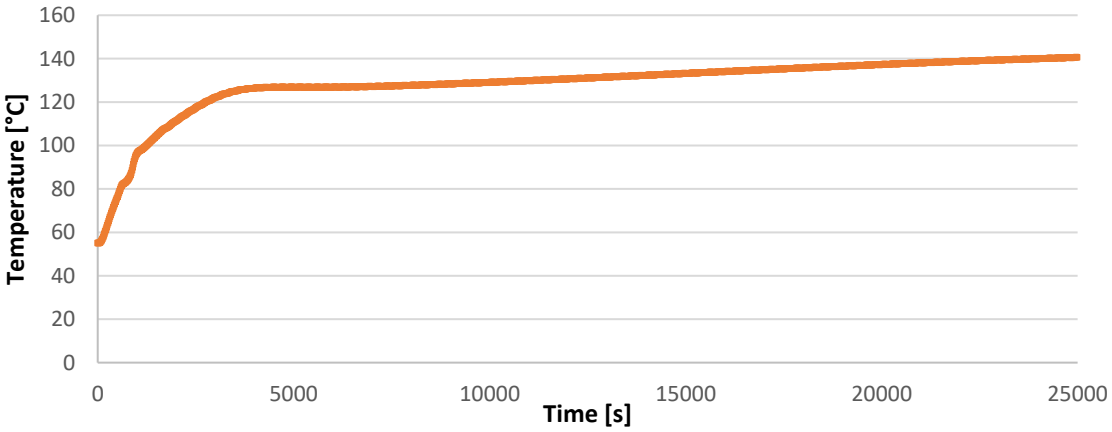

Figure 152: VGO sump temperature

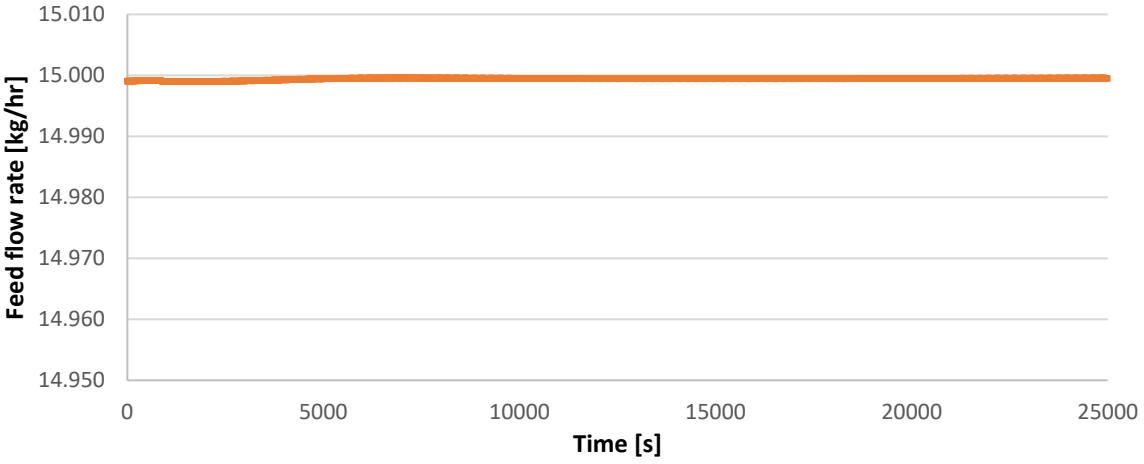

Figure 153: Feed flow rate

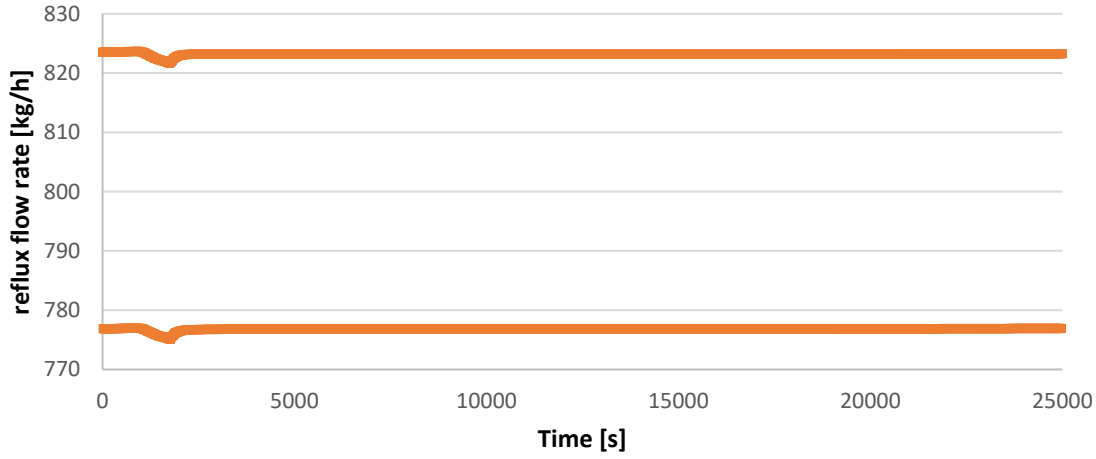

Figure 154: FLP reflux flow rate

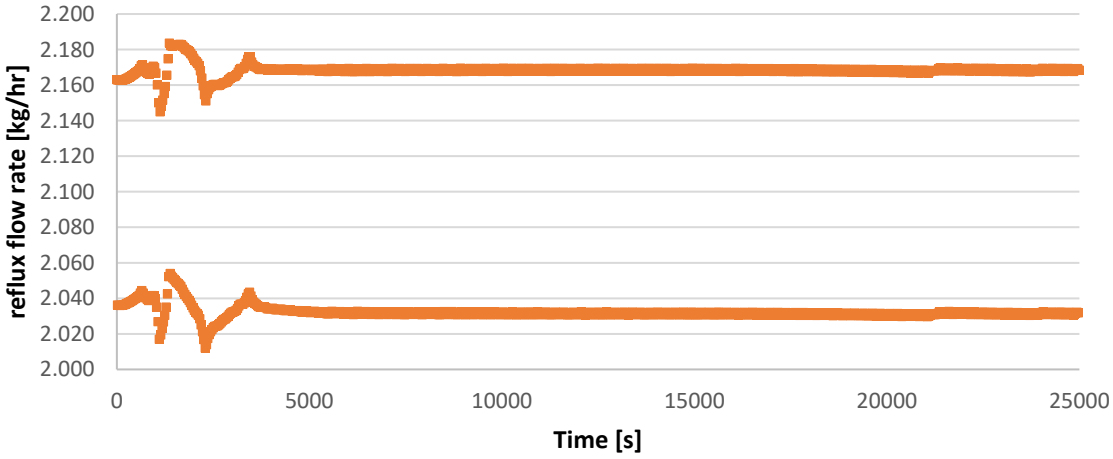

Figure 155: FLL reflux flow rate

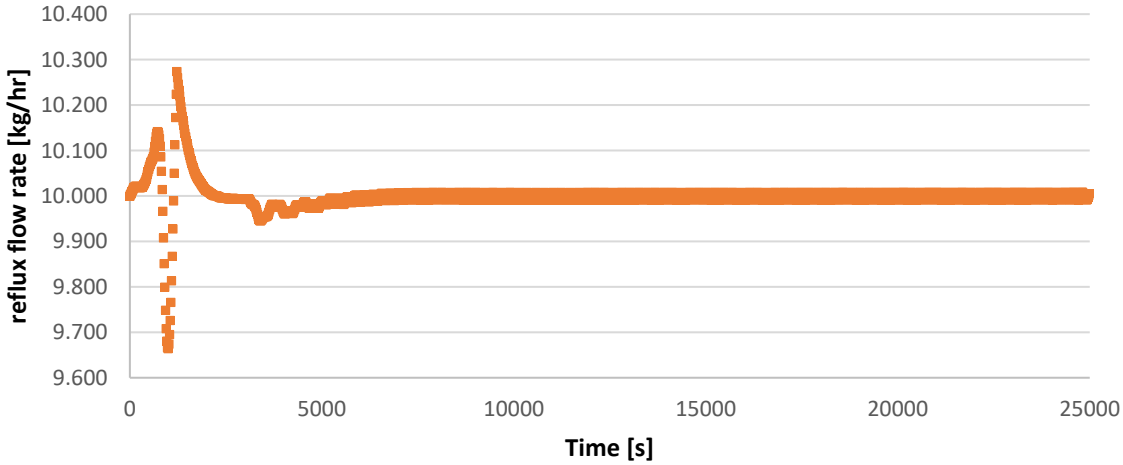

Figure 156: FLS reflux flow rate to FLL pack

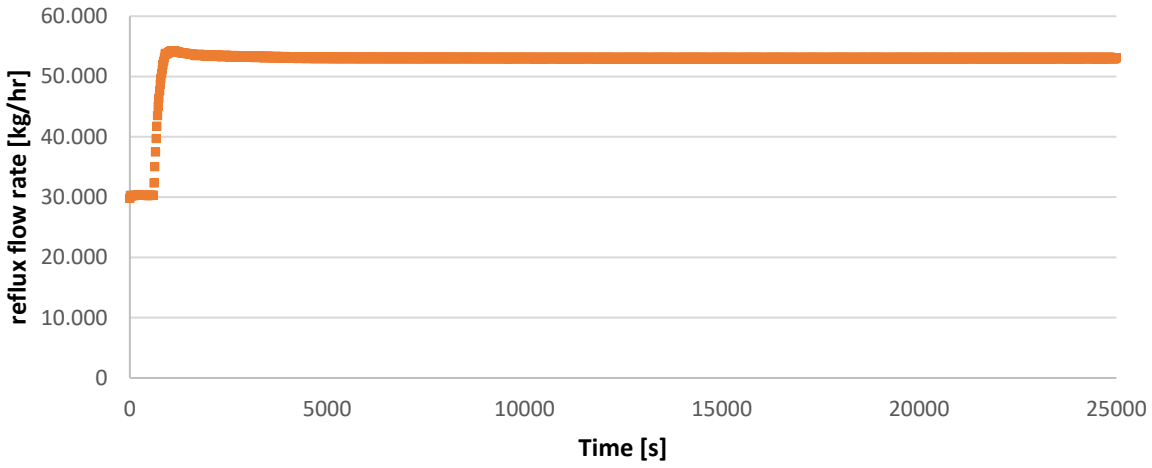

Figure 157: FLS reflux flow rate to FLS pack

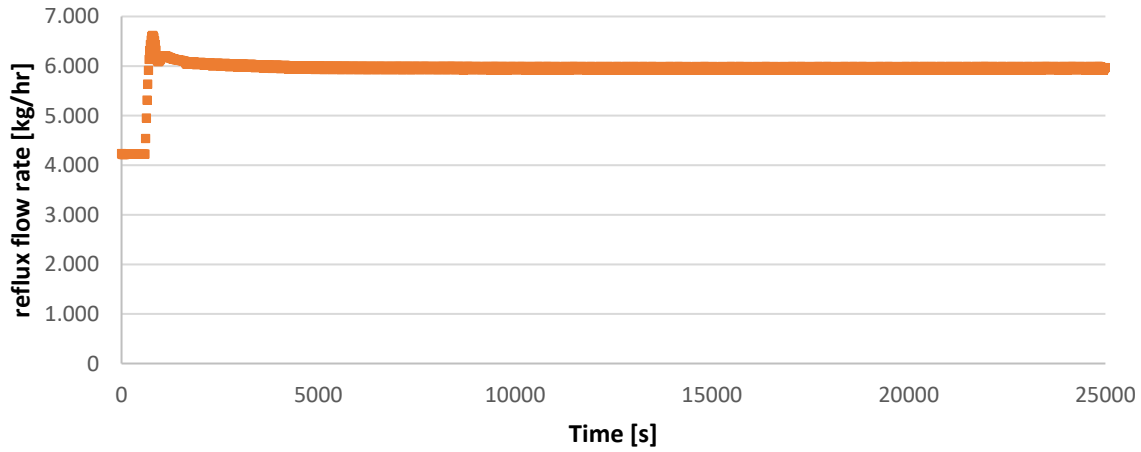

Figure 158: FLS reflux flow rate to fifth pack

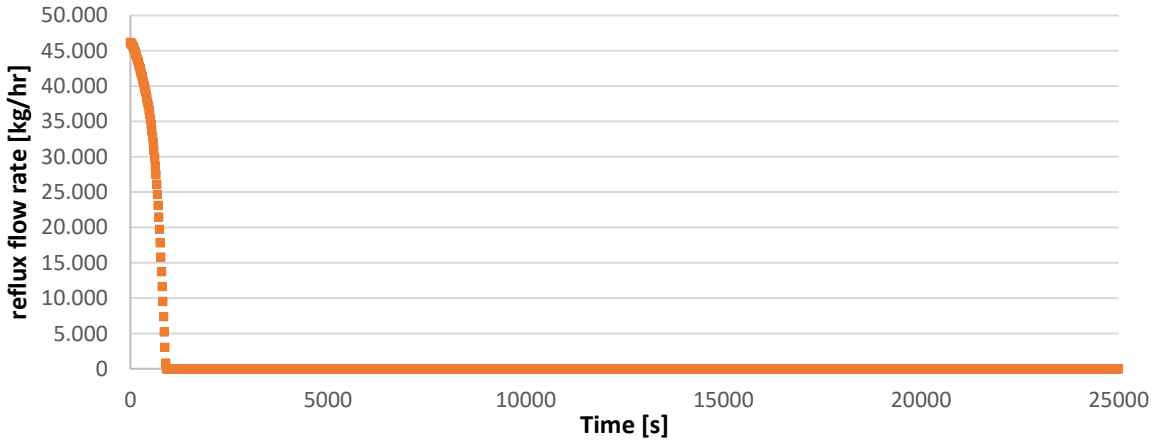

Figure 159: VGO reflux flow rate

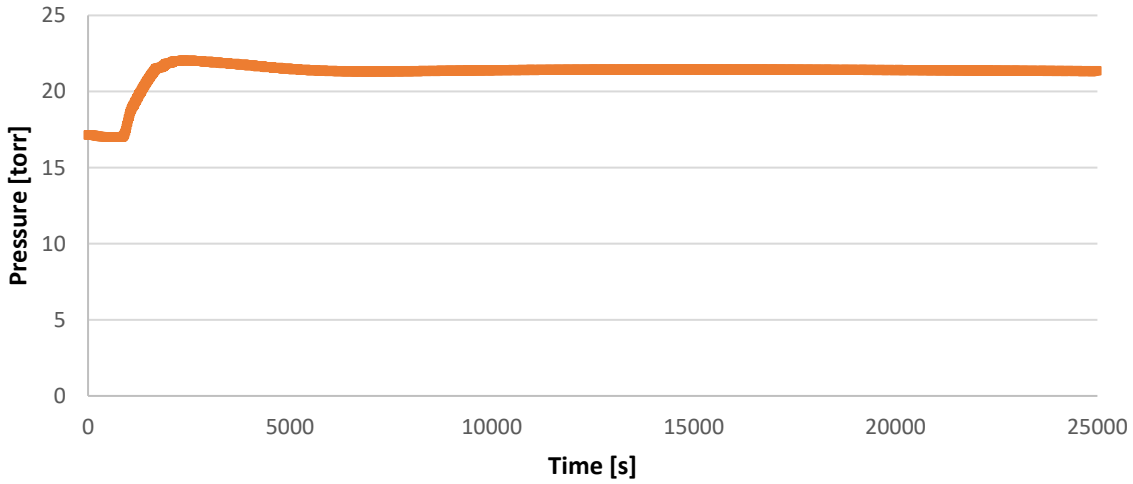

Figure 160: First pack sump pressure

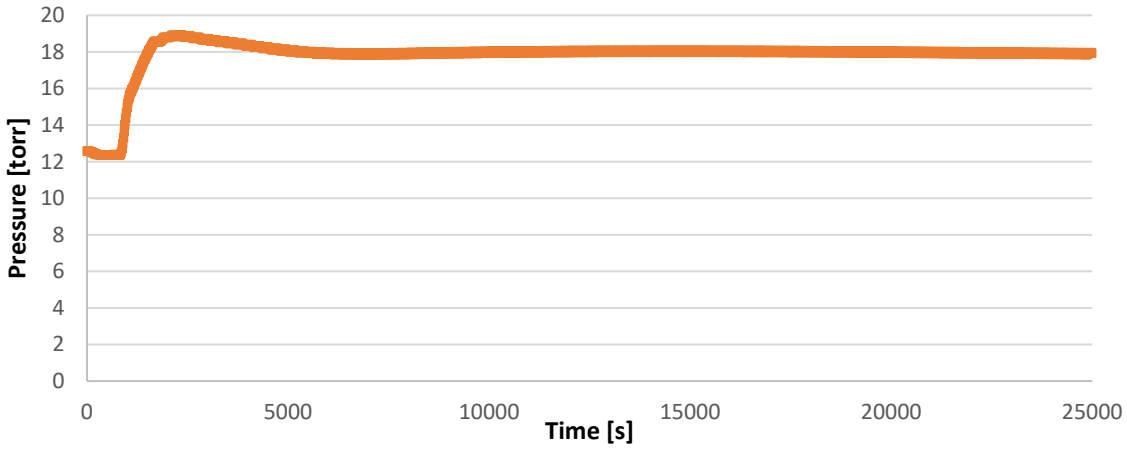

Figure 161: FLL pack sump pressure

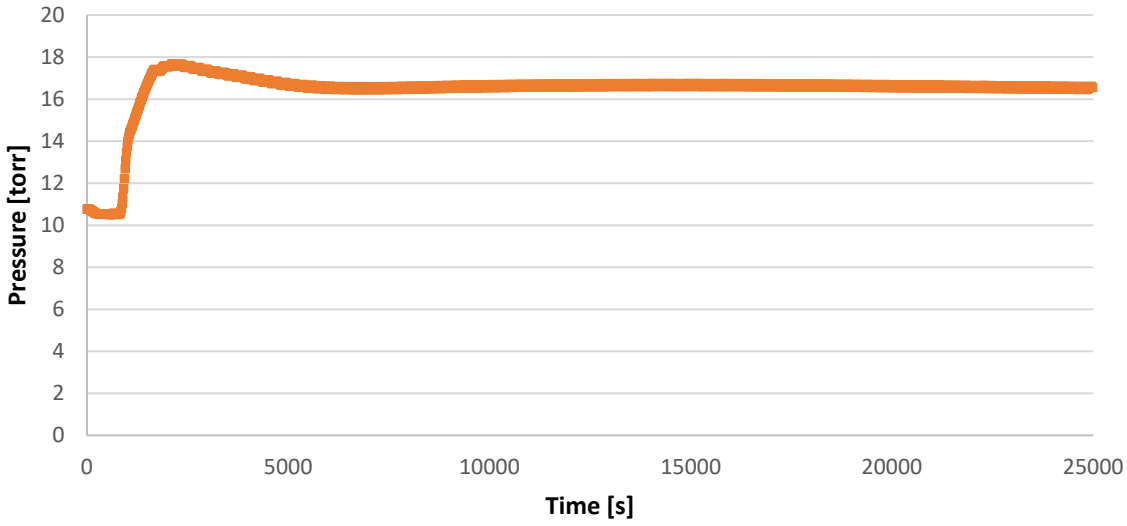

Figure 162: FLS pack sump pressure

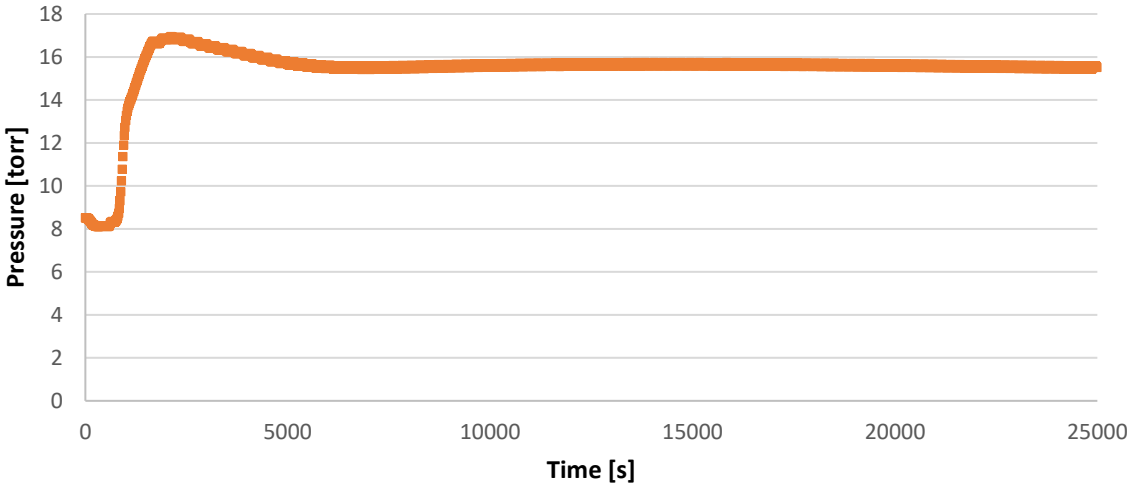

Figure 163: Fifth pack bottom tray pressure

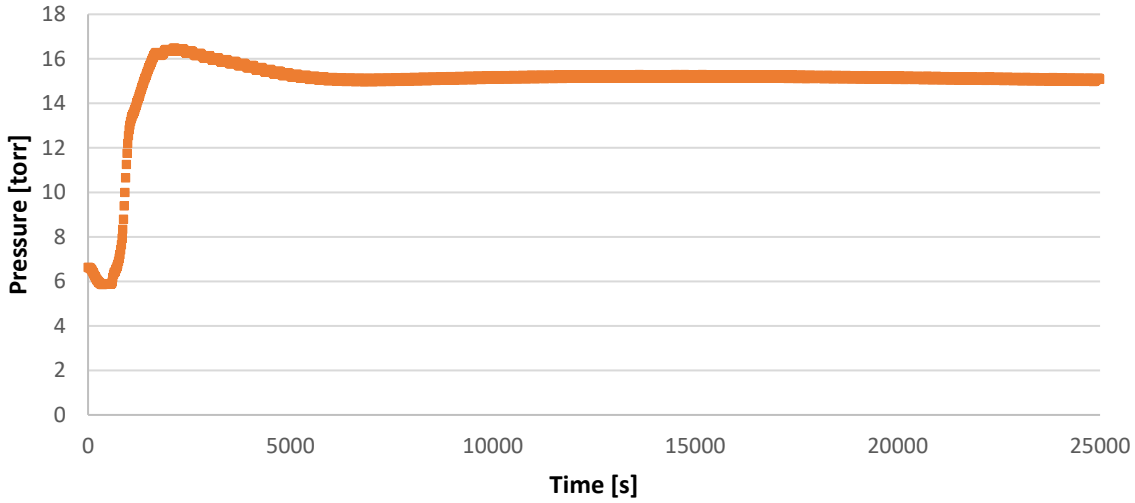

Figure 164: VGO pack sump pressure

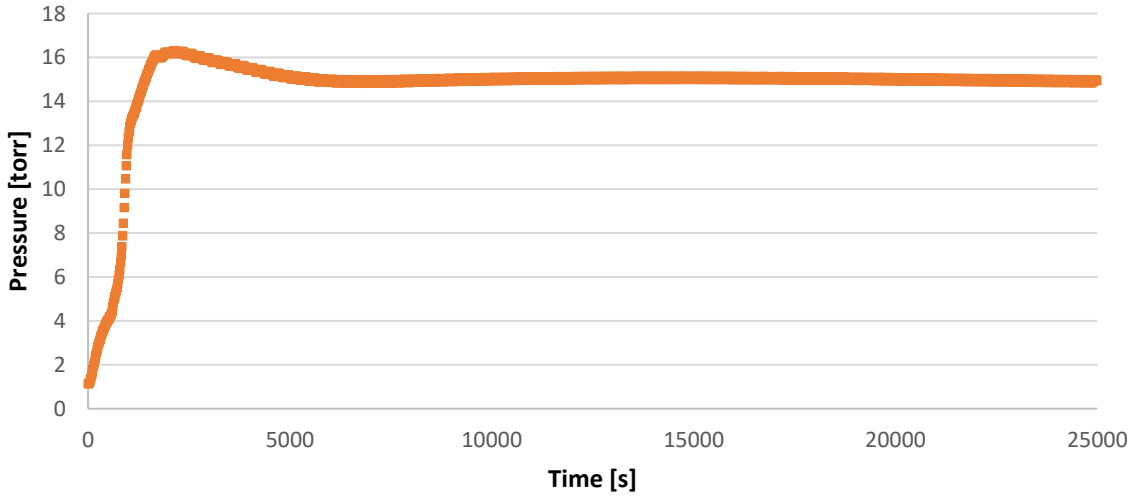

Figure 165: Column top pressure

Even compensating for the loss of E404 by ramping up the other condensers about 20% of the total cooling duty is lost resulting in an overall higher operative temperature and pressure of the column, especially on top. While the temperature difference is drastic for the VGO and fifth pack (respectively ~90°C more for the VGO and ~30°C more for the fifth pack) the difference is not as critical for the rest of the column being in the range of 5°C. The VGO is a secondary product of the column so its specifications are not as important as the ones of the lubricant bases extracted from the 2nd, 3rd and 4th pack. For these reasons there are valid arguments on keeping the column running.

The time each plate takes to cover 95% of the difference between the new stationary temperature and the original stationary temperature is considered the characteristic time of the transient for each of these plates. The same principle is applied when the reverse process is carried out (from new stationary to the old one).

	FLP	FLL	FLS	VGO
Time to Reach new stationary [s]	3832	7875	6265	19092
Of spec mass collected [kg]	2228.5	16336.7	1386.0	506.9

Table 38: Characteristic variables of the accident

As it can be seen in Table 38 the transient is rather fast, being the longest at 3 hour and 38 min for FLL. Integrating by means of trapezoidal rule the product draws it is possible to find the off-spec mass delivered to the storage tanks.

3.9.2. Return to stationary operations

Repristinating the controllers to automatic mode the original stationary conditions of the system can be restored.

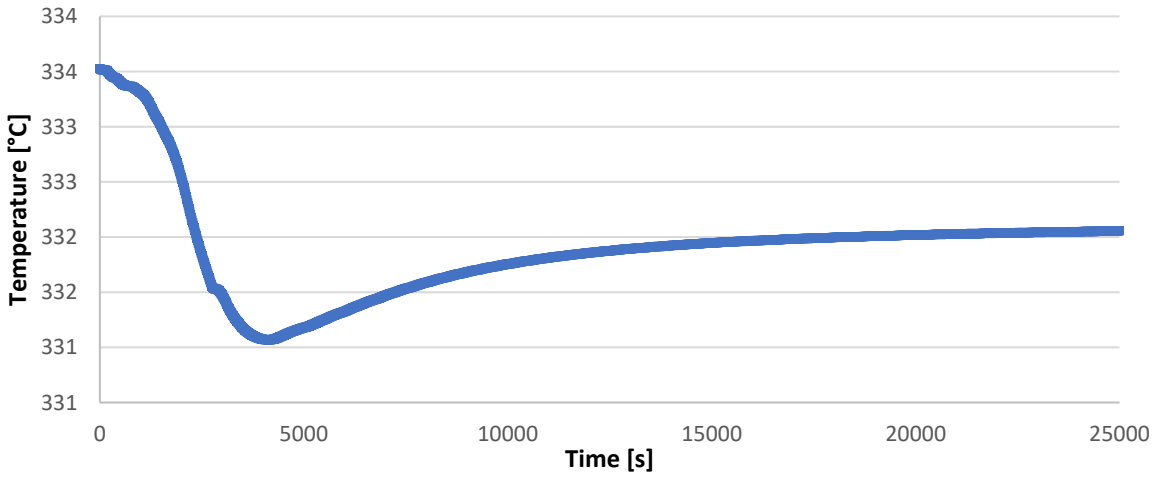

Figure 166: First pack sump temperature

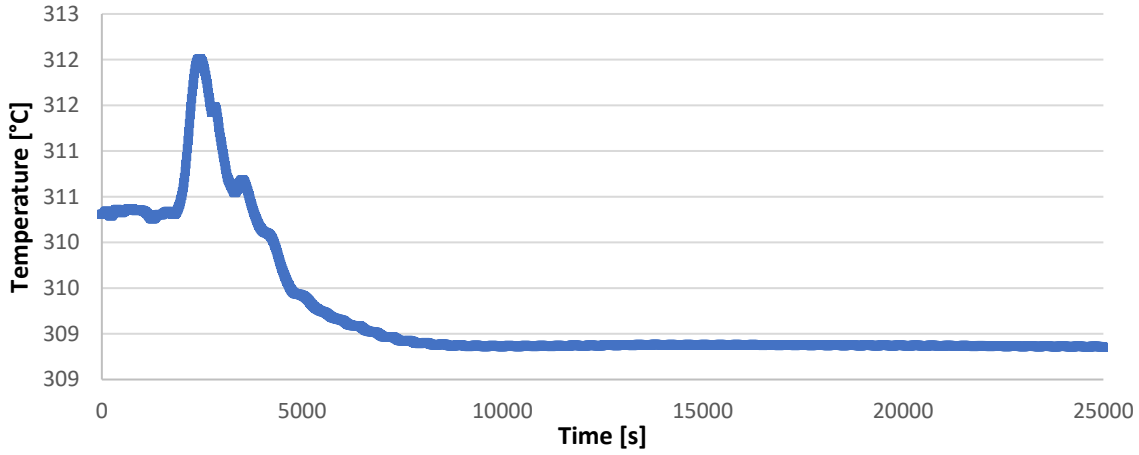

Figure 167: FLP pack sump temperature

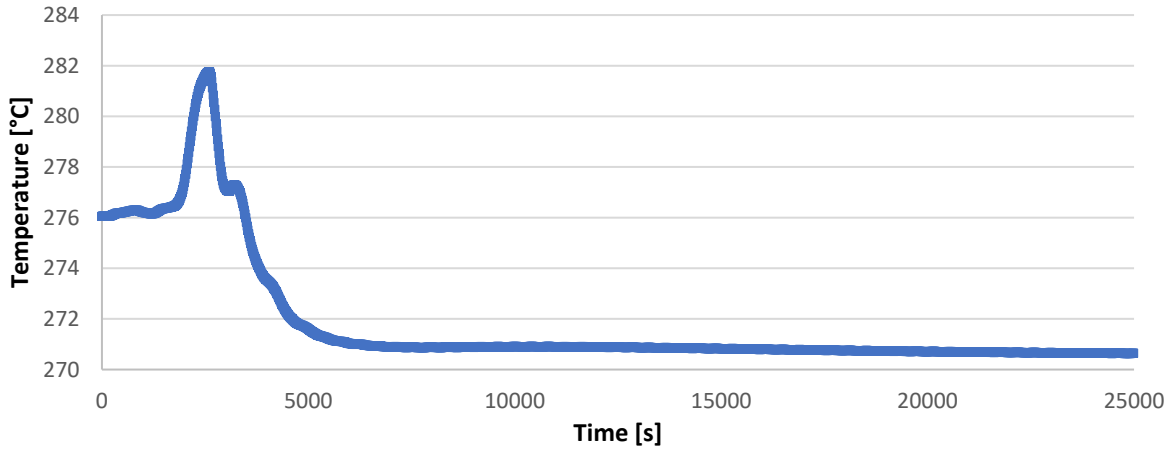

Figure 168: FLL pack sump temperature

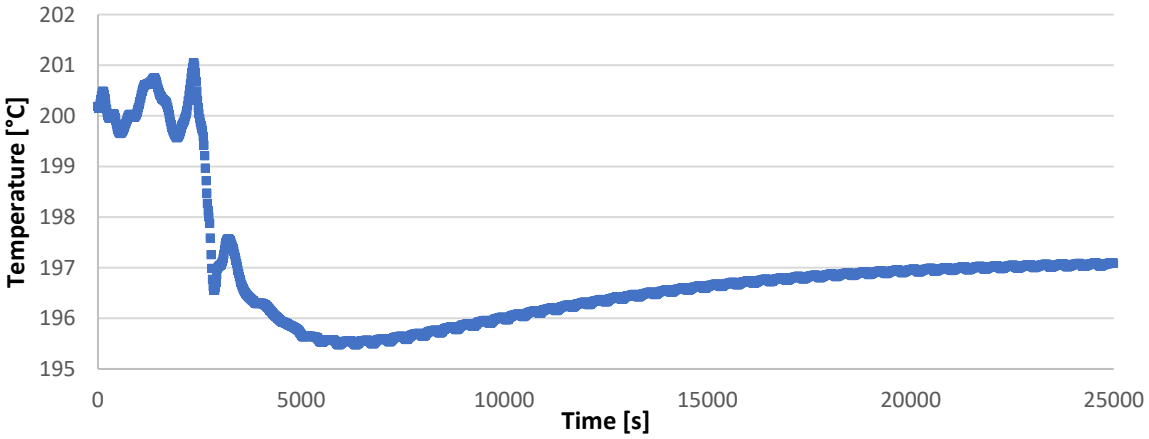

Figure 169: FLS pack sump temperature

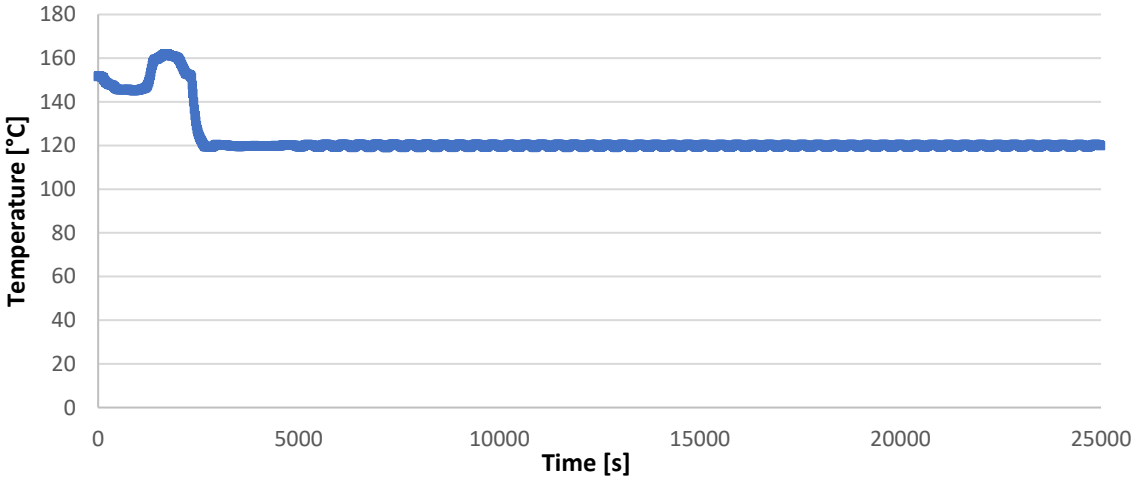

Figure 170: Fifth pack top stage temperature

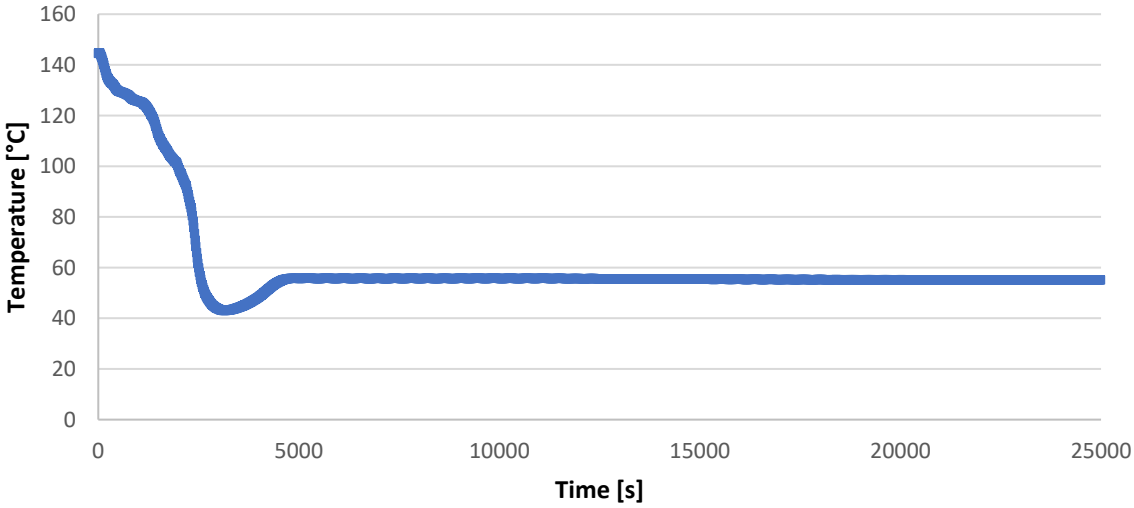

Figure 171: VGO pack sump temperature

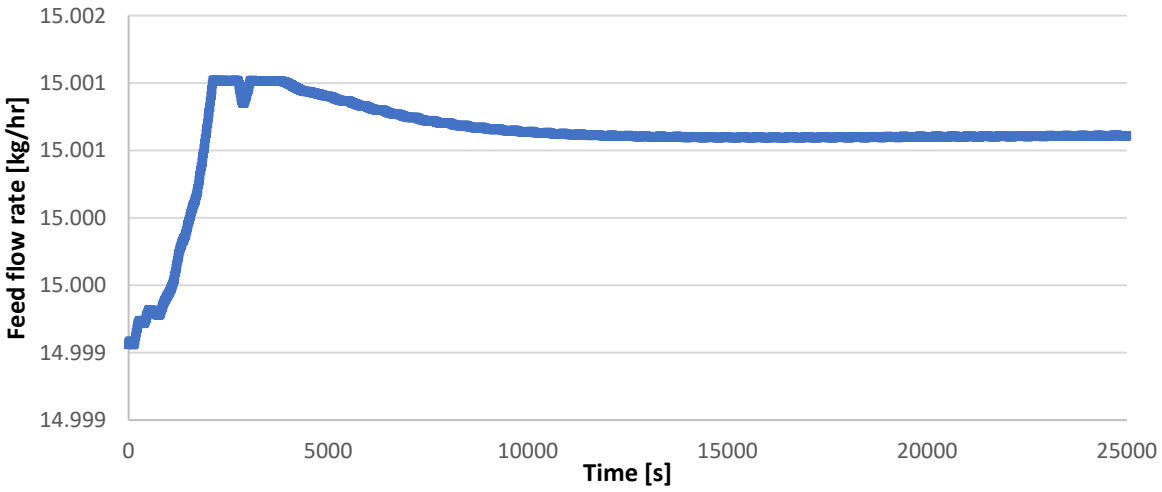

Figure 172: Feed flow rate

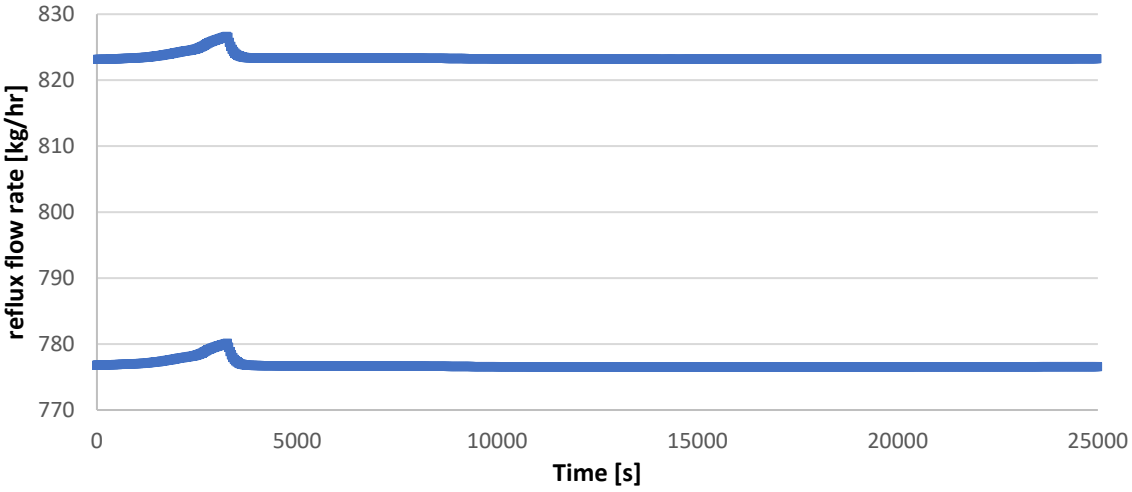

Figure 173: FLP reflux flow rate

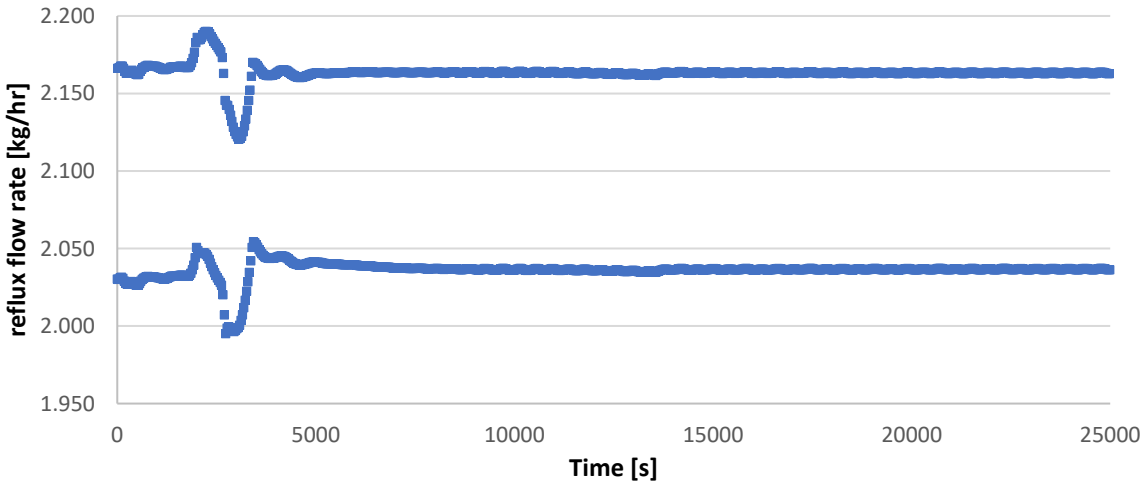

Figure 174: FLL reflux flow rate

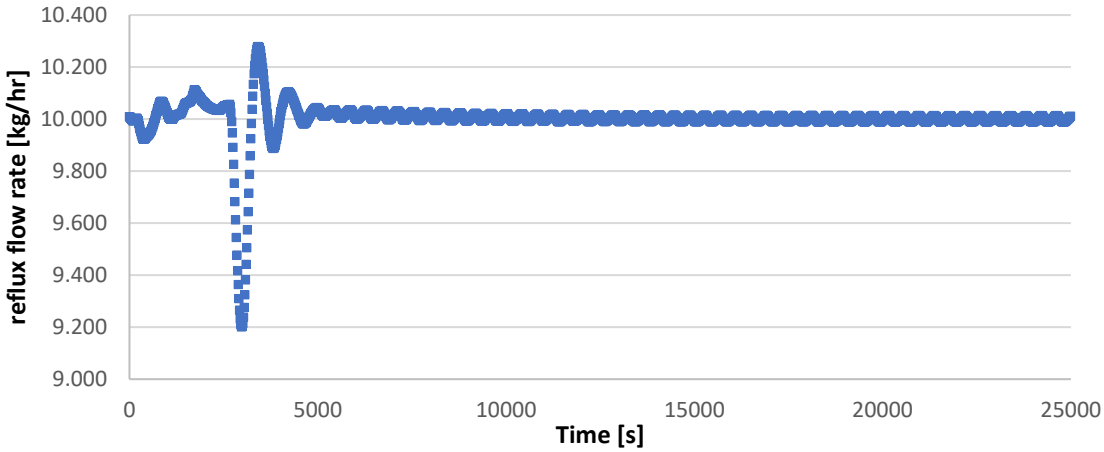

Figure 175: FLS reflux flow rate to FLL pack

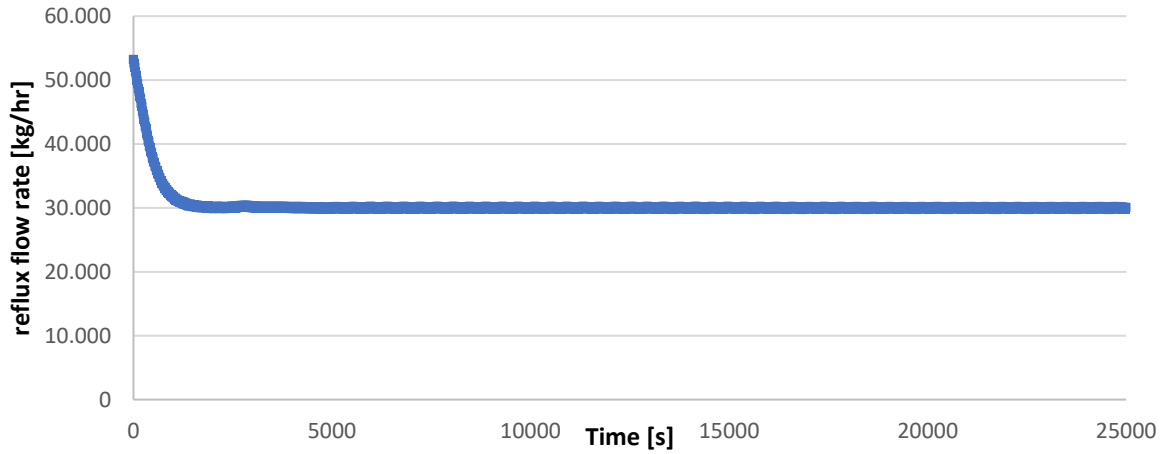

Figure 176: FLS reflux flow rate to FLS pack

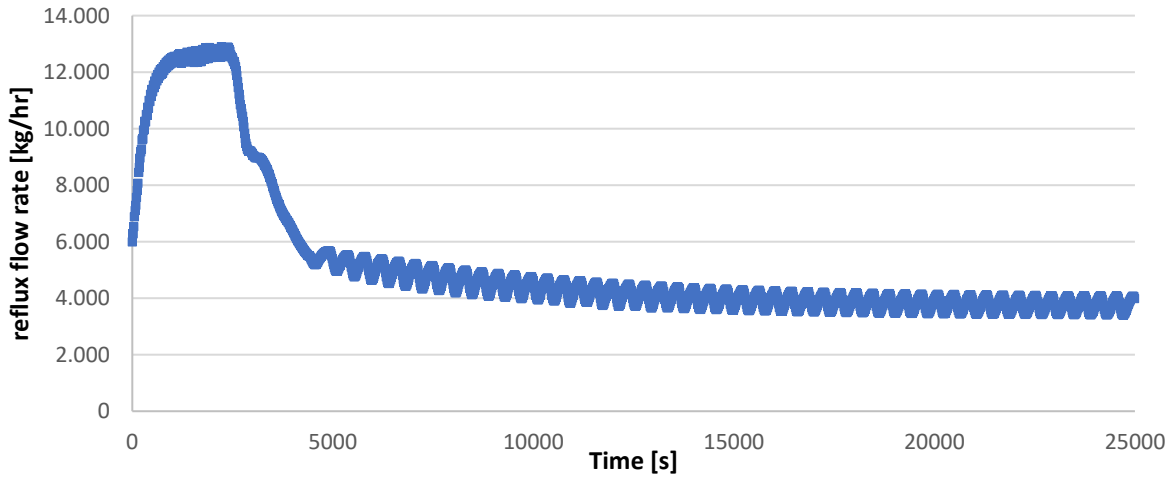

Figure 177: FLS reflux flow rate to fifth pack

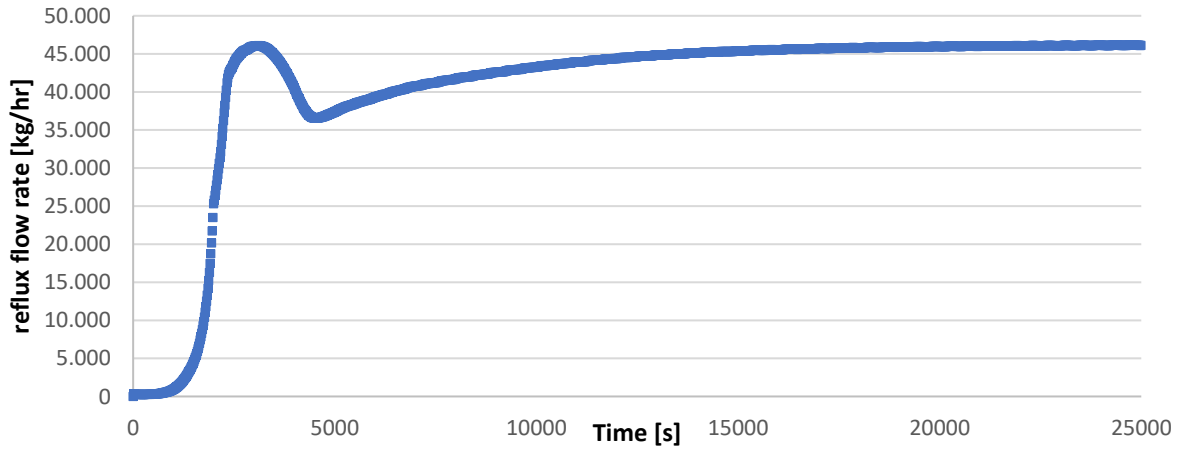

Figure 178: VGO reflux flow rate

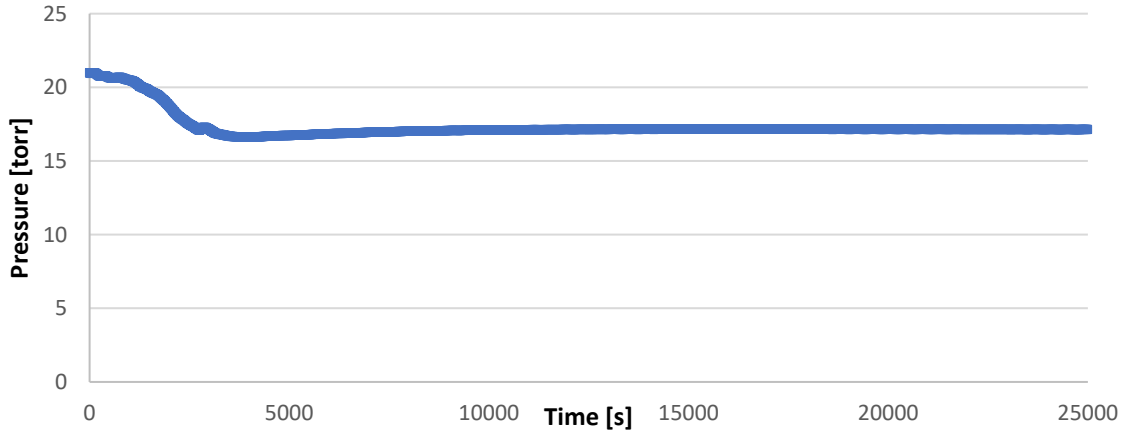

Figure 179: First pack sump pressure

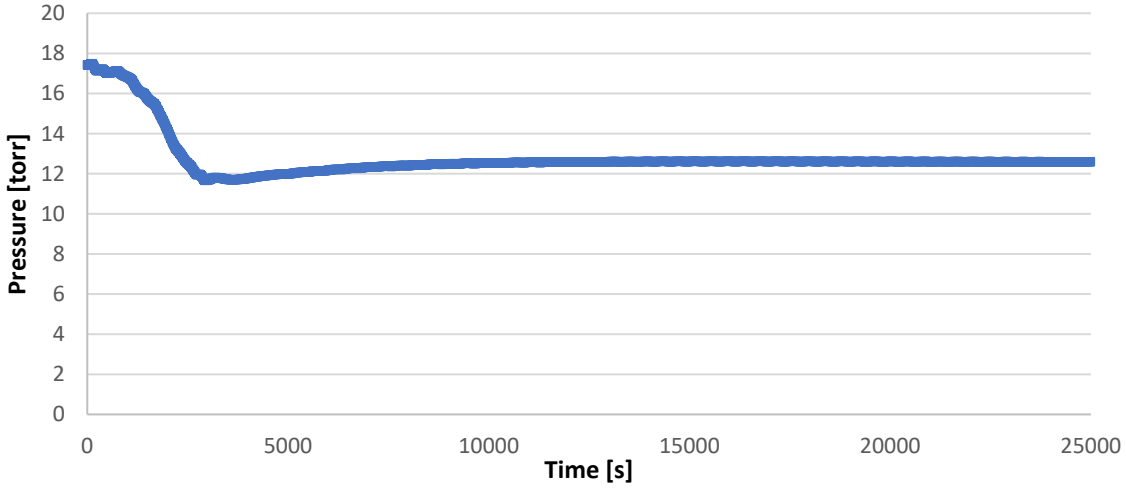

Figure 180: FLL pack sump pressure

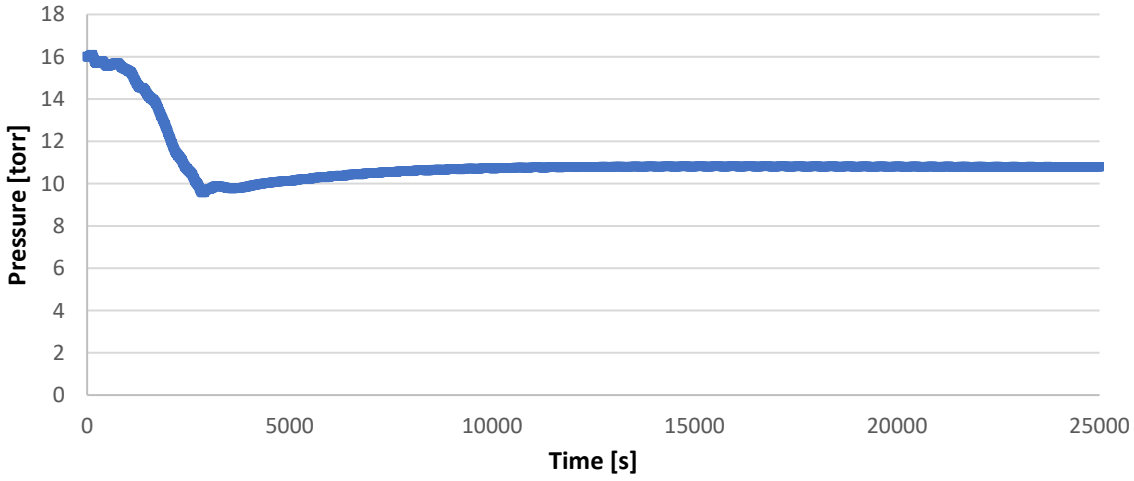

Figure 181: FLS pack sump pressure

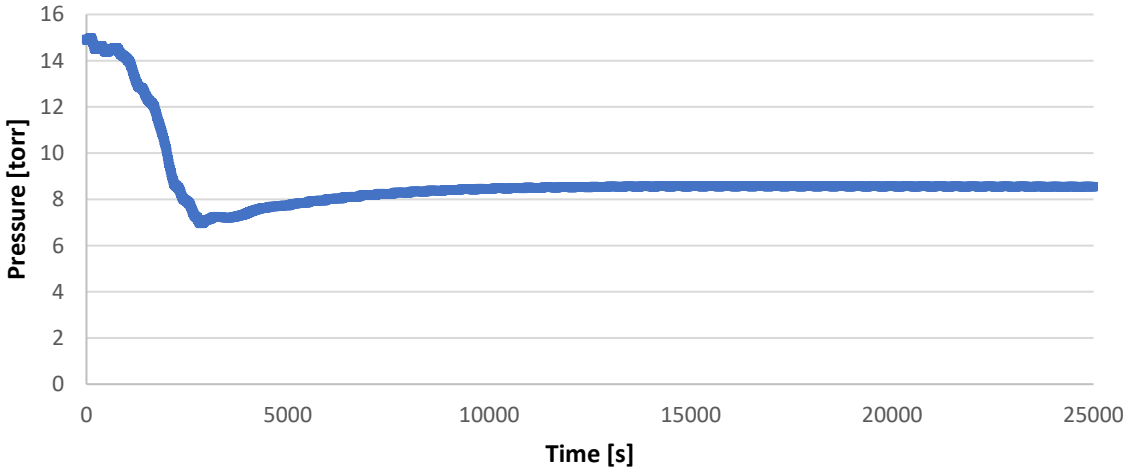

Figure 182: Fifth pack bottom stage pressure

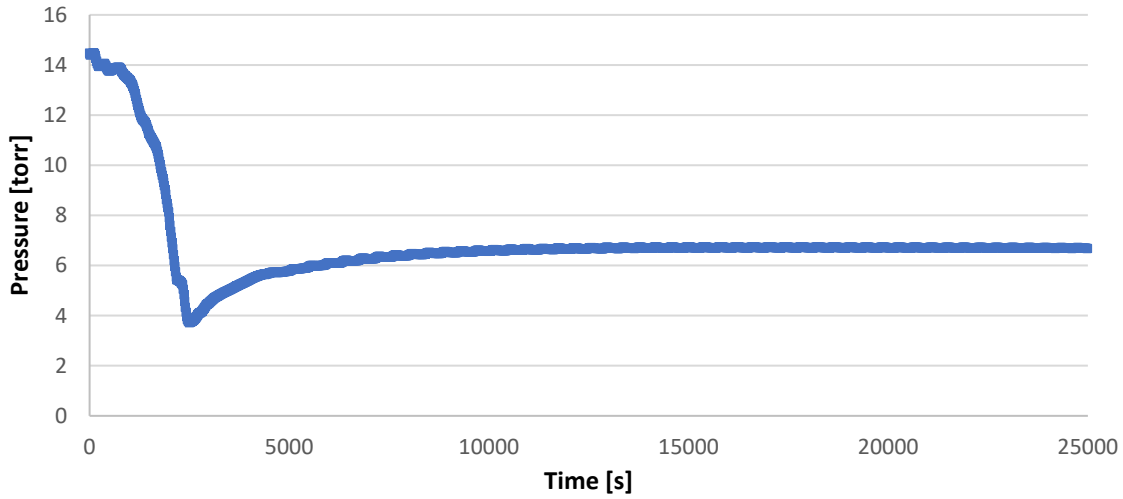

Figure 183: VGO pack sump pressure

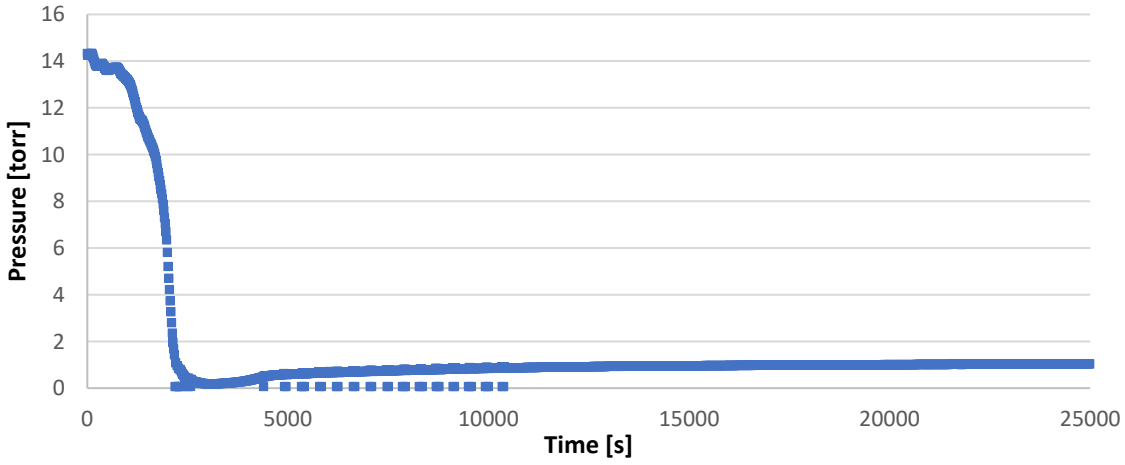

Figure 184: Top column pressure

The characteristic times and quantities are reported in Table 39.

	FLP	FLL	FLS	VGO
Time to repristinate original steady state [s]	7402	11690	20247	4182
Of spec mass collected [kg]	4104.9	16131.4	11631.7	0.2

Table 39: Characteristic variables of the return to stationary

3.9.3. A possible application

This data could be used as an example to compute how much time can the plant be operated before the buffer units are sent off-spec.

Given the following data:

- $\mathbf{m_{os}}$ mass of off-spec product deposited
- $\mathbf{m'_s}$ mass flowrate of products to buffers during normal operations
- $\mathbf{m'_{os}}$ mass flowrate of products to buffers during accident
- $\mathbf{V}$ volume of the buffers
- $\boldsymbol{\rho}$ density of the base oil in the buffer
- $\mathbf{x_s}$ and $\mathbf{x_{os}}$ mass fraction of in spec and off-spec product in the tanks
- $\boldsymbol{\nu_s}$ and $\boldsymbol{\nu_{os}}$ viscosity in spec and out of spec product
- $\boldsymbol{\nu_{min}}$ and $\boldsymbol{\nu_{max}}$ minimum and maximum tolerated viscosities for the product

and applying a mixing rule for viscosity such as the Refutas (2000) [1] the following reasoning can be applied to evaluate how long the plant can be operated out of spec.

The mass fraction of product in-spec in the buffers is going to be:

$$x_s = \frac{V \cdot \rho - m_{os,accident} - m_{of,return} - m'_{os} \cdot t_{os}}{V \cdot \rho}$$

in this calculation it is considered that the tanks can be completely filled after the plant is brought back to nominal conditions, so it is not necessary to know the initial content of product in the tanks.

The Refutas mixing rule is based on the concept of Viscosity Blending Number calculated as follows for each component of the mix:

$$VBN_i = 14.534 \cdot ln\big(ln(\nu + 0.8)\big) + 10.975$$

the VBN of the mixture is then calculated as a weighted average on mass:

$$VBN_{mix} = \sum_{i=0}^{i=N} x_i \cdot VBN_i$$

and the resulting mix viscosity is calculated as inverting the original formula for VBN:

$$\nu_{mixture} = exp\left(exp\left(\frac{VBN_{mixture} - 10.975}{14.534}\right)\right) - 0.8$$

by equating the viscosity of the mixture to the maximum and minimum tolerated viscosities a single equation with the out of spec operation time is obtained. Repeating this procedure for each of the products (the storage tanks are different and so are the properties of each base oil) and taking the smallest time found will permit to estimate the maintenance time available for fixing the problem on E404.

Among the needed variables the mass of off-spec product retrieved during the accident and the return to nominal conditions procedures were found in DynSim as well as the amount of product sent to the buffers during off-spec and nominal operations. The volume of the buffers is known as well as the temperature and thus density of the lube stored. The minimum and maximum tolerated viscosities depend on the client requirements and they will be known.
The viscosity of the stored product has to be normally monitored to guarantee the quality of the product and thus its known. The last variable that must be known is the viscosity of the off-spec product which however is not easily computed. DynSim is not suitable for precise property prediction and viscosity models suffer a lot from this. Rules based on SG were tested and failed due to the fact that a variation of 3% in the SG prediction resulted in a variation of more than 30% in the viscosity. Models based on the properties of the single pseudo-components could not be applied since DynSim does not provide the viscosities of each single pseudo-component.

Moreover, classical models found in literature are made on oils that come from crude and thus have a different composition from the TDA's feedstock, for this reason and the ones mentioned above it is suggested to make a custom model that predicts the viscosity starting from the ASTM D1160 results which can be reliably generated also by DynSim.

3.10. Conclusions

The dynamic model is built respecting both the geometric features of the TDA in situ and the thermodynamic stage characteristics developed in HYSYS. Wherever DynSim requires data which are not available from the plant nor are predicted from HYSYS, they are evaluated separately after a proper bibliographic research. The dynamic and steady state validations of this model show excellent accordance with reality. Such a model is than used both to propose a new Startup procedure and to simulate an incident's consequences and procedure to limit damages.

The new Startup procedure is implemented starting from the one followed by Pieve Fissiraga's operators, especially when external technical issues are involved such as the slow heat up of the furnace. The simulation showed that such new operation can bring the TDA column at operative conditions faster. One of the main differences, which is also the most difficult aspect to implement on the plant, is the use of the high-pressure steam line to heat up the upper part of the column internals, which requires to extend such line to the kettle reboiler E-408 and the production of a high quantity of steam. This last aspect, however, should not be costly since the steam is mostly recovered as showed by the simulation. Since steam recovery from E-408 is also done during normal operation, no technical issues should arise.

As said, in order to evaluate the model's potential, an incident is also simulated. Since DynSim is only able to predict standard operations, anything that involves serial damaging, such as explosions and fires, or leakages cannot be analysed with it. However, failure and malfunctioning of pieces of equipment can be implemented. The case study of the E-404 failure is examined, together with a supporting procedure involving E-408 and E-411. The simulation showed that no dangerous conditions are reached in the column and whereas the ejector system can bear the higher quantity of vapor exiting the column top, no emergency shutdown is required. The products are analysed too. In the hypothesis or reliable deviations of DynSim's specific gravity predictions with the column conditions, the column can run for several days without undermining the products quality, whereas streams are processed and stored with the hypothesis already presented in the previous chapter.

3.11. Model future developments

As pointed out, several aspects of the model can be improved. These modifications require several other data, time to build up and validate such aspects and the use of external tools to build new features in the simulator.

While all the plant column stages are not truly at equilibrium, the column top is the only one which cannot be approximated with satisfactory results, though the consequences on the other parts of the column are little. Since DynSim do not present any features for the representation of vapor-liquid non equilibrium units, an external model has to be built and inserted in the program. As said for the steady state conditions, such stage can be developed as a contact condenser with packings.

Although the furnace implemented in DynSim is satisfactory for the column simulation purposes, it does not permit to properly analyse the real furnace behaviour. This precludes furnace operation optimization and safety analysis. As for the column top, another external model has to be developed. Moreover, a detailed reactive kinetic model may improve furnace transient predictions quality.

Column boundaries can be furtherly developed. Units upstream the furnace are the heated tank TK-401, the preflash unit and the exhaust lubricant feed tank. Downstream the column there are steam strippers and storage tanks, which will provide distilled cuts to the de-waxing and the hydrofinishing units. The ejector group which is located above the column top can also be modelled, to better analyse its operative limits.

Lastly, auxiliary lines can be included, which are inerting utility nitrogen, medium pressure steam to clean up the furnaces and transfer lines of the distilled products for the performance of the wet Startup.

3.12. Model potential applications

Dynamic transient cost analysis and minimization can be performed. By integrating an optimization tool in DynSim, it can be developed an optimal economic scenario compatible with the operative conditions. Costs from utility steam and energy demand together with the products revenues can be accounted for in the following objective function, which has to be maximized:

$$f_{profit} = \sum \int_0^t revenue_i dt - \sum \int_0^t cost_i dt$$

Model predictive control can also be implemented. Even in this case, the integration of an optimization tool is needed to minimize the objective function, which accounts for the controlled variables C, the manipulated variables M and their operative limits, discretized from time 0 to the predictive horizon hp and the control horizon hc:

$$f_{MPC} = \sum_{j}^{Controlled\ variables} \sum_{0}^{hp} \left[w_j * \frac{C_{i,j} - C_{j,set\ point}}{C_{j,set\ point}} + z_j * \left\{ Max\left(0, \frac{C_{i,j} - C_{j,max}}{C_{j,max}}\right) + Min\left(0, \frac{C_{i,j} - C_{j,min}}{C_{j,min}}\right) \right\} \right]$$
$$+ \sum_{j}^{Manipulated\ variables} \sum_{0}^{hc} \left[u_j * \frac{M_{i,j} - M_{j,set\ point}}{M_{j,set\ point}} + l_j \right.$$
$$\left. * \left\{ Max\left(0, \frac{M_{i,j} - M_{j,max}}{M_{j,max}}\right) + Min\left(0, \frac{M_{i,j} - M_{j,min}}{M_{j,min}}\right) \right\} \right] + \sum_{j}^{Manipulated\ variables} \sum_{0}^{hc} \left[n_j * \frac{M_{i,j} - M_{i-1,j}}{M_{j,set\ point}} \right]$$

Lastly, DynSim can be used on concomitance with HYSYS to perform a sensitivity analysis on products viscosity after changing the controlled variables. Considering HYSYS's difficulties in solving systems with a high number of internal recycles, controlled variables can be changed on DynSim in order to identify the wanted operative conditions. Such variables can be implemented in HYSYS to have a better characterisation of the products in the specified steady state. Moreover, the dynamic simulator can evaluate and shorten transients, in order to reduce the total quantity of off spec products.

4. Bibliography

[1] Ullmann's encyclopedia of industrial chemistry, Lubricants, and lubrication.

[2] Bureau Veritas, "www.oil-testing.com," [Online]. Available: https://oil-testing.com/glossary/saybolt-universal-viscosity-suv-or-saybolt-universal-seconds-sus/. [Accessed July 2019].

[3] Wikipedia, "www.wikipedia.org," [Online]. Available: https://en.wikipedia.org/wiki/Viscosity_index. [Accessed June 2019].

[4] CONOU, «Green economy report,» 2017.

[5] Aspentech, "HYSYS operations guide," 2004.

[6] Aspentech, "Aspen physical property system," 2001.

[7] ASTM International, "Standard test method for distillation of petroleum products at reduced pressure," April 2009.

[8] Aspentech , "HYSYS simulation basics," 2004.

[9] C. H. Twu, "An internally consistent correlation for predicting the critical properties and molecular weights of petroleum and coal-tar liquids," *AlChE Journal,* vol. 38, pp. 477-479, 1992.

[10] M. G. K. Byung Ik Lee, "A generalized thermodynamic correlation based on three-parameter corresponding states," *AlChE Journal,* vol. 21, pp. 510-527, 1975.

[11] A. J. Maccone P., "Correlation for saturated liquid densities of Hankinson and Thomson (COSTALD)," *AlChe,* vol. 38, pp. 477-479, 1992.

[12] H. G. Rackett, "Equation of state for saturated liquids," *Journal of chemical engineering data,* vol. 4, 1970.

[13] D. F. Schneider, "Selecting the right hydrocarbon molecular weight correlation," 1998.

[14] W. Shu, "A viscosity correlation for mixtures of heavy oil, bitumen, and petroleum fractions," 1984.

[15] H. S. Naji, "The dead oil viscosity correlations. A C# simulation approach," 2011.

[16] O. P. R. Dohrn, Thermophysical properties: industrial directions, 2002.

[17] G. F. Georgios Kontogeorgis, Thermodynamic Models for Industrial Applications, From Classical and Advanced Mixing Rules to Association Theories, 2010.

[18] J. N. J. Romain Privat, "Thermodynamic models for the prediction of petroleum-fluid phase behaviour," 2012.

[19] B. Cornils, Catalysis from A to Z - A concise Encyclopedia.

[20] P. R. P. David S. J., Handbook of petroleum processing, 2006.

[21] G. L. Lakes, A practical guide for steady state modeling of petroleum processes.

[22] D. W. G. Robert H. Perry, Perry's chemical engineers' handbook, 1997.

[23] ""Statistical analysis of major accidents in petrochemical industry notified to the Major Accident Reporting System"," *Journal of hazardous materials,* 2006.

[24] Noria, "www.machinerylubrication.com," [Online]. Available: https://www.machinerylubrication.com/Read/31107/oil-lubricant-additives. [Accessed July 2019].

[25] T. Bennison, "Prediction of heavy oil viscosity," 1998.

[26] "Statistical analysis of major accidents in petrochemical industry notified to the Major Accident Reporting System," *Journal of Hazardous materials,* 2006.

[27] "Statistical analysis of major accidents in petrochemical industry notified to the Major Accident Reporting System," *Journal of Hazardous materials,* 2006.